NEW MECHANISM-BASED ANTICANCER DRUGS THAT ACT AS ORPHAN

NUCLEAR RECEPTOR AGONISTS

A Dissertation

by

SUDHAKAR REDDY CHINTHARLAPALLI

Submitted to the Office of Graduate Studies of
Texas A&M University
in partial fulfillment of the requirements for the degree of

DOCTOR OF PHILOSOPHY

May 2006

Major Subject: Biochemistry

NEW MECHANISM-BASED ANTICANCER DRUGS THAT ACT AS ORPHAN

NUCLEAR RECEPTOR AGONISTS

A Dissertation

by

SUDHAKAR REDDY CHINTHARLAPALLI

Submitted to the Office of Graduate Studies of
Texas A&M University
in partial fulfillment of the requirements for the degree of

DOCTOR OF PHILOSOPHY

Approved by:

Chair of Committee,	Stephen Safe
Committee Members,	David Peterson
	James Sacchettini
	Robert Burghardt
Head of Department,	Gregory Reinhart

May 2006

Major Subject: Biochemistry

ABSTRACT

New Mechanism-Based Anticancer Drugs That Act as Orphan Nuclear Receptor

Agonists. (May 2006)

Sudhakar Reddy Chintharlapalli, B.V.M., College of Veterinary Science,

Acharya N.G.Ranga Agricultural University, India;

M.S., Texas A&M University-Kingsville

Chair of Advisory Committee: Dr. Stephen Safe

1,1-Bis(3'-indolyl)-1-(*p*-substitutedphenyl)methanes containing *p*-trifluoromethyl (DIM-C-pPhCF$_3$), *p-t*-butyl (DIM-C-pPhtBu), and phenyl (DIM-C-pPhC$_6$H$_5$) substituents have been identified as a new class of peroxisome proliferator-activated receptor γ (PPARγ) agonists that exhibit antitumorigenic activity. In this study, the PPARγ-active compounds decreased HT-29, HCT-15, RKO, HCT116 and SW480 colon cancer cell survival and KU7 and 253JB-V33 bladder cancer cell survival. In HT-29, HCT-15, SW480 and KU7 cells, the PPARγ agonists induced caveolin-1 expression and this induction was significantly downregulated after cotreatment with the PPARγ antagonist GW9662. Since overexpression of caveolin-1 is known to suppress cancer cell and tumor growth, the growth inhibitory effects of the DIM compounds in these cell lines are associated with PPARγ-dependent induction of caveolins. These PPARγ-active compounds did not induce caveolin-1 in HCT-116 cells. However, these compounds induced NSAID-activated gene-1 (NAG-1) and apoptosis in this cell line. This represents a novel receptor-independent pathway for C-DIM-induced growth inhibition

and apoptosis in colon cancer cells. In SW480 colon cancer cells 2.5-7.5 μM C-DIMs induced caveolin-1 whereas high concentrations (10 μM) induced pro-apoptotic NAG-1 expression. In athymic nude mice bearing SW480 cell xenografts DIM-C-pPhC$_6$H$_5$ inhibited tumor growth and immunohistochemical staining of the tumors show induction of apoptosis and NAG-1 expression. Thus, the PPARγ-active compounds induce both receptor-dependent and-independent responses in SW480 cells which are separable over a narrow range of concentrations and this dual mechanism of action enhances their antiproliferative and anticancer activities. Similar results were obtained for another structural class of PPARγ agonists namely 2-cyano-3,12-dioxoolean-1,9-dien-28-oic acid (CDDO) and the corresponding methyl (CDDO-Me) and imidazole (CDDO-Im) esters. Structure-activity studies show that 1,1-bis(3'-indolyl)-1-(*p*-substitutedphenyl)methanes containing *p*-trifluoromethyl (DIM-C-pPhCF$_3$), hydrogen (DIM-C-pPh) and *p*-methoxy (DIM-C-pPhOCH$_3$) substituents activate Nur77 and induce apoptosis in pancreatic, prostate, and breast cancer cell lines. Nur77 agonists activate the nuclear receptor, and downstream responses include decreased cell survival, induction of cell death pathways including tumor necrosis factor related apoptosis-inducing ligand (TRAIL) and PARP cleavage. Nur77 agonists also inhibit tumor growth *in vivo* in athymic nude mice bearing Panc-28 cell xenografts.

DEDICATION

This dissertation is dedicated to my parents
C. ASWATHAPPA & C. LEELAVATHI
Their constant love and care are the cornerstones for where I am and
what I am. My gratitude and my love to them are beyond words.

ACKNOWLEDGEMENTS

TABLE OF CONTENTS

LIST OF FIGURES

XV

LIST OF TABLES

CHAPTER I

INTRODUCTION

Nuclear Receptors

Nuclear receptors comprise a large family of ligand-dependent and independent transcription factors responsible for processes as diverse as organogenesis during development, to governing cyclicity in reproductive tissues. These transcription factors act by transducing the effects of small, lipophilic hormones, synthetic compounds and other endogenous ligands into transcriptional responses (1-4). Nuclear receptors comprise the largest evolutionarily conserved family of transcription factors, found in a variety of animal kingdoms from nematodes to man. More than 5% of our genes are predicted to encode transcription factors underscoring the importance of this family in biology.

In humans, 48 nuclear receptors (Table 1.1) (5) and in mouse 49 nuclear receptors (6) have been identified; this can be compared to 21 nuclear receptor genes in the complete genome of the fly *Drosophila melanogaster* (7) and unexpectedly more than 270 nuclear receptor genes in the worm *Caenorhabditis elegans* (8). This diversity has been organized into a phylogeny-based nomenclature of the form NRxyz, where x is the sub-family, y is the group and z is the gene (9). The nuclear receptor superfamily

_____

This dissertation follows the style of Cancer Research.

includes receptors for steroid hormones [(estrogen receptor (ER), androgen receptor (AR), adrenal glucocorticoid receptor (GR), mineralocorticoid receptor (MR), and progesterone receptor (PR)], nuclear hormones [(vitamin D receptor (VDR), retinoic acid receptor (RAR) retinoid X receptor (RXR), thyroid receptor (TR)], and several orphan nuclear receptors such as [(peroxisome proliferator activated receptors (PPAR)] have also been characterized. Orphan receptors have diverse functions in cells, during development and in adult physiology, however their endogenous ligands are not completely defined. Some orphan receptors such as PPARs are activated by endogenous
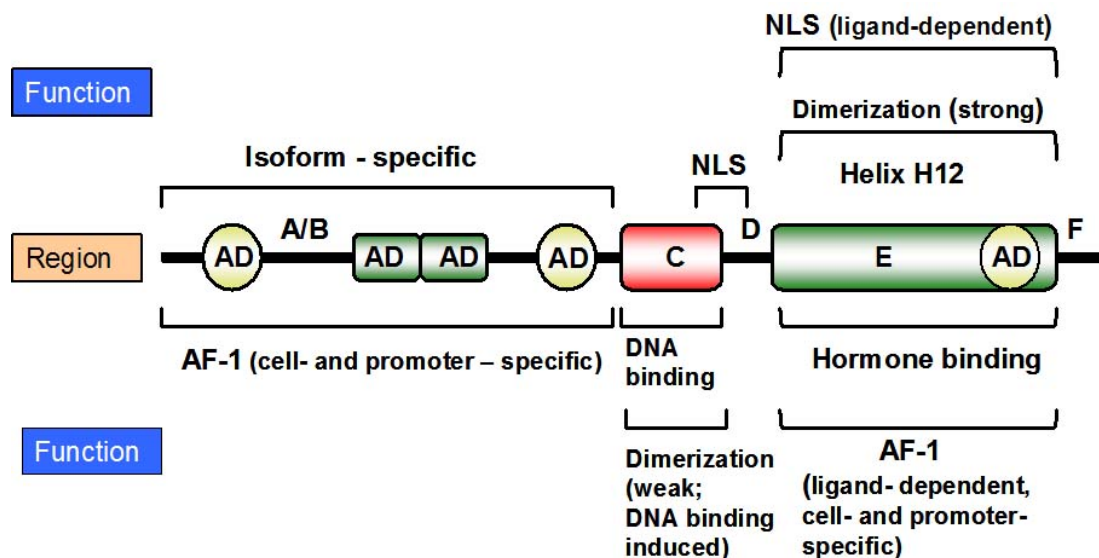
Fig. 1.1. Schematic illustration of the structural and functional organization of nuclear receptors. The evolutionary conserved regions C and E are indicated as boxes and a black bar represents the divergent regions A/B, D and F. Domains functions are described above and below the scheme. Two transcription activation functions(AFs) have been described in several nuclear receptors, a constitutively active AF-1 in region A/B and a ligand inducible AF-2 in region E. Within these activation functions, autonomous transactivation domains (ADs) have been defined in the ER and PR N-terminal regions. In the case of the ER, RXR, TR an autonomous activation domain encompassing helix H12 has been detected at the C-terminal end of the ligand binding domain E (10).

Table 1.1. Human nuclear receptors (10).

Class	Receptor	Subtype	Nomenclature	Ligand	Half-site[1]	Configuration[2]
I	Thyroid hormone receptor	TRα	NR1A1	Thyroid hormone	RGGTCA	IR-0, DR4, ER6,8
		TRβ	NR1A2	Thyroid hormone		
I	Retinoic acid receptor	RARα	NR1B1	Retinoic acid	AGTTCA	IR-0,DR2,5, ER-8
		RARβ	NR1B2	Retinoic acid		
		RARγ	NR1B3	Retinoic acid		
I	Peroxisome proliferators activated receptor	PPARα	NR1C1	Fattyacids, leukotrieneB4, fibrates	AGGTCA	DR-1
		PPARβ	NR1C2	Fattyacids		
		PPARγ	NR1C3	Fattyacids, prostaglandin J2		
I	Reverse erbA	Rev-erbα	NR1D1	Orphan	WAWNAG GTCA	NR
		Rev-erbβ	NR1D2	Orphan		
I	RAR-related orphan receptor	RORα	NR1F1	Cholesterol	WWCWRG GTCA	NR
		RORβ	NR1F2	Retinoic acid		
		RORγ	NR1F3	Retinoic acid		
I	Liver X receptor	LXRα	NR1H3	Oxysterols, T0901317, GW3965	RGKTCA	DR-4
		LXRβ	NR1H2	Oxysterols, T0901317, GW3965		
I	Farnesoid X receptor	FXRα	NR1H4	Bile acids, Fexaramine	AGGTCA	IR-1, DR-5
		FXRβ	NR1H5	Lanosterol		
I	Vitamin D receptor	VDR	NR1I1	1,25-dihydroxy vitamin D3, litocholic acid	RGKTCA	DR-3
I	Pregnane X receptor	PXR	NR1I2	Xenobiotics, pregnenolone 16α–carbonitrile (PCN)	AGTTCA	DR-3
I	Constitutive androstane receptor	CAR	NR1I3	Xenobiotics, Phenobarbital	RGKTCA	DR, IR, ER
II	Human nuclear factor 4	HNF-4α	NR2A1	Orphan	AGGTCA	DR-1
		HNF-4γ	NR2A2	Orphan		

Table 1.1. Continued.

Class	Receptor	Subtype	Nomenclature	Ligand	Half-site[1]	Configuration[2]
II	Testis receptor	TR2 TR4	NR2C1 NR2C2	Orphan Orphan	AGGTCA	DR-1
II	Taillless	TLL	NR2E2	Orphan	AAGTCA	NR
II	Photo-receptor-specific nuclear receptor	PNR	NR2E3	Orphan		
II	Chicken ovalbumin upstream promoter-transcription factor	COUP-TFI COUP-TFII	NR2F1 NR2F2	Orphan Orphan	RGGTCA	DRs, IRs
II	ErbA2-related gene-2	EAR2	NR2F6	Orphan		
III	Estrogen receptor	Erα Erβ	NR3A1 NR3A2	Estradiol-17β, tamoxifen, raloxifene Estradiol-17β, various synthetic compounds	RGGTCA	IR-3
III	Estrogen receptor–related receptor	ERRα ERRβ ERRγ	NR3B1 NR3B2 NR3B3	Orphan Diethylstilbestrol, 4-OH tamoxifen Diethylstilbestrol, 4-OH tamoxifen	TCAGGTCA	NR
III	Glucocorticoid receptor	GR	NR3C1	Cortisol, dexamethasone, RU486	AGAACA	IR-3
III	Mineralocorticoid receptor	MR	NR3C2	Aldosterone, spirolactone	AGAACA	IR-3

Table 1.1. Continued.

Class	Receptor	Subtype	Nomenclature	Ligand	Half-site[1]	Configuration[2]
III	Androgen receptor	AR	NR3C4	Testosterone, flutamide	AGAACA	IR-3
IV	NGF-induced factor B	NGFI-B	NR4A1	Orphan	AAAGGTCA	NR, DR-5, IR-0
IV	Nurr related factor 1	NURR1	NR4A2	Orphan	AAAGGTCA	NR, DR-5, IR-0
IV	Neuron-derived orphan receptor 1	NOR1	NR4A3	Orphan	AAAGGTCA	NR, DR-5, IR-0
V	Steroidogenic factor 1	SF1	NR5A1	Orphan	YCAAGGYCR	NR
V	Liver receptor homologous protein 1	LRH1	NR5A2	Orphan	YCAAGGYCR	NR
VI	Germ cell nuclear factor	GCNF	NR6A1	Orphan	TCAAGGTCA	DR-0
0	Dosage-sensitive sex reversal adrenal hypoplasia congenita critical region on the chromosome, gene 1	DAX-1	NR0B1	Orphan		
0	Short hetero-dimeric partner	SHP	NR0B2	Orphan		

[1] R, purine (adenine or guanine); Y, pyrimidine (thymine or cytosine); W, adenine or thymine; K, guanine or thymine. [2]Hormone response elements are configured as direct repeats (DR), inverted repeats (IR), everted repeats (ER) or nonrepeats (NR) and are spaced by the given number of nucleotides.

and synthetic ligands and these have been referred to as adopted orphan receptors where the identity of true natural ligands in most instances remains to be elucidated.

Despite their functional diversity, molecular cloning and structure/function analyses have revealed that members of the superfamily have a common functional domain structure. This includes a variable N-terminal domain A/B, a well conserved DNA-binding domain (DBD) or region C, a not well conserved linker region D, a conserved domain E that contains the ligand binding domain (LBD) and insome receptors a C-terminal region F whose functions have not been defined (Fig. 1.1).

The hypervariable A/B region often contains an autonomous transcriptional activation function (AF-1) that contributes to constitutive ligand-independent activation by the receptor. The DBD is crucial for recognition of specific DNA sequences and protein:protein interactions. A second transcriptional activation domain (AF-2) in the LBD is essential for ligand-dependent transactivation. The D domain serves as a hinge between the DBD and the LBD and allows rotation of the DBD with respect to the LBD and also often contains nuclear localization signals.

Structural features of specific domains of the nuclear receptor superfamily

The N-Terminal Domain (NTD)

The NTD of many members of the nuclear receptor superfamily contains a powerful transactivation domain, AF-1. Molecular and genetic evidence indicates that this NTD plays an important role in gene regulation (11, 12). Circular dichroism and nuclear magnetic resonance (NMR) studies have shown that the AF-1 region of GR, which is rich in acidic amino acid residues, is largely unstructured in aqueous solution

under a variety of pH conditions (13). However, as many as three segments at the C-terminal end of the AF-1 region exhibit α-helical characteristics in the presence of the strong α-helix stabilizing agent trifluroethanol (TFE). The ability to activate a reporter gene *in vivo* correlates with the ability to form an α-helical conformation, in addition, introduction of helix-breaking proline residues in the potential helix-forming regions of the AF-1 domain of GR greatly disturb the transactivation capacity, suggesting that α-helical structure is important for receptor activity (13, 14). The importance of induction of the α-helical structure in the AF-1 region by TFE is a topic of considerable interest since TFE not only induces α-helical structure in peptides (15) but can also force helicity in peptides. Nevertheless it is unclear whether and under what conditions analogous conformational changes in nuclear receptors occur *in vivo*.

It is not clear how any part of N-terminal region or AF-1 interacts with other proteins to induce transcription. Hypothetically, the transactivation domain is unstructured (16) until it is bound to its putative target factors and interaction of the transactivation domain with these factors by an induced fit mechanism leads to a stabilized structure(17). Functional and physical interaction with the basal transcriptional machinery by the AF-1 domain of GR have been reported (18, 19) and mutants of the AF-1 domain affected these interactions. Interactions with other coactivators, mediators and adaptors are also important (20-22). The data support the idea that conditional folding of the activation domain is an important requirement for its interaction with target factors and subsequent roles in gene regulation (18, 21, 22). However these

concepts are only inferred from experimental data since X-ray crystal structure analysis on the AF-1 domains of nuclear receptors have not been reported.

The DNA-Binding Domain (DBD)

The DBD has the most conserved amino acid sequence among the members of the nuclear receptors superfamily. The DBD consists of two zinc-finger motifs, each containing four highly conserved cysteine residues coordinating binding of a zinc atom (Fig. 1.2). This results in formation of a tertiary structure containing helices that interact specifically with DNA sequences that are organized appropriately in response elements (23-25). In addition to the two zinc fingers that span 60-70 amino acids, this domain is also comprised of a COOH-terminal extension (CTE).

With the use of NMR spectroscopy, the structures of the DBDs of the ER, GR RAR-β, and RXR in solution have been determined (26-29). Crystal structures of the DBDs of the GR and ER complexed with DNA have been reported (16, 23). The central feature of the secondary structure elements within the GR DBD is found in three helical regions. Helices I and III are oriented perpendicular to each other and form the base of a hydrophobic core. NMR studies indicate that helices I and III are both regular α–helices, whereas helix II is somewhat distorted (26). The DBD may be considered as two interdependent subdomains, each consisting of a zinc ion, tetrahedrally coordinated to the sulphurs of four cysteine residues, and an amphipathic helix. The two subdomains differ both structurally and functionally. The helix of the first domain is mainly involved in site-specific recognition based on its interaction with certain bases in the cognate response element hexamer. Also within this helix are the amino acids responsible for

Zinc finger module 1

Zinc finger module 2
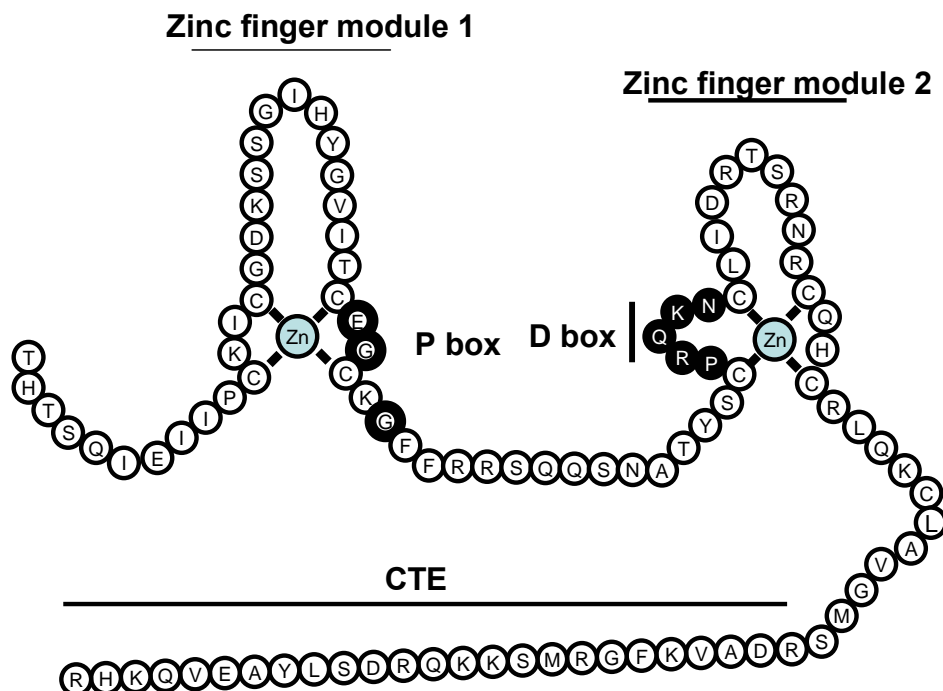
Fig. 1.2. Schematic structure of a nuclear receptor DBD. Amino acid sequences of orphan nuclear receptor DNA-binding domain are shown. The two zinc finger modules as well as CTE are identified. Amino acids in P-box and D-box that are important for the DNA recognition and dimerization, respectively are highlighted (30).

site-specific discrimination of DNA binding. These 3-4 amino acids have been termed the P box (23, 29).

A loop formed in the second subdomain, the so-called D box provides the DBD homodimerization interface, and the helical region is important for less specific DNA interactions. The crystal structure of GR DBD complexed with DNA shows that helix I (the recognition helix) fits into the major groove of the DNA helix and provides critical contacts between three amino acids in the protein helix (23). Helix II which spans the

COOH terminus of the second Zinc finger forms a right angle with the recognition helix.

The hinge region

This region is less conserved in nuclear receptors than the surrounding C and E region. The hinge domain allows DBDs and LBDs to adopt several different conformations without creating any steric hindrance problems. The D region also contains a nuclear localization signal (31). The intracellular localization of nuclear receptors is a result of dynamic equilibrium between nuclear cytoplasmic and cytoplasmic-nuclear shuttling (32). At equilibrium, some steroid receptors (GR, MR and AR) reside in the cytoplasm of cells in absence of ligands and translocate into the nucleus in a ligand-induced fashion. Many other nuclear receptors are in the nucleus in the unbound state and the addition of ligand facilitates interactions with the promoter DNA and transactivation (33, 34).

The Ligand-Binding Domain (LBD)

The LBD is a multifunctional domain that, in addition to the binding of ligand, mediates receptor homo- and heterodimerization, interaction with heat-shock proteins, ligand-dependent transcriptional activity and in some cases, hormone reversible transcriptional repression. For 20 out of the 48 human nuclear receptors the crystal structure of the LBD has been solved (35). These studies have demonstrated that the overall structures of the different receptors are rather similar, suggesting a canonical structure for the different members of the nuclear receptor superfamily (36).

The LBDs are generally composed of a series of 11-12 α-helices (H1-H12) closely folded in a similar manner. There are slight differences in the specific helix

number given for topologically analogous sites when LBDs from different receptors are compared since no universal numbering convention has been adopted. Inspection of helices within the LBDs, show conservation of helical arrangement, with only slight differences, regardless of the numbering system. The structure of the unliganded LBD of the RXR-α revealed that about 65% of the total volume is occupied by 11 α-helices organized in a three layer, antiparallel sandwich and a conserved β–sheet between H5 and H6 (37). A central core layer of three helices is packed between two additional layers to create a cavity, the ligand binding pocket, which accomodates the ligand. This domain is mainly hydrophobic and is buried within the bottom half of the LBD. Contacts with the ligand can be extensive and include different structural elements throughout the LBD.

Similar overall folding was also observed for the structures of the ligand-bound LBDs of TR, RAR-γ, and ERα (38-40) and with the exception of the C-terminal helix their secondary structural features are superimposable (41). However, PPARγ is unique in its overall structure and contains an extra helix designated H2′, and the VDR contains a poorly structured insertion between helices H1 and H3 for which no functional role has been defined (42). Although the secondary structure elements in the unliganded and ligand bound RXR-α and RXR-γ are similar, the bound receptor is more compact. The ligand-bound LBDs of the TR and ER also reveal a more compact structure compared to unliganded RXR-α. Presumably, these differences are due to ligand-induced conformational changes that stabilize the conformation of a large portion of the LBD. The extensive involvement of amino acids from many parts of the LBD to make the

ligand-binding pockets is consistent with the data showing that mutation of several amino acid mutations within the LBD interfered with ligand binding.

The ER LBD was the first nuclear receptor LBD in which the structure of both agonist and antagonist bound complexes have been determined (38). The binding cavity of the LBD bound to the agonist 17 β-estradiol is completely partitioned from the external environment, occupying a relatively large portion of the hydrophobic core of the ER-LBD. This is formed by segments of H3, H6 and H8 and the loop formed by H11 and H12. The antagonist raloxifene binds at the same site but significantly alters the position of helix 12. When the antagonist is bound, the positioning of H12 inhibits interaction of the LBD with coactivators. Thus, the altered LBD surface presumably changes critical protein:protein contacts involving AF2 (H12) and coactivators/corepressors and this accounts for the antagonist activity of raloxifene.

The ligand-inducible activation function has been attributed to the C-terminal part of the LBD (43, 44). For this function to manifest itself, ligand-dependent interactions with a number of putative transcriptional coactivators must occur (45). The region shown by molecular genetics to be essential for AF2 function adopts a helical structure, which corresponds to the C-terminal helix H11 in the unliganded RXR-α LBD structure. This helix is often known as the AF2 activation helix which extends from the core of the LBD, pointing away from the dimer axis at an angle of about 45^{0}. This orientation may be optimal for facilitating interactions with putative intermediary factors (46). The equivalent AF2 activation helix corresponds to the C-terminal amphipathic helix H12 in the liganded RAR, TR, and ER LBDs, and it is positioned as a tight part of

the globular LBD that is different in position from its counterpart in the unliganded RXR (37-40). Deletion and mutational studies have shown that the AF2 activation helix is essential for ligand induced transcriptional activation. It appears that ligand-dependent activation of AF2 induces major conformational changes, required for efficient interactions with transcription factors (47, 48).

The C-terminal F region

The C-terminal F region is not evolutionary conserved and only some receptors possess this domain. The function of the C-terminal sequence is poorly understood, however, recent data suggest that the F-region might play a role in coactivator recruitment to the E-domain and in determining the specificity of the LBD coactivator interface (49, 50).

Hormone Response Elements (HREs)

HREs are specific DNA sequences in target genes that are bound by nuclear receptors in response to steroid hormones to regulate transcription. These elements are normally present in the 5′ regulatory sequences of target genes. HRE's can be located proximal to the translational start site in the distal enhancer region up to several kilobases upstream of the transcriptional start site. The glucocorticoid response element (GRE) was the first HRE identified by mutational analysis of the glucocorticoid-responsive mouse mammary tumor virus (MMTV) gene (51). A deletion or mutation of that sequence eliminated hormone responsiveness. Later it was demonstrated that a short oligonucleotide corresponding to the identified sequence conferred glucocorticoid binding and responsiveness to a heterologous promoter (52). The GRE consisted of two

short, imperfect inverted repeats separated by three nucleotides. Later, response elements for PR, MR and AR were shown to be similar to that of GR (53-57).

A large number of synthetic and naturally occurring HREs were analyzed and a sequence of 6 bp that constitutes the core recognition motif was determined. Two consensus motifs have been recognized, the sequence AGAACA is preferentially recognized by steroid receptors except ER, whereas AGG/TTCA serves as recognition motif for other receptors of the nuclear receptor superfamily (1). Both consensus and variable nonconsensus HREs have been identified. Some monomeric receptors bind to a single hexameric motif, but most nuclear receptors bind as homo- or heterodimers to HREs composed principally of two hexameric half-site core sequences. Modifying the location of the half-sites relative to one another creates diversity among HREs. For dimeric HREs, the half-sites can be configured as palindromes, inverted palindromes or direct repeats (DR) and this influences the receptor dimerization pattern on an HRE.

The nuclear receptor superfamily can be subclassified into at least four categories based on their protein-protein and protein-DNA (HRE) interactions (Fig. 1.3). Class I steroid hormone receptors, form symmetrical head to head arranged homodimers bound to a palindromic HRE (23). Class II receptors are ligand-activated receptors that always

I Steroid receptors (Homodimer)
AR
ER
GR
MR
PR

II RXR:NR receptors (Heterodimer)
RAR   FXR
TR   LXR
VDR   PXR
PPAR EcR

III Orphan receptors (Monomer)
SF-1
ROR
ERR

IV Orphan receptors (Homodimer)
COUP-TF
TR2
HNF4
GCNF
TLX
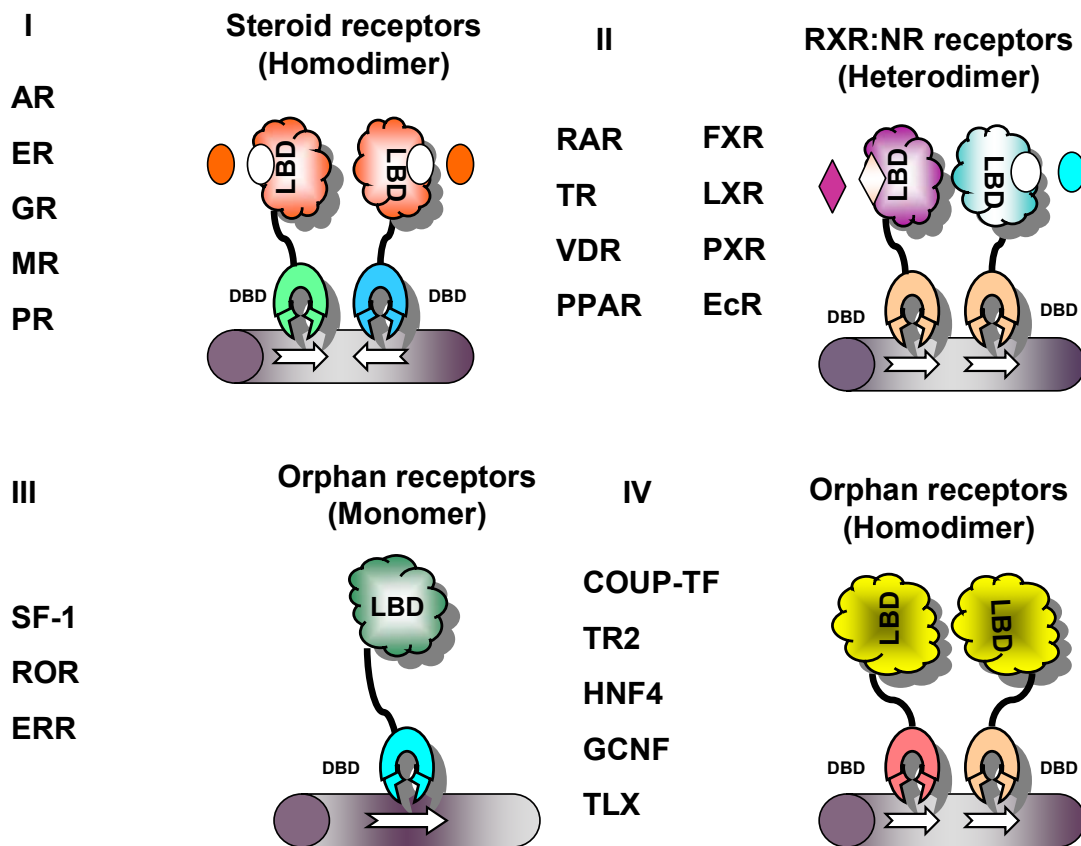
Fig. 1.3. Classification of nuclear receptor family transcription factors. Nuclear receptors can be grouped into four classes according to their ligand binding, DNA binding, and dimerization properties: Steroid receptors, RXR:Nuclear Receptor (NR) heterodimers, RXR heterodimers, homodimeric orphan receptors, and monomeric orphan receptors. Shown are representative receptors for each group (30).

bind to the DR elements arranged asymmetrically in head to tail orientation as a heterodimer with RXR. Class III receptors bind primarily to direct repeats as homodimers and Class IV receptors typically bind to extended core sites as monomers. Most orphan receptors fall into the Class III and IV categories. Further selectivity is

created between HREs by varying the number of neutral base pairs separating the half-site repeats. According to inter-half-site spacing (1-5 bp), these elements are also known as DR1-DR5 (4, 58-60). This is the key identity factor contributing to the binding specificity of different RXR heterodimer pairs and it provides the geometry required for two subunits to specifically interact. Even a single base pair insertion in the inter-half-site spacing displaces the interacting subunits by nearly 3.4 A^0 and reorients them by $\sim35^0$, leading to disruption of important protein-protein and protein-DNA interactions (61). Sequence composition of the spacer nucleotides plays a less critical role in the recognition of HREs by receptors (60, 61).

Molecular mechanisms of transcriptional regulation by nuclear receptors

Nuclear receptor activation is often represented by initial ligand binding to a cytoplasmic receptor complexed with heat shock proteins, which then translocates to the nucleus and binds HREs to activate gene expression. This model is valid only for some steroid hormone receptors (62). Most unbound nuclear receptors are constitutively nuclear and bound to DNA in the absence of ligand, many nuclear receptors act as strong repressors of gene expression (63-67).

Gene expression can be regulated at several different levels, including transcription, translation and posttranslation. Transcription can also be regulated at multiple levels. The transcriptional activity of a gene can be controlled epigenetically via methylation, at the level of its chromatin structure and at the level of the assembly and activity of the initiating and elongating polymerase complexes. The reported effects of nuclear receptors on transcription are so far restricted to the initiation of transcription by

RNA polymerase II (Pol II). Pol II begins transcription with the formation of preinitiation complex in which general transcription factors and Pol II are assembled at the promoter in a defined order. It has been demonstrated that nuclear receptors increase the formation rate of the complex of basal transcription factors and Pol II at the promoter by interacting with specific basal transcription factors including TFIIB, TFIID, and TATA binding protein associated factors (TAFs); however it is evident that a multitude of other factors are involved in these interactions.

Overexpression of the GAL4 transcription factor in yeast squelches the transcription of genes lacking GAL4 response elements. The observation of transcriptional interference or squelching between nuclear receptors provided evidence for the existence of limiting common transcriptional cofactors or adaptors. Meyer *et al* (68) first demonstrated squelching for nuclear receptors by showing that stimulation of transcription of reporter genes by the PR can be decreased by coexpression of ER in the same cell. They also showed that overexpression of ER inhibited transactivation by GR and, as expected these steroid hormone receptors were activated by common coactivators. Squelching experiments also suggested that different types of AFs exist. The two AF domains that were identified in ER and GR differed in their ability to squelch one another (46, 69, 70). For example, the AFs of ER will squelch one another, but the AF-1 of GR will not squelch AF-2 of ER.

Nuclear receptor coactivators, a growing family

Genetic studies demonstrated that transcription cofactors with no specific DNA-binding activity are essential components of transcriptional regulation, and these studies

led to identification of a series of nuclear receptor-interacting coregulator proteins (71). It has been shown that coactivators exhibit some characteristic features. First they must interact with the activation domain of a nuclear receptor directly in a ligand-dependent manner, leading to the enhancement of the receptor activation function. Secondly, a coactivator should also interact with components of the basal transcriptional machinery. Thirdly, some coactivators also exhibit critical enzymatic functions linked to gene regulation, such as the nucleosomal remodeling histone acetyltransferase (HAT) or deacetylase (HDAC) activities. Finally, coactivators alone should not enhance basal transcriptional activity even though they may contain an autonomous activation function (72, 73).

The p160/SRC family

Ligand-induced transactivation function of several nuclear receptors were enhanced by a group of conserved adaptor proteins termed as p160/SRC coactivators. Three distinct but related family members from different species, with each member having a number of splice variants have been identified. These include SRC-1/NCoA-1 (74-76), TIF2/GRIP1/NCoA-2 (74, 76), and p/CIP/ACTR/AIB1/TRAM1/RAC3 (77-79). All three members of the p160/SRC family interact with a broad range of nuclear receptors in a ligand-dependent and independent fashion and enhance nuclear receptor-dependent transcription both *in vitro* and *in vivo* (80).

The p160/SRC proteins contain three distinct functional domains (Fig 1.4). The central nuclear receptor-interaction domain contains three copies of a consensus leucine
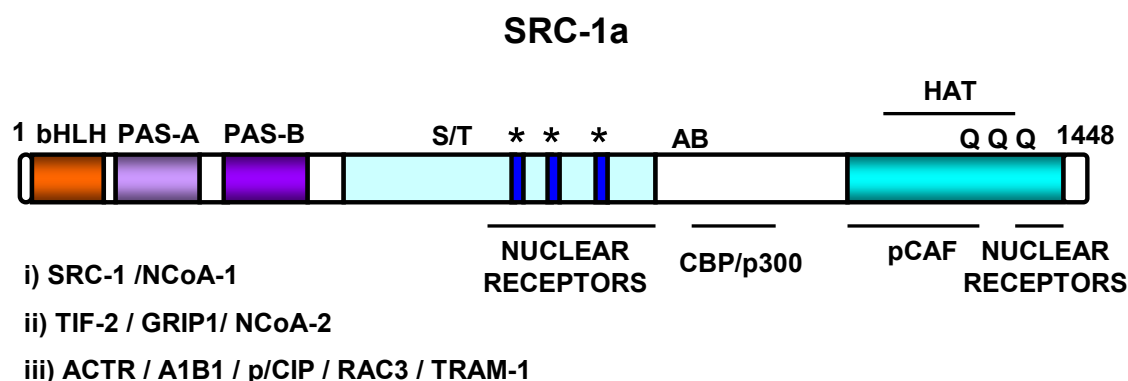
SRC-1a

Fig. 1.4. Structural representation of SRC1a. The structure of SRC1a is representative of a class of highly homologous coactivators. These are divided into three subgroups (i, ii, iii) based on more stringent homology. Asterisks denote LXXLL motifs. bHLH, basic helix-loop-helix; PAS, period/aryl hydrocarbon receptor/single minded; S/T, serine/threonine rich; AB, acidic base; HAT, histone acetyl transferase activity; QQQ, glutamine rich (81).

rich LXXLL signature motifs (NR box) (75, 82). Biochemical and crystallographic studies reveal that the AF2 core (helix 12) undergoes major conformational change upon ligand binding, forming part of a "charged clamp" that accommodates p160/SRC coactivators within a hydrophobic cleft of the receptor LBD, through direct contacts with the LXXLL motifs (83, 84). The N-terminal region of p160 proteins contains a basic helix-loop-helix/Per-Arnt-Sim (bHLH/PAS) domain. This domain plays a role in DNA binding and homo and heterodimerization between proteins containing these motifs (85). These domains have been implicated as potential target sites for other non-nuclear receptor activators (80). The central and the carboxy-terminal regions contain two intrinsic transcriptional activation domains (AD1 and AD2) that retain their activity when transferred to a heterologous DNA binding domain. The AD1 region is responsible for interactions with HAT enzymes, p300 and CREB binding protein (CBP) (76, 86, 87), but does not interact with nuclear receptors (88). The second activation domain (AD2)

located in the C-terminal region of SRC proteins is responsible for interaction with histone methyltransferases, CARM1 and PRMT1 (86, 89).

p160/SRC family members SRC1 and SRC3 (ACTR) possess an intrinsic acetyltransferase activity in their carboxy terminal that is primarily specific for histones H3 and H4 (78, 90). This weaker HAT activity does not appear to be essential for the nuclear receptor-coactivation function (91). Taken together, the data suggest that p160/SRC coactivators effectively target histone modifying enzymes (HATs or histone methyltransferases (HMTs)) to nuclear receptors in a ligand-dependent manner. This results in chromatin remodeling and results in formation of the preinitiation complex, to enhance transcription of target genes.

The CBP/p300 coactivators

CBP and p300 exhibit significant homology and are functionally interchangeable (92), and are referred to as CBP/p300. Although these proteins lack direct DNA-binding activity, they are recruited to specific promoters by forming complexes with sequence-specific transcription factors such as nuclear receptors (80, 93). CBP/p300 coactivators contain several distinct and functionally important domains (Fig. 1.5), including a conserved HAT domain, a centrally located bromodomain that is frequently found in mammalian HATs, three cysteine/histidine (CH)-rich zinc finger domains (CH1, CH2 and CH3), an Ada2 homology domain, which shares extensive homology with the yeast transcriptional coactivator, Ada2p (94) and an SRC/p160 interacting domain (SID). The
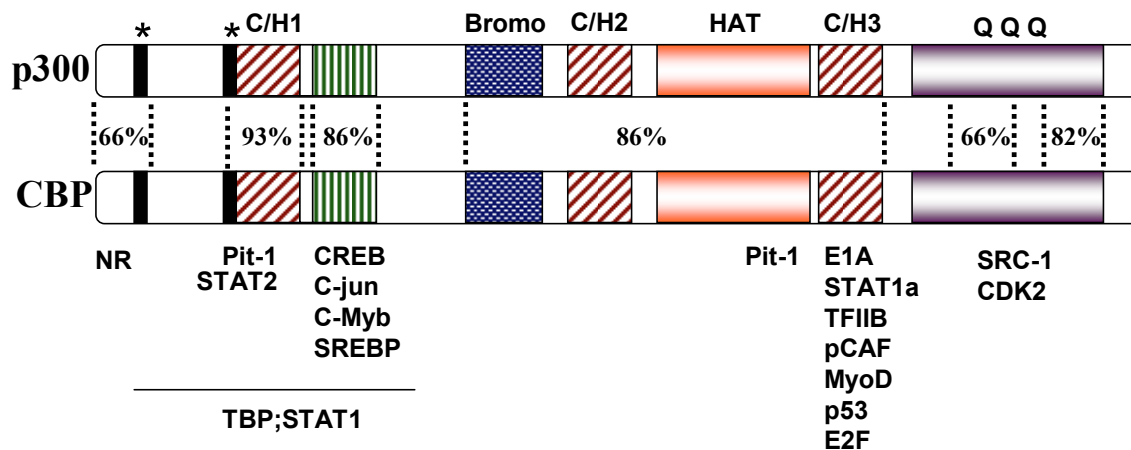
Fig. 1.5. Structural representation of p300/CBP. Factors known to interact with these proteins are shown below the structures. HAT, histone acetyl transferase activity; QQQ, glutamine rich; C/H, cysteine rich; Bromo, bromodomain (81).

CBP/p300 nuclear receptor coactivation function primarily depends on its intrinsic HAT activity (95, 96) since mutations in the HAT domain abolishes its ability to enhance transactivation *in vitro* and *in vivo* (87, 97). CBP/p300 proteins can acetylate all four core histones (98) and form complexes with other HATs, such as p300/CBP associated factor (p/CAF) (99) TFIIB and Pol II via its CH domains (92, 93). The bromodomain plays a role in recognizing different acetylation motifs to facilitate stable CBP/p300 interactions with chromatin (100). The amino terminal regions of CBP/p300 also contain two LXXLL-like motifs that facilitate direct interactions with nuclear receptors (22, 101). However several studies indicate that CBP/p300 is recruited to nuclear receptors by binding to p160/SRC coactivators through its SID domain (102). The recruitment of the nuclear receptor-p160/SRC-CBP/p300 complex to specific target genes results in

histone acetylation of the proximal promoter and this facilitates the ordered recruitment of other types of transcriptional regulatory complexes (103-105).

CARM1

The coactivator arginine methyltransferase 1 (CARM1) enhances transcriptional activation of a broad range of nuclear receptors by physically interacting with the AD2 domain of p160/SRC coactivators (86, 89). CARM1 belongs to a conserved family of protein arginine methyltransferases (PRMT). PRMT catalyzes formation of asymmetric dimethyl arginine residues in proteins by transferring the methyl moiety from S-adenosyl-L-methionine (AdoMet) to the guanidine group of arginine. CARM1 harbors several distinct domains (Fig. 1.6), including the highly conserved central core methyltransferase domain containing the AdoMet and arginine binding sites (106). Mutational analyses shows that a p160/SRC binding site and homo-oligomerization domain significantly overlap with the methyltransferase domain (107). The C-terminal region of CARM1 also contains a strong autonomous activation domain. Recent studies have demonstrated that CARM1 is recruited to promoters through its interaction with CBP/p300 to stimulate nuclear receptor dependent transcription (108). The autonomous C-terminal activation domain synergistically acts with methyltransferase activity to mediate CARM1 coactivator function. The recruitment of CARM1 and arginine-specific H3 methylation results in chromatin remodeling and enhancement of gene transcription (105).

TRAP/DRIP complex

The thyroid hormone receptor-associated protein (TRAP) and vitamin D receptor interacting protein (DRIP) complexes have been isolated based on their ligand-dependent interactions with TR (109, 110) or VDR (111, 112) respectively. Among the several subunits, the 220 kDa component of the TRAP/DRIP complex is unique in that it demonstrates direct ligand-dependent binding to several nuclear receptors, including TRα, VDR, RXRα, RARα, PPARα, PPARγ, ERα and GR (113-115). TRAP220 protein contains three distinct domains (Fig. 1.6) (114). The central nuclear receptor-interaction domain has two LXXLL motifs (NR Box). The two NR boxes show different ligand-dependent affinities for nuclear receptors. NR box 2 preferentially interacts with TRα, VDR and PPARα whereas NR box 1 binds the heterodimerization partner RXRα (114, 116, 117). Although NR box motifs are critical structural features that facilitate ligand-dependent nuclear receptor coactivator interactions (118, 119), a recent study demonstrates that coactivation of ERα by DRIP205 in ZR75 breast cancer cells is complex and involves multiple regions of DRIP205 and ERα (120). Moreover, coactivation of ERα by DRIP205 and interaction of these proteins do not require the NR box motifs of DRIP205 (120). A serine-rich domain followed by a cluster of mixed-charged amino acids is present in the C-terminal of TRAP220 which is responsible for oligomerization and DNA binding. The DRIP complex and p160/CBP share similar nuclear receptor binding determinants but do not bind nuclear receptors simultaneously and constitute functionally distinct complexes (116). A proposed general mode of action is that ligand-mediated association of HAT-containing or HAT- interacting coactivators

24
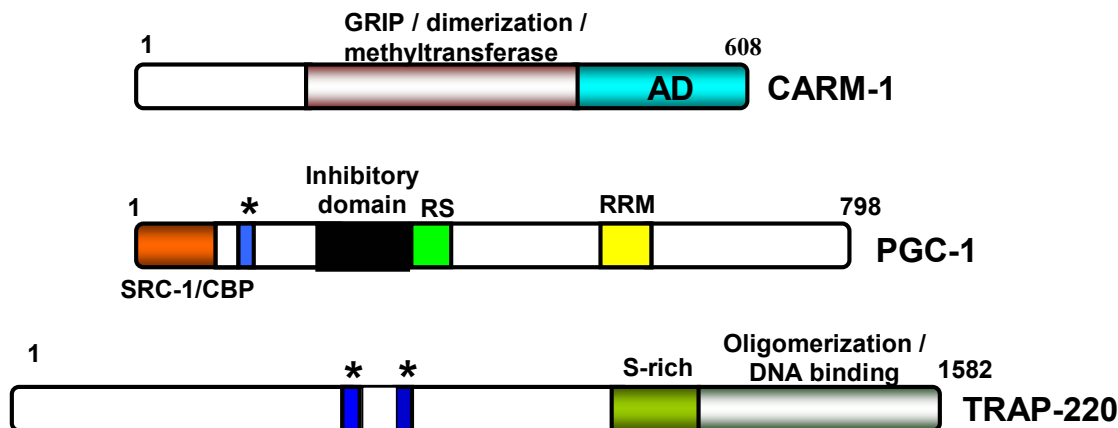
Fig. 1.6. Structural representation of CARM1, PGC-1 and TRAP220. The functional domains/regions are depicted. Asterisks denote LXXLL motifs. AD, transcriptional activation domain; RRM, RNA recognition motif (81).

are exchanged with the TRAP complex which subsequently recruits the transcription factors and Pol II to form a functional preinitiation complex (121).

PGC-1

Peroxisome proliferator-activated receptorγ coactivator-1 (PGC-1) was initially isolated as a coactivator of PPARγ. An isoform of PGC-1, PGC-1α, is preferentially expressed in brown adipose tissue and skeletal muscle and plays a role in adaptive thermogenesis and energy metabolism (122). PGC-1α enhances the transcriptional activation of the uncoupling promoter-1 (UCP-1), and these promoter specific coactivator functions are controlled by external environmental stimuli. PGC-1α contains several distinct domains (Fig. 1.6). A transcriptional activation domain (AD) and an LXXLL motif are present in the amino-terminal region of the protein (123, 124). The

LXXLL motif of PGC-1α mediates ligand-dependent interactions with nuclear receptors, such as ERα (125), ERRα (126), GR (127), PPARα (123), RXR (128), PPARγ (129) and TR (129). PGC-1α also interacts with the SRC-1 and CBP through its N-terminal region (124). An inhibitory domain that represses its transcriptional activation function is also present in PGC-1α. Interactions with transcription factors induces a conformational change in PGC-1α to relieve the inhibitory activity, and enable interaction with other effectors. PGC-1α also associates with Pol II and another isoform of PGC-1, PGC-1β, which is predominantly expressed in heart, adipose tissue, skeletal muscle and brain, and functions as a coactivator for TRβ, PPARα, PPARγ and GR. (130). Unlike PGC-1α, PGC-1β is not induced in response to environmental stimuli.

Other coactivators

In addition to the above mentioned coactivators, nearly 50 other putative coactivators have been identified. Many coactivators have been extensively studied including nuclear receptor interacting factor 3 (NRIF3) (131), nuclear receptor coregulator (NRC) (132), also referred to as activating signal cointegrator-2 (ASC-2) (133), 250-kDa receptor associated protein (RAP250) (134), thyroid hormone receptor-binding protein (TRBP) (135), and PPAR-interacting protein (PRIP) (136). Some of the coactivators such as E6-associated protein (E6-AP), 70-kDa androgen receptor abrogate (ARA70), nuclear receptor coactivator (NCoA62) or NRIF3 interact with AF-2 domain of nuclear receptors in a ligand dependent manner whereas other coactivators such as, p68 interact with AF-1 domains. Recent studies also suggest that cell-specific coactivators may play an important role in gene-specific transcriptional activation. Some

coactivators exhibit a relative preference for a determined group of nuclear receptors. For instance, ARA70 specifically enhances androgen receptor transcriptional responses (137), and four and half LIM domains 2 (FHL2), which has a unique tissue-specific expression pattern, selectively increases androgen receptor-dependent transactivation (138).

One of the more intriguing coactivators is steroid receptor RNA activator (SRA), which selectively enhances the transcriptional activity of the steroid hormone receptors PR, ER, GR and AR but not other nuclear receptors such as TR or RXR (139). Moreover, SRA functions as an RNA transcript and not as a protein. SRA enhances steroid receptor activity in presence of cycloheximide, while other coactivators such as SRC-1 do not. SRA works exclusively through the amino-terminal AF-1 domain and can be detected in a large complex which contains SRC-1 and several other proteins (139).

Although biochemical and functional data strongly suggest that coactivators play a key role in transcriptional regulation by nuclear receptors, coactivator knock-out studies indicate that in addition to their coactivator function they have several other physiological roles. For example, SRC-3 knock-out studies indicate that SRC-3 may play a critical role in overall growth and sexual maturation (140). The organization or expression of nuclear receptor coregulators is also altered in diseases such as X-linked dementia and hypothyroidism, further indicating that they play important physiological roles (141).

Nuclear receptor corepressors

Unliganded nuclear receptors such as RAR and TR bind cis-element in target genes and repress the basal transcription and this led to the discovery of nuclear receptor corepressors. Nuclear receptor corepressor (NCoR) (64) and silencing mediator for retinoic acid and thyroid hormone receptors (SMRT) (63) were originally isolated as factors associated with the hinge domain of the unliganded TR and RAR. These interactions are disrupted upon binding of their respective ligands. Other studies have shown that NCoR and SMRT interact with other nuclear receptors, including VDR, PPARδ, and LXR, and with orphan nuclear receptors such as COUP-TF, RORα and DAX (80). NCoR and SMRT also interact with steroid hormone receptors, including AR, ER and PR (142-146) but only when these receptors are bound to their corresponding antagonists. These studies demonstrate that NCoR and SMRT are common corepressors of nuclear receptors.

NCoR and SMRT contain distinct functional domains including C-terminal receptor interaction domains (RIDs) that are responsible for nuclear receptor binding (Fig. 1.7). RIDs contain a consensus sequence of LXXI/HIXXXI/L (CoRNR box) (147, 148), representing an extended helix compared to the coactivator LXXLL helix (75, 82), which interacts with specific residues in the same receptor pocket required for coactivator binding. Multiple distinct domains responsible for repression are also present in the amino-terminal ends of corepressors and through these repression domains (RD),
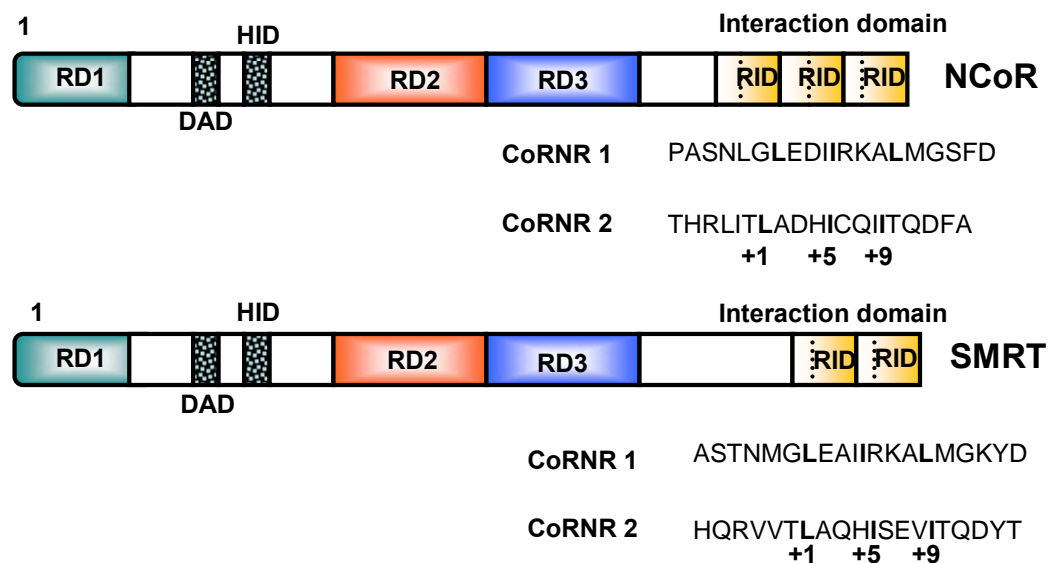
Fig. 1.7. Structural representation of corepressors, NCoR and SMRT. The N-terminal region contains multiple repression domains (RDs). The receptor interacting domains (RIDs) in the C-terminal region each contain a conserved CoRNR are shown with the conserved LXXXIXXXL sequence in bold. The N-terminal portion of the corepressors also harbors the two matched SANT domains in the DAD and HID (81).

NCoR and SMRT associate with HDAC leading to targeted hypoacetylation of histones and repressed gene expression (147, 149). Two distinct SANT (SWI/ADA2/NCoR/TFIIIB) domains have been identified in the amino-terminal regions of corepressor proteins such as SWI/SNF, Ada, NCoR and TFIIIB and both NCoR and SMRT also contain a SANT domain. In addition NCoR and SMRT have a conserved deacetylase domain (DAD) which is critical for interaction of corepressors with HDAC3 and for activating the HDAC enzyme complex (150). The conserved SANT domain is a part of a histone interaction domain (HID) and serves to increase the affinity of the active corepressor/HDAC complex for histones (151).
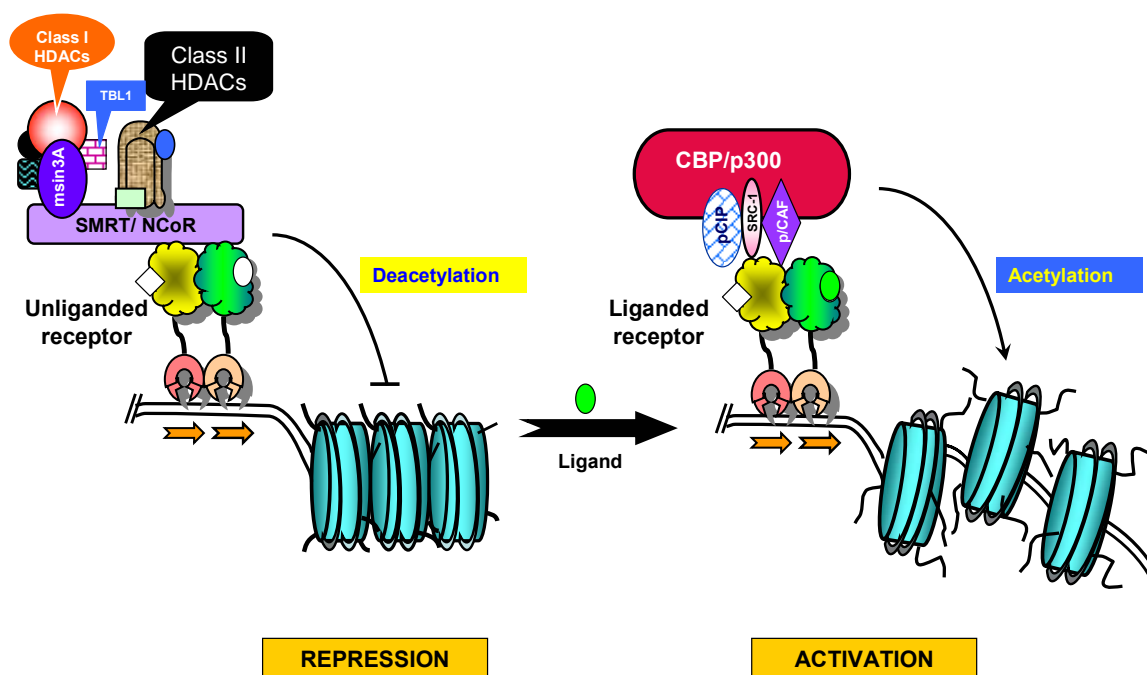
Fig. 1.8. Coactivator and corepressor complexes and histone acetylation. In the absence of ligand, the nuclear hormone receptor heterodimer is associated with corepressor complexes. The corepressors (NCoR/SMRT) recruit histone deacetylases (HDACs) either directly or through interaction with Sin3. Deacetylation of histone tails leads to chromatin compaction and transcriptional repression. Ligand binding causes the release of corepressor cmplex and the AF-2-dependent recruitment of a coactivator complex that contains at least p160 coactivators (SRC-1) and CBP/p300. All of these proteins possess histone acetyltransferase (HAT) activity that allows chromatin decompaction and gene activation (30).

NCoR and SMRT use multiple complimentary mechanisms to repress transcription. Both NCoR and SMRT are not only associated with multiple members of the HDAC family (HDACs 3,4, 5, and 7), but also interact with HDAC 1 and 2 via Sin3 (152). These interactions combined with HDAC activating and enhancing functions of the DAD and HID domains, cooperatively repress nuclear receptor interactions with specific response elements by antagonist bound nuclear receptors or by unliganded nuclear receptors.

Coactivators and corepressors have an important function in ligand-dependent activation of nuclear receptors. In brief, ligand binding results in the release of HDAC-containing corepressor complexes and recruitment of SRC-1, which then serves as a platform to recruit CBP. These factors and associated proteins induce HAT-dependent remodeling of nucleosomal structures and facilitate replacement of SRC-1/CBP with TRAP/DRIP complexes which in turn recruit the Pol II complex required for nuclear receptor mediated transactivation (Fig. 1.8).

Orphan Nuclear Receptors

Most nuclear receptors are orphan receptors for which endogenous ligands were not initially identified. Orphan nuclear receptors are often defined as gene products that embody structural features of nuclear receptors and these genes were identified without any prior knowledge of their association with a putative ligand (153). Recently novel ligands have been identified for a number of these receptors including RXR (154), PPAR (155), farnesoid X receptor (FXR) (156, 157), liver X receptor (LXR) (158) and pregnane X receptor (PXR) (159) and this has led to characterization of their functional roles and an understanding their significance in metabolic regulation (160). It is not known whether unliganded orphan receptors exert their diverse actions in a ligand-independent manner or if they are regulated by unidentified endogenous compounds. Since orphan nuclear receptors occur in nearly all species examined and outnumber the steroid/nonsteroid hormone receptors, they probably represent an ancient and complex class of regulatory proteins that participate in multiple physiological functions.

Most orphan nuclear receptors possess the functional domains that have been characterized for other nuclear receptors, however, some orphan receptors have very short N-terminal regions, and lack an AF-1, while Rev-Erbα and –β lack the conserved AF-2. Some members possess either a conserved DBD or LBD, but not both. Both DAX-1 and SHP lack a "typical" nuclear receptor DBD (161), however, DAX-1 binds hairpin loop structures via its unique amino-terminal domain (161). Other serum and cellular binding proteins (such as retinol-binding protein, cellular retinoic acid binding protein) and intracellular receptors (such as aryl hydrocarbon receptor) bind small lipophilic ligands using structures unrelated to the LBD of nuclear receptors.

The PPAR family

Peroxisome proliferator-activated receptors (PPARs) are a subgroup of ligand-activated orphan nuclear receptors responsible for regulation of diverse cellular events ranging from glucose and lipid homeostasis to cell differentiation and apoptosis (162). Peroxisome proliferation occurs only in rodents as a consequence of the activation of PPARs by specific molecules called peroxisome proliferators (PPs) (163). Three related PPAR isotypes have been identified in vertebrates, including xenopus, mouse, rat, hamster, and human (164-170). They have been named PPARα, PPAR β, and PPAR γ based on their initial identification in *Xenopus* (171) and the mammalian PPARα and PPAR γ equivalents were easily identified (Fig. 1.9). The third PPAR isotype exhibited lower homology to xenopus PPAR β and was alternatively called PPARδ, FAAR, or NUCI. The chromosomal localization of human (hu) PPARα was mapped to chromosome 22 slightly telomeric to a linkage group of six genes and genetic markers

that are located in the general region 22q12-q13.1(169). The huPPAR γ gene is located on chromosome 3 at position 3p25, close to RARβ and TRβ, which are at positions 3p24 and 3p21, respectively(170). Finally, huPPAR β has been assigned to chromosome 6, at position 6p21.1-p21.2 (172). These three isotypes have distinct tissue distribution and biological activities. PPARα is expressed in liver, intestine, pancreas, kidney, muscle, heart, skeletal muscle, adrenals and cells from the vascular wall, and regulates fatty acid uptake and oxidation in the liver (173). PPAR γ is mainly expressed in adipose tissues where it plays a role in lipid metabolism, and expression has been observed in intestine, mammary gland, endothelium, liver, skeletal muscle, prostate, colon and other cell types, including monocytes, macrophages/foam cells and type2 alveolar pneumocytes. PPARγ regulates not only systemic glucose and lipid homeostasis, but also has a role in the biology of monocytes, cell-cycle regulation, cancer development and treatment (163, 173, 174). PPAR β is expressed in a wide range of tissues including embryonic kidney, small intestine, heart, adipose tissue, skeletal muscle and developing brain, with a less-defined function (163). PPARγ is involved in keratinocyte differentiation, wound healing and in mediating very low-density lipoprotein (VLDL) signaling of macrophages (175).

The PPAR response element (PPRE) was first characterized using synthetic oligonucleotides and was defined as a direct repeat of two core recognition motifs AGGTCA separated by one nucleotide, DR1 (176). All PPREs fulfill these DR1 criteria,
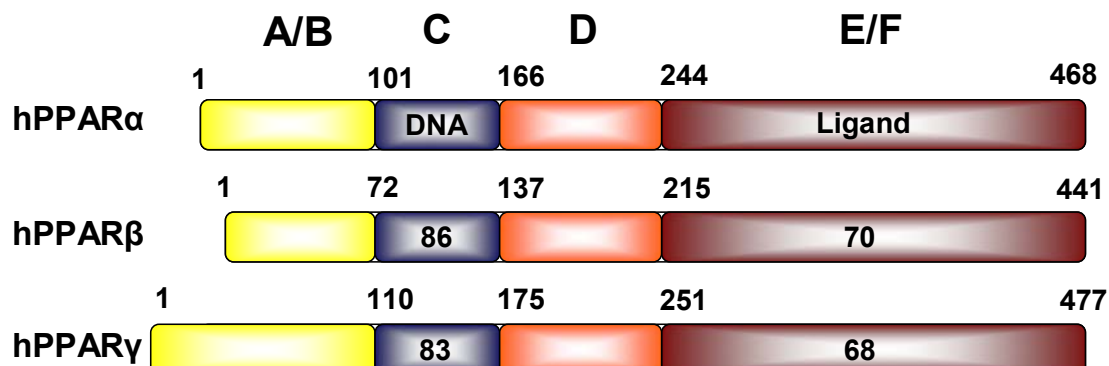
Fig. 1.9. General structure of PPARs. Schematic representation of the domain structure of PPARs, which is similar to other members of the nuclear receptor family. The numbers within each domain correspond to the percentage of aminoacid sequence identity of human PPARβ and PPARγ relative to PPARα (177).

and this distinguishes PPREs from other direct repeat response elements for the TR/RAR class of receptors. PPARs do not bind as a monomer or homodimer but are dependent on RXR as DNA-binding partner. Based on more extensive analysis of PPREs in several gene promoters (178-181) three additional properties can be added to the definition of a DR1; an extended 5′ half-site, an imperfect core DR1, and an adenine as the spacing nucleotide between the two hexamers giving the following consensus PPRE 5′-AACTAGGNCA A AGGTCA-3′. These properties most likely add discriminating parameters that contribute to PPAR:RXR binding selectivity vs. the homo- and heterodimers formed by other members of the superfamily, some of which also recognize a DR1 type element. PPAR interacts with the upstream extended core hexamer of the DR1, whereas RXR occupies the downstream motif (179, 182). This represents a reversed polarity compared to the VDR:RXR bound to DR3, where RXR occupies the

upstream core hexamer of the direct repeat. This difference in binding polarity between PPAR:RXR and VDR:RXR is determined in part by the 5'-extended half-site in the PPRE. The inability of PPARs to bind as monomers has been attributed to the N-terminal region of these proteins since PPARα in which the A/B domain has been deleted binds as a monomer to a PPRE. These changes in the DNA binding of this truncated PPAR might reflect evolutionary changes in which PPAR has functionally diverged from its monomeric cousins such as NGFI-B, ROR and RevErbAα (183).

PPARγ

PPARγ is the most extensively studied of the three PPAR subtypes (Fig.1.10), and there is a remarkable conservation of this receptor across different species (184). In contrast to the mouse which has only two PPARγ isoforms (185) humans express three PPARγ isoforms, namely i.e. PPARγ1, PPARγ2 (186) and PPARγ3 (187). Alternate transcription start sites and alternate splicing generate three PPARγ mRNAs, which differ at their 5' ends.

The three PPARγ mRNAs have specific and distinct expression patterns (186, 187). PPARγ1 and PPARγ3 mRNAs give rise to an identical protein product, (i.e. PPARγ1), and PPARγ2 encodes for the PPARγ2 protein, which in humans contains 28 additional amino acids at the N-terminus. PPARγ1 is broadly expressed but at low levels. Both PPARγ2 and PPARγ3 are highly expressed in adipose tissue, and PPARγ3 is also expressed in macrophages. To date, functional differences between PPARγ isoforms have not been determined.
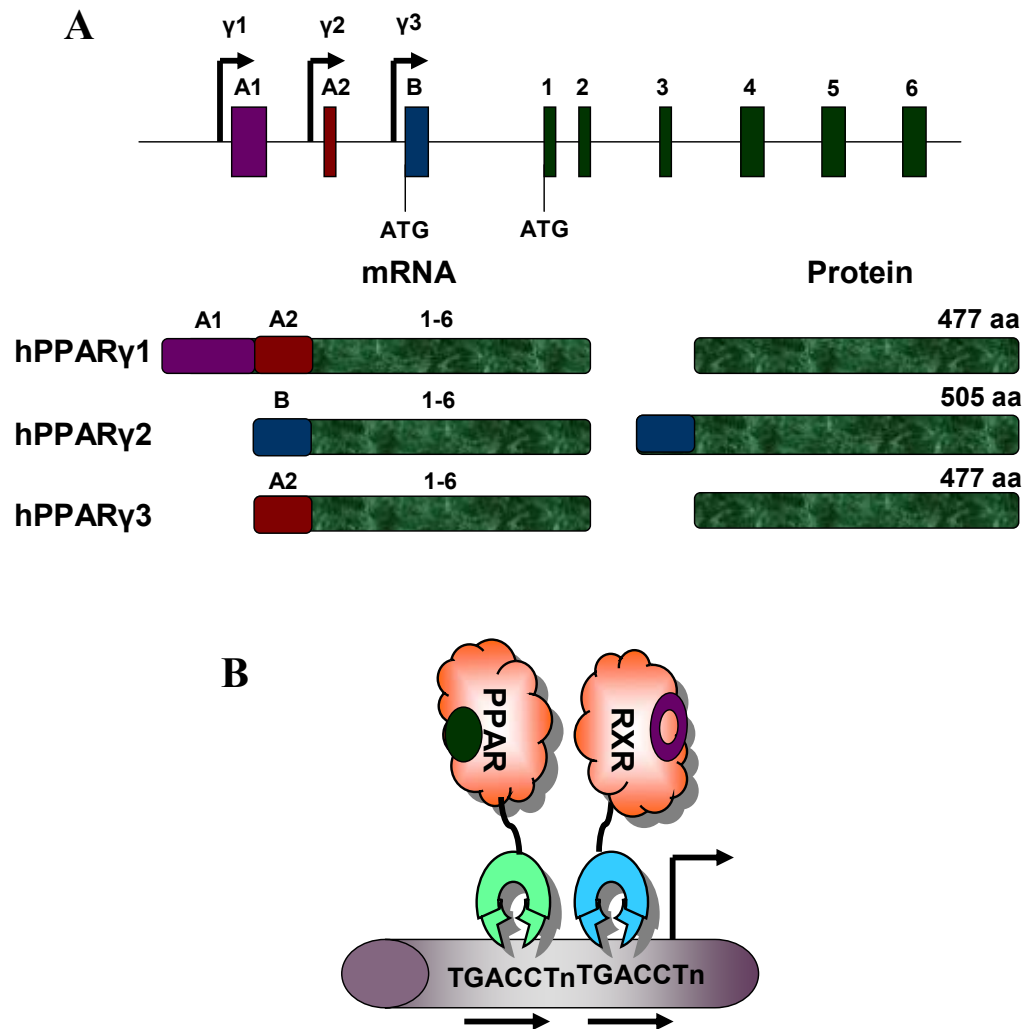
Fig. 1.10. Structural representation of PPARγ. A. Structure of PPARγ gene and the PPARγ mRNA and protein. The three promoters and the different exons are indicated. The three mRNA species give rise to two different PPARγ proteins. B. Basic mechanism of action PPARs. Upon ligand binding, PPARs form heterodimeric complex with RXR, that binds to the PPRE and drives the transcription of target genes (177).

PPARγ ligands

Natural PPARγ ligands. Endogenous PPARγ ligands include a variety of lipophilic compounds such as long-chain polyunsaturated fatty acids and several eicosanoids. PPARγ is bound and activated by essential fatty acids like arachidonic acid, gamolenic acid, docasahexanoic acid, and eicosapentaenoic acid, as well modified oxidized lipids 9- and 13-hydroxyoctadecadienoic acid (9- and 13-HODE) and 12- and 15- hydroxyeicosatetraenoic acid (12- and 15- HETE) (Fig.1.11) (184).

15-deoxy-$\Delta^{12, 14}$-PGJ$_2$ (15d- PGJ$_2$) is the naturally occurring PPARγ agonist that has been most commonly used experimentally (188). This cyclopentenone-derived prostaglandin (PG) was first discovered in 1983, following incubation of PGD$_2$ for extended periods in the presence of albumin (189). In 1995 two groups simultaneously reported that PGJ$_2$ activated PPARγ and it was subsequently hypothesized that 15d-PGJ$_2$ may serve as an endogenous PPARγ ligand.

15d- PGJ$_2$ activates PPARγ but in order for this compound to be an endogenous ligand it has to induce PPARγ-dependent responses at physiological concentrations. However, the concentrations of 15d- PGJ$_2$ required to activate PPARγ are generally in the low μM range whereas physiological levels of 15d- PGJ$_2$ are in the low nM range (190). It has been demonstrated *in vitro* that albumin-catalyzed dehydration of PGD$_2$ yields PGJ$_2$, and further dehydration of PGJ$_2$ results in formation of 15-dPGJ$_2$. However, there is no evidence for enzymatic formation of these prostaglandins *in vivo*. Bell-Parikh and his colleagues used a highly sensitive liquid chromatography/tandem mass

15-deoxy-Δ12, 14-PGJ2

Hexadecyl azelaoyl phosphatidylcholine (azPC)

9-HODE

13-HODE
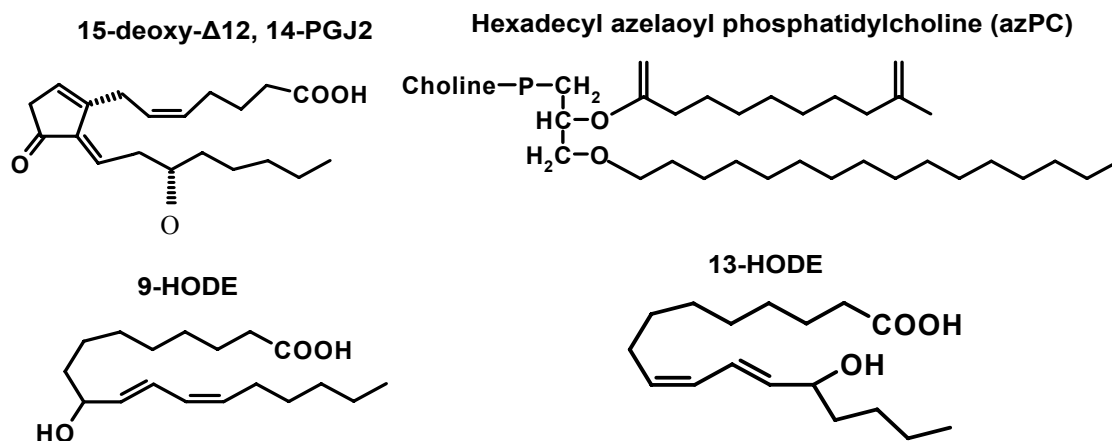
Fig. 1.11. Chemical structures of naturally occuring PPARγ ligands (191).

spectrometry assay for detecting 15-dPGJ$_2$. They reported that 15dPGJ$_2$ can be synthesized *in vivo* but the levels are not sufficient for this compound to be an endogenous PPARγ ligand (192). However 15-dPGJ$_2$ is the most potent natural ligand for this receptor and commonly used as a PPARγ agonist (188).

15-dPGJ$_2$ has been used extensively to define PPARγ-dependent responses however, it is important to note that 15-dPGJ$_2$ can induce a variety of PPARγ-independent effects and induce many growth inhibitory responses in cells devoid of the receptor (193). Many of the PPARγ-independent effects are mediated through covalent binding of 15-dPGJ$_2$ to proteins; the cyclopentenone ring of 15-dPGJ$_2$ readily reacts with nucleophiles such as cysteinyl thiol groups of proteins. For example, 15-dPGJ$_2$ not only inhibits NF-κB activation via PPARγ but also through two distinct PPARγ-independent mechanisms. First, 15-dPGJ$_2$ inhibits nuclear factor (NF)-κB activation by inhibiting the binding of NF-κB to promoter elements (194). Secondly, 15-dPGJ$_2$ also interrupts NF-

κB-dependent gene transcription by covalently binding to IκB kinase thus preventing IκB degradation and nuclear uptake of NF- κB (194, 195).

Synthetic PPARγ ligands. In addition to the natural PPARγ agonists, a wide range of synthetic ligands have also been developed. The most widely used synthetic agents belong to the thiazolidinedione (TZD) class of antidiabetic drugs, also referred to as glitazones and these include ciglitazone, troglitazone, pioglitazone, rosiglitazone and LY171.833 (Fig.1.12). Pioglitazone (Actos), rosiglitazone (Avandia) and troglitazone (Rezulin) sensitise patients to insulin and lower blood glucose levels and have been used clinically to treat type 2 diabetes (196). Troglitazone was recently removed from the market due to idiosyncratic hepatotoxicity, which resulted in liver failure in extreme cases. Several other structurally distinct ligands, such as the derivative of 2,3-disubstituted indole-5-acetic acid called GW0207 or non- thiazolidinedione tyrosine based compounds are potent and selective PPARγ agonists (184).

Non-steroidal anti-inflammatory drugs such as indomethacin, ibuprofen, fenoprofen and fulfenamic acid are also PPARγ agonists, and this might explain the anti-inflammatory effects of these drugs at concentrations that are substantially higher than those required to inhibit prostanoid synthesis (197). The synthetic triterpenoid 2-cyano-3,12-dioxooleana-1,9-dien-28-oic acid (CDDO) binds PPARγ and induces differentiation and inhibits proliferation of a variety of cancer cells and CDDO also exhibits anti-inflammatory activity (198). Our laboratory has characterized a series of 1,1-bis(3'-indolyl)-1-(p-substitutedphenyl)methanes (C-DIM) containing

troglitazone

rosiglitazone

pioglitazone

ciglitazone

LY 171883

GW 0072

englitazone

GI 262570

CDDO
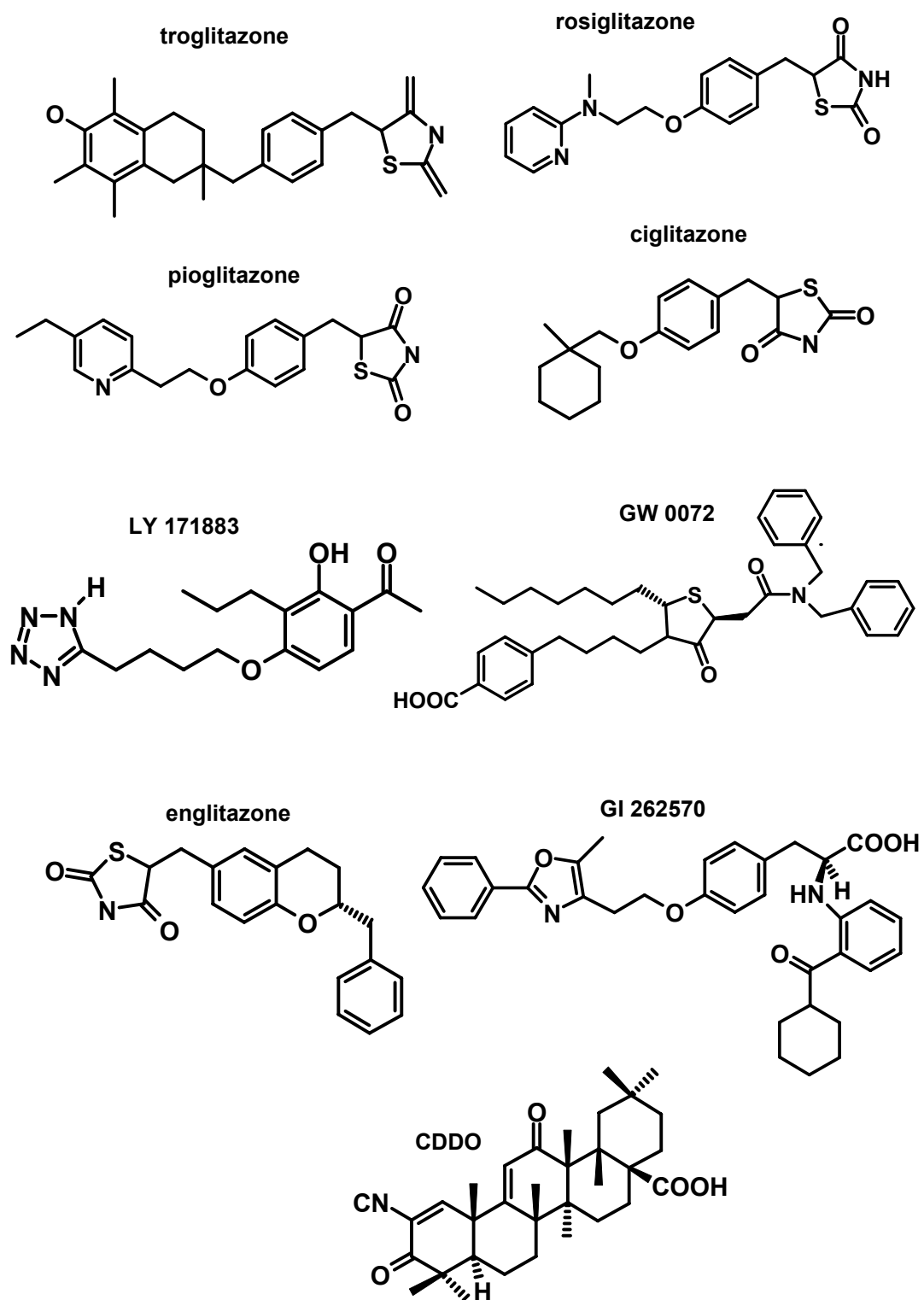
Fig. 1.12. Chemical structures of synthetic PPARγ ligands (199).

p-triflouromethyl, p-t-butyl and p-phenyl substituents that also activate PPARγ and these compounds inhibit MCF-7 breast cancer cell growth and Go/G1-S phase progression and induce differentiation in 3T3-L1 preadipocytes and apoptosis (200).

PPARγ ligands activate transcription of many genes that are important for lipid metabolism and transport, and these includes lipoprotein lipase (LPL), adipsin, fatty acid binding protein, acyl-CoA synthase, and fatty acid transport protein-1 (FATP-1). Furthermore ligand-activated PPARγ mediates differentiation of preadipocytes to adipocytes (201-203). PPARγ ligands also repress expression of some genes. For example, in monocytes and macrophages, PPARγ agonists decrease expression of cytokines such as IL-4, proinflammatory molecules including TNF, IL-1, as well as inducible nitric oxide synthase (193, 204-207). Proinflammatory transcription factors such as AP1, Stat, and NF-κB are also inhibited by PPARγ agonists. The mechanisms for these responses are unclear, however gene repression induced by these compounds may be PPARγ -independent.

The activity of PPARγ is controlled by ligands and interactions with various co-factors. In the inactive (unliganded) state PPARγ is complexed with corepressors such as NCoR and SMRT. Upon ligand binding PPARγ undergoes conformational changes that lead to release of repressors and subsequent binding to coactivators. Many PPARγ interacting coactivators have been identified including SRC-1, TIF-2, CBP/p300, TRAP220 and PGC-1 (208). Kodera *et al* showed that the endogenous ligand 15-dPGJ$_2$ induced a different set of coactivator interactions compared to the synthetic ligand

troglitazone and this may explain some of the ligand-dependent selective activation of PPARγ (209).

X-ray crystal structure of PPARγ LBD

Nuclear receptors exhibit a common structural three-dimensional fold, which consists of an antiparallel α-helical sandwich of 12 helices organized in three layers with a central hydrophobic pocket. Upon ligand binding, the swinging of helix 12 or activation function helix (HAF) closes the ligand binding pocket like a lid, in a so-called "mouse trap model" (37, 39, 40). The x-ray crystal structure of the human apo-PPARγ reveals an overall fold similar to that of the above mentioned LBDs from helix 3 to the C-terminus (84, 210, 211). However there are certain distinct differences. Similar to the holoforms of PPAR and other nuclear receptors, the core AF-2 activation domain in the apo-PPARs is folded against the ligand binding pocket. An additional helix, called helix 2′, which is found between the first β-strand and helix 3 together with the helix 2, provides an easy access to the hydrophoblc pocket for ligands (212). The region between the helix 2′ and helix 3 is the most thermally mobile loop and undergoes structural changes upon ligand binding. The ligand binding pocket is buried in the bottom half of the LBD and is unusually large, approximately 1300 $\mathring{A}^3$ (84, 211), and the ligand occupies only 30-40% of this pocket. The LBD of PPARs is large and more accessible than observed for other known LBDs. For example the cavity in TR is approximately 600 $\mathring{A}^3$ and most of this volume is occupied by T3 which has a volume of 530 $\mathring{A}^3$ (40)). Two histidine residues, H323 and H449, participate in fixation of the thiazolidinedione head group (84). These key interactions along with the relatively free non-specific

interactions associated with the hydrophobic regions of the ligands can occur within the large binding cavity and may explain the promiscuous ligand binding behavior of PPARγ. Therefore the different functional activities of a specific ligand may be related to different conformations in the ligand binding cavity (210). The extra helix 2′ and the tertiary placement of helix 2 provides ready access of PPARγ to structurally diverse ligands and this is consistent with the low affinity interactions of this receptor with multiple natural ligands (84).

Four amino acids, namely aspartic acid 243 (D243) at the N terminus of the first β-sheet, arginine 288 (R288), glutamic acid 291 (E291) and glutamic acid 295 (E295) in helix 3, are the critical determinants of the ligand entry site (84). E291 and E295 are conserved in all known PPARs, whereas D243 and R288 are only conserved in the γ-isotype, suggesting that these latter positions might be involved in isotype- and species specific ligand selectivity. The crystal structure also shows coiled-coil interactions between helix 10 of two PPARγ molecules forming a homodimer, which is reinforced by salt bridges involving helices 9 and 10. While PPARγ homodimers do not occur *in vivo*, these observations are similar to those described for RXR homodimers (37) and reflect the type of contacts involved in formation of the PPARγ:RXR heterodimer. Consistent with these observations, a deletion of helix 10 and HAF of PPARα abolishes heterodimerization with RXRα (213).

Alternative pathways for activation of PPARγ

Activation by phosphorylation. In addition to ligand-dependent activation, many nuclear receptors including PPARγ are activated by phosphorylation. Transfection

studies in CV1 and HepG2 cells revealed that insulin increases the transcriptional activity of PPARγ by nearly two-fold (214). Insulin induces phophorylation of two mitogen-activated protein (MAP) kinase sites in the A/B domain of PPARγ (215). The results of cotransfection experiments in chinese hamster ovary (CHO) cells that express the insulin receptor, showed the insulin and the PPARγ agonist TZD synergistically induced expression of the PPARγ –responsive target gene aP2 and this effect was partially inhibited by addition of a MAP kinase inhibitor (216). Enhanced PPARγ – dependent activity was observed in cells transfected with purified MAP kinase (216). In contrast the growth factors such as epidermal growth factor (EGF) and platelet-derived growth factor (PDGF) decrease the transcriptional activity of PPARγ while increasing the phosphorylation of PPARγ through MAP kinase signaling (217, 218). How the same changes in phosphorylation can result in activation or inhibition of PPARγ signaling, depending on the action of either insulin or growth factor is unclear but may involve either specific pleiotropic actions or activation of different kinase pathways by these hormones. For example, the insulin mediated up-regulation of phosphoenolpyruvate carboxykinase (PEPCK) gene expression does not require the activation of MAP kinase but relies on the phosphatidylinositol 3-kinase (PI3K) signaling pathway (219).

Activation by RXR agonists. PPARγ forms a permissive heterodimer with RXR in which either partner can regulate the transcriptional activity of the DNA-bound complex by interacting with its own cognate ligand, or both ligands. The response of ligands in both receptors is essentially additive. Thus, both the natural (9-*cis*-retinoic acid (9-*cis*-RA)) and synthetic RXR ligands,(LG1069, LG 100268), activate a PPRE-

dependent liver fatty acid binding protein or aP2, in a PPAR:RXR dependent manner (176, 220-223). Activation of PPAR:RXR by the RXR agonist 9-*cis*-RA signal is consistent with the observation that RXR agonists also display antidiabetic activities comparable to those observed thiazolidinediones (224). The *in vivo* actions of RXR ligands are not PPARγ-specific since these compounds also activate PPARα inducible genes (225).

Physiological effects of PPARγ

PPARγ is necessary and sufficient for differentiating adipocytes. PPARγ regulates adipocyte-specific expression of the fatty acid-binding protein aP2 by directly interacting to the *cis* PPRE aP2 gene promoter (226). Ligand activated PPARγ induces differentiation of fibroblasts into adipocytes (202). PPARγ heterozygous null mice have decreased amounts of adipose tissue (227-229) and expression of PPARγ dominant-negative mutants in 3T3-L1 cells inhibited their differentiation into adipocytes (230, 231). PPARγ regulates numerous genes involved in lipid metabolism in adipocytes including aP2 (201), PEPCK (232), acyl-CoA synthase (233) and LPL (203). PPARγ also controls the expression of genes involved in lipid uptake into adipocytes such as FATP-1 (234) and CD36 (235) and all these genes contain a PPRE in their regulatory regions.

PPARγ is also associated with several genes that affect insulin action. PPARγ agonists inhibit expression of TNFα, a pro-inflammatory cytokine, in adipocytes of obese rodents (236) and also inhibit TNFα-induced insulin resistance (237). PPARγ agonists also induce expression of c-CBL-associated protein which plays a positive role

in insulin signaling (238). Thus PPARγ agonists enhance or partially mimic certain actions of insulin and these activities form the basis for their use as antidiabetic agents (239). Although TZDs show a positive correlation between their binding affinity for PPARγ and their antihyperglycaemic activity, their activation of PPARγ is not sufficient to explain their biological effects. For example, PPARγ is predominantly expressed in adipose tissue compared to liver or muscle suggesting that adipose tissue is a major site of action of PPARγ agonists. However in aP2/DTA mice, whose white and brown fat is virtually eliminated by fat specific expression of diphtheria toxin A chain, troglitazone alleviated hyperglycaemia, and decreased elevated insulin levels without affecting PPARγ mRNA levels in liver, suggesting an adipose tissue-specific and PPARγ-independent response (240).

PPARγ agonists also induce rapid effects that do not correlate with their affinity for PPARγ, suggesting a PPARγ independent mechanism. For example, rosiglitazone and troglitazone rapidly inhibited LPL activity in adipocyte cell lines, increased lipase mRNA levels in undifferentiated adipocytes but had no effect on mRNA or protein expression of LPL in differentiated cells (241). The effects of PPARγ agonists on cholesterol levels may be receptor independent. TZDs inhibit cholesterol biosynthesis in CHO ovary cells, HepG2 hepatocarcinoma cells, 3T3-L1 adipocytes within 2 hr after treatment and these effects are reversed within 1 hr after the drug was withdrawn. Neither actinomycin D nor cycloheximide affected the inhibition of cholesterol synthesis by TZDs, suggesting that this inhibitory response did not require de novo mRNA or protein synthesis (242).

PPARγ and inflammation

The potential involvement of PPARγ in inflammatory processes was first suggested by the inhibition of the pro-inflammatory cytokine TNFα. PPARγ agonists also inhibit macrophage (differentiated monocyte) activation and limit their production of cytokines. Treatment of monocytes with PPARγ agonists inhibits production of TNFα, IL-1β and IL-6 (204) and PPARγ agonists induce a resting phenotype and down-regulate inducible nitric oxide synthase (iNOS) (207, 243), gelatinase B and scavenger receptor A genes in macrophages (207). These processes may be mediated by a direct transcriptional effect of PPARγ, which interferes with NF-κB, activating protein-1 (AP-1), and signal transducers and activators of transcription (STAT) transcription factors that regulate cytokine gene expression (207, 243).

The anti-inflammatory effects of PPARγ agonists in these studies are often observed at concentrations higher than their EC_{50} values for binding to or activating PPARγ (184). For example, concentrations of troglitazone and rosiglitazone required for inhibition of iNOS were 15- to 60-fold (for troglitazone) and 650-fold (for rosiglitazone) higher than their corresponding EC_{50} values for activating PPARγ (244). Although this suggests that these responses are PPARγ-independent more direct evidence comes from studies which show that PPARγ antagonists do not block the anti-inflammatory effects of these TZDs. For example, high concentrations of rosiglitazone increased lipopolysaccharide stimulated prostanoid synthesis; however, PPARγ antagonists did not reverse this effect (245). Moreover studies from PPARγ null cells provide additional evidence that TZD-induced anti-inflammatory responses were

PPARγ-independent since inhibition of iNOS by TZDs were obsereved in both PPARγ null cells and macrophages (246).

PPARγ and atherosclerosis

Treatment of monocytic cells with PPARγ agonists induce lipid accumulations reminiscent of those found in foam cells of the atherosclerotic plaque and activation of PPARγ /RXR heterodimer enhances macrophage differentiation. Exposure of human monocytes or monocytic cell lines to oxidized LDL (oxLDL) but not regular LDL not only induces PPARγ expression (247) but also provides the cells with two PPARγ ligands i.e 9-HODE and 13-HODE, both oxidative metabolites of linoleic acid present in oxLDL (248). Activated PPARγ induces oxLDL receptor, CD36 and fatty acid translocase (FAT) expression through a PPRE in CD36/FAT gene promoter thereby establishing a positive feedback loop leading to foam cell formation (248). Consistent with this hypothesis PPARγ is expressed at moderately high levels within the atherosclerotic plaques of mice (248) and humans (249, 250) and mice carrying the targeted deletion of CD36 are partially protected from atherosclerosis (251). These data suggest a complex function of PPARγ in macrophage and foam cell formation with a predominantly pro-atherogenic activity. However, this pro-atherogenic activity may be neutralized by the effects of PPARγ in vascular smooth muscle cells, where PPARγ inhibits expression of metalloproteinase 9 and reduces cell migration (252). Furthermore, using LDL receptor knockout mice as a model for atherogenesis, LDL-deficient mice, like their human counterparts, are hypercholesterolemic and prone to atherosclerosis when fed diets rich in fat and cholesterol. However administration of two

different classes of synthetic PPARγ ligands, rosiglitazone and a non-TZD tyrosine analog decreased atherosclerotic lesions (34). These studies provide direct experimental evidence that PPARγ activation can inhibit or reverse atherosclerosis in a well-characterized model for this disease.

PPARγ and cancer

The proliferation advantage of cancer cells over their normal counterparts is at least, in part, because of their inability to undergo terminal differentiation, they remain in a proliferative state and continue to grow. The effects of PPARγ agonists on cancer was based on results showing that PPARγ ligands inhibited cell proliferation while inducing adipocyte differentiation (253-256). Moreover PPARγ is overexpressed in most tumor samples and cancer cells lines (257). PPARγ agonists inhibit proliferation of transformed cells mainly by cell cycle arrest or by inducing differentiation and/or apoptosis.

Cell cycle. Studies based in several tumor cell lines have implicated a role for PPARγ in cell cycle arrest. It was initially observed that ligand activation of PPARγ induces cell cycle withdrawal of preadipocytes via suppression of the transcriptional activity of E2F/DP DNA-binding complex (258). Decreased E2F/DP activity is in part mediated by PPARγ through down-regulation of the protein phosphotase 2A (PP2A) (259). E2F/DP activity can also be inhibited by the activation of retinoblastoma protein (RB) and PPARγ ligands inhibit phosphorylation of RB in vascular smooth muscles cells, therefore maintaining RB in its hypophosphorylated form and abrogating the G1 to S phase transition (260).

Morrison and Farmer also suggested a role for PPARγ in up-regulating the cyclin-dependent kinase inhibitors (CDKIs) p18 and p21 during adipogenesis (261). Thus PPARγ ligands control genes that are involved in the negative regulation of cell cycle and similar responses were also observed in pancreatic cancer cell lines (262). However, the specific growth regulatory pathways that are affected by PPARγ agonists are highly variable even among cells derived from a common tumor type. TGZ inhibited growth of six of nine pancreatic cancer cell lines, by G1 phase cell cycle arrest through the up-regulation of p21 mRNA and protein expression (262). In the Panc-1 pancreatic cancer cell line , TZD-dependent growth inhibition of G1 phase arrest was accompanied by increased expression of p27 but not p21 (262, 263). A dose dependent cytostatic effect of TZD was observed in different hepatoma cell lines including HLF, HuH-7, HAK-1B, and HAK-5 cells, and the G0 to G1 cell cycle arrest was related to alterations in p21 protein expression. HLF hepatoma cells, which are deficient in RB, responded more profoundly to TGZ, which induced expression of p21, p27 and p18, suggesting that these CDKIs may be involved in TGZ-induced cell cycle arrest in human hepatoma cell lines (264).

Hupfeld and Weiss reported that TZDs inhibit vascular smooth muscle cell growth by decreasing cyclin D1 and cyclin E levels, suggesting another possible mechanism for TZD action (265). MCF-7 breast cancer cell growth and G1-S phase progression was inhibited by troglitazone treatment, and cells accumulated in the G1 phase by modulating RB phosphorylation and decreasing cyclin D1 expression (266). CDK-dependent activity was also decreased by troglitazone and overexpression of

cyclinD1 partially rescued MCF-7 cells from troglitazone mediated G1 cell cycle arrest (266). PPARγ activation inhibits proliferation of several other malignant cells from different lineages such as liposarcoma (267), prostate carcinoma (268), colorectal carcinoma (269-271), non-small cell lung carcinoma (272), bladder cancer cells (273) and gastric carcinoma cells (274).

Differentiation. PPARγ induces differentiation pathways beyond adipocytes and overexpression of PPARγ induces differentiation of hepatocytes, myoblasts and several other cell types including mammary and colon epithelium (202). Furthermore, treatment of human primary liposarcoma cells with pioglitazone induced terminal differentiation (275). PPARγ agonists induce upregulation of several differentiation markers such as carcinoembryogenic antigen, E-cadherin and alkaline phosphotase in pancreatic cancer cell lines (276). Ligand-dependent activation of PPARγ induced apoptosis in malignant rat and human glioma cells and also induced transient expression of the glioma redifferentiation marker N-cadherin (277).

In the colon, levels of PPARγ mRNA are nearly equivalent to that found in adipocytes (186) with the highest levels of receptor expressed in the post-mitotic, differentiated epithelial cells facing the lumen (278). Consistent with this expression pattern, exposure of human colon cancer cells to PPARγ agonists induces growth inhibition associated with a delay in G1 phase of the cell cycle and an increase in several markers of differentiation, including caveolin-1 and caveolin-2, which exhibit tumor suppressor activity, and some members of the keratin and CEA families (269, 270, 279). Levels of caveolin-1 and 2 also increase during differentiation of pre-adipocytes to

adipocytes (280, 281). Breast adenocarcinoma and colon adenocarcinoma cells, where caveolin expression is normally downregulated, express a functional PPARγ with transcriptional activity (278, 282). These cells undergo differentiation *in vitro* upon treatment with PPARγ agonists (271, 283, 284). The ability of PPARγ to promote lineage-specific differentiation and the fact that caveolins are characteristic markers for terminally differentiated cells raised the hypothesis that PPARγ transcriptionally regulates caveolin expression. Burgermeister *et al.* have shown that PPARγ induces caveolin gene expression in human adenocarcinoma cells and this may have important applications in the context of cancer differentiation therapy (285).

Apoptosis. PPARγ ligands induce apoptotic cell death in a wide variety of experimental cancer models both *in vitro* and *in vivo* (286-289) including ER negative MDA-MB-231 and ER positive MCF-7 breast cancer cells (290). Treatment of MCF-7 cells with troglitazone irreversibly inhibited the growth and induced apoptosis, and this was accompanied by a dramatic decrease of anti apoptotic bcl-2 protein levels (291). Inhibition of RNA or protein synthesis abrogates apoptosis induced by 15d-PGJ$_2$ in breast cancer cells. Additionally, 15d- PGJ$_2$-induced caspase activation is inhibited by caspase inhibitors, showing that de novo gene transcription was necessary for induction of apoptosis in breast cancer cells (292).

PPARγ ligands such as 15d- PGJ$_2$, LY171 833 and ciglitazone inhibited proliferation and induced cell death in human (U87MG and A172) and rat (C6) glioma cell lines. This cell death was characterized by DNA fragmentation and nuclear condensation which are the hallmarks of apoptosis. In contrast, primary murine

astrocytes were not affected by treatment with ciglitazone (293). PPARγ ligand-induced apoptotic cell death in the glioma cells was accompanied by transient upregulation of proapoptotic proteins Bax and Bad. Upregulated expression of Bad and Bax induce apoptosis by enhanced release of mitochondrial cytochrome C and subsequent activation of several effector caspases. In addition, inhibition of Bax expression by specific antisense oligonucleotides protected glioma cells against PPARγ mediated apoptosis, indicating an essential role of Bax in this process (293). PPARγ activation by troglitazone also leads to increased caspase 3 activity in human liver-cancer cells (294) and in human malignant astrocytoma cell lines (277).

Shimada and coworkers noted that troglitazone-induced cell death in colon cancer cells was inhibited by pan-caspase inhibitors (295). Furthermore, ciglitazone - induced apoptosis in human pancreatic cell lines is blocked by the pan-caspase inhibitor ZVAD-FMK but not by a specific caspase-3 inhibitor (296). Moreover, treatment of human liver cancer cell lines (294) and human thyroid carcinoma cells (297) with PPARγ agonists did not increase in Bax protein levels, suggesting that PPARγ agonists induce several different apoptotic pathways. TNF related apoptosis inducing ligand (TRAIL) is a member of TNF family of cytokines that induces apoptosis and both natural and synthetic PPARγ agonists sensitize tumor cells but not normal cells to apoptosis induction by TRAIL. PPARγ ligands selectively reduce levels of FLICE-inhibitory protein (FLIP), an apoptosis-suppressing protein that blocks early events in TRAIL/TNF family death receptor signaling. PPARγ ligands induced ubiquitination and

proteasome-dependent degradation of FLIP, without concomitant decreases in FLIP mRNA (298).

PPARγ-independent actions. PPARγ agonists inhibit proliferation of several types of cancer cells, however, the role of PPARγ remains controversial and in many cases the compounds induce receptor-independent effects. The sensitivity of cancer cell lines to PPARγ agonist induced growth inhibition does not correlate with levels of PPARγ protein in these cells. For example glitazone resistance occurs even in tumors with high PPARγ concentration (eg, breast-tumor cells) (284). Homologous recombination was used to create embryonic stem cells with a null mutation for PPARγ and these stem cells could be differentiated into macrophages when treated with glitazones (193). Troglitazone induced cell cycle arrest and subsequent cell death and this was associated with downregulation of c-myc, c-myb and cyclin D2 expression. These genes lack a PPRE in their promoter regions , indicating that these responses were not directly mediated through PPARγ (299). Similar results were observed in human leukemia cell line (KU812) suggesting that troglitazone-mediated growth suppression was PPARγ-independent and was associated with decreased cyclin E levels and hyperphosphorylation of RB (300).

In human glioblastoma T98G cells, TZD induced cell cycle arrest and apoptosis, and the fomer response was associated with increased p27 levels, whereas apoptosis was mediated by downregulation of anti-apoptotic Bcl2 and upregulation of pro-apoptotic Bax and caspase-3 activation. None of these responses were blocked in cells treated with a specific PPARγ antagonist (301). The mechanisms by which PPARγ agonists induce

glioma toxicity were also investigated in another study using rosiglitazone and ciglitazone. The rapidity of the mitochondrial damage caused by PPARγ agonists and the failure to revert the cytotoxic effects using the specific PPARγ antagonist GW9662 suggested a receptor-independent action (302).

Troglitazone inhibited growth of HCT-116 colon cancer cells by expression of nonsteroidal anti-inflammatory drug-activated gene-1 (NAG-1), most likely via direct activation of the transcription factor early growth response-1 (EGR-1) (303). This induction was not blocked by a PPARγ antagonist, thus providing another mechanism by which TZD can cause growth inhibition. In MCF-7 breast cancer cell lines, troglitazone-induced apoptosis was dependent upon GADD45 expression. Regulation of GADD45 by troglitazone occurred at the transcription level and was associated with MAPK activation. In the same studies neither rosiglitazone nor pioglitazone induced GADD45 expression indicating a receptor independent action (304).

The triterpenoid CDDO inhibits the growth of ovarian cancer cells that express PPARγ, but the effects of CDDO were not blocked after co-treatment with a PPARγ antagonist T007, suggesting that the growth inhibition was a PPARγ independent response (305). Another PPARγ agonist, methylene-sustituted diindolylmethane inhibited the G0/G1-S phase progression in MCF-7 and several cancer cell lines by downregulation of cyclin D1. The PPARγ inhibitor T007 did not affect downregulation of cyclin D1 indicating that this response was also PPARγ independent (200).

More direct evidence of PPARγ independent effects comes from receptor knockout studies. Embryonic stem cells induced tumor growth was inhibited by

troglitazone and ciglitazone in both PPARγ (-/-) and PPARγ (+/+) mice, confirming the receptor independent actions of PPARγ agonists. These compounds blocked the G1/S phase transition by inhibiting translation initiation as a consequence of partial depletion of intracellular calcium stores. This resulted in activation of PKR, a kinase that phosphorylates the alpha subunit of eukaryotic initiation factor 2, thus rendering it inactive (306).

Indirect and direct evidence suggest that many of the anticancer activities of PPARγ ligands are PPARγ-independent, however the mechanisms of receptor-independent pathways warrant further study. Although PPARγ is well characterized, there are still numerous challenges ahead before modulators of this receptor will be adopted for therapeutic applications in treating cancer. This will require development of selective PPARγ modulators with minimal side effects and an increased understanding of both receptor-dependent and independent pathways.

Nerve growth factor-inducible gene B (NGFI-B) family

Three orphan receptors, (Nur77 (NGFI-Bα, TR$_3$, NAK1), Nurr1 (NGFI-Bβ), NOR-1 (NGFI-Bγ)) (Fig.1.13) have been characterized as a distinct family (NGFI-B) based on their strong sequence homologies. Since different nomenclature has been used to describe these genes, for convenience this group will be referred as the Nur77 receptor subfamily and use the terminology for the mouse homolog genes for Nurr77 and Nurr1 and the human homolog for NOR-1. The rat homolog of Nur77, NGFI-B was the first of these proteins discovered when it was identified in the rat pheochromocytoma cell 12 (PC12) following differentiation after treatment with nerve growth factor (NGF) (307).

Later, the mouse homolog Nur77 (nuclear receptor-77) was identified in fibroblasts (308). Nurr1 (Nor-related factor-1), was the second gene in this subfamily discovered while screening a mouse brain cDNA library with COUP-TF, another orphan nuclear receptor as a probe (309). Subsequently, other Nurr1 homologs were identified in the rat (RNR-1 and Hzf-3) (310, 311) and the human (NOT) (312). The final member of this subclass, NOR-1 (nuclear derived orphan receptor-1), was isolated from cultured rat forebrain neurons undergoing apoptosis (313).

Nur77 receptor subfamily members are highly expressed in adult nervous system where they are induced as part of the immediate early response to stimuli such as growth factors, membrane depolarization, and seizures (308, 309, 314, 315). The pattern of expression of the Nur77 subfamily members is broad. In adult rodents, Nur77 is expressed in the adrenal, thyroid, and pituitary glands, as well as the liver, testis, ovary, thymus, muscle, lung, and ventral prostate (307, 316, 317). Nur77 expression is upregulated in T cells undergoing apoptosis (318, 319). Nurr1 is expressed in the adult liver (310) as well as the pituitary gland, thymus, and osteoblasts (312, 317). NOR-1 is expressed at high levels in the pituitary gland and at intermediate or low levels in the adrenal glands, heart, skeletal muscle, thymus, kidney, epididymis, and submandibular glands (313, 320, 321).

Similar to other nuclear receptors, Nur77 family members consists of an N-terminal AF1 transactivation domain, a DBD with two zinc fingers, and a C-terminal putative LBD. While Nur77, Nurr1 and NOR-1 share this tripartite structure and a high degree of structural homology. Strong sequence homologies are found in central DBD

where all the three receptors share greater than 90% homology (307, 309, 313). Strong homologies (59-65%) are also found in the putative LBD (307, 309, 313). The N-terminal regions of these receptors are more distinctive and only approximately 30% homology is found (307, 309, 313). In comparison, these three proteins only share homologies of 40-60% and 20-30% in the DBD and LBD respectively with other members of the nuclear receptor superfamily (307, 308).

Nur77 subfamily members bind DNA as monomers, as homodimers, or as heterodimers with RXR. Nur77 binds to monomeric response elements (NBREs) containing the 5'-extended core motif, AAAGGTCA. This is an artificial DNA sequence selected from random oligomer library on the basis of the ability of this sequence to bind Nur77 (322). Nur77 site specificity is determined by DNA-protein contacts between nucleotides located 5' to the core motif contained in the NBRE and the CTE (323-325). On the contrary Nur77 binds the Nur response element (NuRE) palindromic DNA motif as homo- and heterodimers with other Nur77 subfamily members. NuRE was initially identified in the pro-opiomelanocortin (POMC) gene promoter (326). The homodimer binding site consists of two inverted NBREs separated by 6 bp that confer high responsiveness to Nur77.

Ligands for members of the Nur77 subfamily have not been identified. However Nur77 and Nurr1 (but not NOR-1) bind to DR5 response elements as heterodimers with
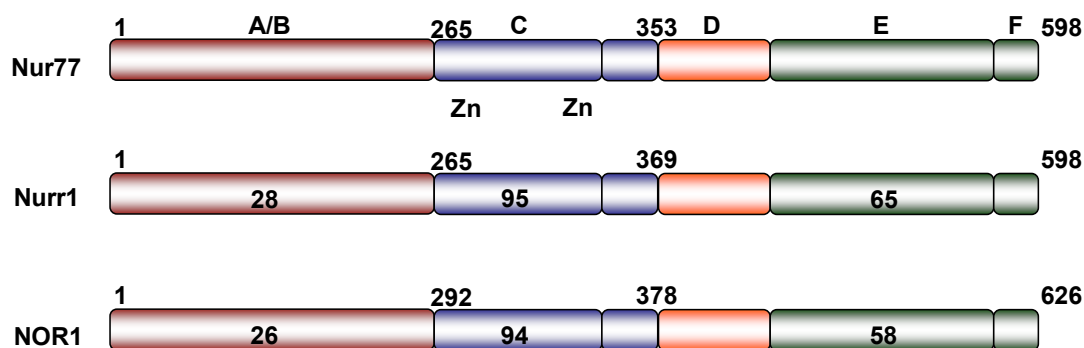
Fig. 1.13. Domain structure and the percent of amino acid identity with the corresponding region of human Nur77 (327).

RXR and, the heterodimer complex is efficiently induced by rexinoids (328, 329). Transcription of Nurr1-RXR heterodimers by rexinoids has been reported when synthetic reporters containing multiple copies of monomeric NBRE are used in cotransfection assays (330). In this case, activation by the heterodimeric complex occurs in the absence of direct DNA binding by the RXR moiety. In addition, the activity of Nur77 subfamily members appears to be regulated by posttranslational modifications, which may be induced via ligand-independent pathways activated by growth factors. Nur77 nuclear localization, DNA-binding affinity, and transcriptional activity can be modulated by phosphorylation of the receptor protein (331-335). Regulation of the NGFI-B heterodimeric complexes activity by rexinoids and covalent modifications does not exclude the existence of the NGFI-B-specific ligands since other RXR-receptor heterodimers can be activated by ligands for both receptors. Recent studies reports that 6-mercaptopurine activates both Nurr1 and Nor-1 through their respective N-terminal

AF-1 domains (336, 337). These results suggest that some activities of 6-mercaptopurine and other antimetabolite drugs may be mediated through NGFI-B proteins.

The physiological roles for NGFI-B proteins are not fully understood; however, gene targeting knockout experiments demonstrate several important functions for these proteins which correlate, in part, with other *in vitro* and *in vivo* studies. For example mice lacking Nurr1 die soon after birth and Nurr1 mutant mice fail to generate midbrain neurons with a dopaminergic phenotype, and midbrain dopamine precursor cells degenerate as brain development progresses (338, 339). Since loss of midbrain dopaminergic neurons is associated with the etiology of Parkinson's disease, the use of the putative NGFI-B ligands or specific rexinoids could provide a novel therapeutic avenue for treatment of this disease. A recent study reports that NOR-1 knockout animals die at gestation day 5, demonstrating an important role for this protein in early embryogenesis (340). In contrast, Nur77 knockout mice do not exhibit a specific phenotype, and this may be related to coexpression of both Nur77/Nor1 which exhibit some overlapping functions (341).

Nur77 and T-cell apoptosis

Immature T-cells expressing a T cell receptor (TCR) that binds to self peptides and major histocompatibility complexes undergo apoptosis during T-cell development. The removal of potentially autoreactive T-cells from the population of T-cells by apoptosis is defined as negative selection. Nur77 was rapidly induced in T-cell hybridomas undergoing TCR-mediated cell death. Expression of dominant negative Nur77 protein or antisense Nur77 mRNA blocked the TCR-mediated apoptosis of these

cells (318, 319). Furthermore, thymocytes undergoing TCR-mediated apoptosis also express high levels of Nur77, suggesting that Nur77 might play a role in thymocytes negative selection. Transgenic mice expressing a dominant negative Nur77 protein blocked TCR mediated apoptosis and prevented clonal deletion of self-reactive T cells (342, 343). In contrast, overexpression of full-length Nur77 in the thymus resulted in massive apoptosis. These results suggest that thymocyte negative selection depends on Nur77. However Nur77 deficient mice did not show any defect in thymocyte negative selection (341). The normal thymic phenotype in Nur77 $^{-/-}$ mice may be due to functional redundancy of NOR-1 in the thymus. NOR-1 and Nur77 exhibit similar tissue expression patterns and overexpression induces massive thymocyte apoptosis (344). A clear functional role of Nur77/NOR-1 in thymocyte negative selection requires the generation of mice lacking both Nur77 and NOR-1. Besides its role in TCR-mediated lymphocyte cell death, Nur77 is also involved in T cell hybridoma cell death induced by thapsigargin (345), suggesting that Nur77 may regulate some shared death pathways in both types of apoptosis.

TCR activation, Nur77/NOR-1 expression and apoptosis are calcium-dependent and treatment with calcium ionophores and phorbol esters mimics TCR activation while inhibition of calcineurin, a calcium/calmodulin-dependent phosphotase, by cyclosporine A blocks apoptosis (346). Using promoter deletional analysis, two myocyte enhancer factor 2 (MEF2) sites were identified as TCR-regulated transcriptional elements in the Nur77 promoter region (346). Studies have shown that TCR activation elevates intracellular calcium levels that cause dissociation of MEF2 from Cabin1, an inhibitor of

MEF2 activity. After dissociation from Cabin1, MEF2 binds MEF2 sites in the Nur77 promoter and induces expression of Nur77 (347).

Nur77 and cancer

Nur77 is involved in induction of apoptosis in various cancerous cell types. Nur77 is not only rapidly induced during apoptosis of immature thymocytes and T-cell hybridomas but also in lung cancer cells treated with synthetic retinoids (348) and prostate cancer cells (LNCaP) treated with different retinoids and apoptotic inducers such as phorbol-12-myristate-13-acetate (TPA) and TNFα (349). Li and coworkers demonstrated that Nur77 regulates apoptosis through a mechanism that is independent of transcriptional regulation (350). In response to apoptotic stimuli, Nur77 is translocated from the nucleus to the cytoplasm, where it targets mitochondria and induces cytochrome c release and apoptosis. It was also shown that Nur77 lacking the DBD localized exclusively in the cytoplasm where it is associated with mitochondria and induced apoptosis indicating that this response was independent of activation of the nuclear receptor (350). Lin *et al* showed that Nur77 interacts with Bcl-2 through its LBD and this interaction is required for Nur77-dependent mitochondrial targeting and apoptosis. Interestingly, Nur77 binds to the Bcl-2 N-terminal loop, resulting in a conformational change in Bcl-2, which converts it from a pro-apoptotic to an anti-apoptotic protein (351).

The role Nur77 plays in apoptosis in colon carcinoma cells appear to be different from that reported in prostate cancer cells. Apoptosis induced by butyrate, the anti-inflammatory drug, sulindac and 5-flourouracil (5-FU) in colon cancer cells results in

nuclear-cytosol translocation of Nur77 which does not associate with mitochondria (352). Thus, although Nur77 translocation from the nucleus may be an apoptotic signal for colon cancer cells, it appears that the mitochondria are not directly targeted. Instead, the trigger for the apoptotic cascade may involve recruitment of other proapototic molecules.

In contrast, other studies support a role of nuclear Nur77 in mediating the effects of apoptosis inducers. For example, TPA induces Nur77 expression in LNCaP cells and the apoptotic response is linked to the induction of E2F1 through direct interaction of Nur77 with a NBRE in the E2F1 promoter (353). Overexpression of E2F1 through induction by Nur77 can induce apoptosis in several systems (353). Thus it is clear that Nur77 can induce apoptosis by multiple mechanisms which not only depend on cell context but also on the apoptosis-inducing agent.

CHAPTER II

1,1-BIS(3'-INDOLYL)-1-(*p*-SUBSTITUTEDPHENYL)METHANES INDUCE

PEROXISOME PROLIFERATOR-ACTIVATED RECEPTOR γ-MEDIATED

GROWTH INHIBITION, TRANSACTIVATION AND DIFFERENTIATION

MARKERS IN COLON CANCER CELLS*

Introduction

Peroxisome proliferator-activated receptors (PPARs) are ligand-activated transcription factors and members of the nuclear receptor (NR) family (354-356). Ligand-bound PPARs form nuclear heterodimers with retinoid X receptors (RXRs) which modulate transcription by interactions with cognate PPAR response elements in target gene promoters. PPARγ has been extensively investigated and ligands for this receptor typically induce adipocyte differentiation and mediate tissue-specific anti-inflammatory responses. Synthetic thiazolidinediones (TZDs), such as rosiglitazone and pioglitazone, are PPARγ agonists that have been developed for treatment of insulin-resistant Type 2 diabetes (354-357).

Ikezoe and coworkers (257) reported expression of wild-type PPARγ mRNA in tumors from multiple tissues including lung, breast, colon, prostate, osteosarcomas,

---

acute myelogenous leukemia, adult T-cell leukemia, glioblastomas, B-cell acute lymphoblastic leukemia, non-Hodgkin's lymphoma, and myelodisplastic syndrome. In addition, PPARγ mRNA was also expressed in 71 different cancer cell lines derived from hematopoietic and non-hematopoietic (lung, duodenal, prostate, breast, glioblastomas and colon) tumors. Surprisingly, the reported PPARγ mutations in colon cancer (358) were not observed in the 10 colon cancer cell lines and 58 clinical samples examined in this study.

Studies in this laboratory have characterized a series of 1,1-bis(3'-indolyl)-1-(*p*-substitutedphenyl)methanes [methylene or C-substituted diindolylmethanes (DIMs)] that activate PPARγ-dependent transactivation and inhibit growth of MCF-7 breast cancer cells (359). Compounds containing *p*-CF$_3$ (DIM-C-pPhCF$_3$), *p*-*t*-butyl (DIM-C-pPhtBu), and *p*-phenyl (DIM-C-pPhC$_6$H$_5$) were the most potent activators of PPARγ and inhibitors of cell growth. Growth inhibition by C-substituted DIMs in MCF-7 cells was associated, in part, with proteasome-dependent downregulation of cyclin D1.

A recent study reported that several colon cancer cells expressed either wild-type or mutant PPARγ containing a point mutation at codon 422 (K422Q) (360). HCT-15 and other cells that express mutant PPARγ were resistant to the growth inhibitory and differentiation-inducing effects of rosiglitazone, whereas these responses were induced by rosiglitazone in cells (e.g. HT-29) expressing wild-type PPARγ. Results of this study show that PPARγ-active C-substituted DIMs induce PPARγ-dependent transactivation and differentiation-induced genes/proteins in both rosiglitazone-responsive (HT-29) and -nonresponsive (HCT-15) colon cancer cell lines. Caveolin 1 and caveolin 2 proteins

were induced by rosiglitazone only in HT-29 cells, whereas C-substituted DIMs induced these proteins in both HT-29 and HCT-15 cells. The cell context-dependent growth inhibitory responses of rosiglitazone and PPARγ-active C-substituted DIMs correlated with induction of caveolins which exhibit tumor suppressor activity.

Materials and Methods

Cell lines and reagents

Human colon carcinoma cell lines RKO, DLD1, SW480 were provided by M.D. Anderson Cancer Center; HT-29 and HCT-15 were obtained from American Type Culture Collection (Manassas, VA). RKO, DLD1, SW480 and HT-29 cells were maintained in Dulbecco's Modified Eagle's Medium nutrient mixture F-12 Ham (DMEM:Ham's F-12; Sigma, St. Louis, MO) with phenol red supplemented with 0.22% sodium bicarbonate, 0.011% sodium pyruvate and 5% fetal bovine serum (FBS) and 10ml/L of 100X antibiotic antimycotic solution (Sigma). HCT-15 cells were maintained in RPMI-1640 medium (Sigma) supplemented with 0.22% sodium bicarbonate, 0.011% sodium pyruvate, 0.45% glucose, 0.24% HEPES, 10% FBS and 10ml/L of 100X Antibiotic Antimycotic solution (Sigma). Cells were maintained at 37°C in the presence of 5% CO_2. Rosiglitazone was purchased from LKT Laboratories Inc. (St. Paul, MN). Antibodies for PPARγ (sc-7273), Sp1 (sc-59), bcl-2, bax, PARP, cyclin D1 (sc-718), p21 (sc-756), p27 (sc-528) and caveolin 1 (sc-894) were purchased from Santa Cruz Biotechnology (Santa Cruz, CA). Keratin-18 antibody was purchased from NeoMarkers (Fremont, CA). Caveolin 2 antibody was obtained from Transduction Laboratories (Lexington, KY). Reporter lysis buffer and luciferase reagent for luciferase studies were

purchased from Promega (Madison WI). β-Gal reagent was obtained from Tropix (Bedford, MA). Lipofectamine™ reagent and Plus™ reagent were supplied by Invitrogen (Carlsbad, CA). Western lightning™ chemiluminiscence reagent were from PerkinElmer Life Sciences (Boston, MA). The C-substituted DIMs were prepared in this laboratory by condensation of indole with *p*-substituted benzaldehydes, and compounds were > 95% pure by gas chromatography-mass spectrometry.

Plasmids

The Gal4 reporter containing 5X Gal4 DBD (Gal4Luc) was kindly provided by Dr. Marty Mayo (University of North Carolina, Chapel Hill, NC). Gal4DBD-PPARγ construct (gPPARγ) was a gift of Dr. Jennifer L. Oberfield (Glaxo Wellcome Research and Development, Research Triangle Park, NC). The PPARγ-VP16 fusion plasmid (VP-PPARγ) contained the DEF region of PPARγ (amino acids 183-505) fused to the pVP16 expression vector and the GAL4-coactivator fusion plasmids pM-SRC1, pMSRC2, pMSRC3, pM-DRIP205and pM-CARM-1 were kindly provided by Dr. Shigeaki Kato (University of Tokyo, Tokyo, Japan).

Transfection and luciferase assay

Colon cancer cells were plated in 12-well plates at 1 x 10^5 cells/well in DME-F12 media supplemented with 2.5% charcoal-stripped FBS. After growth for 16 hr, various amounts of DNA, i.e. Gal4Luc (0.4 μg), b-gal 0.04 μg), VP-PPARγ (0.04 μg), pM SRC1 (0.04 μg), pMSRC2 (0.04 μg), pMSRC3 (0.04 μg), pMDRIP205 (0.04 μg) and pMCARM-1 (0.04 μg) were transfected by Lipofectamine or Lipofectamine Plus (Invitrogen) according to the manufacturer's protocol. After 5 hr of transfection, the

transfection mix was replaced with complete media containing either vehicle (DMSO) or the indicated ligand for 20-22 hr. Cells were then lysed with 100 ml of 1 X reporter lysis buffer and 30 µl of cell extract were used for luciferase and β-Gal assays. Lumicount was used to quantitate luciferase and β-Gal activities, and the luciferase activities were normalized to β-Gal activity.

Cell proliferation assay

Cells were plated at a density of 2 x 10^4/well in 12-well plates and replaced the next day with DMEM:Ham's F-12 media containing 2.5% charcoal-stripped FBS and either vehicle (DMSO) or the indicated ligand and concentration. Fresh media and compounds were added every 48 hr. Cells were counted at the indicated times using a Coulter Z1 cell counter. Each experiment was done in triplicate and results are expressed as means ± SE for each determination.

Fluorescence-activated cell-sorting analysis

HT-29 and HCT-15 cells were synchronized in serum-free media for 3 days and then treated with either the vehicle (DMSO) or the indicated compounds for 24 hr. Cells were trypsinized, centrifuged, and resuspended in staining solution containing 50 µg/ml propidium iodide, 4 mM sodium citrate, 30 units/ml RNase, and 0.1% Triton X-100. After incubation at 37°C for 10 min, sodium chloride was added to give a final concentration of 0.15 M. Cells were analyzed on a FACS Calibur flow cytometer (Becton Dickinson Immunocytometry Systems, San Jose, CA), using CellQuest (Becton Dickinson) acquisition software. PI fluorescence was collected through a 585/42nm bandpass filter, and list mode data were acquired on a minimum of 20,000 single cells

defined by a dot plot of PI width *versus* PI area. Data analysis was performed in ModFit LT (Verity Software House, Topsham, ME) using PI width *versus* PI area to exclude cell aggregates.

Western blot analysis

HT-29 and HCT-15 cells were seeded in DMEM:Ham's F-12 media containing 2.5% charcoal-stripped FBS for 24 hr and then treated with either the vehicle (DMSO) or the indicated compounds. For the apoptosis experiments, cells were treated for 72 hr with various compounds. Western blot analysis of whole cell lysates was determined as previously described (359, 361). Band intensities were evaluated by scanning laser densitometry (Sharp Electronics Corporation, Mahwah, NJ) using Zero-D Scanalytics software (Scanalytics Corporation, Billerica, MA).

Statistical analysis

Statistical differences between different groups were determined by ANOVA and Scheffe's test for significance. The data are presented as mean ± standard deviation for at least 3 separate determinations for each treatment.

Results

Inhibition of colon cancer cell growth by rosiglitazone and PPARγ-active C-substituted DIMs

The effects of rosiglitazone, DIM-C-pPhCF$_3$, DIM-C-pPhtBu and DIM-C-pPhC$_6$-H$_5$ on the growth of HT-29, HCT-15, SW480 and RKO colon cancer cells are summarized in Figure 2.1 and Table 2.1. The results obtained in HT-29 and HCT-15 cells which express wild-type and mutant (K422Q) PPARγ (360) are illustrated in

Figures 2.1A and 2.1B. Rosiglitazone significantly inhibited growth of HT-29 cells at

concentrations of 1, 5 and 10 µM; however, the concentration required for 50%

Table 2.1. Percentage inhibition of SW480 and RKO colon cancer cell growth (6 days)

by rosiglitazone and PPARγ-active C-substituted DIMs.[a]

Treatment (µM)	SW480	RKO
Rosiglitazone		
1	7.85 ± 0.92	0.39 ± 1.73
5	8.13 ± 1.34	2.79 ± 2.89
10	7.75 ± 2.21	2 ± 1.55
DIM-C-pPhCF$_3$		
1	$22.35 \pm 3.87*$	4.36 ± 0.18
5	$104.83 \pm 0.29*$	$101.65 \pm 0.06*$
10	$104.93 \pm 0.25*$	$101.71 \pm 0.09*$
DIM-C-pPhtBu		
1	1.43 ± 3.47	3.22 ± 1.70
5	$65.52 \pm 1.85*$	$41.04 \pm 1.76*$
10	$102.03 \pm 0.37*$	$103.82 \pm 0.06*$
DIM-C-pPhC$_6$H$_5$		
1	2.184 ± 2.44	6.34 ± 2.20
5	$24.328 \pm 1.67*$	$39.77 \pm 2.33*$
10	$103.91 \pm 0.08*$	$102.83 \pm 0.052*$

[a] Cells were treated with different concentrations of the test compounds, and cell numbers were determined as described in the Materials and Methods, and the percent inhibition of cell growth was compared to DMSO (set at 100%). Results are means ± SD for 3 replicate determinations for each treatment group, and significant ($p < 0.05$) inhibition (*) is indicated.
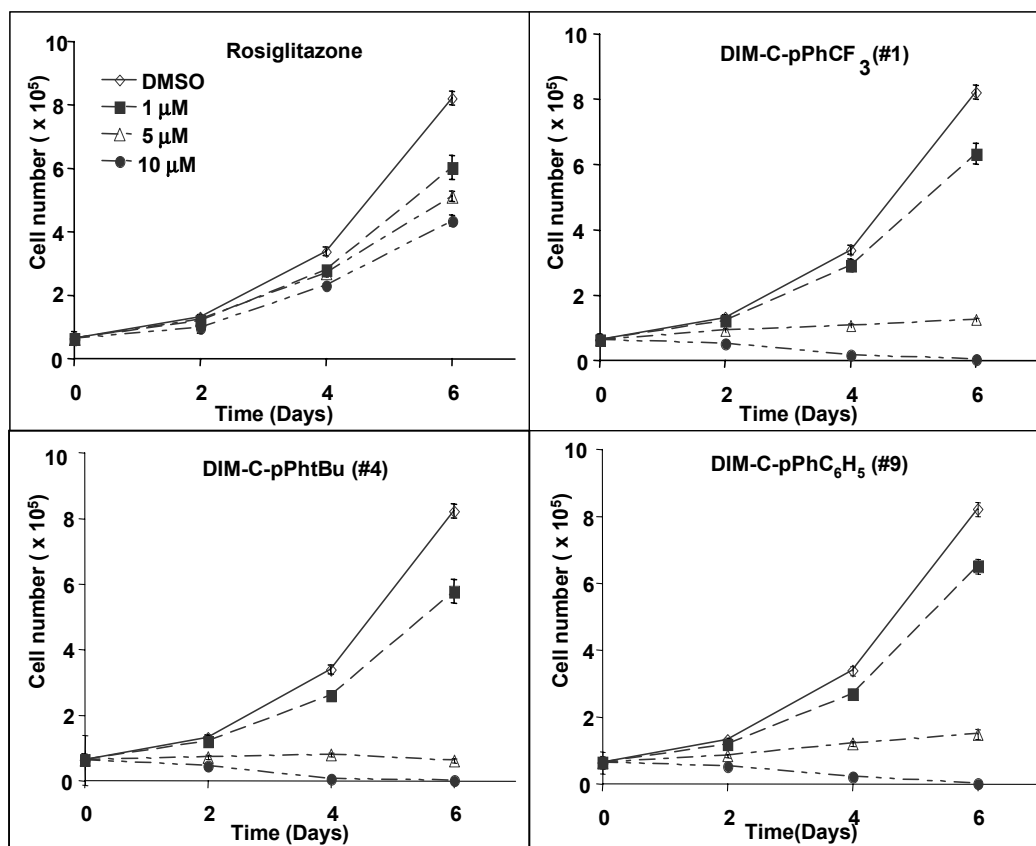
Fig. 2.1. Growth inhibition studies. HT-29 [A] and HCT-15 [B] colon cancer cells were treated with 1 - 10 µM rosiglitazone, DIM-C-pPhCF$_3$, DIM-C-pPhtBu and DIM-C-pPhC$_6$H$_5$ for 6 days, and cell numbers were determined using a Coulter Counter as described in the Materials and Methods. Results are expressed as means ± SE for 3 separate determinations at each time point.

B   **HCT-15**
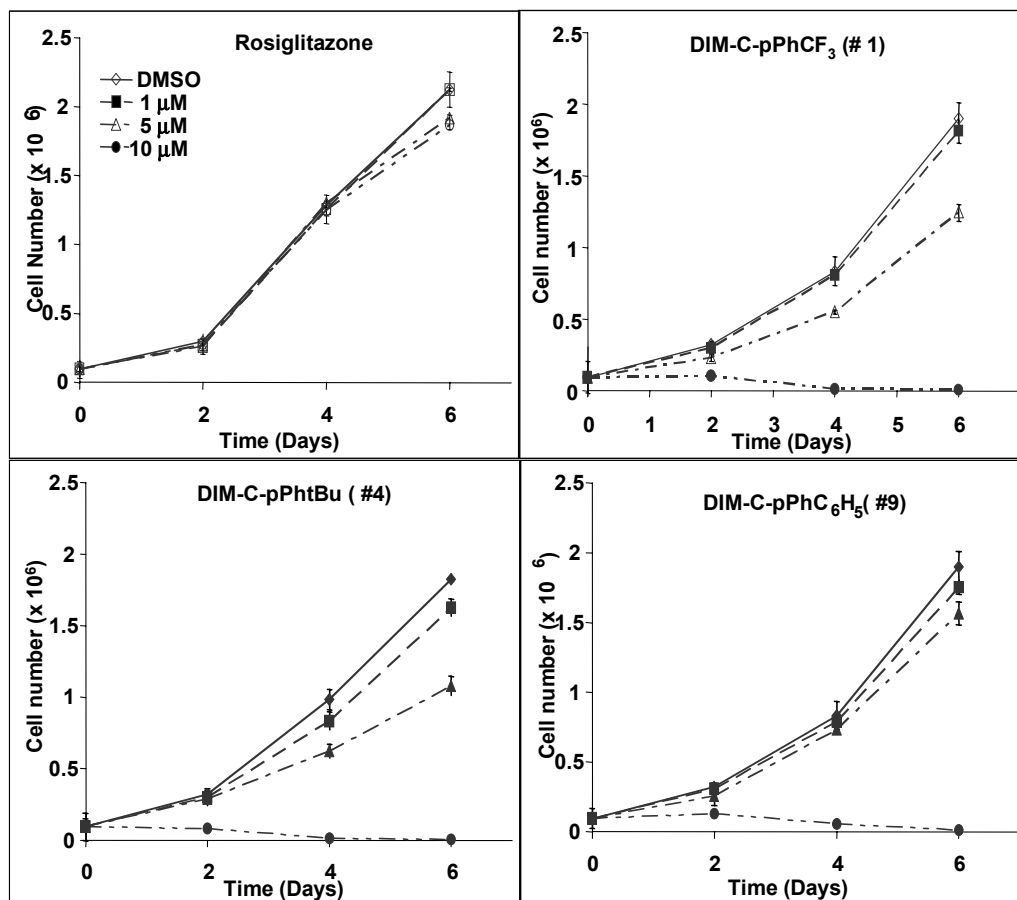
Fig. 2.1 Continued
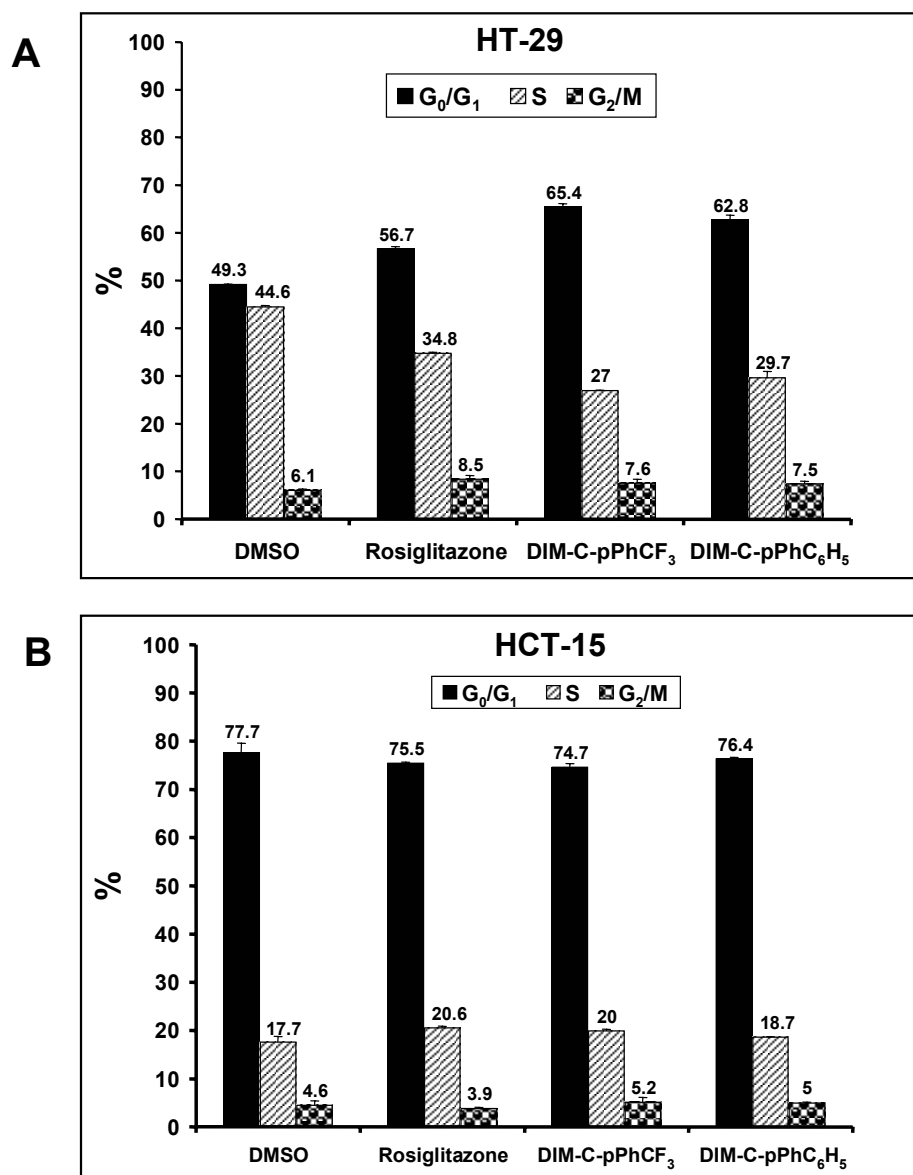
Fig. 2.2. FACS analysis. HT-29 [A] and HCT-15 [B] cells were growth arrested for 3 days and then treated for 24 hr with 10 μM rosiglitazone, DIM-C-pPhCF$_3$ or DIM-C-pPhC$_6$H$_5$ and analyzed by FACS analysis as described in the Materials and Methods. Results of a single experiment are presented and were also observed in two (HT-29) or three (HCT-15) separate studies.

inhibition of cell growth (IC_{50}) was > 10 µM. In contrast, 1 µM concentrations of DIM-C-pPhCF$_3$, DIM-C-pPhtBu and DIM-C-pPhC$_6$H$_5$ significantly ($p < 0.05$) inhibited growth of HT-29 cells, and IC_{50} values were < 5 µM for all three compounds. Rosiglitazone did not inhibit proliferation of HCT-15cells (360); the PPARγ-active C-substituted DIMs all significantly inhibited growth at 5 or 10 µM concentrations, and IC_{50} values were < 10 µM. The results in Table 2.1 show that rosiglitazone treatment (1 - 10 µM) minimally affected growth of SW480 or RKO cells, whereas IC_{50} values for the PPARγ-active C-substituted DIMs varied from 1 - 5 or 5 - 10 µM with DIM-C-pPhCF$_3$ as the most potent compound in both cell lines.

HT-29 and HCT-15 cells were cultured in serum-free media for 3 days and then grown in 2.5% charcoal-stripped serum and treated with DMSO (solvent control), 10 µM rosiglitazone, DIM-C-pPhCF$_3$ or DIM-C-pPhC$_6$H$_5$. Three days after treatment, the percentage distribution of cells in G$_0$/G$_1$, S and G$_2$/M phases was determined by FACS analysis (Fig. 2.2). The PPARγ agonists decreased the percentage of HT-29 cells in S phase and increased the percentage in G$_0$/G$_1$. Rosiglitazone did not affect the percentage of HCT-15 cells in G$_0$/G$_1$, S or G$_2$/M phase of the cell cycle, and this was consistent with the failure of this compound to inhibit proliferation of this cell line (Fig. 2.1B). Surprisingly, 10 µM DIM-C-pPhCF$_3$ and DIM-C-pPhC$_6$H$_5$ also did not alter the percentage distribution of HCT-15 cells in G$_0$/G$_1$, S or G$_2$/M phase, even though both compounds significantly inhibited growth of these cells (Fig. 2.1). Previous studies with HCT-15 cells showed that the PPARγ agonists BRL 49653 did not inhibit growth of

these cells or block $G_0/G_1 \rightarrow S$ phase progression (362).

PPARγ-dependent transactivation and coactivator interactions by rosiglitazone, DIM-C-

pPhCF$_3$, DIM-C-pPhtBu and DIM-C-pPhC$_6$H$_5$

PPARγ is expressed in SW480, RKO, HT-29 and HCT-15 cells, and ligand-dependent activation of PPARγ in HCT-15 and HT-29 colon cancer was determined in cells transfected with chimeric PPARγ-GAL4 and a GAL4 response element plasmid (pGAL4) containing 5 tandem GAL4 response elements linked to a luciferase reporter gene (Figs. 2.3A and 2.3B). Rosiglitazone (1 - 10 µM) and 1 - 10 µM DIM-C-pPhCF$_3$, DIM-C-pPhtBu and DIM-C-pPhC$_6$H$_5$ induced reporter gene activity in HCT-15 and HT-29 cells, and similar results were observed in RKO and SW480 cells. The magnitude of the induction responses were < 6-fold in the HCT-15 and HT-29 cells, and the relative potencies of the individual compounds were variable and dependent on cell context. DIM-C-pPhCH$_3$ exhibited lower activity in the transactivation assays in the colon cancer cells as previously reported in breast cancer cell lines (359). Results in Figures 2.3C and 2.3D show that induction of luciferase activity by rosiglitazone and PPARγ-active C-substituted DIMs in HT-29 and HCT-15 cells transfected with PPARγ-GAL4/pGAL4 was inhibited by GW9662, a PPARγ antagonist. Results summarized in Figure 2.3E show that 7.5 µM GW9662 also significantly blocks the growth inhibitory effects of 2.5, 5.0 or 7.5 µM DIM-C-pPhC$_6$H$_5$ in HCT-15 cells. In contrast, GW9662 alone was growth inhibitory in HT-29 cells. These data confirm the role of PPARγ in mediating inhibition of HCT-15 cell growth by DIM-C-pPhC$_6$H$_5$.

A
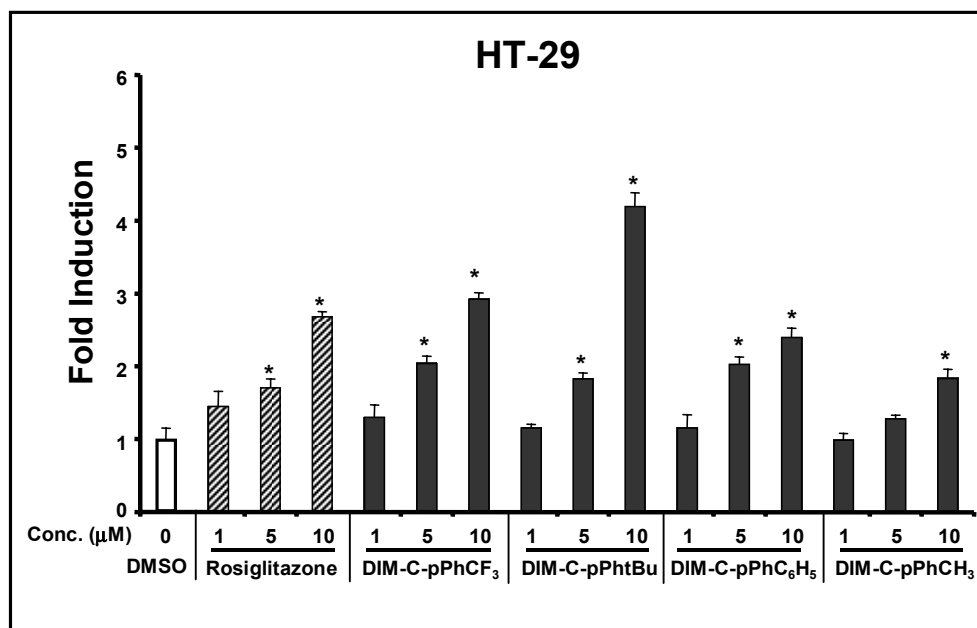
Fig. 2.3. Ligand-induced activation of PPARγ, and effects of PPARγ antagonists. [A] Ligand-dependent activation of PPARγ-GAL4/pGAL4 in HT-29 cells. Cells were transfected with PPARγ-GAL4/pGAL4, treated with 1, 5 or 10 µM of the PPARγ agonists, and luciferase activity was determined as described in the Materials and Methods. Results of all transactivation studies in this Figure are presented as means ± SE for at least 3 separate determinations for each treatment group and significant ($p < 0.05$) induction compared to solvent (DMSO) control is indicated by an asterisk. [B] Ligand-dependent activation of PPARγ-GAL4/pGAL4 in HCT-15 cells. This experiment was carried out as described in Figure 2.3A. Inhibition of transactivation in HT-29 [C] and HCT-15 [D] cells by GW9662. Cells were transfected with PPARγ-GAL4/pGAL4, treated with 10 µM rosiglitazone or PPARγ-active C-substituted DIMs alone or in combination with 5 or 10 µM GW9662, and luciferase activities were determined as described in Figure 2.3A. Significant ($p < 0.05$) inhibition of induced transactivation by GW9662 is indicated (**). [E] Inhibition of HCT-15 cell growth by DIM-C-pPhC$_6$H$_5$: effects of GW9662. The effects of DIM-C-pPhC$_6$H$_5$ alone and in combination with GW9662 on proliferation of HCT-15 cells were determined as described in the Materials and Methods and outlined in the caption for Figure 2.1. Significant ($p < 0.05$) inhibition of cell proliferation (*) and antagonism of this response by GW9662 (**) are indicated.

B
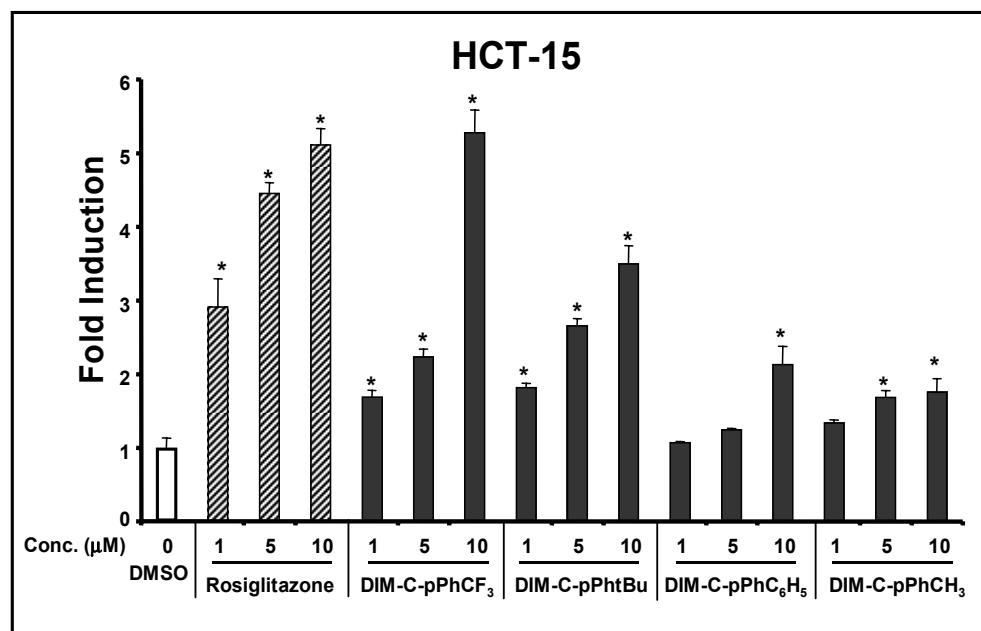
C
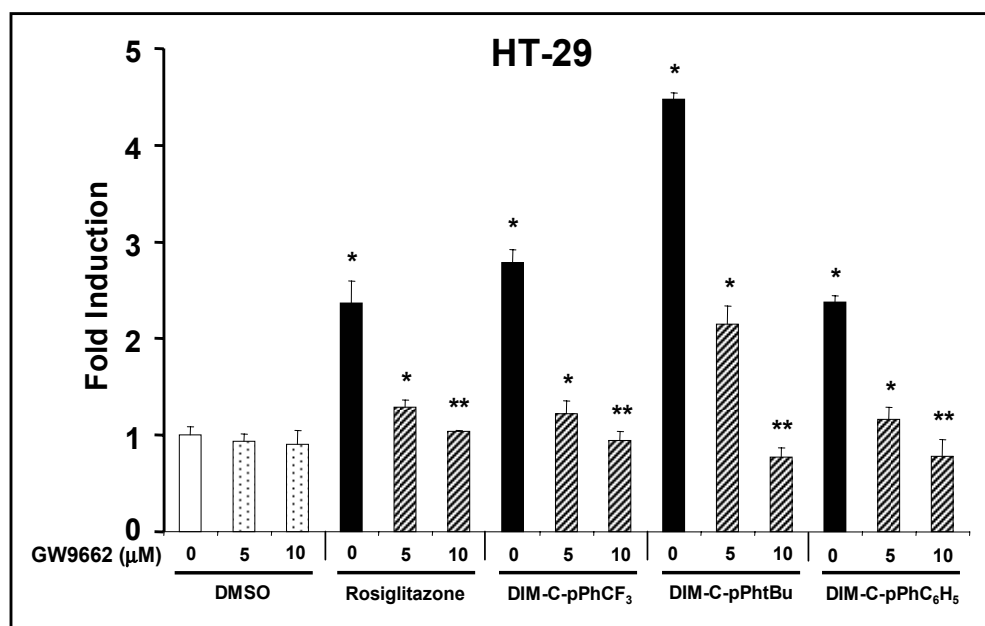
Fig. 2.3 Continued

D
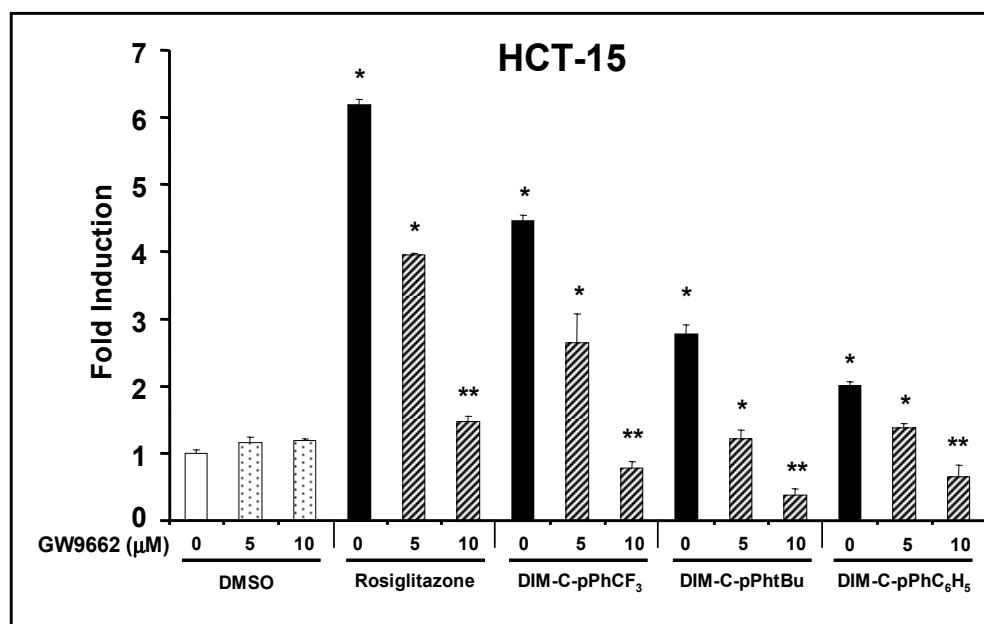
E
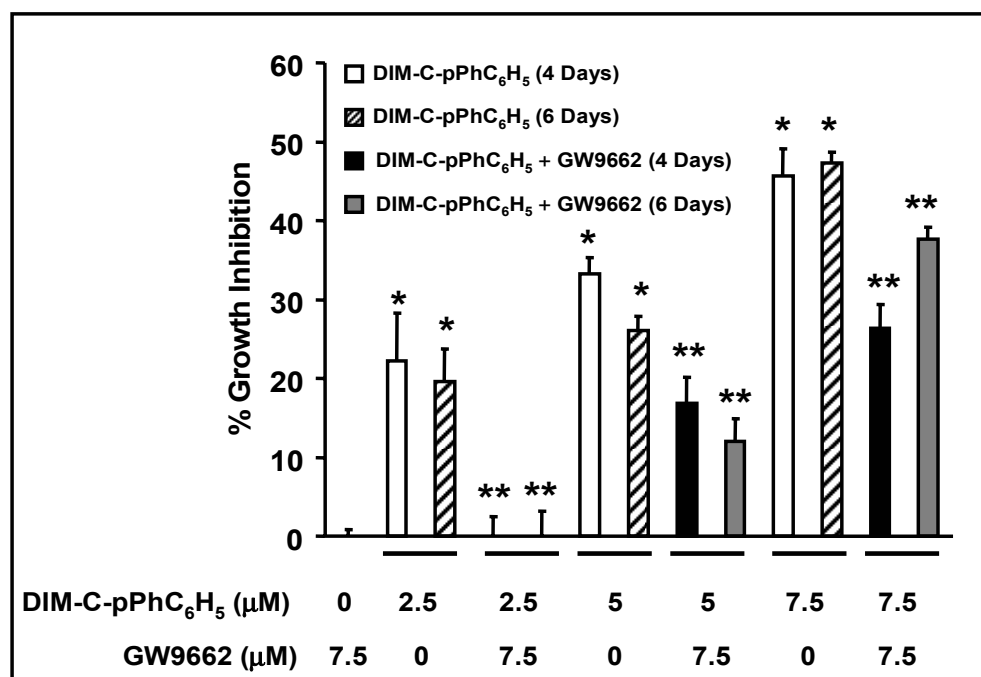
Fig. 2.3 Continued

A previous report (363) showed that 15-deoxy-Δ12,14-prostaglandin J2 (PGJ2) but not TZDs induced transactivation in a mammalian two-hybrid assay in COS-1 cells transfected with VP-PPARγ and GAL4-coactivator chimeras (coactivators = SRC-1, SRC-2, SRC-3 and DRIP205/TBP/TRAP220). Therefore, we investigated ligand-dependent interactions of VP-PPARγ with chimeric GAL4-coactivator in colon cancer cells transfected with the pGAL4-luc reporter gene construct (Fig 2.4). PPARγ-active C-substituted DIMs and rosiglitazone induced transactivation in HT-29 cells transfected with VP-PPARγ and GAL4-PGC-1, and minimal interactions were observed using chimeric proteins containing SRC-1, SRC-2, SRC-3, DRIP205 or CARM-1. DIM-C-pPhCF$_3$ also induced transactivation (< 2-fold) in cells transfected with GAL4-SRC-3 and DIM-C-pPhC$_6$H$_5$ did not significantly induce activity in cells transfected with GAL4-PGC-1. PPARγ-active C-substituted DIMs induced transactivation in HCT-15 cells transfected with GAL4-PGC-1 and with one exception (DIM-C-pPhtBu/GAL4-SRC2), minimal interactions with other coactivators were observed. In SW480 and RKO colon cancer cells, a variable pattern of PPARγ-coactivator interactions were observed and the PPARγ-active C-substituted DIMs but not rosiglitazone induced interactions with PGC-1.

Modulation of cell cycle proteins, differentiation markers and apoptosis by PPARγ agonists

The effects of rosiglitazone and PPARγ-active C-substituted DIMs on
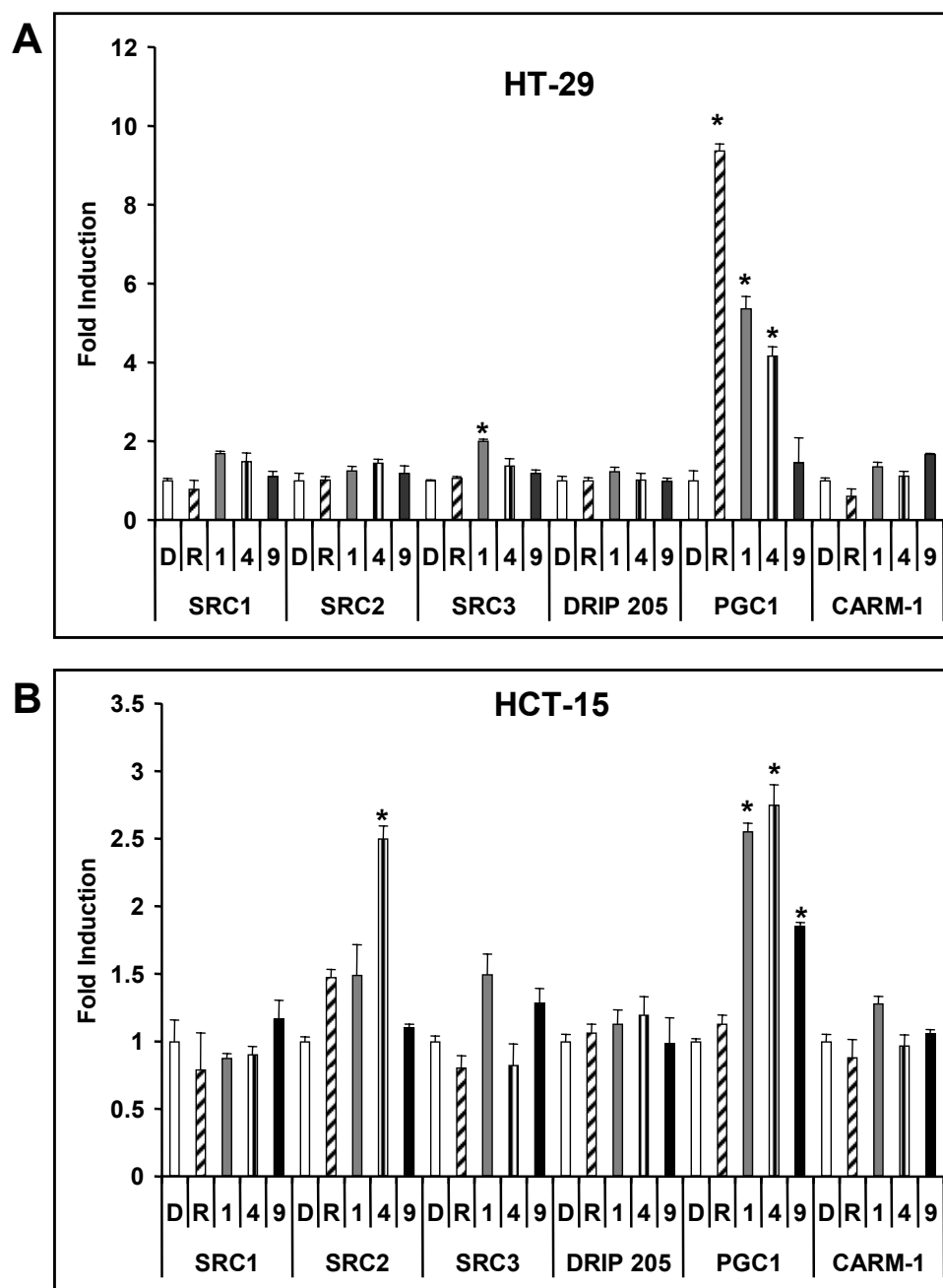
Fig. 2.4. Ligand-induced PPARγ-coactivator interactions. HT-29 [A] and HCT-15 [B] were transfected with VP-PPARγ, coactivator-GAL4/pGAL4, treated with 10 μM rosiglitazone, DIM-C-pPhCF$_3$ (#1), DIM-C-pPhtBu (#4) or DIM-C-pPhC$_6$H$_5$ (#9), and luciferase activity was determined as described in the Materials and Methods. Results are expressed as means ± SE for 3 replicate determinations for each treatment group, and significant (p < 0.05) induction is indicated by an asterisk.
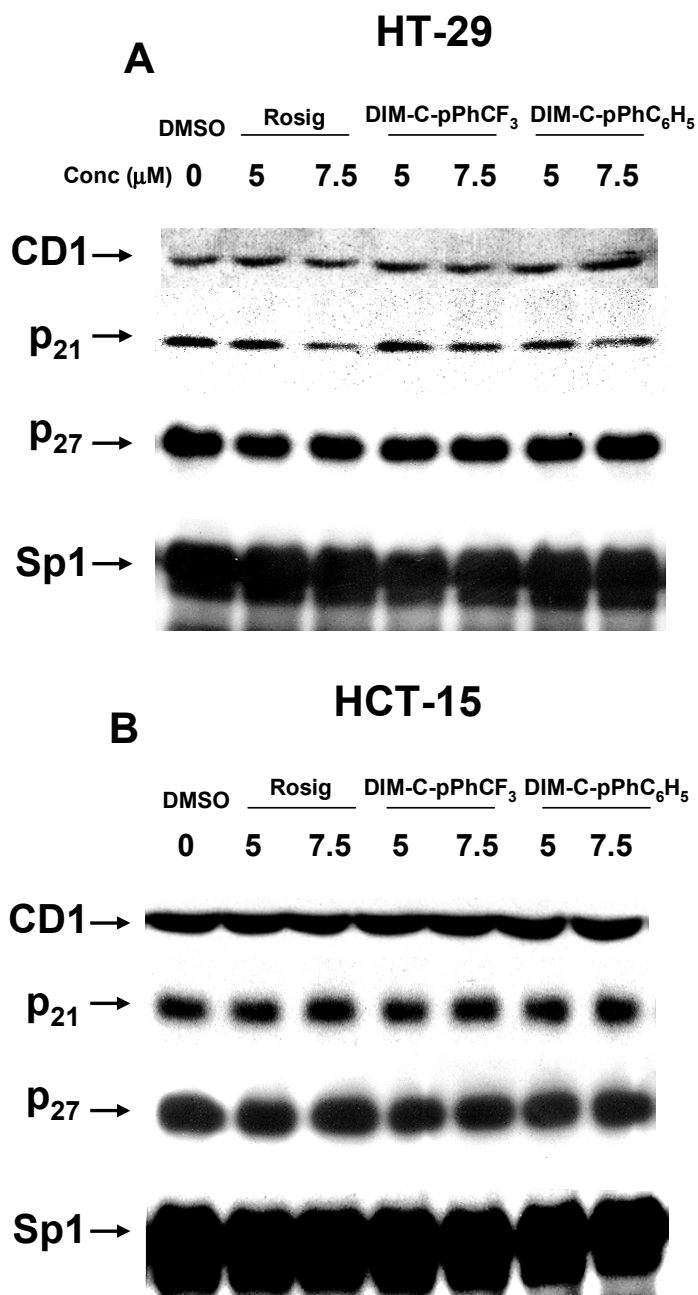
Fig. 2.5. Modulation of cell cycle proteins. HT-29 [A] or HCT-15 [B] cells were treated with 5.0 or 7.5 μM rosiglitazone, DIM-C-pPhCF$_3$ or DIM-C-pPhC$_6$H$_5$ for 24 hr, and whole cell lysates were analyzed by Western blot analysis as described in the Materials and Methods. Cyclin D1, p21 and p27 protein levels were similar in all treatment groups in duplicate experiments after treatment for 24 hr.

cyclin D1, p21 and p27 protein expression were investigated in HT-29 and HCT-15 after treatment with DMSO (control) and 5 or 7.5 µM concentrations of these compounds for 24 hr. The results show that none of the treatments significantly affected levels of cyclin D1, p21 or p27 proteins (Fig. 2.5), and protein levels at other time points (6 and 12 hr) were also unchanged.

PPARγ agonists induce genes associated with differentiation in preadipocytes and cancer cell lines, and results in Figure 2.6 show that keratin 18 is constitutively expressed in both HT-29 and HCT-15 cells. In the former cell line, 5 and 7.5 µM rosiglitazone, DIM-C-pPhCF$_3$ and DIM-C-pPhC$_6$H$_5$ significantly induced keratin 18 protein and a maximal 2-fold induction response was observed for 7.5 µM DIM-C-pPhC$_6$H$_5$. Rosiglitazone and PPARγ-active C-substituted DIMs also induced a 2.5- to 3-fold increase in keratin 18 protein in HCT-15 cells showing that induction of this differentiation marker did not correlate with expression of wild-type or mutant PPARγ. A recent report showed that caveolins 1 and 2 were induced by TZDs in HT-29 cells (364). Rosiglitazone, DIM-C-pPhCF$_3$ and DIM-C-pPhC$_6$H$_5$ also significantly induced caveolins 1 and 2 in this cell line, and protein levels were increased by 5- to 9-fold after treatment for 72 hr. Similar results were observed in HT-29 cells treated for only 48 hr with the PPARγ agonists. In contrast, DIM-C-pPhCF$_3$ and DIM-C-pPhC$_6$H$_5$, but not rosiglitazone, induced caveolins 1 and 2 in HCT-15 cells after treatment for 72 hr (Figs. 2.7C and 2.7E). Induction of caveolins 1 and 2 by DIM-C-pPhCF$_3$ and DIM-C-pPhC$_6$H$_5$ in HT-29 and HCT-15 cells was inhibited by cotreatment with the PPARγ agonist
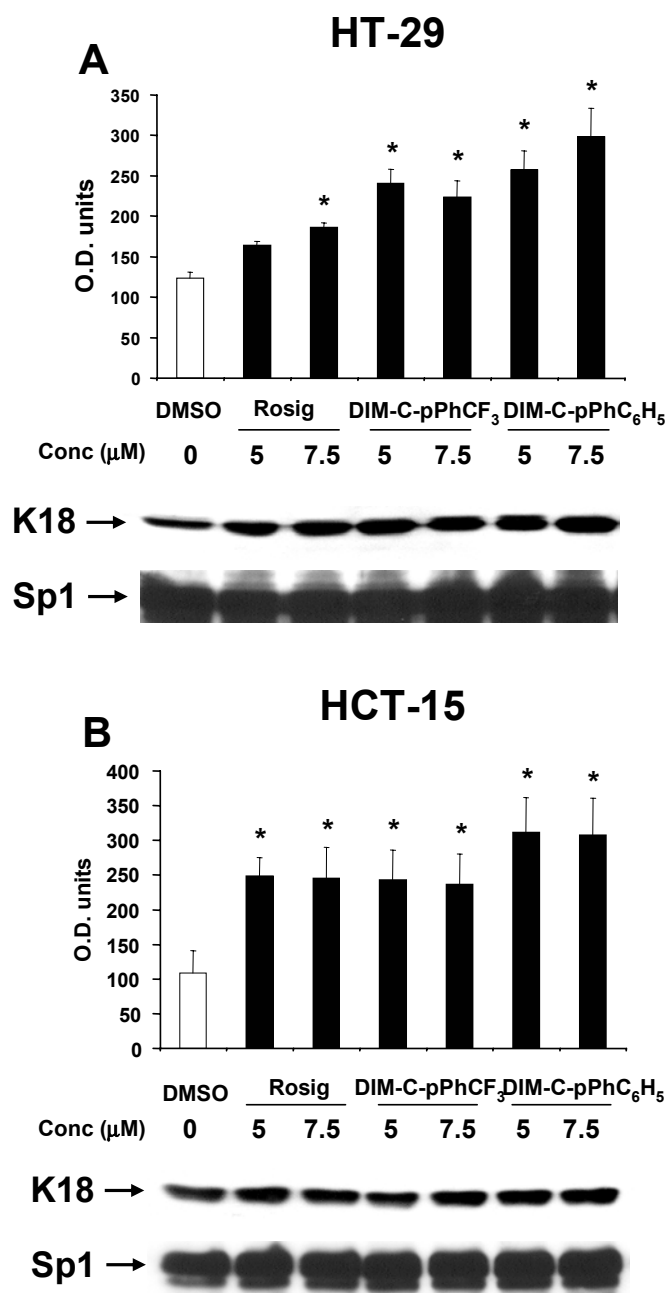
Fig. 2.6. Expression of keratin 18. HT-29 [A] and HCT-15 [B] cells were treated with 5.0 or 7.5 μM rosiglitazone, DIM-C-pPhCF$_3$ or DIM-C-pPhC$_6$H$_5$ for 3 days, and whole cell lysates were analyzed by Western blot analysis as described in the Materials and Methods. Keratin 18 levels in each treatment group were quantitated relative to an Sp1 protein loading control, and results are expressed as means ± SE for 3 replicate determinations for each treatment group. Significant (p < 0.05) induction is indicated by an asterisk.
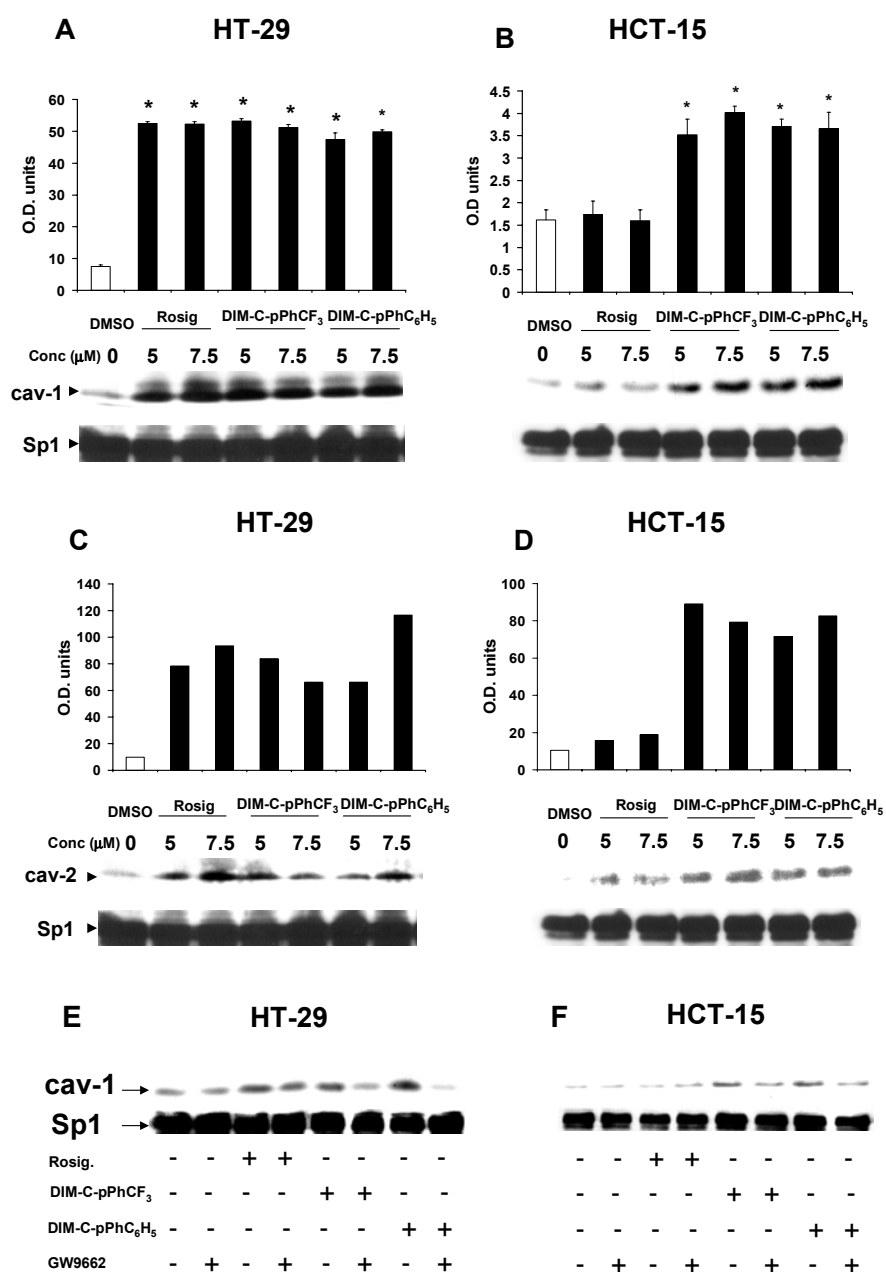
Fig. 2.7. Expression of caveolin 1 and caveolin 2. HT-29 [A] and HCT-15 [B] cells were treated with 5.0 or 7.5 μM rosiglitazone, DIM-C-pPhCF$_3$ or DIM-C-pPhC$_6$H$_5$ for 3 days, and whole cell lysates were analyzed by Western blot analysis as described in the Materials and Methods. Using a similar approach, caveolin 2 protein levels were determined in HT-29 [C] and HCT-15 [D] cells. Results are expressed as means ± SE for 3 replicate determinations [A, B] or averages of two determinations [C, D], and significant (p < 0.05) induction (*) [A, B] was determined as outlined in Figure 6. Inhibition of caveolin 1 induction in HT-29 [E] and HCT-15 [F] cells by GW9662. The experiment was carried out as described in Figures 7A and 7B; however, cells were also treated with the PPARγ agonists (7.5 μM) in combination with GW9662. Comparable results were observed in duplicate experiments.

A   **B**

DMSO   1   4   9   ROSI   MG132   DMSO   1   4   9   ROSI   MG132

PARP 112
PARP 85

bcl2

bax

N.S.
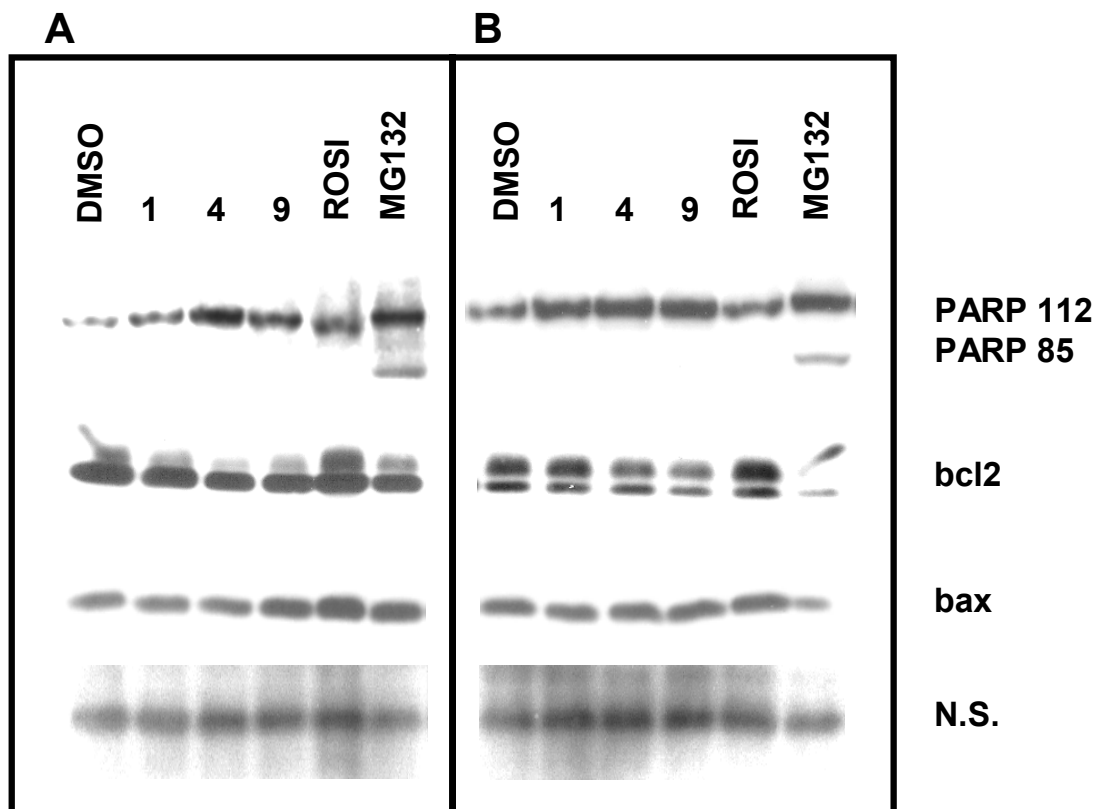
Fig. 2.8. Effects of PPARγ agonists on apoptosis. HCT-15 [A] or HT-29 [B] cells were treated with DMSO, 10 μM DIM-C-pPhCF$_3$ (1), DIM-C-pPhtBu (4), DIM-C-pPhC$_6$H$_5$ (9), or rosiglitazone for 72 hr or 10 μM MG132 for 20 hr, and whole cell lysates were analyzed by Western blot analysis for PARP112/85, bcl-2, bax or a non-specific (NS) (loading control) protein. Similar results were observed in duplicate analyses.

GW9662; similar inhibition was observed for rosiglitazone in HT-29 cells (Figs. 2.7E and 2.7F). Since caveolin 1 exhibits tumor suppressor and growth inhibitory activities, the results suggest that induction of caveolins may be important for the antiproliferative effects of PPARγ-active C-substituted DIMs and rosiglitazone in colon cancer cells (Fig. 2.1).

PPARγ agonists also induce apoptosis in some cancer cell lines (254, 365, 366), and therefore this response was also investigated in HT-29 and HCT-15 cells. PPARγ-active compounds (10 μM) did not induce PARP cleavage (a marker of apoptosis) or alter levels of bax or bcl-2 protein expression in HCT-15 or HT-29 cells (Fig. 2.8). In contrast, the proteasome inhibitor MG132 induced PARP cleavage in both cell lines but did not affect levels of bcl-2 or bax proteins. Thus, differences in the observed antiproliferative activities of rosiglitazone and PPARγ C-substituted DIMs in HT-29 and HCT-15 cells (Fig. 2.1) was not due to apoptosis or modulation of cell cycle proteins but correlated with their cell context-dependent differential induction of caveolins 1 and 2, but not keratin 18.

Discussion

PPARγ is overexpressed in multiple tumor types (257) and studies in several laboratories have demonstrated that PGJ2 and TZDs inhibit growth of human cancer cell lines *in vitro* and also in xenograft models *in vivo* (359-361, 367, 368). Two reports (368, 369) showed that treatment of Min mice, which express a mutated inactive form of the adenomatous polyposis coli (APC) tumor suppressor gene, with troglitazone or BRL-49653 induced colon polyp formation. These results contrast with xenograft studies

where PPARγ agonists inhibit colon tumor growth (367). Moreover, a recent study reported that 100 or 200 ppm pioglitazone and bezafibrate in the diet of *Apc*-deficient mice reduced intestinal polyps and hyperlipidemia (370). Another study used PPARγ$^{+/-}$/Min mice and their crosses to show that inhibition of colon carcinogenesis in these mice by PPARγ agonists is Apc-dependent (371).

Recent studies in this laboratory showed the C-substituted DIMs inhibited growth and $G_0/G_1 \rightarrow S$ progression of MCF-7 breast cancer cells and activated PPARγ-dependent transactivation (359). The growth-inhibitory properties of rosiglitazone and three PPARγ-active C-substituted DIMs (DIM-C-pPhCF$_3$, DIM-C-pPhtBu and DIM-C-pPhC$_6$H$_5$) were also determined in HT-29, HCT-15, SW480 and RKO colon cancer cell lines. At concentrations of 10 μM rosiglitazone significantly inhibited growth of HT-29 cells (IC$_{50}$ > 10 μM) but not the other cell lines, whereas the PPARγ-active C-substituted DIMs inhibited growth of all four colon cancer cell lines with IC$_{50}$ values between 1 - 10 μM. The growth inhibitory effects of DIM-C-pPhC$_6$H$_5$ were inhibited by GW9662 in HCT-15 cells (Fig. 2.3E). A recent report showed that troglitazone inhibited growth and induced differentiation genes in HCT-15 cells (372). However, these responses were observed using 50 μM troglitazone, suggesting that activation of some mutant (K422Q) PPARγ-dependent responses in HCT-15 cells may be observed with higher concentrations of thiazolidinediones.

Rosiglitazone and the PPARγ-active C-substituted DIM activated PPARγ-GAL4/pGAL4-luc in all four cell lines (Fig. 2.3) with variable potencies, and

transactivation was inhibited after cotreatment with the PPARγ antagonist GW9662. The pattern of coactivator-PPARγ interactions in HT-29 and HCT-15 cells paralleled, in part, their responsiveness to the growth inhibitory effects of rosiglitazone and the PPARγ-active C-substituted DIMs (Fig. 2.4). Both structural classes of PPARγ agonists induced interactions between VP-PPARγ and GAL4-PGC-1 in HT-29 cells, whereas only the C-substituted DIMs induced the same interaction in HCT-15 cells (Fig. 2.4). In contrast, the pattern of coactivator-PPARγ interactions in SW480 and RKO cells was more complex and minimal induction was observed for rosiglitazone in both cell lines. The differences in rosiglitazone-induced transactivation in the mammalian two-hybrid assay in HT-29 and HCT-15 were observed using VP-PPARγ (wild-type) in both cell lines. This suggests that differences in PGC-1-PPARγ interactions in HT-29 and HCT-15 cells are not due to expression of the PPARγ mutant (K422Q) in the latter cell line but related to differential expression in the two cell lines of other nuclear cofactors required for this response. Although PPARγ-active C-substituted DIMs preferentially induce PPARγ-PGC-1 interactions in HT-28 and HCT-15 cells, this was not uniformly observed for all ligands in these cells (Fig. 2.4). For example, DIM-C-pPhC$_6$H$_5$ inhibits HT-29 and HCT-15 cell growth (Fig. 2.1), induces caveolins 1/2 (Fig. 2.7), and both responses are inhibited by the PPARγ agonist GW9662 (Figs. 2.3E, 2.7E and 2.7F). In contrast, 10 μM DIM-C-pPhC$_6$H$_5$ does not induce transactivation in the mammalian two-hybrid assay in HT-29 cells using GAL4-PGC-1 and VP-PPARγ (Fig. 2.4). Current studies are investigating expression of PGC-1 and other coactivators and their role in

PPARγ-dependent transactivation and growth inhibition in HT-29 and HCT-15 cells.

We further investigated the role of wild-type vs. mutant (K422Q) PPARγ expression in mediating ligand-dependent responses in HT-29 and HCT-15 cells by examining their effects on proteins critical for cell cycle progression and differentiation. In HT-29 cells, treatment with rosiglitazone or PPARγ-active C-substituted DIMs inhibited $G_0/G_1 \rightarrow S$ phase progression (Fig. 2.2A). These effects were not observed in HCT-15 cells (Fig. 2.2B) and may be due to the high percentage of cells in G_0/G_1 with or without treatment (> 74%). Despite differences in FACS analysis, neither rosiglitazone or the PPARγ-active C-substituted DIMs significantly changed levels of the cell cycle regulatory proteins p27, p21 or cyclin D1 in HT-29 or HCT-15 cells (Fig. 2.5). Moreover, we did not observe PPARγ agonist-dependent induction of apoptosis in either cell line (e.g. Fig. 2.8) suggesting that the antiproliferative effects (Fig. 2.1) are not dependent on modulation of cell cycle proteins or induction of apoptosis in HT-29 or HCT-15 cells.

PPARγ agonists also induce genes/proteins associated with differentiation in colon cancer cells (360, 364, 370, 373, 374). For example, troglitazone induced villin and intestinal alkaline phosphatase mRNA levels in several colon cancer cell lines (374), and TZDs and PGJ2 induced caveolin 1 and caveolin 2 protein expression in HT-29 cells (364). Keratin 18 and 20 proteins and CEACAM6 mRNA levels were minimally expressed in HCT-15 cells but were not affected by treatment with rosiglitazone; however, after transfection of HCT-15 cells with wild-type PPARγ, rosiglitazone induced these responses (360). A direct comparison of PPARγ agonist-induced

expression of differentiation markers in HCT-15 vs. HT-29 cells has not been previously reported. The results in Figure 6 show that rosiglitazone, DIM-C-pPhCF$_3$ and DIM-C-pPhC$_6$H$_5$ significantly induced keratin 18 in both HT-29 and HCT-15 cells, indicating that keratin 18 protein induction was independent of PPARγ agonist structure and expression of wild-type or mutant (K422Q) PPARγ. In contrast, induction of caveolin 1 and caveolin 2 in HT-29 and HCT-15 was dependent on both ligand structure and cell context (Fig. 2.7). Rosiglitazone induced caveolins 1 and 2 in HT-29 but not in HCT-15 cells, whereas PPARγ-active C-substituted DIMs induced caveolins 1 and 2 in both HT-29 and HCT-15 cells and these responses were inhibited after cotreatment with GW9662. This pattern of induced caveolin expression parallels the growth inhibitory effects of rosiglitazone and PPARγ-active C-substituted DIMs in HT-29 and HCT-15 cells (Fig. 2.1), suggesting that induced caveolin 1 and caveolin 2 expression may contribute to growth inhibition of colon cancer cells. This observation is consistent with a report by Bender and coworkers (375) showing that overexpression of caveolin 1 in HT-29 or DLD (HCT-15) cells significantly decreased their tumorigenicity in athymic nude mouse xenograft models.

In summary, this study demonstrates the PPARγ-active C-substituted DIMs induce PPARγ-dependent transactivation in colon cancer cells expressing wild-type (HT-29) or mutant (K422Q) (HCT-15) PPARγ. Moreover, these compounds also inhibit growth of HT-29 and HCT-15 cells, whereas equivalent concentrations of rosiglitazone are active only in the former cell line. The enhanced growth inhibitory activity of PPARγ-active C-substituted DIMs vs. rosiglitazone in HCT-15 cells correlated with the

induction of caveolins 1 and 2 by the former compounds and not by rosiglitazone (Fig. 2.7). Current studies are focused on the mechanisms of the growth inhibitory effects of this new class of PPARγ agonists in other colon cancer cell lines and the role of caveolins and other genes/proteins in mediating PPARγ-dependent antitumorigenic activities.

CHAPTER III

INHIBITION OF BLADDER TUMOR GROWTH BY 1,1-BIS(3'-INDOLYL)-1-(*p*-SUBSTITUTEDPHENYL)METHANES: A NEW CLASS OF PEROXISOME PROLIFERATOR-ACTIVATED RECEPTOR γ AGONISTS

Introduction

Metastatic UC of the bladder is typically treated with various combinations of systemic chemotherapy (376-379). However, almost all patients with distant metastatic bladder cancer are dead within 1 to 2 years, despite treatment with the most effective regimens available (377, 378). Since the mid-1980s, the standard treatment for metastatic UC has been a combination of methotrexate, vinblastine, adriamycin and cisplatin. Recently, several novel combination regimes has been reported; however, there is no compelling evidence of enhanced patient survival with these treatments (380-382). An improved understanding of the biology of malignancy will provide novel therapeutic approaches.

One such strategy is targeted therapy which involves modulation of specific genes/pathways that are upregulated in cancer cells compared to normal tissues and can lead to decreased cancer cell survival and/or death. The peroxisome proliferator-activated receptor γ (PPARγ) is a ligand-activated receptor and a member of the nuclear receptor superfamily of transcription factors. PPARγ, PPARα and PPARβ/δ are differentially expressed in normal tissues/organs and play diverse roles in metabolism, anti-inflammatory responses, and differentiation (355, 356, 383-385). Synthetic PPARγ agonists such as the thiazolidinediones (TZDs) are now widely used for treatment of

insulin-resistant Type II diabetes. PPARγ is highly expressed in tumor samples from different sites and, in one study, wild-type PPARγ mRNA was observed in multiple tumors and in 34 hematopoeitic cancer cell lines as well as several lung (385), colon (385), duodenal (376), prostate (380), breast (379), and glioblastoma (377) cell lines (257). PPARγ has also been detected in bladder tumors and bladder cancer cell lines (386-389), and PPARγ is expressed in the epithelium but not surrounding smooth muscle or interstitium (387).

PPARγ is an excellent target for cancer chemotherapy not only due to its elevated expression in tumors but also for the induced responses which include decreased cell survival and G_0/G_1 to S phase progression, increased differentiation and apoptosis (254, 360-366, 390-392). Research in this laboratory has identified a new class of PPARγ agonists from a series of 1,1-bis(3'-indolyl)-1-(*p*-substitutedphenyl)methanes where the PPARγ-active compounds contain *p*-trifluromethyl (DIM-C-pPhCF$_3$), *p*-*t*-butyl (DIM-C-pPhtBu), and *p*-phenyl DIM-C-pPhC$_6$H$_5$) substituents (359, 391-395). The PPARγ-active methylene-substituted diindolylmethanes (C-DIMs) inhibit growth and/or induce apoptosis in breast, pancreatic and colon cancer cell lines and leukemia cells, and this study investigates their effects on bladder cancer cells *in vitro* and bladder tumors *in vivo*. The PPARγ-active C-DIMs inhibit growth of KU7 bladder cancer cells and induce the tumor suppressor caveolin-1 but do not affect expression of cyclin D1, p21 or p27. In contrast, induction of p21 but not caveolin-1 was observed in 253JB-V33 cells. C-DIM compounds also inhibit growth of orthotopic and subcutaneous bladder tumors (KU7) in athymic nude mice, and this was accompanied by enhanced expression of

caveolin-1 in the tumors. These data demonstrate that PPARγ-active C-DIMs exhibit antitumorigenic activity for bladder cancer, and current studies are evaluating these compounds for future clinical applications.

Materials and Methods

Cell lines, antibodies, plasmids and reagents

KU7 and 253JB-V33 bladder cancer cell lines were obtained from American Type Culture Collection (Manassas, VA). Cells were maintained in RPMI 1640 (Sigma-Aldrich, St. Louis, MO) supplemented with 0.22% sodium bicarbonate, 0.011% sodium pyruvate, 0.45% glucose, 0.24% HEPES, 10% FBS, and 10 mL/L of 100x antibiotic antimycotic solution (Sigma-Aldrich). Cells were maintained at 37°C in the presence of 5% CO_2. Antibodies for cyclin D1 (sc-718), p27 (sc-528), phospho-Akt (sc-7985R), Akt (sc-8312), Sp1 (PEP2), and caveolin 1 (sc-894) were purchased from Santa Cruz Biotechnology (Santa Cruz, CA). Monoclonal β-actin was purchased from Sigma-Aldrich. Reporter lysis buffer and luciferase reagent for luciferase studies were supplied by Promega (Madison, WI). β-Galactosidase (β-Gal) reagent was obtained from Tropix (Bedford, MA) and Lipofectamine reagent was purchased from Invitrogen (Carlsbad, CA). Western Lightning chemiluminescence reagent was from Perkin-Elmer Life Sciences (Boston, MA). Rosiglitazone was purchased from LKT Laboratories, Inc. (St. Paul, MN). The C-substituted DIMs were prepared in this laboratory as previously described (359, 393-395). The Gal4 reporter containing 5x Gal4 response elements (pGal4) was kindly provided by Dr. Marty Mayo (University of North Carolina, Chapel

Hill, NC). Gal4DBD-PPARγ construct was a gift of Dr. Jennifer L. Oberfield (GlaxoSmithKline Research and Development, Research Triangle Park, NC).

Transfection and luciferase assay

KU7 or 253JB-V33 cells (1 x 10^5 cells/well) were plated in 12-well plates in DMEM:Ham's F-12 media supplemented with 2.5% charcoal-stripped FBS. After 16 hr, various amounts of DNA [*i.e.* pGal4 (0.4 µg), β-gal (0.04 µg), PPARγ-GAL4 (0.04 µg)] were transfected by Lipofectamine (Invitrogen) according to the manufacturer's protocol. After 5 hr, the transfection mix was replaced with complete media containing either vehicle (DMSO) or the indicated ligand for 20 to 22 hr. Cells were then lysed with 100 µL of 1x reporter lysis buffer, and cell extracts (30 µL) were used for luciferase and β-gal assays. A Lumicount luminometer (PerkinElmer Life and Analytical Sciences) was used to quantitate luciferase and β-gal activities, and the luciferase activities were normalized to β-gal activity.

Cell proliferation assay

The bladder cancer cells (2 x 10^4/well) were plated in 12-well plates and allowed to attach for 24 hr. The medium was changed to DMEM:Ham's F-12 media containing 2.5% charcoal-stripped FBS and either vehicle (DMSO) or the indicated compounds were added. Fresh media and compounds were added every 48 hr, and cells were then trypsinized and counted after 96 and 144 hr using a Coulter Z1 cell counter. Each experiment was determined in triplicate, and results are expressed as means ± SE for each determination.

Western blot analysis

The bladder cells cells were seeded in DMEM:Ham's F-12 media containing 2.5% charcoal-stripped FBS for 24 h and treated with either the vehicle (DMSO) or the compounds for different times as indicated. Cells were collected by scraping in 150 µL high salt lysis buffer (50 mM HEPES, 0.5 M NaCl, 1.5mM $MgCl_2$, 1 mM EGTA, 10% (v/v) glycerol, 1% (v/v) Triton-X-100 and 5 µL/ml of Protease Inhibitor Cocktail (Sigma). The lysates were incubated on ice for 1 hr with intermittent vortexing followed by centrifugation at 40,000 *g* for 10 min at 4°C. Samples were boiled for 3 min at 100°C prior to electrophoresis, protein concentrations were determined, and 60 µg protein applied per lane. Samples were subjected to SDS-PAGE on 10% gel at 120 V for 3 to 4 hr. Proteins were transferred onto polyvinylidene membranes (PVDF; Bio-Rad, Hercules, CA) by semidry electroblotting in a buffer containing 25 mM Tris, 192 mM glycine and 20% methanol for 1.5 hr at 180 mA. The membranes were blocked for 30 min with 5% TBST-Blotto (10 mM Tris-HCl, 150 mM NaCl (pH 8.0), 0.05% Triton X-100 and 5% non-fat dry milk) and incubated in fresh 5% TBST-Blotto with 1:1000 primary antibody overnight with gentle shaking at 4°C. After washing with TBST for 10 min, the PVDF membrane was incubated with secondary antibody (1:5000) in 5% TBST-Blotto for 90 min. The membrane was washed with TBST for 10 min and incubated with 10 ml of chemiluminiscence substrate (PerkinElmer Life Sciences) for 1.0 min and exposed to Kodak X-OMAT AR autoradiography film (Eastman Kodak, Rochester, NY).

Animal experiments

Male athymic BALB/c nude mice, 4-6 weeks old, were purchased from the Animal Production Area of the National Cancer Institute, Frederick Cancer Research Facility (Frederick, MD). The mice were housed in laminar flow cabinets under specific pathogen-free conditions. Animals were maintained in facilities approved by the American Association for Accreditation of Laboratory Animal Care and in accordance with current regulations and standards of the United States Department of Agriculture, Department of Health and Human Services, and NIH. Mice were acclimatized for 2 weeks and their use in these experiments was approved by the M. D. Anderson Cancer Center Institutional Animal Care and Use Committee. We implanted the highly tumorigenic human cell carcinoma cell line, KU7 (1 million cells/injection), into the subcutis of athymic nude mice for the heterotopic xenograft experiment and into the bladder wall for the orthotpic xenograft experiment. One week later, mice were treated (10 per treatment group) with placebo or DIM-C-pPhCF$_3$ (60 mg/kg/dose on days 1, 3 and 5). Treatment was continued for 4 weeks, then the animals were sacrificed. Tumor volumes were measured and tumor kinetics were established in the various groups. Apoptosis and proliferation were subsequently evaluated in tumor sections using immunohistochemical techniques.

Immunohistochemistry

For immunohistochemical (IHC) analysis, frozen tissue sections (8 μm thick) were fixed with cold acetone, chloroform/acetone, and acetone. Tissue sections (5 μm thick) of formalin-fixed, paraffin-embedded specimens were deparaffinized in xylene

followed by treatment with a graded series of alcohol [100%, 95%, and 80% ethanol/double-distilled H_2O (v/v)] and rehydrated in PBS (pH 7.5). Antigen retrieval for paraffin-embedded tissues was performed with pepsin (Biomeda, Foster City, CA) for 15 min at 37°C. Endogenous peroxidase was blocked by the use of 3% hydrogen peroxide in PBS for 10 min. The samples were washed thrice with PBS and incubated for 20 min at room temperature with a protein blocking solution containing 5% normal horse serum and 1% normal goat serum in PBS (pH 7.5). Excess blocking solution was drained, and the samples were incubated for 18 hr at 4°C with one of the following: a 1:100 dilution of mouse monoclonal anti-PCNA antibody (DAKO, Carpinteria, CA); or 1:100 dilution of caveolin-1 antibody. The samples were then rinsed four times with PBS and incubated for 60 min at room temperature with the appropriate dilution of the secondary antimouse IgG (Jackson ImmunoResearch Laboratory). The slides were rinsed with PBS and incubated for 5 min with diaminobenzidine (Research Genetics). The sections were then washed with PBS (3X), counterstained with Gill's hematoxylin (Biogenex Laboratories, San Ramon, CA), and again washed with PBS (3X). The slides were mounted using a water and alcohol-based mounting medium (Universal mount, Research Genetics).

TUNEL assay

Frozen tissue sections fixed and treated as above were washed with PBS containing 0.1% Brij (v/v). Terminal deoxynucleotidyl transferase (Tdt)-mediated nick end labeling (TUNEL) was performed using a commercial kit (Promega, Madison, WI) according to the manufacturer's instructions with the following modifications. Samples

were fixed with 4% paraformaldehyde (methanol-free) for 10 min at room temperature, washed with PBS, and permeabilized by incubating with 0.2% Triton X-100 in PBS (v/v) for 15 min. The samples were incubated with equilibration buffer (from the kit). Reaction buffer containing equilibration buffer (45 µL), nucleotide mix (5 µL), and Tdt (1 µL) was added to the sections and incubated in a humidified chamber for 1 hr at 37°C protected from light. The reaction was terminated by immersing the samples in 2x SSC [30 mM NaCl, 3 mM sodium citrate (pH 7.2)] for 15 min followed by three washes to remove unincorporated fluorescein-dUTP. Background reactivity was determined by processing the slides in the absence of Tdt (negative control). Nuclei were stained with PI (1 µg/mL) for 10 min. Fluorescent bleaching was minimized with an enhancing reagent (Prolong; Molecular Probes, Eugene, OR). Immunofluorescence microscopy was performed using a Zeiss Plan-Neofluar lens on an epifluorescence microscope equipped with narrow bandpass excitation filters mounted in a filter wheel (Ludl Electronic Products, Hawthorne, NY) to individually select for green, red, and blue fluorescence. Images were captured using a cooled CCD camera (Photometrics, Tucson, AZ). DNA fragmentation was detected by localized green fluorescence within the nucleus of apoptotic cells.

Quantification of cell proliferation and apoptosis in in vivo *tissue samples*

Cell proliferation and apoptosis were determined by IHC of tissue sections with anti-PCNA antibodies and TUNEL assay. The tissue was photographed using a cooled CCD Optotronics Tec 470 camera linked to a computer and digital printer. The intensity of the immunostaining was quantified in five different areas of each sample by an image

analyzer using Optimas image analysis software program (Media Cybernetics) to obtain an average measurement. The density of proliferative cells and apoptotic cells was expressed as an average number of the five highest areas identified within a single x200 field.

Statistical analyses

Statistical analysis was performed using SPSS (SPSS Inc., Chicago, IL) and Instat3 (San Diego, CA) software. For *in vitro* data, analysis of variance was performed, and *t*-tests with the Bonferroni correction were used to evaluate for significant differences between the treated cells at each drug concentration and untreated control cells. Tumor weights as well as expression intensities of TUNEL and PCNA counts were compared by unpaired Student's *t*-test. For the primary end point of tumor size the sample size of 10 mice/treatment group were expected to have >90% power to detect a minimum difference of 24 mm^3 in tumor size at a statistical significance level of 0.05%. Statistical significance for this study was set at two-sided p < 0.05.

Results

Decreased cell survival and activation of PPARγ

The effects of PPARγ-active C-DIMs and rosiglitazone, a widely used TZD on survival of KU7 and 253JB-V33 bladder cancer cell lines was investigated. Results in Figure 3.1 illustrate the survival of KU7 cells after treatment with solvent (DMSO; set at 100% survival), 1 - 10 μM rosiglitazone DIM-C-pPhCF$_3$, DIM-C-pPhtBu and DIM-C-pPhC$_6$H$_5$ for 48 hr. Decreased survival of cells treated with rosiglitazone was not observed at the highest concentration (10 μM), whereas 1, 5 and 10 μM concentrations

of the PPARγ-active C-DIMs significantly decreased cell survival. Moreover, 10 µM of the C-DIM compounds also induced cell death after treatment for 48 hr since the number of cells remaining was lower than the initial number of seeded cells (day 0). We also examined KU7 cell survival after 96 and 144 hr and the results were similar to those observed after 48 hr; 10 µM rosiglitazone also decreased (10 - 25%) cell survival at the longer time points (Fig. 3.1).   We also examined the comparative effects of rosiglitazone, DIM-C-pPhCF$_3$, DIM-C-pPhtBu and DIM-C-pPhC$_6$H$_5$ on 253JB-V33 cell survival, and the results after treatment for 48 hr are summarized in Figure 3.2. Rosiglitazone at the highest concentration exhibited minimal effects on cell survival, whereas 5 and 10 µM of the C-DIM compounds significantly decreased cell survival and, after 96 or 144 hr, both concentrations also induced cell death. Based on their cell growth curves, the IC$_{50}$ values for growth inhibition by the PPARγ-active C-DIMs ranged between 5- 10 and 1 - 5 µM in KU7 and 253JB-V33 cells, respectively, and the IC$_{50}$ value for rosiglitazone was > 10 µM in both cell lines.

KU7
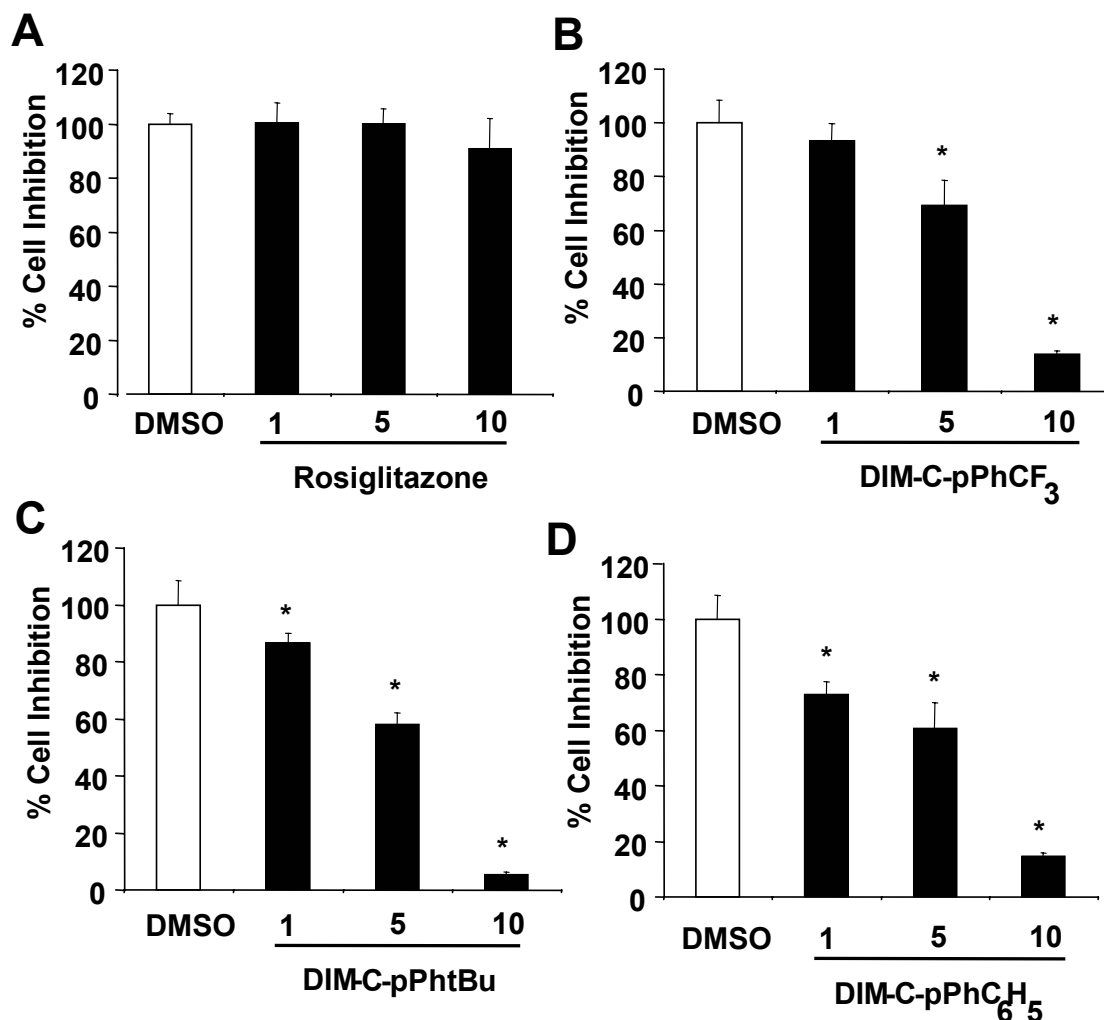
Fig. 3.1. KU7 cell survival curves. KU7 cells were treated with DMSO and different concentrations of [A] rosiglitazone, [B] DIM-C-pPhCF$_3$, [C] DIM-C-pPhtBu, and [D] DIM-C-pPhC$_6$H$_5$ for 48 hr, and the percent survival was determined as described in the Materials and Methods. The number of cells in the DMSO treatment group was set at 100%. Results are expressed as means $\pm$ SE for three replicate treatments for each concentration and significantly ($p < 0.05$) decreased cell survival is indicated by an asterisk. Ten μM concentrations of the C-DIM compounds significantly ($p < 0.05$) induced cell death [i.e. the number of cells in the treatment groups were lower than the original number of seed cells (at time 0)].

253JB-V
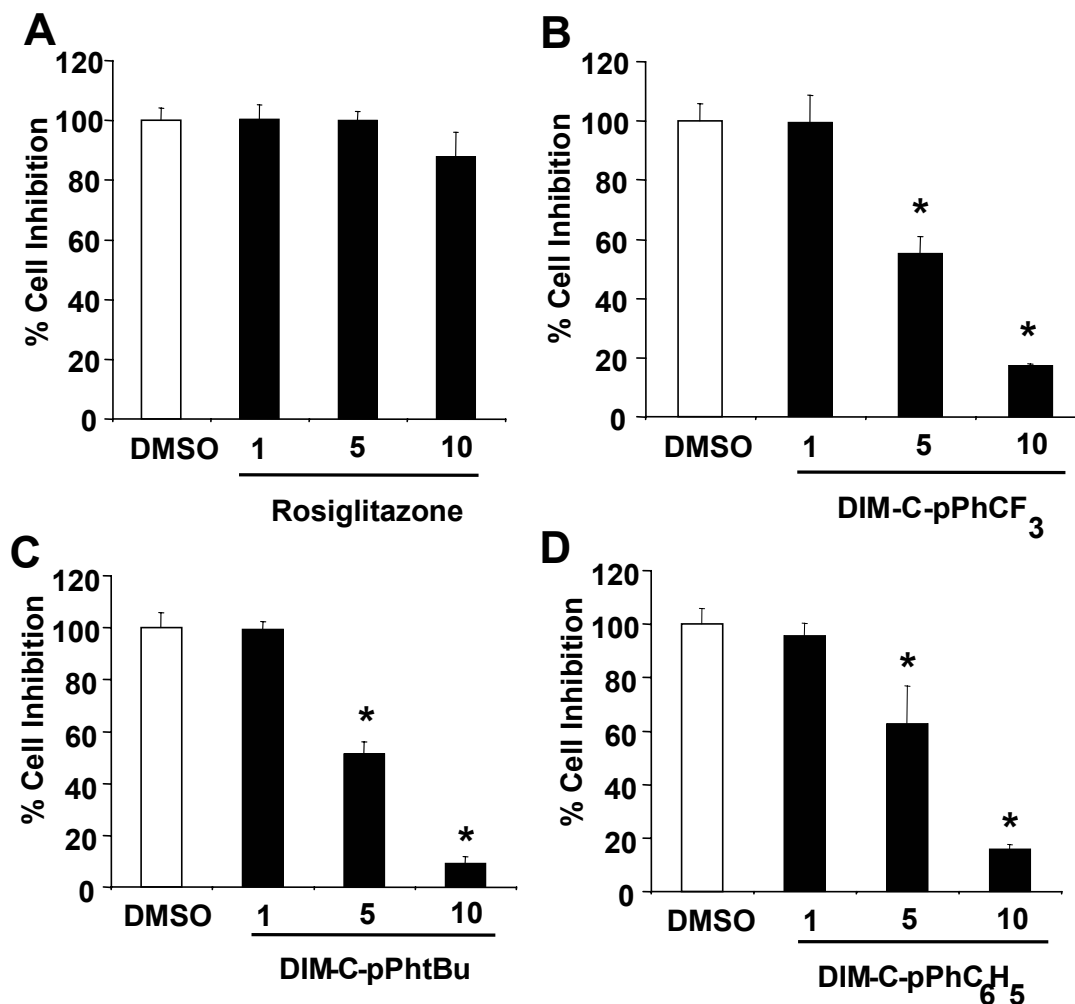
Fig. 3.2. 253JB-V33 survival curves. 253JB-V33 cells were treated with DMSO and 1, 5 or 10 μM [A] rosiglitazone, [B] DIM-C-pPhCF$_3$, [C] DIM-C-pPhtBu, and [D] DIM-C-pPhC$_6$H$_5$ for 48 hr, and percent survival of cells in the treated groups [relative to DMSO (100%)] was determined as described in the Materials and Methods. Results are expressed as means ± SE for three replicate determinations for each treatment group, and significantly (p < 0.05) decreased cell survival is indicated by an asterisk. After 48 hr, cell death was observed for 10 μM concentrations of the C-DIMs and, after 144 hr, 5 μM concentrations also induced death.

We also examined PPARγ activation in both cancer cell lines treated with DMSO, rosiglitazone or the C-DIMs and transfected with the GAL4-PPARγ/GAL4-luc constructs. The results in KU7 cells show that rosiglitazone and the C-DIMs caused a concentration-dependent increase in transactivation (Fig. 3.3A). These compounds also induced transactivation in 253JB-V33 cells (Fig. 3.3B) and the fold-induction was higher for rosiglitazone compared to the C-DIMs. A concentration-dependent response was not observed for the latter compounds, and this may be due, in part, to their potent growth inhibitory effects at 5 and 10 µM concentrations in 253JB-V33 cells (Fig. 3.2).

Effects of rosiglitazone and C-DIMs on cell cycle proteins and caveolin-1

In some cancer cell lines, PPARγ agonists modulate genes/proteins involved in G_0/G_1 to S cell cycle progression, and results in Figure 3.4A summarize the effects of rosiglitazone and C-DIMs on cyclin D1 (CD1), p27 and p21 expression in KU7 cells (Sp1 serves as a loading control). CD1 and p27 levels were unaffected by the treatment, whereas increased expression of p21 protein was concentration-independent. In contrast, the C-DIM compounds but not rosiglitazone induced p21 expression in 253JB-V33 cells (Fig. 3.4B), whereas CD1 and p27 were unaffected by the treatments. The upregulation of p21 expression in 253JB-V33 cells by the C-DIMs has previously been reported for the same compounds in Panc-28 cells (394) and is consistent with their growth-inhibitory effects (Fig. 3.2). Previous studies in several colon cancer cell lines related the growth inhibitory effects of C-DIMs to the induction of caveolin-1 (393) which has been shown to inhibit growth of some colon cancer cells. The effects of rosiglitazone and the PPARγ-active C-DIMs on caveolin-1 expression were further
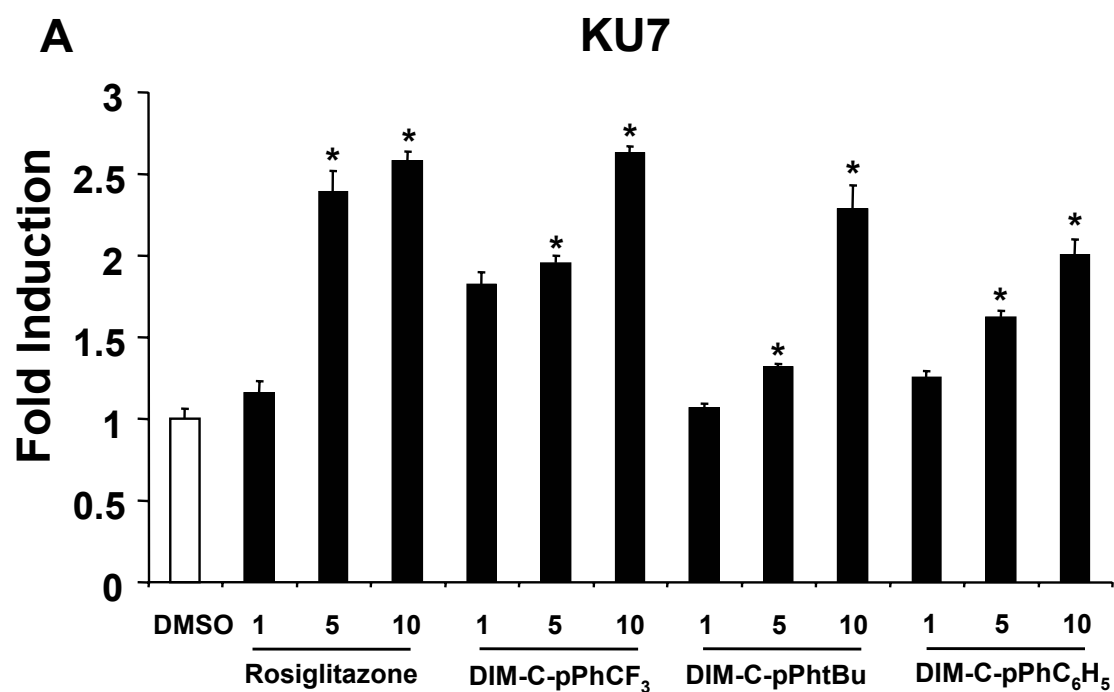
Fig 3.3. Activation of PPARγ-GAL4/pGAL4 by C-DIM compounds and rosiglitazone. [A] KU7 and [B] 253JB-V33 bladder cancer cells were transfected with PPARγ-GAL4/pGAL4, treated with DMSO or different concentrations of the test compounds, and luciferase determined as described in the Materials and Methods. Results are expressed as means ± SE for at least three replicate determinations for each treatment group and significant ($p < 0.05$) induction is indicated by an asterisk.
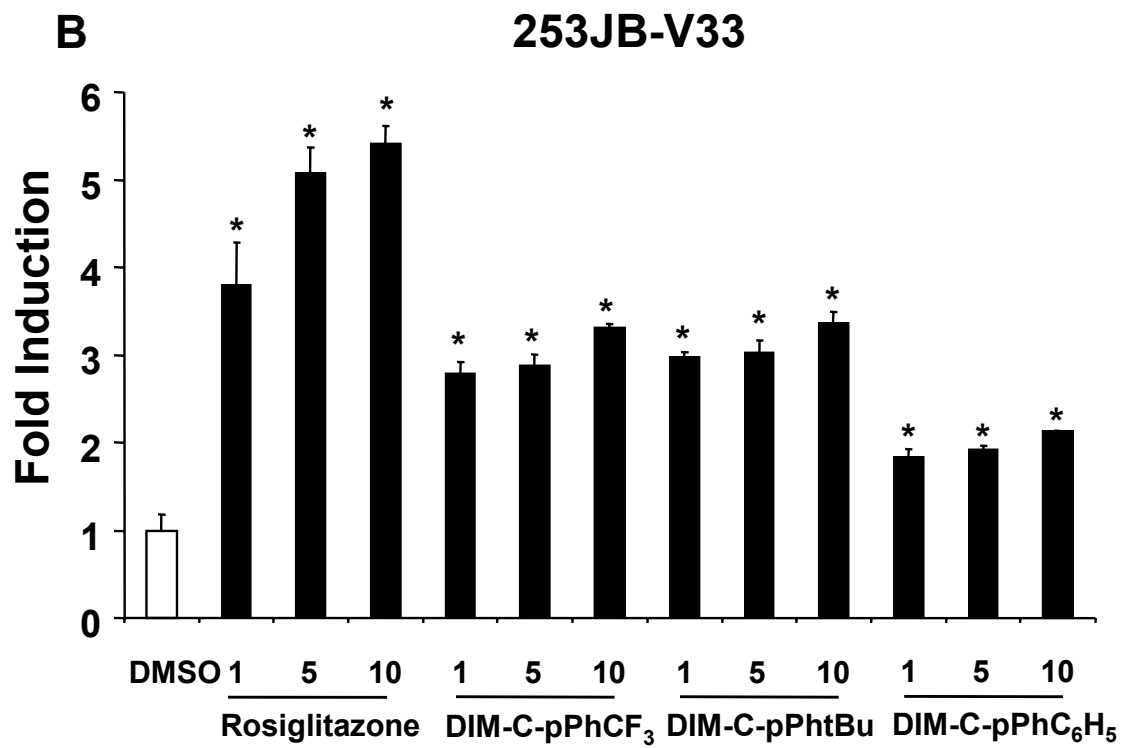
Figure 3.3 Continued
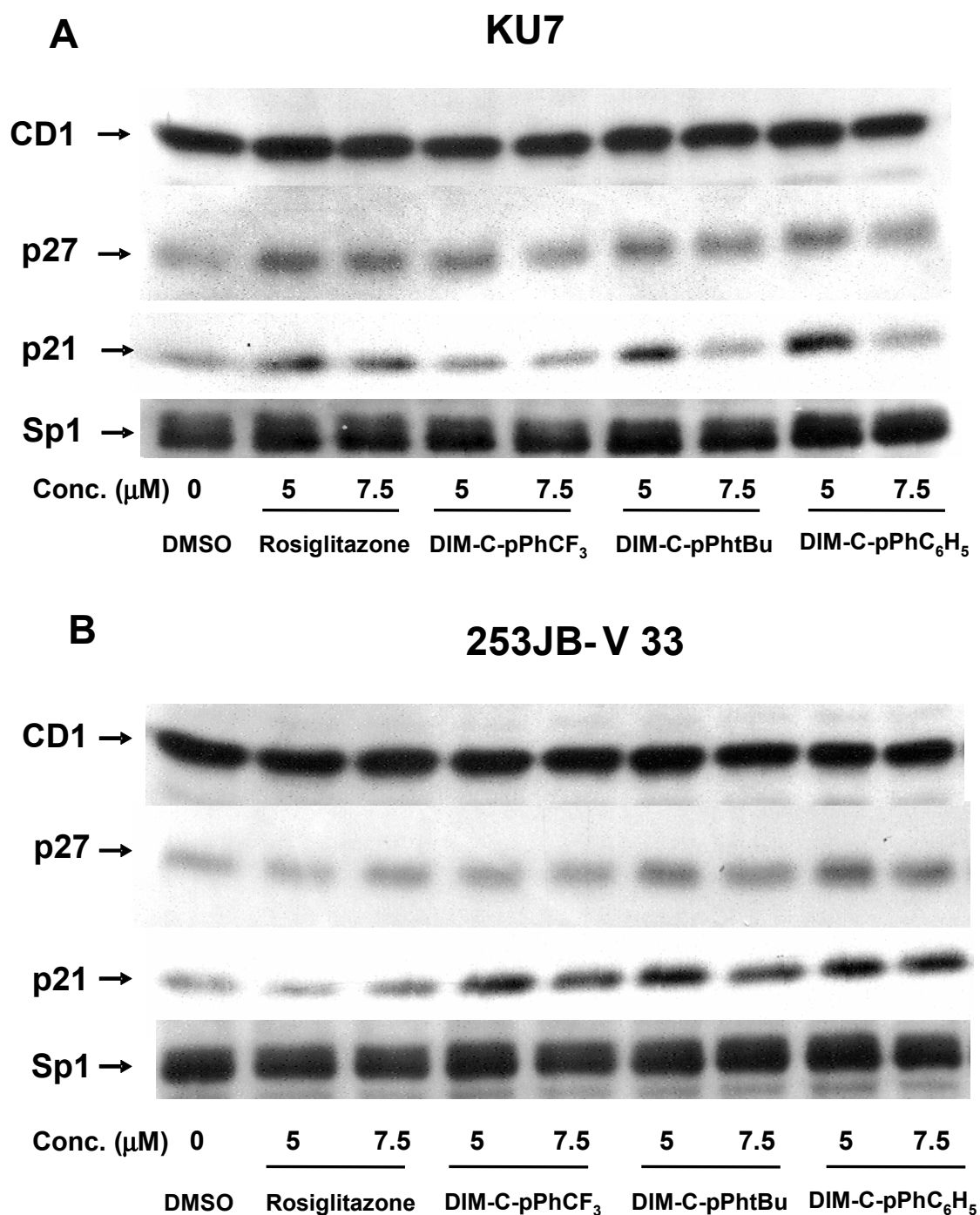
Fig. 3.4. Effects of C-DIM compounds on cell cycle protein expression. [A] KU7 and [B] 253JB-V33 cells were treated with DMSO or 5.0 and 7.5 µM of the PPARγ-active C-DIMs and rosiglitazone for 24 hr. Whole cell lysates were analyzed in a Western blot assay as described in the Materials and Methods. Sp1 protein serves as a loading control.

investigated in KU7 (Fig. 3.5A) and 253JB-V33 (Fig. 3.5B) cells. The C-DIM compounds (but not rosiglitazone) induced approximately a 3- to 4-fold increase in caveolin-1 protein expression, and this was comparable to the response induced in colon cancer cells (393). In contrast, constitutive caveolin-1 protein expression was relatively high in 253-JB-V33 cells and neither rosiglitazone or C-DIMs significantly enhanced levels of this protein. The role of PPARγ in mediating induction of caveolin-1 was investigated in KU7 cells treated with 5 and 7.5 μM DIM-C-pPhCF$_3$ alone or in combination with the PPARγ antagonist GW9662 (Fig. 3.5C). The results show that induction of caveolin-1 by PPARγ-active C-DIMs was inhibited after cotreatment with GW9662, and these results are similar to those observed in colon cancer cells (393). There is also evidence that the PPARγ-active compounds including C-DIMs enhance phosphatidylinsositol-3-kinase (PI3-K) activity in colon cancer cell lines [(396) and unpublished observations], and the results in Figure 3.5C confirm that DIM-C-pPhCF$_3$ and DIM-C-pPhC$_6$H$_5$ also induced PI3-K-dependent phosphorylation of Akt. The compounds did not affect Akt protein. Thus, PPARγ-active C-DIMs decreased survival of KU7 and 253-JB-V33 cells and this correlated with increased expression of caveolin-1 and p21, respectively, in these cell lines. These results are another example of the cancer cell context-dependent differences in the growth inhibitory pathways induced by C-DIMs and other PPARγ agonists.

A   **KU7**

Cav-1 →

Sp1 →

Conc (μM)	0	5	7.5	5	7.5	5	7.5	5	7.5
	DMSO	Rosiglitazone		DIM-C-pPhCF$_3$		DIM-C-pPhtBu		DIM-C-pPhC$_6$H$_5$	
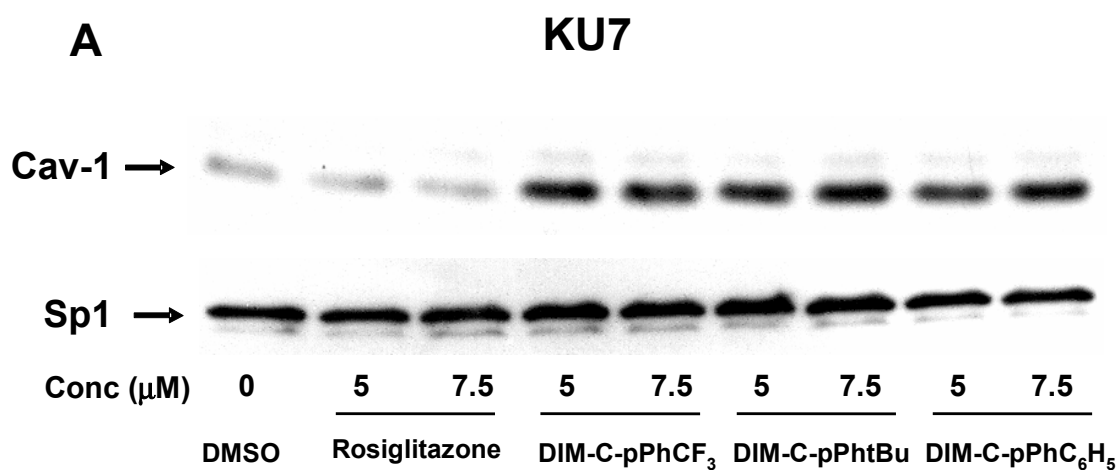
Fig. 3.5. Induction of caveolin-1 by C-DIM compounds. [A] KU7 and [B] 253JB-V33 cells were treated with DMSO or 5.0 and 7.5 μM PPARγ-active C-DIMs and rosiglitazone for 72 hr. Whole cell lysates were analyzed for caveolin-1 in a Western blot assay as described in the Materials and Methods. Sp1 protein served as loading control. [C] Effects of the PPARγ agonist GW9662. KU7 cells were treated with DIM-C-pPhCF$_3$ or DIM-C-pPhC$_6$H$_5$ alone or in combination with 10 μM GW9662 and analyzed in a Western blot assay for caveolin-1, Akt, phospho-Akt (pAkt) and β-actin (loading control) as described in the Materials and Methods.

B   **253JB-V33**

Cav-1 →

Sp1 →

Conc (μM)	0	5	7.5	5	7.5	5	7.5	5	7.5
	DMSO	Rosiglitazone		DIM-C-pPhCF₃		DIM-C-pPhtBu		DIM-C-pPhC₆H₅	

C

DIM-C-pPhCF$_3$ (μM)	-	-	5	5	7.5	7.5	-	-	-	-
DIM-C-pPhC$_6$H$_5$ (μM)	-	-	-	-	-	-	5	5	7.5	7.5
GW9662 (μM)	-	10	-	10	-	10	-	10	-	10

Cav-1 →

β-Actin →

pAkt →

Akt →
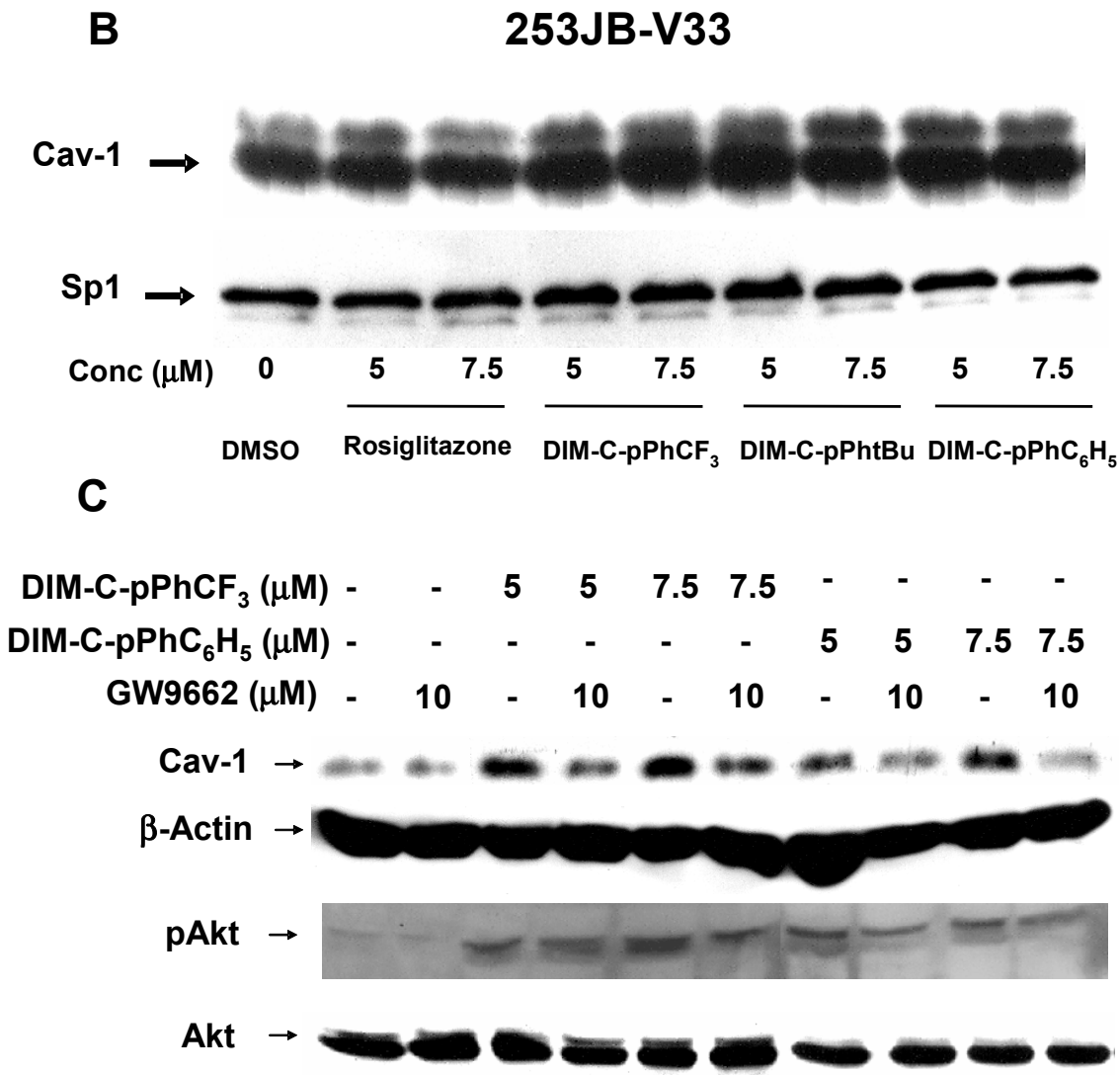
Fig. 3.5 Continued

Effects of PPARγ-active C-DIMs on bladder tumor growth in vivo

To confirm whether our *in vitro* data are comparable in an *in vivo* model for bladder cancer, the human UC cell line KU7 was implanted into the orthotopic bladders of athymic nude mice. To establish tumor kinetics, another *in vivo* experiment was bladder cancer, the human UC cell line KU7 was implanted into the orthotopic bladders of athymic nude mice. To establish tumor kinetics, another *in vivo* experiment was performed using subcutaneously implanted tumors. No toxicity was seen in mice treated with DIM-C-pPhCF$_3$ as demonstrated by weighing the mice. Tumor growth was substantially inhibited with DIM-C-pPhCF$_3$ compared with controls in both orthotopic and subcutaneous tumors (Fig. 3.6A). *In vivo*, growth of orthotopic and subcutaneous tumors was significantly inhibited by DIM-C-pPhCF$_3$ (32% and 60% growth inhibtion) when compared to control. Mean tumor weights of mice in control and DIM-C-pPhCF$_3$-treated groups were 265 mg and 191 mg in the orthotopic model compared with 997 mg and 398 mg in the s.c.model, respectively. DIM-C-pPhCF$_3$ significantly inhibited cell proliferation in both orthotopic and subcutaneous bladder tumors by 26% and 55%, respectively (Fig. 3.6B). However, tumors obtained from mice in the treatment group displayed low levels of apoptosis that were not appreciably different from those in controls. Furthermore, DIM-pPhCF$_3$ significantly induced expression of caveolin in both orthotopic and subcutaneous bladder tumors by 30% and 25%, respectively (Fig. 3.7) and these *in vivo* results complement *in vitro* studies (Fig. 3.5) which showed upregulation of caveolin-1 protein expression.
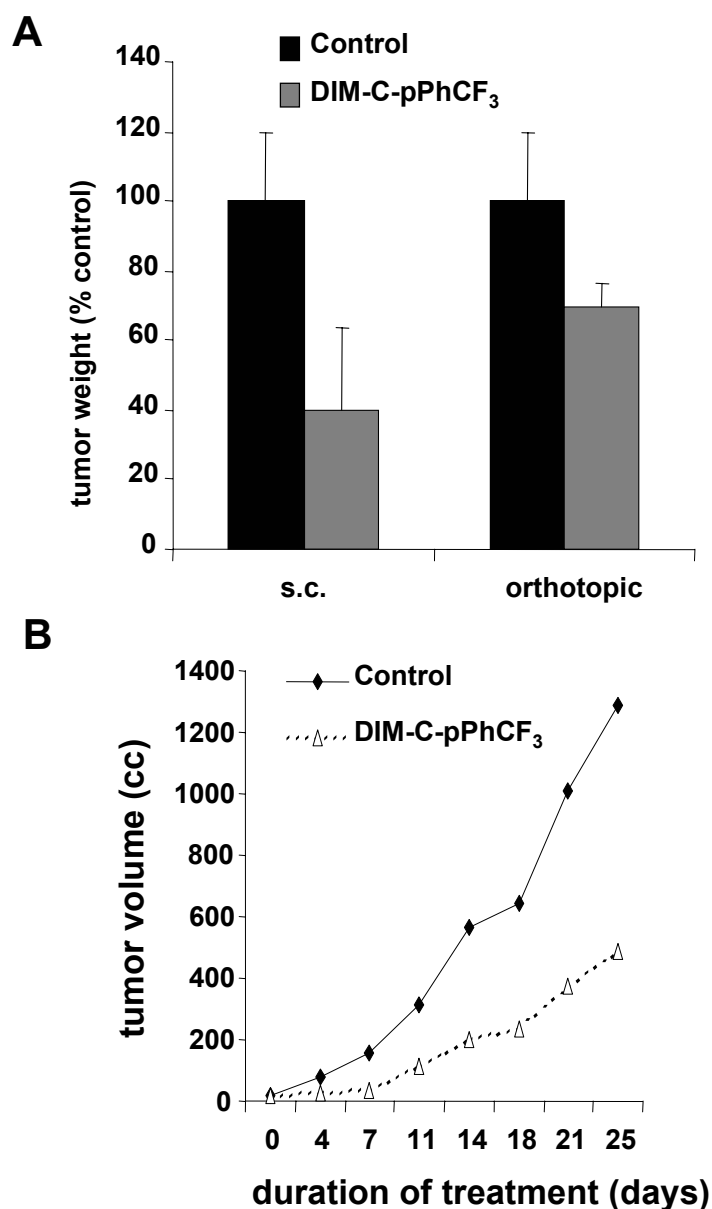
Fig. 3.6. DIM-C-pPhCF$_3$ inhibits bladder tumor growth. Inhibition of [A] orthotopic and [B] subcutaneous bladder tumor growth. KU7 cells (1×10^6 cells/injection) were administered to athymic nude mice via subcutaneous (sc) injection or by direct injection into the bladder wall as described in the Materials and Methods. Mice were administered DIM-C-pPhCF$_3$ (60 mg/kg) three times each week (days 1, 3 and 5) for 4 weeks. Tumor weights at the end of the treatment are summarized in [A] and tumor volumes in the subcutaneous group are given in [B]. [C] Proliferation index and apoptosis were determined as described in the Materials and Methods.

C

Fig. 3.6 Continued

113
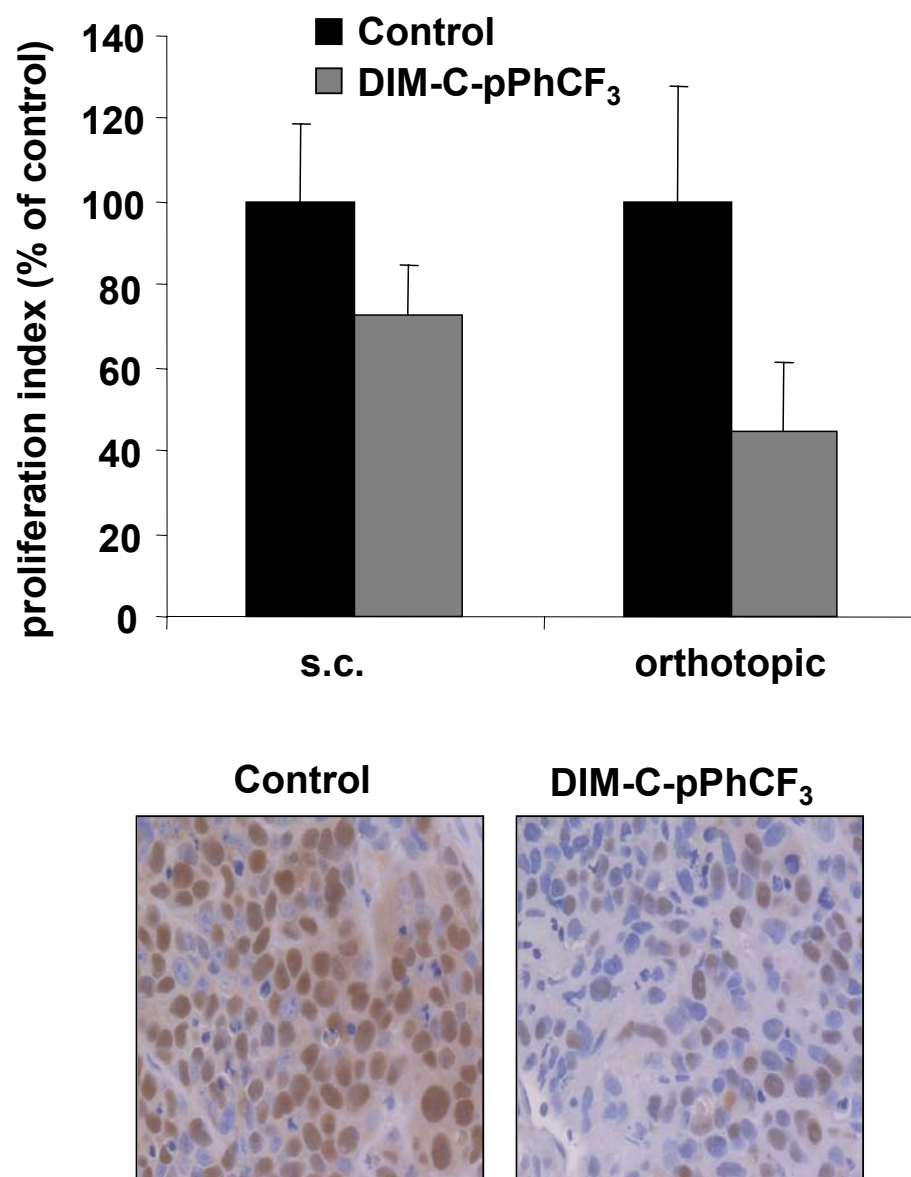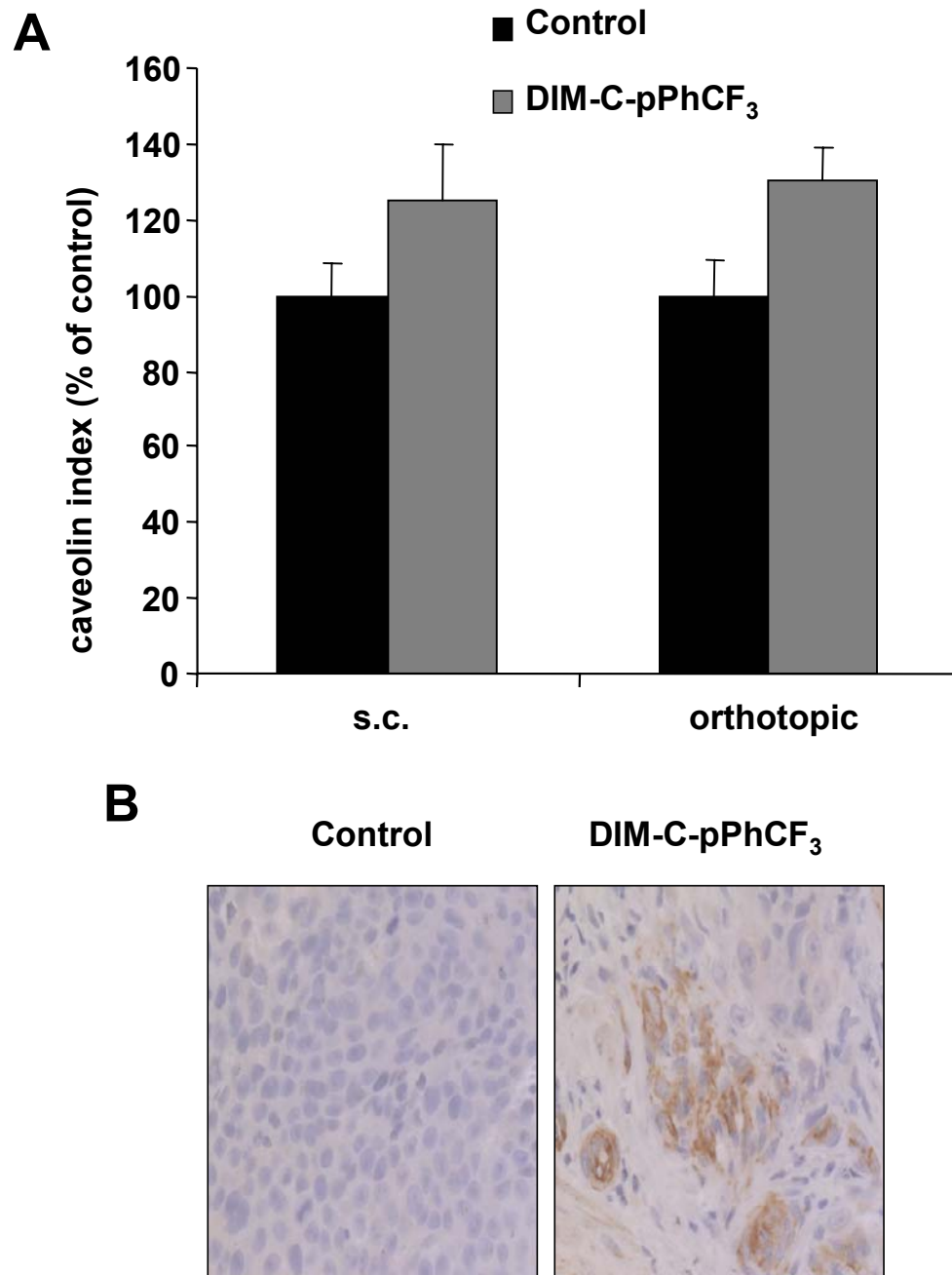
Fig. 3.7. Induction of caveolin-1 in bladder tumors by DIM-C-pPhCF$_3$. The caveolin-1 index [A] and immunostaining [B] of bladder tumors for caveolin-1 expression was determined as described in the Materials and Methods.

Discussion

The potential anticarcinogenic activities of different structural classes of PPARγ agonists have been investigated in various cancer cell lines *in vitro* and *in vivo* models (254, 359, 362-366, 391-395). PPARγ agonists induce genes and activities linked to differentiation, growth inhibition, and apoptosis; however, the induced responses are highly variable and dependent on ligand structure and cell context. Moreover, there is evidence that the effects induced by these compounds may be PPARγ-dependent or -independent. For example, the PPARγ agonists troglitazone and 15-deoxy$^{\Delta 12,14}$-prostaglandin J2 (PGJ2) induce the NSAID-activated gene (*NAG-1*) in HCT-116 colon cancer cells by receptor-independent and -dependent pathways, respectively (397). PPARγ-active C-DIMs induce p21 expression in Panc-28 but not other pancreatic cell lines, and this response was PPARγ-dependent. Rosiglitazone induced caveolin-1 in HT-29 colon cancer cells expressing wild-type PPARγ but not in HCT-15 cells which express a mutant (K422Q) form of this receptor (393). In contrast, PPARγ-active C-DIMs induce caveolin and other genes associated with differentiation in colon cancer cells expressing either wild-type or mutant PPARγ (393). A recent study showed that 2-cyano-3,12-diooxoolean-1,9-dien-oic acid (CDDO) and related PPARγ agonists also induced caveolin-1 in colon cancer cells and this was inhibited by PPARγ antagonists, whereas higher concentrations of CDDO induced apoptosis and this response was receptor independent (396).

Bladder cancer cells also overexpress PPARγ (386-389). One study showed that although PGJ2 and TZDs both decreased cell survival, there were significant differences in the responsiveness of bladder cancer cells to these compounds (389). For example, the IC_{50} value for growth inhibition by troglitazone and pioglitazone was > 50 μM in 253J bladder cancer cells; IC_{50} values in T24, RT4 and IT-1 cells were ≤ 30, 15 and 10 μM, respectively (389). Both PPARγ-active C-DIMs and rosiglitazone activated PPARγ (Fig. 3.3), and the C-DIMs decreased cell survival (Figs. 3.1 and 3.2) in KU7 and 253JB-V33 cells. KU7 cells were less responsive than 253JB-V33 cells to the growth inhibitory effects of ≤ 10 μM C-DIMs, whereas ≤ 10 μM rosiglitazone was relatively ineffective in both cell lines. Thus, as previously reported in colon cancer cells (393), PPARγ-active C-DIMs were more potent than rosiglitazone as inhibitors of bladder cancer cell growth.

The modulation of cell cycle genes (p21) associated with G_0/G_1 to S phase progress, and the induction of caveolin-1 have been linked to PPARγ-dependent inhibition of Panc-28 pancreatic and HT-29/HCT-15 colon cancer cell growth after treatment with C-DIMs (393, 394). Differences in activation of specific PPARγ-dependent "growth inhibitory" genes by C-DIMs in these cell lines was also observed 253JB-V33 and KU7 cells in which C-DIMs induced p21 and caveolin-1, respectively (Figs. 3.4 and 3.5). The reason for cell context-dependent regulation of p21 and caveolin-1 by C-DIM compounds is unknown; however, based on results of ongoing studies with colon cancer cells, the fold-induction of caveolin-1 is inversely related to

constitutive levels of this protein. Thus, high basal expression of caveolin-1 in 253JB-V33 cells (Fig. 3.5) may preclude further induction of this protein.

We further investigated the *in vivo* anticarcinogenic activity of DIM-C-pPhC$_6$H$_5$ and DIM-C-pPhCF$_3$ by implanting the highly tumorigenic KU7 cell line into the orthotopic bladder of athymic nude mice and also in a subcutaneous implant model using the same cell line. Both PPARγ agonists inhibited tumor growth in the orthotopic and subcutaneous implant models in athymic nude mice. DIM-C-pPhCF$_3$ significantly inhibited tumor growth in both models, whereas initial *in vivo* studies with DIM-C-pPhC$_6$H$_5$ were not completed due, in part, to formulation problems. We also demonstrated that for DIM-C-pPhCF$_3$ there was a significantly increased expression of caveolin-1 in the orthotopic (30%) and subcutaneous (25%) bladder cancer models, and these *in vivo* responses (Fig. 3.7) correlated with induced expression of caveolin-1 in KU7 cancer cells (Fig. 3.5A). Thus, PPARγ-active C-DIMs inhibit growth of bladder cancer cells *in vitro* and bladder tumors in both an orthotopic and subcutaneous *in vivo* mouse models. We also observed the somewhat paradoxical induction of PI3-K activity by PPARγ-active C-DIMs in KU7 cells (Fig. 3.5), and a previous study also showed that the triterpenoid PPARγ agonist CDDO also induced this kinase pathway in SW-480 colon cancer cells (396). Although PI3-K has been linked to cell survival pathways, increased PI3-K-dependent activity and caveolin-1 expression sensitizes HeLa and 293 cells to the cytotoxicity of arsenite and hydrogen peroxide (398) and L929 cells to tumor necrosis factor α-induced cell death (399). Thus, activation of PI3-K and induction of caveolin-1 expression may be an important element in the antitumorigenic activity of

PPARγ-active C-DIMs. Current studies are investigating other receptor-dependent and -

independent pathways responsible for the anticancer activities of these compounds, and

their application in the treatment of bladder and other cancers.

CHAPTER IV

1,1-BIS(3'-INDOLYL)-1-(*p*-SUBSTITUTEDPHENYL)METHANES ARE

PEROXISOME PROLIFERATOR-ACTIVATED RECEPTOR γ AGONISTS BUT

DECREASE HCT-116 COLON CANCER CELL SURVIVAL THROUGH

RECEPTOR-INDEPENDENT ACTIVATION OF EARLY GROWTH

RESPONSE-1 AND NAG-1*

Introduction

NSAID-activated gene-1 (NAG-1) is a transforming growth factor β (TGFβ)-like secreted protein and was initially characterized as a p53-regulated gene (400, 401). Overexpression of NAG-1 in breast cancer cells resulted in growth arrest and apoptosis, and similar results were also observed in colon cancer cells (401, 402). Baek, Eling and their coworkers have extensively investigated the induction of NAG-1 by several different structural classes of drugs and chemoprotective phytochemicals in HCT-116 colon and other cancer cell lines (303, 402-413). Chemicals that induce NAG-1 expression in cancer cell lines generally inhibit growth and/or induce apoptosis in these cells, and these effects are due, in part, to induction of NAG-1 protein. In addition to NSAIDs, other agents that induce NAG-1 include phorbol esters, cyclooxygenase

---

inhibitors, genistein, plant polyphenolics, diallyl disulfide, retinoids, indole-3-carbinol (I3C), diindolylmethane (DIM), and peroxisome proliferator-activated receptor γ (PPARγ) agonists (303, 402-413).

Several mechanisms of NAG-1 induction have been described and these are dependent not only on the structure or class of inducing agents but also on cell context. For example, diallyl disulfide and genistein are antitumorigenic components of garlic and soy, and their induction of NAG-1 in HCT-116 cells is p53-dependent (405, 407). In contrast, induction of NAG-1 by indole-3-carbinol and diindolylmethane (DIM), two anticarcinogenic components in cruciferous vegetables, is p53-independent in the same cell line (414). Two PPARγ agonists, 15-deoxy-$\Delta^{12,14}$-prostaglandin J2 (PGJ2) and troglitazone, also induce NAG-1 expression in HCT-116 cells, and the PPARγ antagonist 2-chloro-5-nitrobenzanilide (GW9662) inhibits the induction response by PGJ2 but not troglitazone (303). It was also shown that the PPARγ-independent activation of NAG-1 by troglitazone is due to induction of early growth response gene (Egr-1) which in turn activates NAG-1 (303, 397).

Recent studies in this laboratory have identified 1,1-bis-(3'-indolyl)-1-(p-substitutedphenyl)methanes [methylene-substituted DIMs (C-DIMs)] as PPARγ agonists, and the most active compounds contain p-trifluoromethyl (DIM-C-pPhCF$_3$), p-t-butyl (DIM-C-pPhtBu), and phenyl (DIM-C-pPhC$_6$H$_5$) (359, 393-395). These PPARγ agonists decrease survival and induce apoptosis in breast, leukemia, pancreatic and colon cancer cells. In the latter two cell lines, growth inhibition is associated with receptor-dependent activation of p21 (394) and the tumor suppressor gene caveolin-1 (393).

There is also evidence that decreased cancer cell survival induced by these compounds is also receptor-independent (359, 395). The PPARγ-active methylene-substituted diindolylmethanes (C-DIMs) also decrease cell survival and induce apoptosis in HCT-116 cells but do not induce caveolin-1, as previously reported in HT-29 and HCT-15 colon cancer cells (393). In contrast, these compounds induce NAG-1 in HCT-116 cells and this response is not inhibited by PPARγ antagonists. Like troglitazone, the PPARγ-active C-DIMs also induce Egr-1 which in turn interacts with proximal (GC-rich) Egr-1 motifs in the NAG-1 gene promoter. However, in contrast to troglitazone, the C-DIM compounds induce Egr-1 through a phosphatidylinositol-3-kinase (PI3K)-dependent pathway which in turn activates serum response elements in the Egr-1 promoter. This represents a novel pathway for induction of Egr-1 and NAG-1, and these responses contribute to the induction of growth inhibition and apoptosis by the PPARγ-active C-DIMs in colon cancer cells. Moreover, these results also distinguish the mode of action of these C-DIM analogs from that of troglitazone and DIM and identify an important PPARγ-independent mode of action.

Materials and Methods

Cell lines

HCT-116 (human colon carcinoma cell line) and LNCap (human prostate cancer cell line) were obtained from American Type Culture Collection (Manassas, VA). HCT-116 and LnCap cells were maintained in RPMI 1640 (Sigma-Aldrich, St. Louis, MO) supplemented with 0.22% sodium bicarbonate, 0.011% sodium pyruvate, 0.45% glucose,

0.24% HEPES, 10% FBS, and 10 mL/L of 100x antibiotic antimycotic solution (Sigma-Aldrich). Cells were maintained at 37°C in the presence of 5% CO_2.

Antibodies and reagents

Antibodies for poly(ADP-ribose) polymerase (sc-8007), cyclin D1 (sc-718), p27 (sc-528), phospho-Akt (sc-7985R), Akt (sc-8312) p53 (sc-126) and caveolin 1 (sc-894) were purchased from Santa Cruz Biotechnology (Santa Cruz, CA), NAG-1 from Upstate Biotechnology (Lake Placid, NY), and Egr-1 from Cell Signaling Technology, Inc. (Beverly, MA). Monoclonal β-actin antibody was purchased from Sigma-Aldrich. Reporter lysis buffer and luciferase reagent for luciferase studies were supplied by Promega (Madison, WI). β-Galactosidase (β-Gal) reagent was obtained from Tropix (Bedford, MA) and Lipofectamine reagent was purchased from Invitrogen (Carlsbad, CA). Western Lightning chemiluminescence reagent was from Perkin-Elmer Life Sciences (Boston, MA). Rosiglitazone was purchased from LKT Laboratories, Inc. (St. Paul, MN). The C-substituted DIMs were prepared in this laboratory as previously described (359, 393) and the Egr-1 constructs were kindly provided by Mr. C.-C. Chen and Mrs. W.-R. Lee (Texas A&M University).

Plasmids

The Gal4 reporter containing 5x Gal4 response elements (pGal4) was kindly provided by Dr. Marty Mayo (University of North Carolina, Chapel Hill, NC). Gal4DBD-PPARγ construct (gPPARγ) was a gift of Dr. Jennifer L. Oberfield (GlaxoSmithKline Research and Development, Research Triangle Park, NC). PPRE-luc construct contains three tandem PPREs with a minimal TATA sequence in pGL2 (359,

393). pNAG-1A - pNAG-1D, pNAG-1Dm1, pNAG-1Dm2 and pNAG-1Dm3 were generated previously (397, 403). pEGR-1A - pEGR-1E constructs containing Egr-1 promoter inserts have also previously been described (415).

Transfection and luciferase assay

HCT-116 cells (1×10^5 cells/well) were plated in 12-well plates in DMEM:Ham's F-12 media supplemented with 2.5% charcoal-stripped FBS. After 16 hr, various amounts of DNA [*i.e.* Gal4Luc (0.4 µg), β-gal (0.04 µg), PPRE-Luc (0.04 µg)] and 0.25 µg of the NAG-1/EGR-1 constructs were transfected by Lipofectamine (Invitrogen) according to the manufacturer's protocol. Five hours after transfection, the transfection mix was replaced with complete media containing either vehicle (DMSO) or the indicated ligand for 20 to 22 hr. Cells were then lysed with 100 µL of 1x reporter lysis buffer, and 30 µL of cell extract were used for luciferase and β-gal assays. A Lumicount luminometer (PerkinElmer Life and Analytical Sciences) was used to quantitate luciferase and β-gal activities, and the luciferase activities were normalized to β-gal activity.

Cell proliferation assay

HCT-116 cells (2×10^4/well) were plated in 12-well plates. After cell attachment for 24 hr, the medium was changed to DMEM:Ham's F-12 media containing 2.5% charcoal-stripped FBS and either vehicle (DMSO) or the indicated compound. Fresh media and compounds were added every 48 hr, and the cells were then trypsinized and counted at the indicated times using a Coulter Z1 cell counter. Each experiment was done in triplicate, and results are expressed as means ± SE for each determination.

Western blot analysis

HCT-116 cells were seeded in DMEM:Ham's F-12 media containing 2.5% charcoal-stripped FBS for 24 h and then treated with either the vehicle (DMSO) or the compounds for different times as indicated. Cells were collected by scraping in 150 μL high salt lysis buffer (50 mM HEPES, 0.5 M NaCl, 1.5mM $MgCl_2$, 1 mM EGTA, 10% (v/v) glycerol, 1% (v/v) Triton-X-100 and 5 μL/ml of Protease Inhibitor Cocktail (Sigma). The lysates were incubated on ice for 1 hr with intermittent vortexing followed by centrifugation at 40,000 *g* for 10 min at 4°C. Before electrophoresis, the samples were boiled for 3 min at 100°C, the amounts of protein was determined and 60 μg protein applied per lane. Samples were subjected to SDS-PAGE on 10% gel at 120 V for 3 to 4 hr. Proteins were transferred onto polyvinylidene membranes (PVDF; Bio-Rad, Hercules, CA) by semidry electroblotting in a buffer containing 25 mM Tris, 192 mM glycine and 20% methanol for 1.5 hr at 180 mA. The membranes were blocked for 30 min with 5% TBST-Blotto (10 mM Tris-HCl, 150 mM NaCl (pH 8.0), 0.05% Triton X-100 and 5% non-fat dry milk) and incubated in fresh 5% TBST-Blotto with 1:1000 (for caveolin 1, p27 and cyclin D1), 1:250 (for PARP), 1:500 (for NAG-1 and Egr-1), 1:5000 (for β-actin) primary antibody overnight with gentle shaking at 4°C. After washing with TBST for 10 min, the PVDF membrane was incubated with secondary antibody (1:5000) in 5% TBST-Blotto for 90 min. The membrane was washed with TBST for 10 min and incubated with 10 ml of chemiluminiscence substrate (PerkinElmer Life Sciences) for 1.0 min and exposed to Kodak X-OMAT AR autoradiography film (Eastman Kodak, Rochester, NY).

Chromatin immunoprecipitation (ChIP) assay

HCT-116 cells (2×10^7) were treated with Me_2SO (time 0), or DIM-C-pPhC$_6$H$_5$ (20 μM) for 1 or 2 hr. Cells were then fixed with 1.5% formaldehyde, and the cross-linking reaction was stopped by addition of 0.125 M glycine. After washing twice with phosphate-buffered saline, cells were scraped and pelleted. Collected cells were hypotonically lysed, and nuclei were collected. Nuclei were then sonicated to desired chromatin length (~500 bp). The chromatin was pre-cleared twice by addition of protein A-conjugated beads (PIERCE), and then incubated at 4°C for 1 hr with gentle agitation. The beads were pelleted, and the pre-cleared chromatin supernatants were immunoprecipitated with antibodies specific to IgG, Sp1, Sp3, Sp4 (Santa Cruz Biotechnology), and Egr-1 (Cell Signaling Technology) at 4°C overnight. Protein-antibody complexes were collected by addition of protein A-conjugated beads at room temperature for 1 hr. Beads were extensively washed; the protein-DNA crosslinks were eluted and reversed. DNA was purified by phenol extraction/ethanol precipitation followed by PCR amplification. The NAG-1 primers are: 5' - TAC TGA GGC CCA GAA ATG TG - 3' (forward), and 5' - GAG CTG GGA CTG ACC AGA TG - 3' (reverse). These primers amplify a 211-bp region of the human NAG-1 promoter containing two Sp1/Egr-1 binding sites. The positive control primers are: 5' - TAC TAG CGG TTT TAC GGG CG - 3' (forward), and 5' - TCG AAC AGG AGG AGC AGA GAG CGA - 3' (reverse), which amplify a 167-bp region of human glyceraldehydes-3-phosphate dehydrogenase (GAPDH) gene. The negative control primers are: 5' - ATG GTT GCC ACT GGG GAT CT - 3' (forward), and 5' - TGC

CAA AGC CTA GGG GAA GA - 3' (reverse), which amplify a 174-bp region of human CNAP1 exon. PCR products were resolved on a 2% agarose gel in the presence of 1:10 000 SYBR gold (Molecular Probes, Eugene, OR).

Statistical analysis

Statistical significance was determined by analysis of variance and Scheffe's test, and the levels of probability are noted. The results are expressed as means ± SE for at least three separate (replicate) experiments for each treatment.

Results

Studies in this laboratory have characterized selected C-DIMs as PPARγ agonists that inhibit growth of colon and other cancer cell lines through receptor-dependent and -independent pathways (359, 393-395). Results illustrated in Figure 4.1 show that three PPARγ-active C-DIM compounds, namely DIM-C-pPhCF$_3$, DIM-C-pPhtBu and DIM-C-pPhC$_6$H$_5$, decreased HCT-116 colon cancer cell survival at concentrations of 1 - 10 μM after treatment for 48 or 96 hr. Treatment for 96 hr resulted in cell death using 10 μM concentrations (i.e. cell numbers were lower than the initial number of seeded cells). In contrast, 10 μM rosiglitazone decreased cell survival but did not induce cell death, which is observed only at higher concentrations of this compound. Previous studies in colon cancer cells show that PPARγ-active C-DIMs induced transactivation in cells transfected with PPRE-luc or GAL4-PPRγ/pGAL4-luc constructs (393). In HCT-116 cells, PPARγ-active C-DIMs induced a concentration-dependent increase in transactivation in cells transfected with PPRE-luc, and 10 μM rosiglitazone also increased activity but with lower fold-inducibility (Fig. 4.2A). The same compounds

also induced transactivation in HCT-116 cells transfected with GAL4-PPARγ/GAL4-luc constructs and treated with 5 and 10 μM of the C-DIMs, and cotreatment with the PPARγ antagonist GW9662 significantly inhibited this response (Fig. 4.2B). These results confirm that PPARγ-active C-DIMs induce receptor-dependent transactivation in HCT-116 cells, and this complements results of recent studies that show similar response in HT-29 and HCT-15 colon cancer cell lines (393). Treatment of HCT-116 cells for 24 hr with 2.5, 5.0 and 7.5 μM DIM-C-pPhCF$_3$, DIM-C-pPhtBu or DIM-C-pPhC$_6$H$_5$ did not affect expression of cyclin D1 or p27 proteins (Fig. 4.3A). PPARγ agonists frequently affect expression of these proteins in other cancer cell lines (255, 361, 390, 391, 394, 416, 417); however, the results (Fig. 4.3A) are comparable to those observed for the same compounds in HT-29 and HCT-15 cells (393). The growth inhibitory effects of these compounds in HT-29 and HCT-15 cells are associated with receptor-dependent activation of the tumor suppressor gene caveolin-1 (393) which inhibits colon cancer cell growth. However, in HCT-116 cells, treatment with 5, 10 or 15 μM DIM-C-pPhCF$_3$ or DIM-C-pPhC$_6$H$_5$ for 72 hr did not affect caveolin-1 protein expression (Fig. 4.3B). Moreover, unlike HT-29 and HCT-15 cells, relatively high levels of caveolin-1 were detected in solvent (DMSO)-treated HCT-116 cells. Other PPARγ agonists such as PGJ2 and troglitazone, induce the TGFβ-like protein NAG-1 in HCT-116 cells (397, 407), and therefore induction of NAG-1 protein and apoptosis by PPARγ-active C-DIMs was investigated in HCT-116 cells treated with relatively high concentrations (10 - 20 μM) over 24 hr. The results (Fig. 4.3C) show that NAG-1 protein expression was not
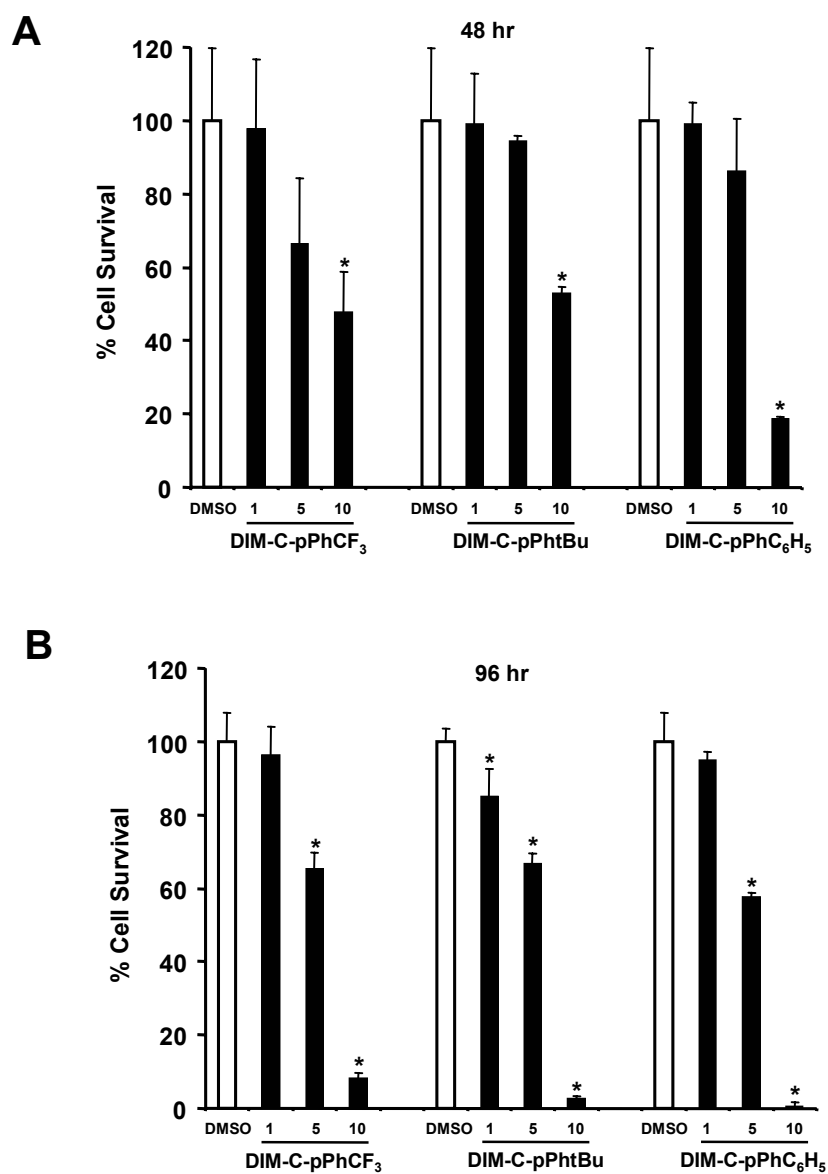
Fig. 4.1. PPARγ-active C-DIMs decrease HCT-116 cancer cell survival. HCT-116 cells were treated for 48 [A] or 96 [B] hr with DMSO or different concentrations of C-DIMs, and cell numbers as a percentage of DMSO-treated cells were determined as described in the Materials and Methods. Results are expressed as means ± SE for three separate determinations for each treatment group and a significant (p < 0.05) decreased in cell survival is indicated with an asterisk.
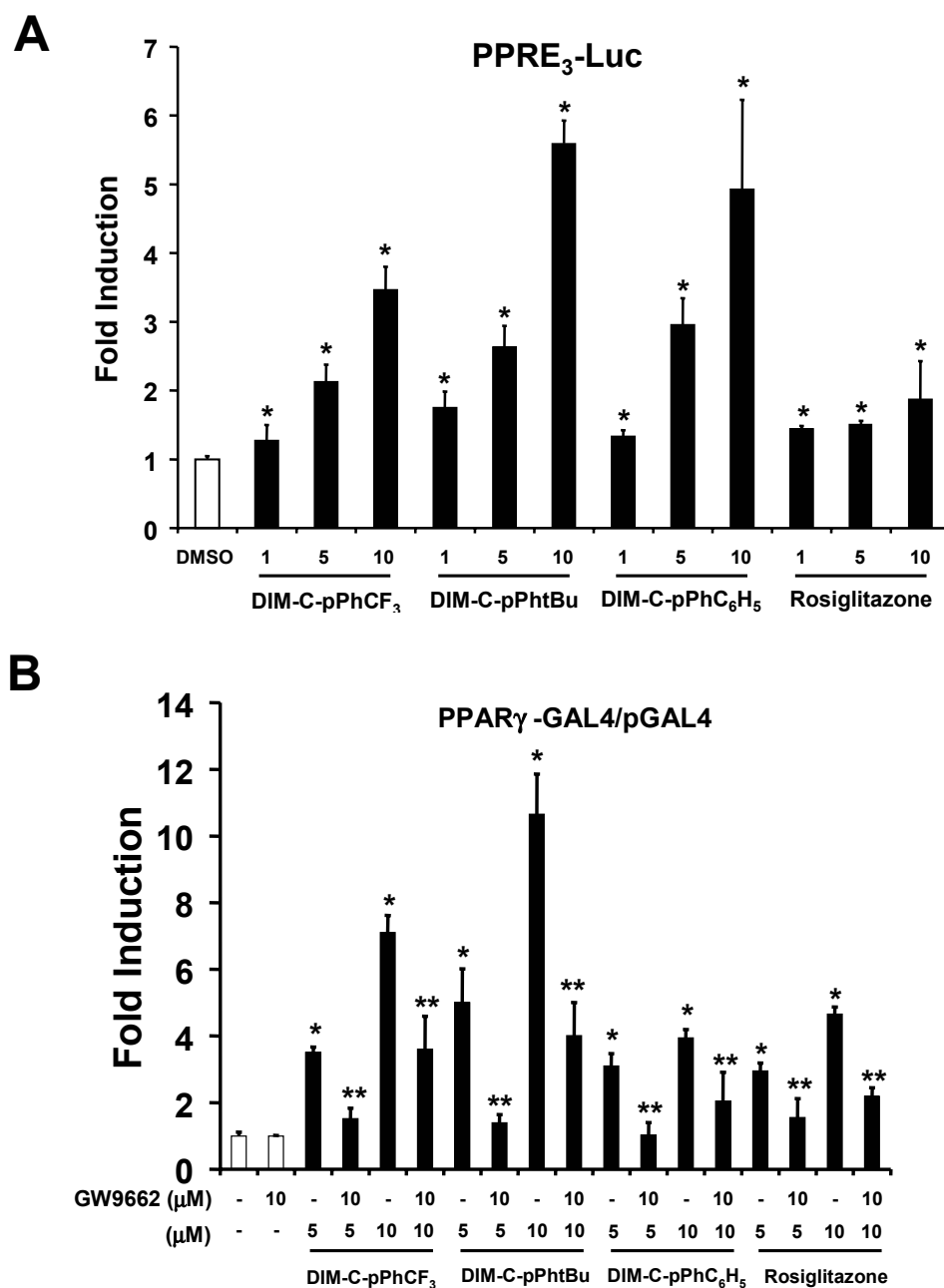
Fig. 4.2. Activation of PPARγ-dependent transactivation. HCT-116 cells were transfected with PPRE$_3$-luc [A] or PPARγ-GAL4/pGAL4 [B], treated with DMSO, different concentrations of C-DIMs or rosiglitazone alone or in combination with GW9662, and luciferase activity was determined as described in the Materials and Methods. Results are expressed as means ± SE for replicate determinations for each treatment group, and significant (p < 0.05) induction (*) or inhibition after cotreatment with GW9662 (**) are indicated.

A   **HCT-116 (24 hr)**

B   **HCT-116 (72 hr)**
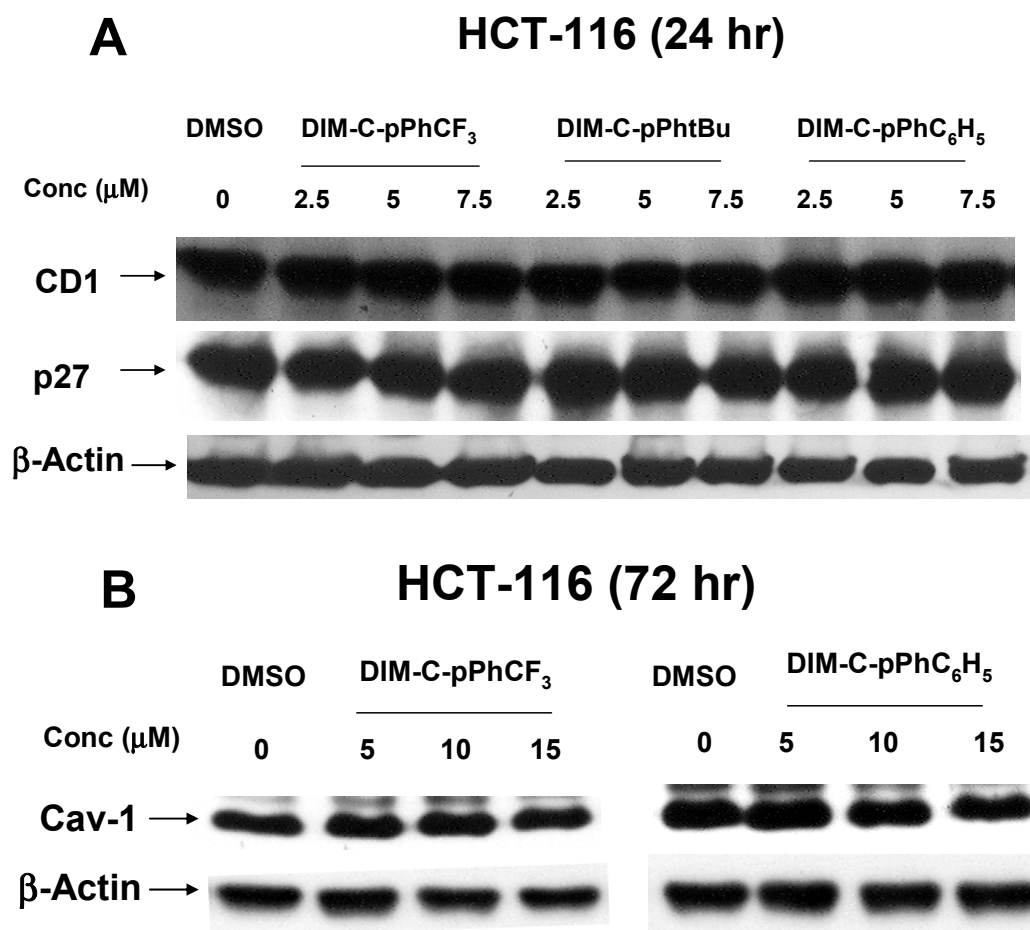
Fig. 4.3. Modulation of cell cycle proteins, caveolin-1, PARP cleavage, and NAG-1 by PPARγ-active C-DIMs. HCT-116 cells were treated with DMSO or different concentrations of C-DIMs and analyzed for cyclin D1 (CD1)/p27 [A], caveolin-1 [B], PARP cleavage/NAG-1 and CD1 [C], and NAG-1 [D] by Western blot analysis as outlined in the Materials and Methods. Treatment times were varied and similar results were observed in duplicate experiments for [A] - [D].

130
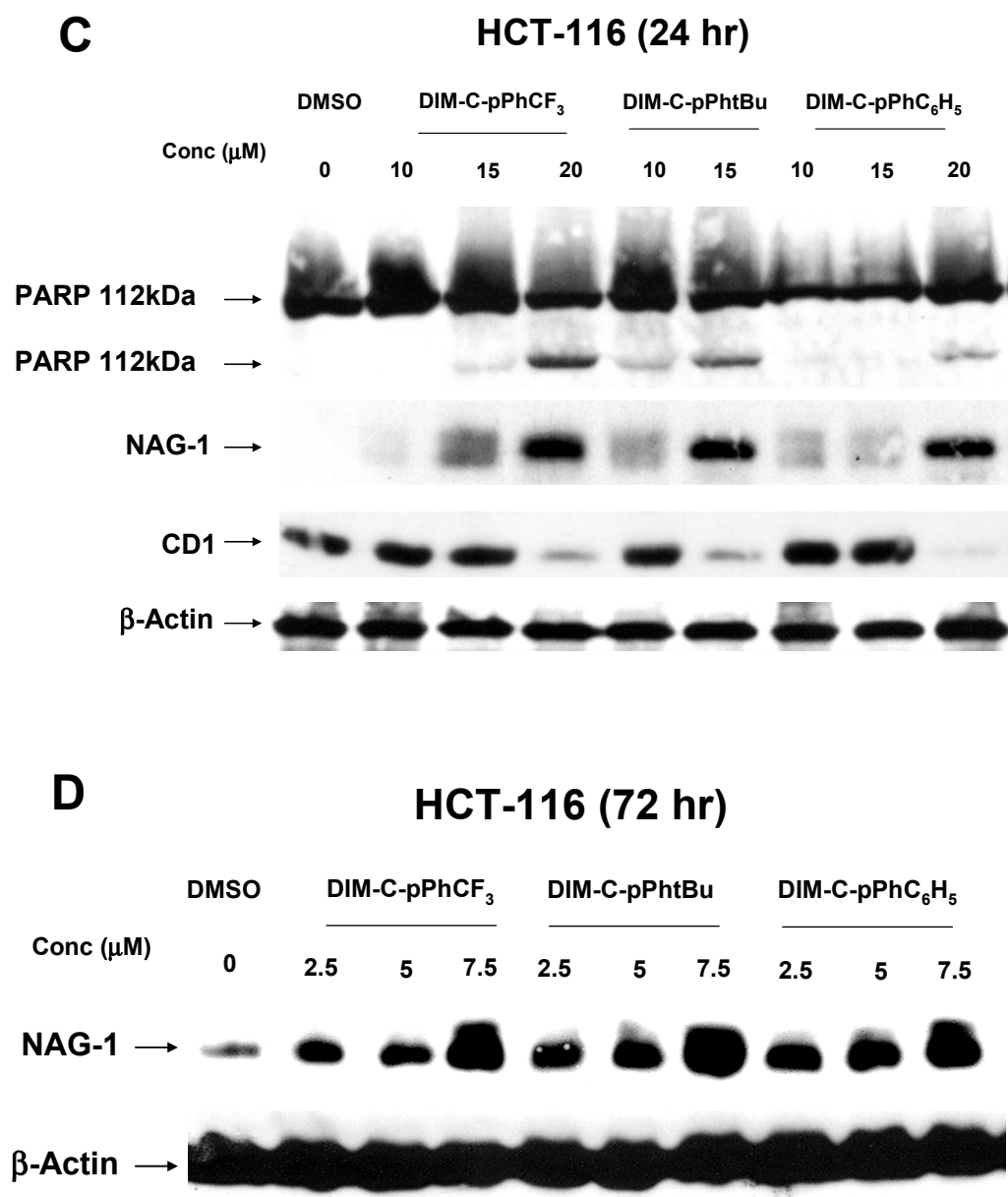
Fig. 4.3 Continued

detectable in solvent-treated cells; however, treatment with 10 - 20 μM DIM-C-pPhCF₃, DIM-C-pPhtBu or DIM-C-pPhC₆H₅ induced NAG-1 protein expression. We also observed induction of NAG-1 by C-DIMs in LNCaP cells as previously described for other NAG-1 inducers (408). The induction of NAG-1 in HCT-116 cells was accompanied by activation of apoptosis as indicated by PARP cleavage. In contrast, p27 expression was unaffected by this treatment and cyclin D1 was downregulated only at the highest dose level. The coordinate induction of NAG-1 and apoptosis in HCT-116 cells by PPARγ-active C-DIMs after treatment for 24 hr is consistent with the effects of these compounds on decreased cell survival (Fig. 4.1). However, the induction of NAG-1 by PPARγ-active C-DIMs was not strictly a high dose effect since treatment of HCT-116 cells with 2.5, 5.0 and 7.5 μM DIM-C-pPhCF₃ and DIM-C-pPhC₆H₅ for 72 hr show that NAG-1 protein was induced at concentrations as low as 2.5 μM (Fig. 4.3D).

The concentration-dependent effects of DIM-C-pPhCF₃ and DIM-C-pPhC₆H₅ on induction of NAG-1 and other proteins that are often induced along with NAG-1 were determined in HCT-116 cells after treatment for 24 hr (Fig. 4.4A). NAG-1 protein levels were elevated at concentrations as low as 7.5 μM. After 24 hr, maximal induction was observed at concentrations ≤ 15 μM and this was accompanied by PARP cleavage. Induction of NAG-1 by some compounds is accompanied by increased expression of p53 protein (405, 407) or ATF3 (411, 414), and the PPARγ-active C-DIMs induced the latter protein but not p53. Although other PPARγ agonists induce NAG-1, the role of the receptor in mediating these responses is structure dependent since studies with PPARγ antagonists showed that induction of NAG-1 by PGJ2 and troglitazone was

HCT-116

A

B
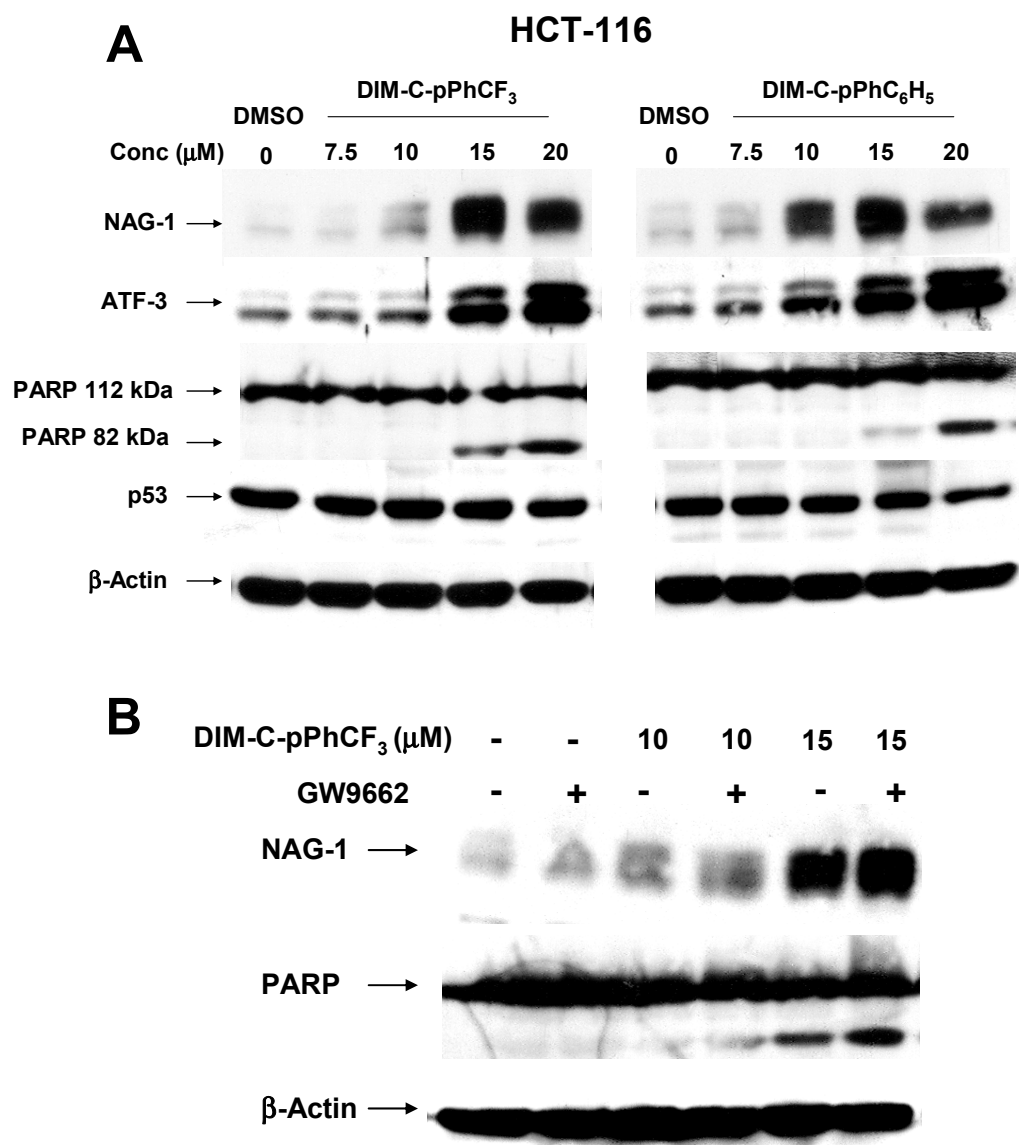
Fig. 4.4. Induction of NAG-1 and related proteins by C-DIMs and the role of PPARγ. [A] Induction of NAG-1 and related proteins by C-DIMs. HCT-116 cells were treated with DMSO or 7.5 - 20 μM C-DIMs for 24 hr and proteins were analyzed by Western immunoblot analysis as described in the Materials and Methods. [B]/[C] Role of PPARγ in activation of NAG-1/PARP cleavage by C-DIMs. HCT-116 cells were treated for 24 hr with DMSO, 10 or 15 μM C-DIMs alone or in combination with 10 μM GW9662 and whole cell lysates were analyzed by Western immunoblot analysis as described in the Materials and Methods. [D] Role of PPARγ in mediating C-DIM-induced cell survival. Cell survival data (after 96 hr) were obtained as described in Figure1, and the effects of C-DIMs alone or in combination with GW9662 were determined. No significant ($p < 0.05$) effects on cell survival were observed in cells treated with D-DIMs plus GW9662. Experiments illustrated in [B] - [D] were also determined using the PPARγ antagonist T007 and similar results were obtained.

C

DIM-C-pPhC$_6$H$_5$ (μM)   –   –   10   10   15   15
GW9662   –   +   –   +   –   +

NAG-1 →

PARP →

β-Actin →

D   **96 hr**

GW9662 (10 μM) – + – + – + – +   – + – + – + – +   – + – + – + – +
DMSO 1 5 10   DMSO 1 5 10   DMSO 1 5 10

DIM-C-pPhCF$_3$ **DIM-C-pPhtBu**   **DIM-C-pPhC$_6$H$_5$**
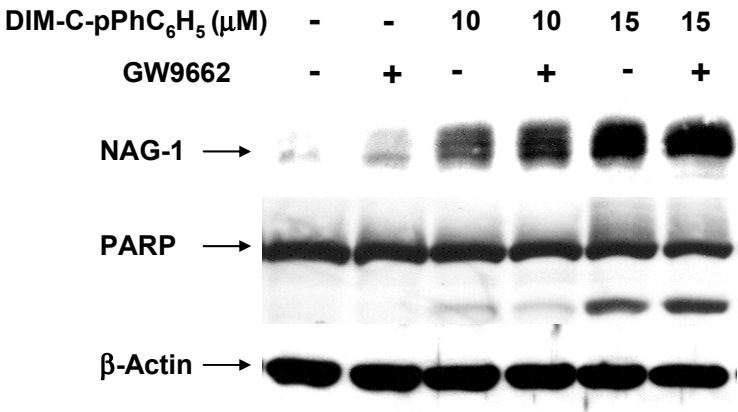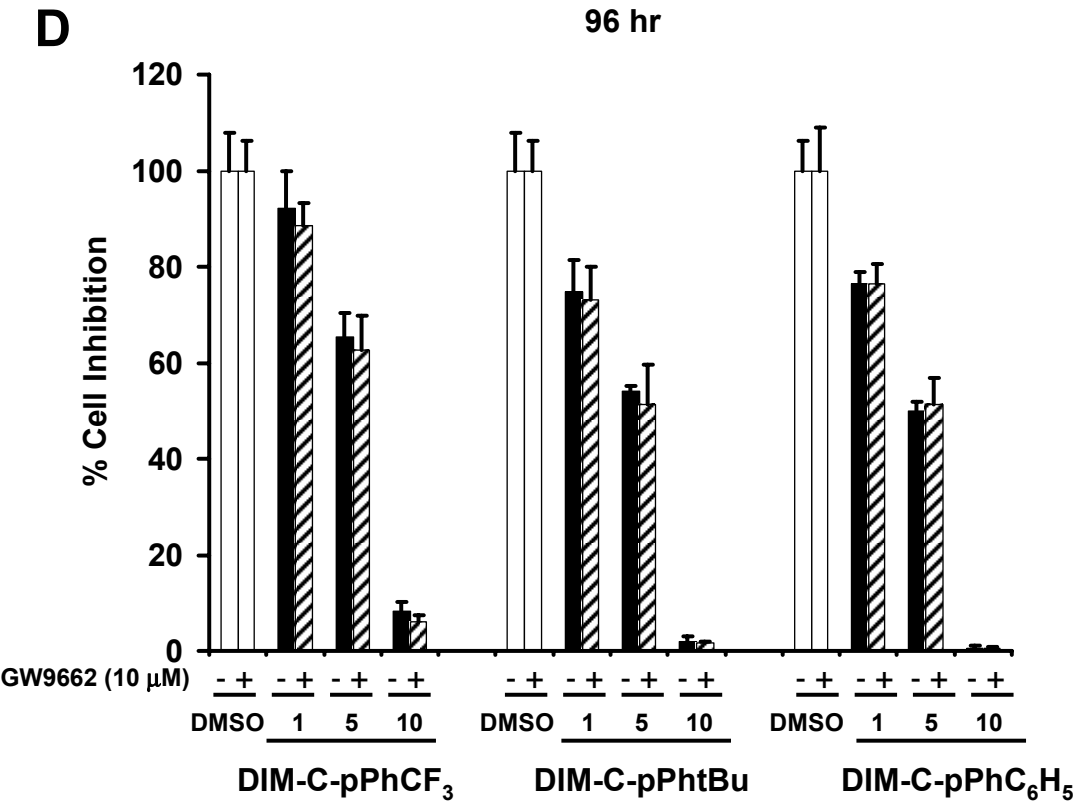
Fig. 4.4 Continued

PPARγ-dependent and -independent, respectively (303). Treatment of HCT-116 cells with DIM-C-pPhCF$_3$ (Fig. 4.4B) or DIM-C-pPhC$_6$H$_5$ (Fig. 4.4C) alone or in combination with the PPARγ antagonist GW9662 shows that induction of NAG-1 or apoptosis by the C-DIM compounds is not inhibited by GW9662. We have also repeated the same experiment with another PPARγ antagonist, 2-chloro-5-nitro-*N*-4-pyridinyl-benzamide (T007) and observed no inhibition of the C-DIM-mediated induction of NAG-1 or PARP cleavage. In addition, GW9662 did not affect decreased HCT-116 cell survival after treatment with the C-DIM compounds for 96 hr (Fig. 4.4D). Apoptosis (PARP cleavage) was induced by PPARγ-active C-DIMs at concentrations as low as 10 μM (after 24 hr); this was more pronounced after 48 hr and correlated with the cell survival results (Fig. 4.1). Thus, like troglitazone, the PPARγ-active C-DIMs induce NAG-1 and apoptosis in HCT-116 cells via a PPARγ-independent pathway.

Previous reports have linked the anticarcinogenic activity of troglitazone to induction of both NAG-1 and Egr-1 and enhanced Egr-1 expression has been linked to upregulation of NAG-1 in HCT-116 cells (303, 397, 411). The results in Figure 4.5A show that both DIM-C-pPhCF$_3$ and DIM-C-pPhC$_6$H$_5$ induce Egr-1 and NAG-1 proteins in HCT-116 cells; however, the temporal expression of both proteins is different. Egr-1 is maximally induced within 2 hr after treatment and levels then decline 4 to 24 hr after treatment. In contrast, induction of NAG-1 protein increases over the 24 hr treatment period and the highest levels are observed after 24 hr. The temporal sequence of C-DIM-induced NAG-1 and Egr-1 expression is comparable to that observed for

troglitazone in HCT-116 cells except that the time-course for induction of both proteins

is somewhat delayed (397).
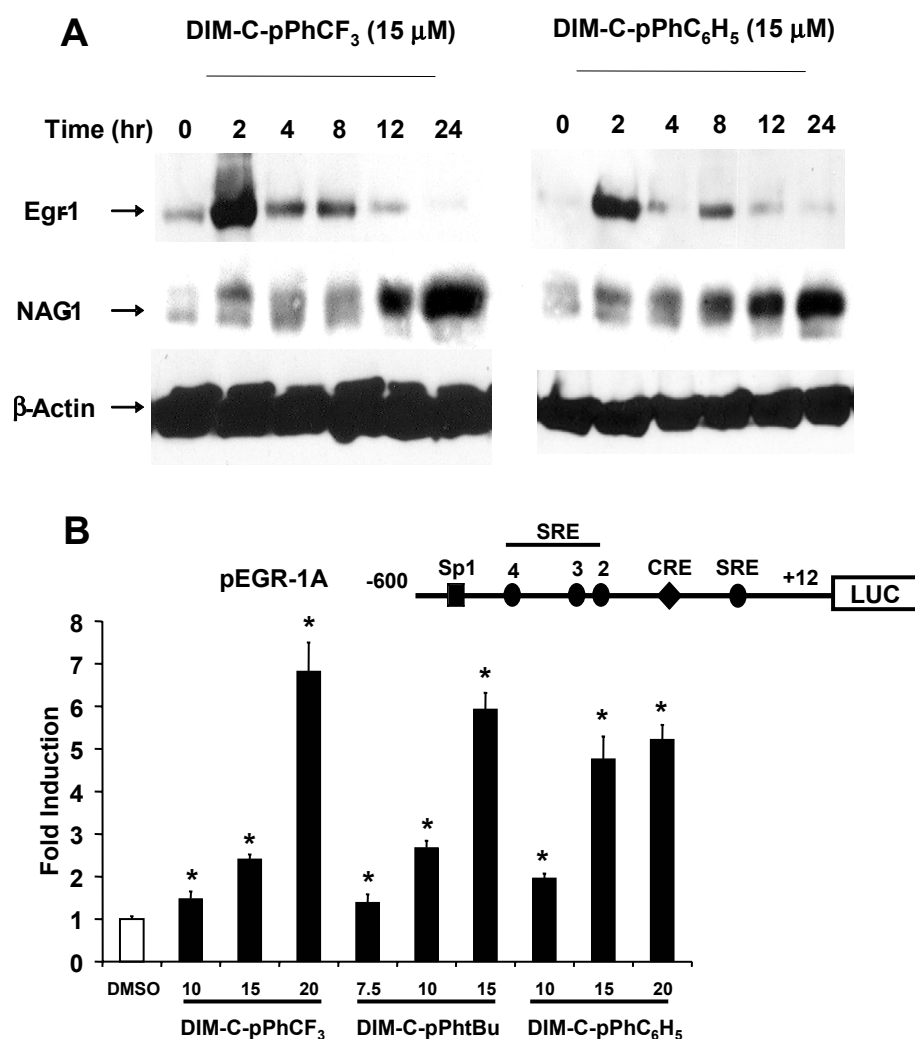
Fig. 4.5. Induction of Egr-1 protein/reported gene activity by C-DIMs. [A] Time course induction of NAG-1 and Egr-1. HCT-116 cells were treated with DMSO or 15 μM C-DIMs for up to 24 hr, and whole cell lysates were analyzed for Egr-1, NAG-1 and β-actin (control) by Western immunoblot analysis as described in the Materials and Methods. Activation of EGR-1A [B], EGR-1B [C], EGR-1C [D], EGR-1D [E], and EGR-1E [F] by C-DIMs. HCT-116 cells were transfected with the various constructs treated with DMSO or C-DIMs and luciferase activity determined as described in the Materials and Methods. Results are expressed as means ± SE for three replicate determinations for each treatment group, and significant (p < 0.05) induction is indicated by an asterisk.
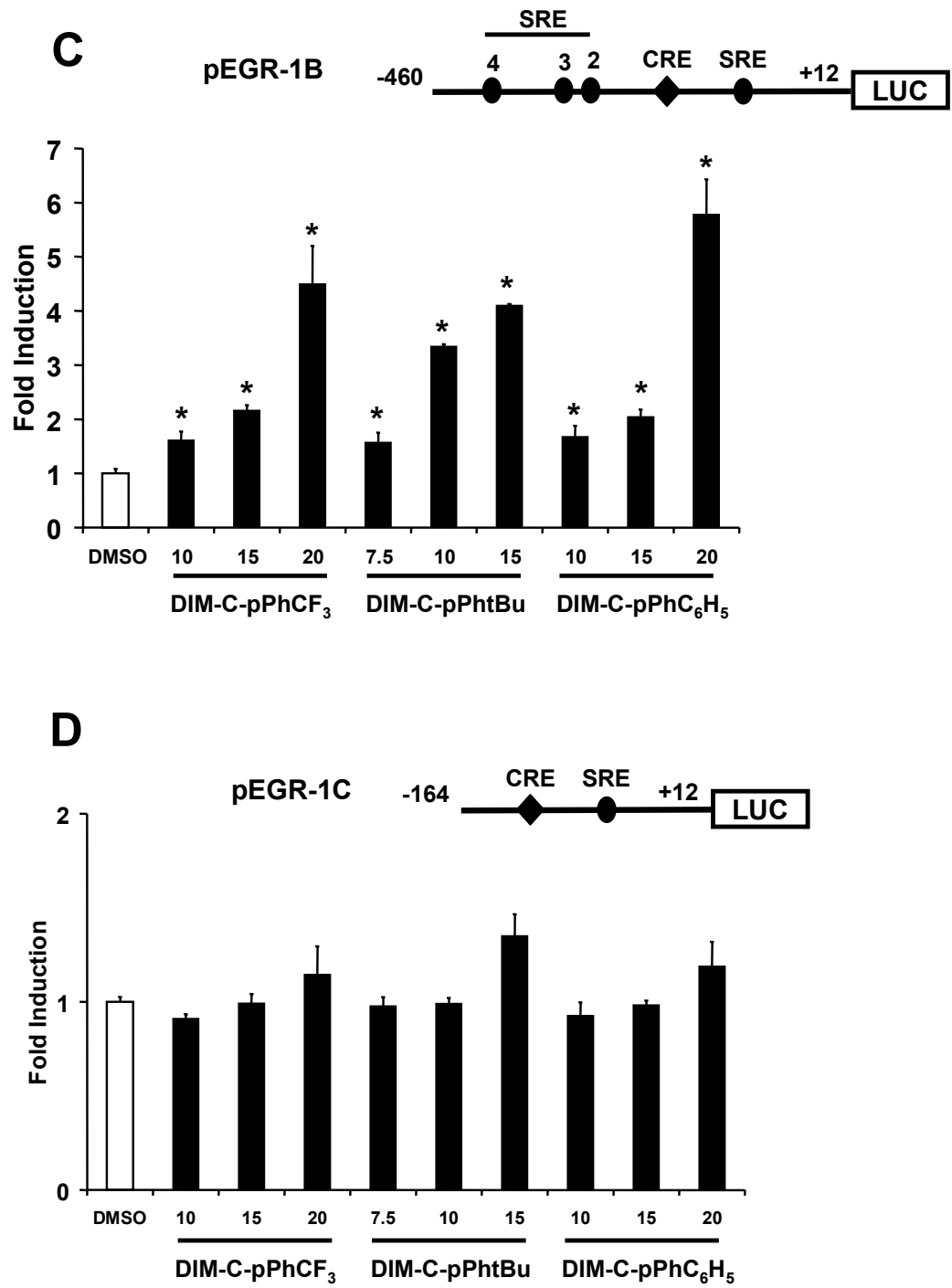
Fig. 4.5 Continued
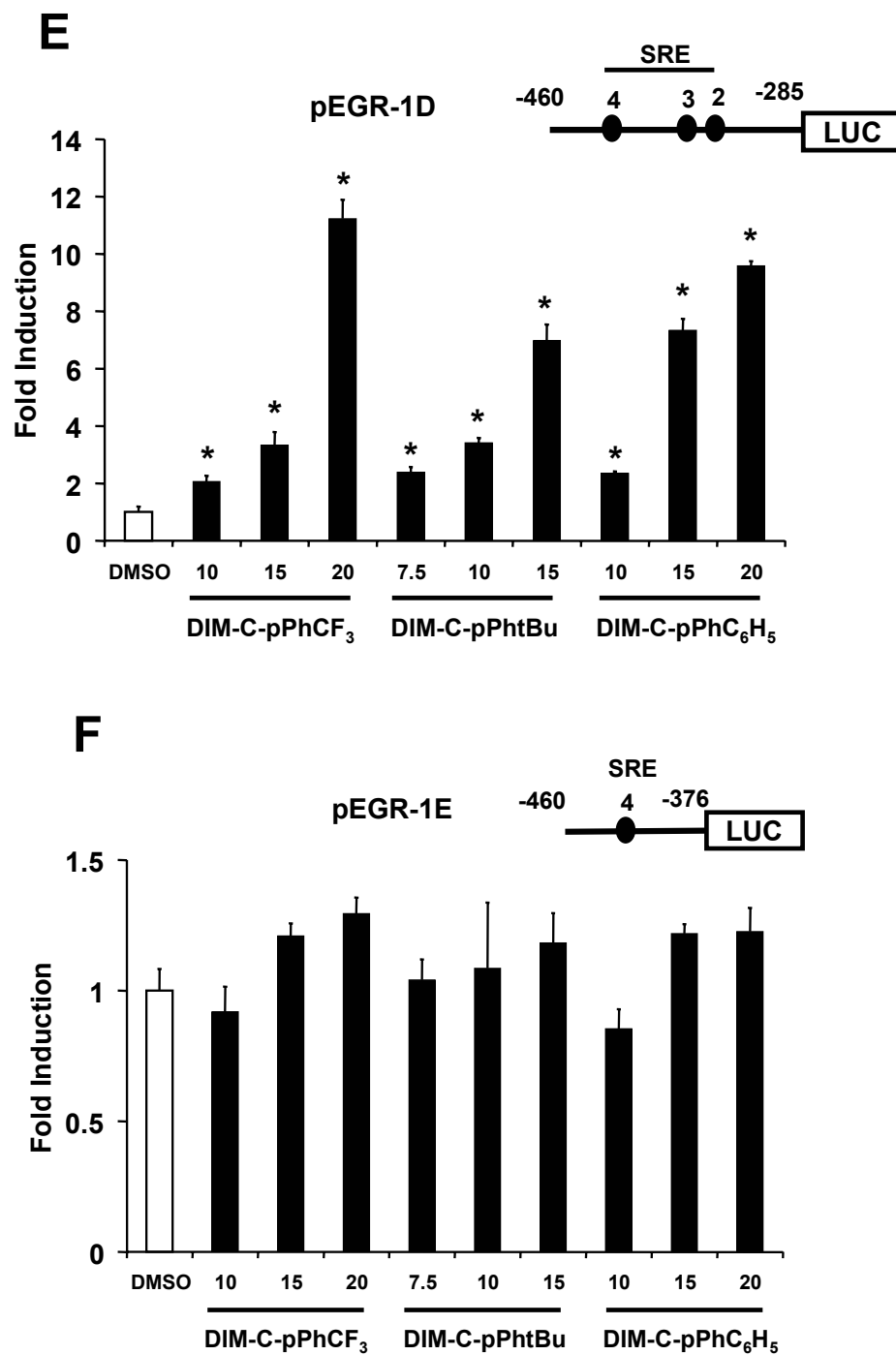
Fig. 4.5 Continued

We also investigated the effects of the PPARγ-active C-DIMs on transactivation in cells transfected with constructs containing -600 to +12 (pEGR-1A), -460 to +12 (pEGR-1B), and -164 to +12 (pEGR-1C) Egr-1 promoter inserts (Figs. 4.5B – 4.5D). All three compounds induced transactivation in cells transfected with pEGR-1A and pEGR-1B but not pEGR-1C, suggesting that SRE2-4 motifs within the -460 to -164 region of the promoter were required for activation of Egr-1. Further deletion of the 3' region of the promoter was investigated in cells transfected with pEGR-1D (-480 to -285) and pEGR-1E (-480 to -376). The C-DIM compound induced transactivation only in cells transfected with pEGR-1D and not pEGR-1E demonstrating that the minimal region of the Egr-1 promoter required for transactivation (-376 to -285) contained SRE3 and SRE2.

The potential role of Egr-1 in mediating induction of NAG-1 was further investigated in HCT-116 cells transfected with a series of constructs containing the -3500 to +41 (pNAG-1A), -1086 to +41 (pNAG-1B), -474 to +41 (pNAG-1C), and -133 to +41 (pNAG1D) NAG-1 promoter inserts (Figs. 4.6A – 4.6D). The results show that the C-DIM compounds induce transactivation in HCT-116 cells transfected with all four constructs. Previous studies show that the -73 to -44 region of the NAG-1 gene promoter contains two GC-rich Sp1 binding sites that overlap two Egr-1 sites (303, 402, 403). Therefore, cells were transfected with pNAG-1D or constructs containing a single Egr-1 site mutation (pNAG-1Dm1 and pNAG-1Dm2) or both sites mutated (pNAG-1Dm3). The results (Fig. 4.6E) show that C-DIM-induced transactivation was decreased in cells transfected with pNAG-1Dm1 and pNAG-1Dm2 and no significant induction
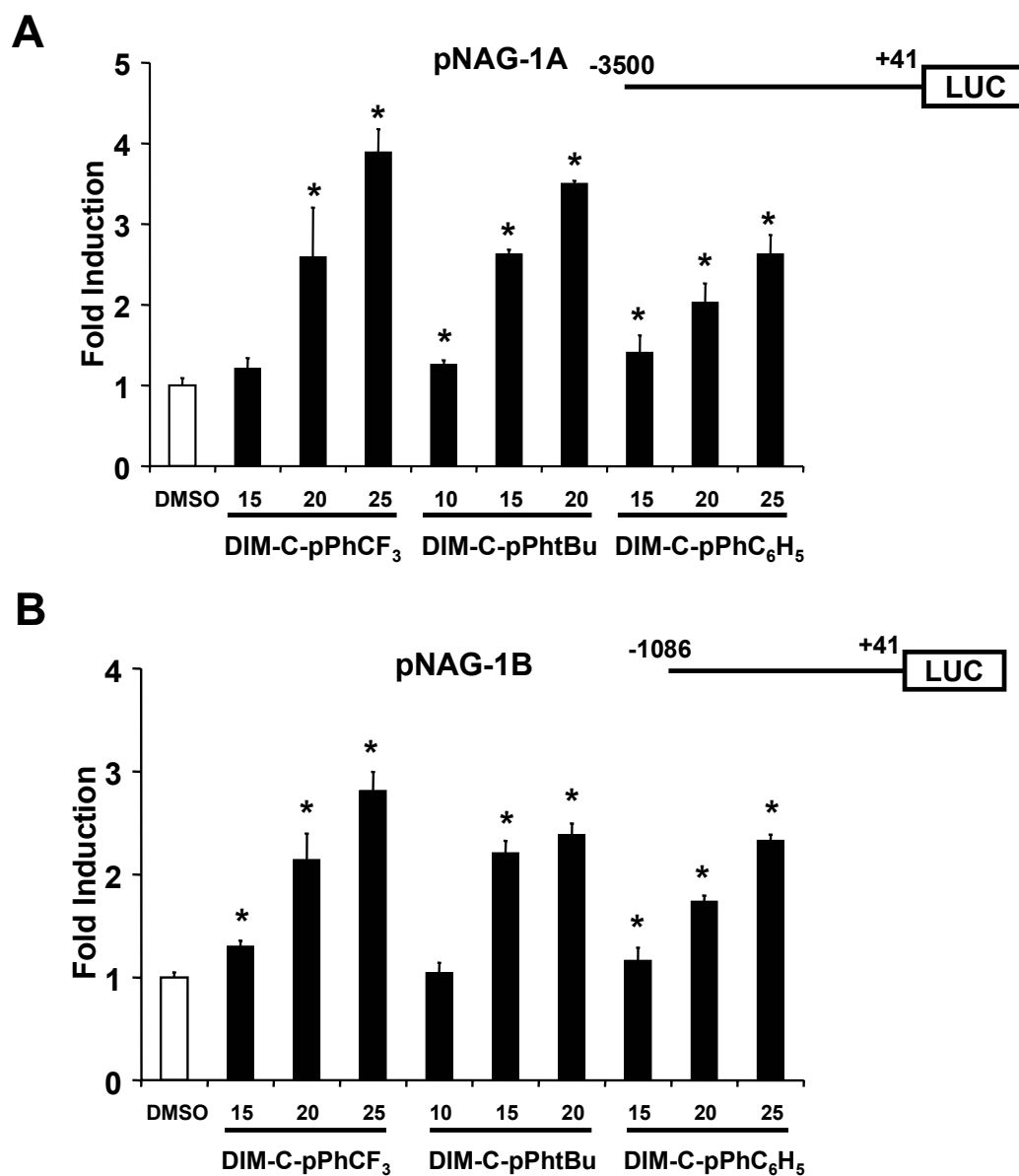
Fig. 4.6. Activation of NAG-1 promoter constructs by C-DIMs and Egr-1. HCT-116 cells were transfected with pNAG-1A [A], pNAG-1B [B], pNAG-1C [C], pNAG-1D [D], or pNAG-1D mutants [E], treated with DMSO or C-DIMs, and luciferase activity determined as described in the Materials and Methods. Results in [A] - [E] are expressed as means ± SE for three replicate determinations for each treatment group, and significant (p < 0.05) induction is indicated by an asterisk.
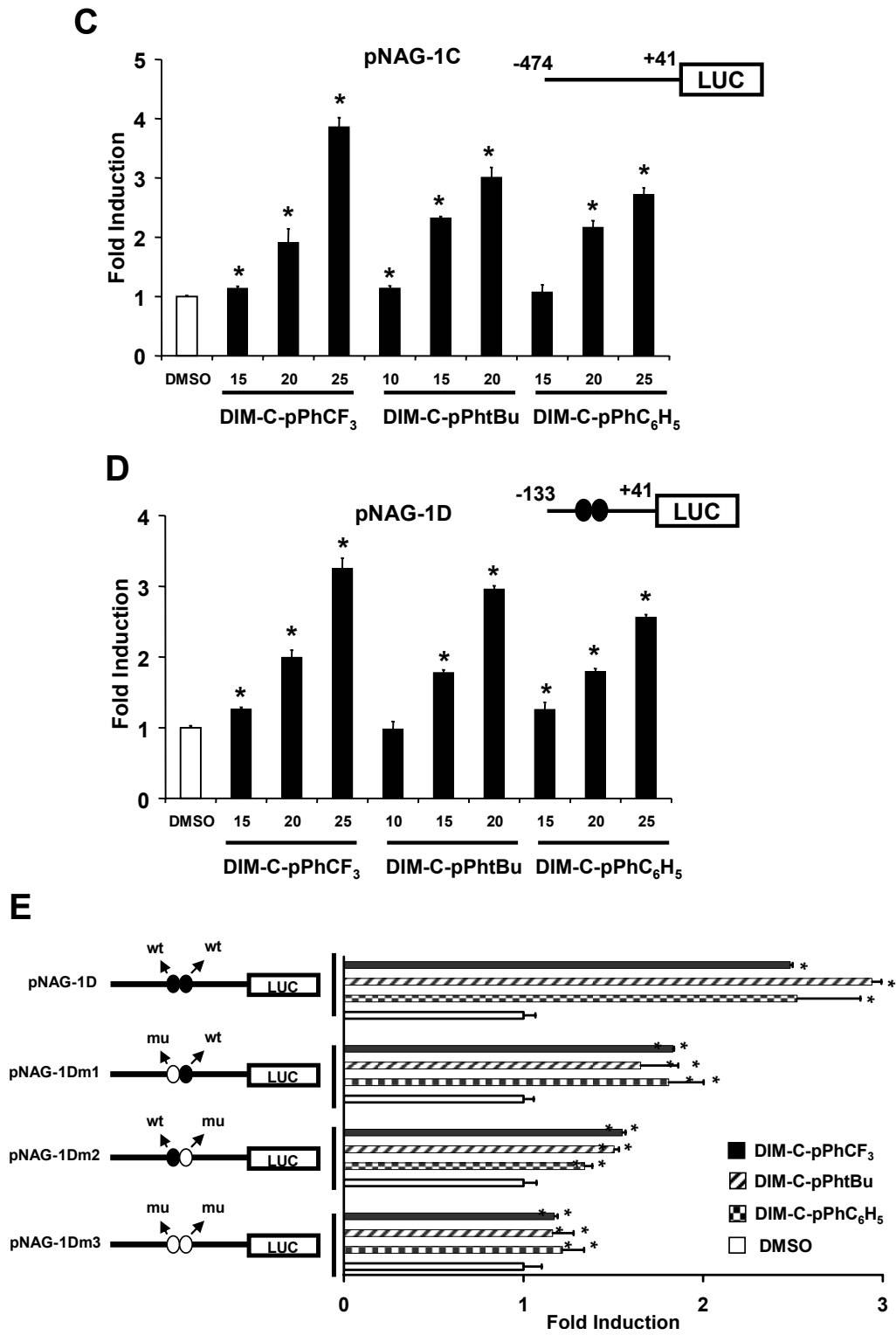
Fig. 4.6 Continued

was observed in cells transfected with pNAG-1Dm3. Thus, mutation of the Egr-1 sites resulted in loss of inducibility of the NAG-1 constructs. Moreover, in cells transfected with pNAG-1D, cotransfection with Egr-1 expression plasmid also induces transactivation (Fig. 4.7A). These results are consistent with a mechanism of NAG-1 induction by C-DIMs which involves initial activation of Egr-1 which in turn activates the NAG-1 promoter through proximal Egr-1 motifs. We also investigated interactions of Egr-1 with the NAG-1 promoter in a ChIP assay with PCR primers that target the proximal region of the NAG-1 promoter that contain the Egr-1 motifs. HCT-116 cells were treated with DMSO or 20 μM DIM-C-pPhC$_6$H$_5$ for 1 or 2 hr; cells were then crosslinked with formaldehyde and the ChIP assay procedure was used to determine interactions of Sp proteins and Egr-1 with the NAG-1 promoter (Fig. 4.7B). The results show binding of Sp1, Sp3 and Sp4 proteins to the NAG-1 promoter and the band intensities are increased after treatment with DIM-C-pPhC$_6$H$_5$. Similar results were observed for Egr-1 suggesting that induction of Egr-1 protein (Fig. 4.5) facilitates recruitment of Egr-1 and Sp proteins to the NAG-1 promoter. As a control experiment for the ChIP assay, the binding of TFIIB to the GAPDH promoter, but not exon 1 of the CNAP1 gene, is illustrated in Figure 4.7C as previously described (394).

Egr-1 is an immediate early gene that is activated by multiple factors in different cell lines, including UV light, ER stress, hormones, phorbol esters, and troglitazone (303, 397, 412, 418-423), and many of the responses involve activation of kinases. Moreover, troglitazone activates Egr-1 and NAG-1 in HCT-116 cells through activation of the mitogen-activated protein kinase (MAPK) pathway (303, 397). The role of
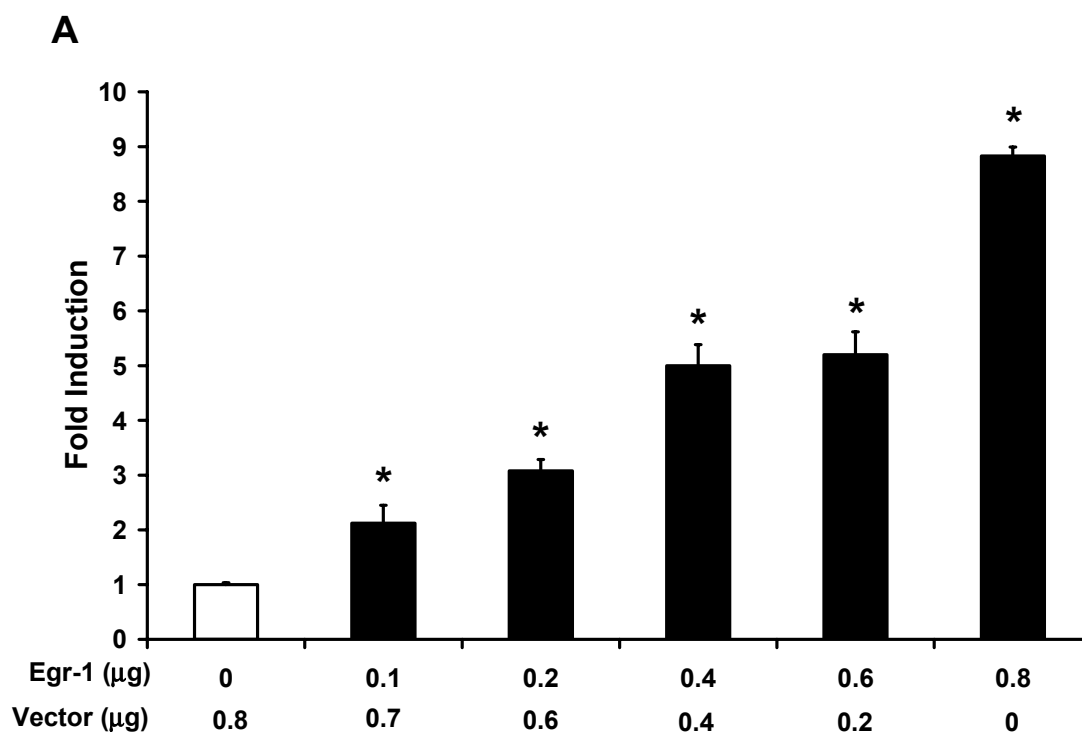
Fig. 4.7. Activation of NAG-1 by Egr-1. [A] Activation of NAG-1 promoter constructs by Egr-1 expression plasmid. HCT-116 cells were transfected with pNAG-1D and different amounts of Egr-1 expression plasmid (or empty vector to maintain a constant amount of transfected DNA), and luciferase activity determined as described in the Materials and Methods. Results are expressed as means ± SE for three replicate determinations for each group, and significant (p < 0.05) induction compared to empty vector is indicated by an asterisk. [B] ChIP assay. HCT-116 cells were treated with DMSO or 20 μM DIM-C-pPhC$_6$H$_5$, and interactions of various proteins with the NAG-1 promoter were determined in a ChIP assay as described in the Materials and Methods. [C] Control binding of TFIIB. The control ChIP assay illustrates binding of TFIIB to the GAPDH promoter but not to exon 1 of the CNAP1 gene (negative control).

B

NAG-1 promoter

DMSO	1hr	2hr	
			Input
			IgG
			Sp1
			Sp3
			Sp4
			Egr-1

-73 ~ -51

-200

+11

⬤ Sp1/Egr-1 binding site   ⇄ primers

C

Negative Ctrl (CNAP1)

DMSO	1hr	2hr	
			Input
			IgG
			TFIIB

Positive Ctrl (GAPDH)

DMSO	1hr	2hr	
			Input
			IgG
			TFIIB
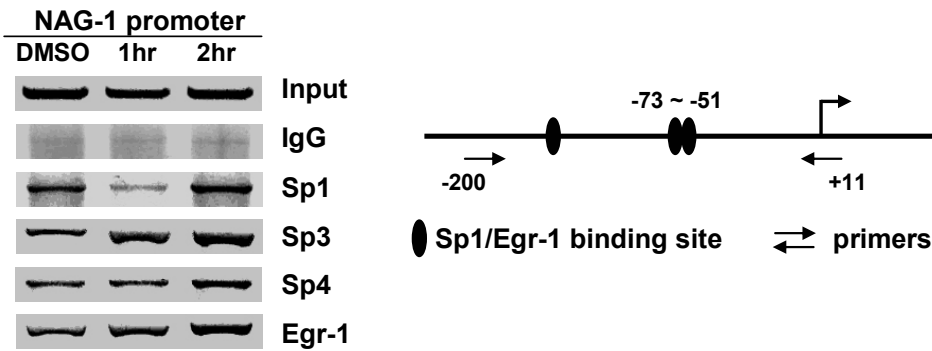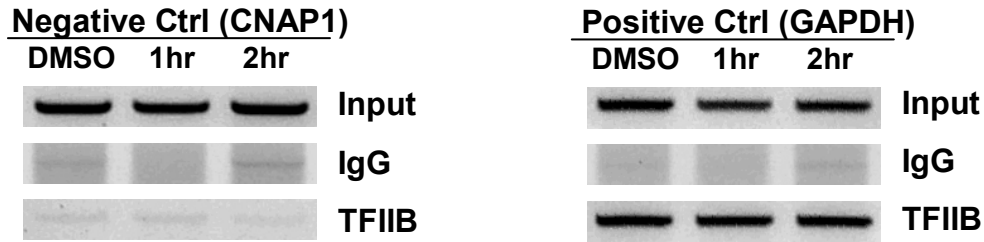
Fig. 4.7 Continued
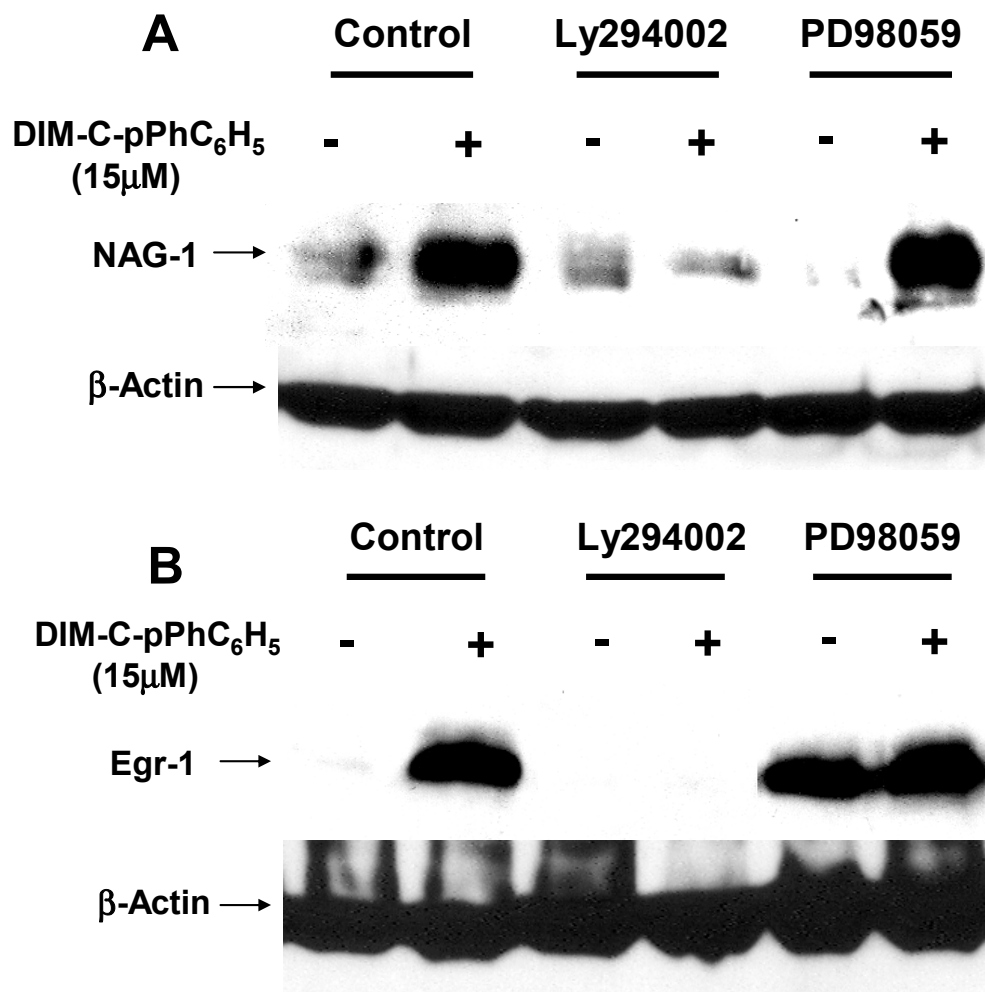
Fig. 4.8. C-DIM compounds activate PI3-K in HCT-116 cells. Effects of kinase inhibitors on induction of NAG-1 [A] or Egr-1 [B] by C-DIMs. HCT-116 cells were treated with DMSO, C-DIMs alone or in combination with 20 μM PD98059 or 20 μM LY294002 for 24 [A] or 2 [B] hr, and whole cell lysates were analyzed by Western immunoblot analysis as described in the Materials and Methods. Similar results were observed using DIM-C-pPhCF$_3$ or DIM-C-pPhtBu. [C] Inhibition of pEGR-1D activation by LY294002. HCT-116 cells were transfected with pEGR-1D, treated with 10 or 15 μM C-DIM compounds alone or in combination with 20 μM LY294002 and luciferase activity determined as described in the Materials and Methods. Results are expressed as means ± SE (triplicate). Significant (p < 0.05) induction by C-DIMs and inhibition by LY294002 are indicated by (*) and (**), respectively. [D] Activation of Akt phosphorylation by C-DIMs. HCT-116 cells were treated with the C-DIM compounds for different periods of time, and whole cell lysates were analyzed by Western blot analysis for phospho-Akt and Akt as described in the Materials and Methods. Results shown in the bar graph are means of two duplicate determinations.
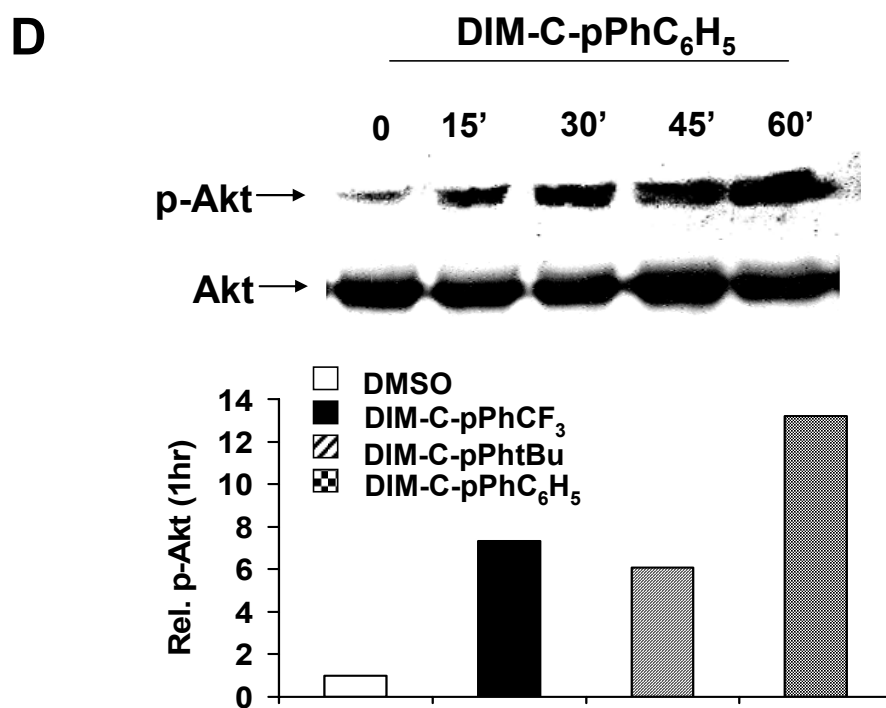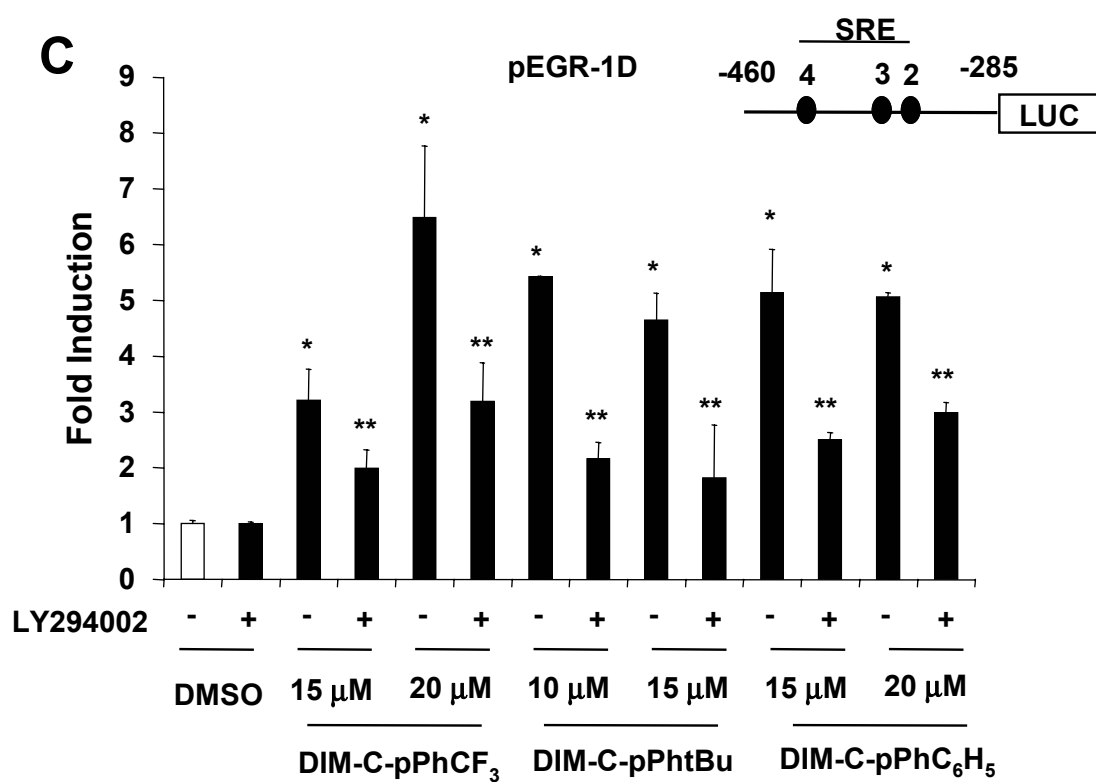
Fig. 4.8 Continued

kinases in activation of NAG-1 by C-DIM compounds was therefore investigated in HCT-116 cells treated with 15 μM DIM-C-pPhC$_6$H$_5$ for 24 hr in the presence or absence of PD98059 or LY294002 which inhibit MAPK and PI3-K-dependent phosphorylation, respectively. The results showed that induction of NAG-1 protein by DIM-C-pPhC$_6$H$_5$ was inhibited by LY294002 but not PD98059 (Fig. 4.8A); similar inhibitory responses were also observed for induction of Egr-1 (Fig. 4.8B). Interestingly, PD98059 alone also induced Egr-1 (Fig. 4.8B) but not NAG-1 (Fig 4.8A), suggesting that Egr-1 alone is not sufficient for activation of NAG-1. The inhibitory effects of LY294002 suggest that the C-DIM compounds induce PI3-K. Moreover, in cells transfected with pEGR-1D, induction of luciferase activity by the C-DIM compounds was inhibited by cotreatment with LY294002 (Fig. 4.8C). The results in Figure 4.8D show the time-dependent induction of Akt phosphorylation by DIM-C-pPhC$_6$H$_5$ and a similar induction response was observed for DIM-C-pPhCF$_3$ and DIM-C-pPhtBu. Activation of PI3-K was time-dependent since induction of Akt phosphorylation was not observed after treatment for 2 hr. These results demonstrate that PPARγ-active C-DIMs coordinately induce Egr-1 and NAG-1 through a novel pathway which involves initial PI3-K-dependent activation of Egr-1 through SRE3 and SRE2 motifs on the Egr-1 promoter.

Discussion

PPARγ-active C-DIMs and other PPARγ agonists inhibit growth and induce apoptosis in several different cell lines, and these responses are both receptor-dependent and -independent (254, 359, 361, 390, 391, 393-395, 416-418). For example, studies in this laboratory have demonstrated that induction of p21 in Panc-28 cells and upregulation of caveolin-1 in HT-29 and HCT-15 cells is PPARγ-dependent and inhibited by PPARγ antagonists or by PPARγ knockdown with small inhibitory RNAs (393, 394). In contrast, induction of apoptosis and downregulation of cyclin D1 in breast cancer cells was PPARγ-independent (359). The interplay between receptor-dependent and -independent pathways has also been reported for the potent triterpenoid-derived PPARγ agonist 2-cyano-3,12-dioxooleana-1,9-dien-28-oic acid and related compounds in HCT-15, HT-29 and SW-480 colon cancer cells (396). At lower growth-inhibitory concentrations, CDDO induced caveolin-1, and this response was inhibited in cells cotreated with the PPARγ antagonist T007. In contrast, at higher concentrations, caveolin-1 expression was decreased and apoptosis was induced and this latter response was receptor-independent and not inhibited by T007. The type of differential concentration-dependent induction of PPARγ-dependent and -independent responses has also been observed for PPARγ-active C-DIM compounds in SW-480 cells.

In this study, we have investigated the effects of PPARγ-active C-DIMs in HCT-116 cells and, as previously reported in HCT-15 and HT-29 cells (393), these compounds decrease HCT-116 cell survival (Fig. 4.1), activate PPARγ-dependent transactivation (Fig. 4.2), and p21, p27 and cyclin D1 levels were unchanged except for

downregulation of cyclin D1 at high concentrations (Fig. 4.3). In contrast to observations in HT-29 and HCT-15 cells (393), the PPARγ-active compounds did not induce caveolin-1 in HCT-116 cells (Fig. 4.3), and this may be due, in part, to the relatively high constitutive expression of caveolin-1 in this cell line. Thus, the growth inhibitory responses of C-DIMs in HCT-116 cells must be related to activation of other pathways. Previous studies in HCT-116 cells have reported that several different structural classes of growth inhibitory/antitumorigenic compounds, including the PPARγ agonists PGJ2 and troglitazone, and DIM induced NAG-1 expression and this protein exhibits both growth inhibitory and pro-apoptotic activity (303, 397, 402-414). Our results show that PPARγ-active C-DIMs also induce NAG-1 protein expression in HCT-116 cells (Figs. 4.3 and 4.4), and this is consistent with their growth inhibitory (Fig. 4.1) and apoptotic (Figs. 4.3 and 4.4) effects in HCT-116 cells. It was also shown that induction of NAG-1 and apoptosis in HCT-116 cells by DIM-C-pPhCF$_3$ and DIM-C-pPhC$_6$H$_5$ was not inhibited by the PPARγ antagonists GW9662 or T007 and the PPARγ antagonists also did not affect C-DIM-induced growth inhibition (Fig. 4.4). Thus, induction of NAG-1 by PPARγ-active C-DIMs and troglitazone was receptor-independent, and this was in contrast to induction of NAG-1 by PGJ2 since this response was inhibited by a PPARγ antagonist (303).

Induction of NAG-1 by troglitazone was linked to activation of the tumor suppressor gene Egr-1 which in turn directly activates NAG-1 promoter constructs. The C-DIM compounds also rapidly activate Egr-1 protein expression in HCT-116 cells and maximal induction was observed within 2 hr after treatment, whereas NAG-1 protein

expression is increased with time over 24 hr (Fig. 4.5A). In contrast, DIM induced NAG-1 but did not affect Egr-1 expression in HCT-116 cells (414), and this clearly differentiated between diarylmethane (DIM) from the triarylmethane (C-DIM) compounds. Constructs containing Egr-1 promoter inserts (Figs. 4.5B – 4.5E) are also activated by the C-DIM compounds, and the minimal promoter region required for transactivation contains SRE3 and SRE2 which have previously been identified as critical *cis*-elements required for activation of Egr-1 (415). Moreover, these compounds also activate NAG-1 promoter constructs (Fig. 4.6) and deletion/mutation analysis of the NAG-1 promoter indicates that mutation of the proximal Egr-1 sites resulted in loss of C-DIM-induced transactivation (Fig. 4.6E). These results, coupled with the observed interactions of Egr-1 with the NAG-1 promoter in a ChIP assay (Fig. 4.7), clearly link the induction of NAG-1 by C-DIMs to the rapid induction of Egr-1 which subsequently activates NAG-1 expression in HCT-116 cells.

Thus, the induction of NAG-1 by PPARγ-active C-DIMs and troglitazone in HCT-116 cells is receptor-independent and also involves Egr-1 induction. However, induction of NAG-1 protein and reporter gene activity by troglitazone was inhibited by the MAPK inhibitor PD98059 suggesting that this response may be due, in part, to induction of Egr-1 through activation of kinases by troglitazone (303). Kinase-dependent activation of NAG-1 by C-DIMs was further investigated by determining the effects of PI3-K and MAPK inhibitors on induction of NAG-1 and Egr-1 proteins and reporter gene activity (pEGR-1D) in HCT-116 cells (Figs. 4.8A – 4.8C). The results show that PI3-K, and not MAPK inhibitors, block induction of NAG-1 and Egr-1

proteins and induction of transactivation in cells transfected with pEGR-1D, and this was consistent with the identification of kinase-responsive SRE3 and SRE2 as critical *cis*-elements in the Egr-1 promoter that are required for C-DIM-dependent activation of the Egr-1 constructs (Fig. 4.5). Kinase-mediated activation of Egr-1 is highly variable and dependent on cell context (415, 418-424); however, it is apparent from this study that activation of Egr-1 by C-DIMs is PI3-K-dependent, whereas troglitazone activation of Egr-1/NAG-1 was linked to a MAPK pathway (303). In this study, 20 μM LY294002 alone did not affect NAG-1 or Egr-1 protein expression, but inhibited induction of these proteins by PPARγ-active C-DIMs (Fig. 4.8), and induction of Egr-1-derived promoter constructs by DIM-C-pPhtBu was also inhibited by LY294002. In contrast, a recent study reported that higher concentrations of LY294002 (50 μM) induced NAG-1 protein expression and this was linked to activation of GSK-3β through dephosphorylation of this protein (412). Thus, PI3-K plays a pivotal role in activation of Egr-1 (and NAG-1) by the C-DIM compounds, whereas inactivation of PI3-K after treatment with high concentrations of LY294002 results in GSK-3β-dependent activation of NAG-1 (412).

In summary, our results show that PPARγ-active C-DIMs induce both NAG-1 and Egr-1 in HCT-116 cells through receptor-independent pathways. NAG-1 upregulation is linked to prior PI3-K-dependent induction of Egr-1 which directly activates NAG-1 through interaction with Egr-1 *cis*-elements in the NAG-1 promoter. It is also possible that the decreased HCT-116 cell survival and apoptosis observed after treatment with the C-DIM compounds is due, in part, to activation of other Egr-1-dependent genes which mediate the apoptotic and growth inhibitory effects (425). The

induction of PI3-K by the C-DIM compounds (Fig. 4.8D) is somewhat paradoxical since this kinase is linked to cell survival pathways. However, recent studies have demonstrated that activation of PI3-K can sensitize caveolin-1-expressing HeLa and 293 cells to the cytotoxicity of arsenite and hydrogen peroxide (398). Moreover, caveolin-1 and PI3-K also sensitize L929 cells to tumor necrosis factor-α-induced cell death, and it was postulated that this may be due to Akt-dependent inactivation of forkhead transcription factors (399). Although the C-DIM compounds do not induce caveolin-1 in HCT-116 cells, the high endogenous expression of caveolin-1 in these cells (Fig. 4.3B) coupled with the induction of PI3-K may also contribute to the decreased HCT-116 cell survival and apoptosis after treatment with the C-DIMs. Thus, like other PPARγ agonists, the C-DIM compounds activate receptor-independent responses that contribute to their effectiveness as a new class of drugs with potential clinical applications for cancer chemotherapy.

CHAPTER V

1,1-BIS(3'-INDOLYL)-1-(*p*-SUBSTITUTEDPHENYL)METHANES INHIBIT COLON CANCER CELL AND TUMOR GROWTH THROUGH PEROXISOME PROLIFERATOR-ACTIVATED RECEPTOR γ-DEPENDENT AND - INDEPENDENT PATHWAYS

Introduction

Peroxisome proliferator-activated receptor γ (PPARγ) is a member of the nuclear receptor superfamily of ligand-activated transcription factors (354-356, 383-385). Although the endogenous ligand for PPARγ has not been determined, several endogenous molecules such as 15-deoxy-$\Delta^{12,14}$-prostaglandin J2 (PGJ2), other prostaglandin-derived compounds, fatty acids, and flavonoids activate PPARγ. It has recently been reported that nitrolinoleic acid, a stress-induced fatty acid oxidation product may be an endogenous PPARγ agonist (426). Several different structural classes of PPARγ agonists have been synthesized and these include thiazolidinediones (TZDs), 2-cyano-3,12-dioxoolean-1,9-dien-28-oic acid (CDDO) and related triterpenoids, 3-benzyl and acyl-substituted indoles, substituted chromane carboxylic acids and phosphonophosphates (427-432). Among the synthetic PPARγ agonists, the TZDs are now being extensively used as insulin-sensitizing agents for treatment of type II diabetes (354, 356). PPARγ is highly expressed in many tumor samples and cancer cells lines derived from hematopoietic and non-hematopoietic tumors (257), and several studies show that PPARγ agonists inhibit growth and/or induce apoptosis in multiple cancer cell

lines and in *in vivo* tumor models (254, 255, 303, 359-362, 365-367, 370, 372-374, 391, 393, 397, 416, 433-435).

Research in this laboratory has identified a new structural class of 3,3'-diindolylmethane (DIM) analogs. Several methylene-substituted DIMs (C-DIMs) including 1,1-bis(3'-indolyl)-1-(p-substitutedphenyl)-methanes containing trifluoromethyl (DIM-C-pPhCF$_3$), t-butyl (DIM-C-pPhtBu), and phenyl (DIM-C-pPhC$_6$H$_5$) substituents activate PPARγ in several cancer cell lines including colon cancer cells (359, 393-395). The effects of these compounds depend on cell context and this is commonly observed for other PPARγ agonists. The PPARγ-active C-DIMs inhibit growth and/or induce apoptosis in cancer cells; in HT-29 and HCT-15 colon cancer cells, these compounds induce caveolin-1, whereas p21 is induced in Panc28 pancreatic cancer cells and both responses are inhibited by PPARγ antagonists (393, 394). In contrast, induction of cyclin D1 downregulation and apoptosis in breast cancer cells (359) and induction of nonsteroidal anti-inflammatory drug (NSAID) activated gene-1 (NAG-1) are PPARγ-independent (436, 437).

In this study, we show that PPARγ-active C-DIMs inhibit growth of SW480 colon cancer cells and this is associated with PPARγ-dependent induction of caveolin-1 and receptor-independent activation of both NAG-1 and PARP cleavage. Moreover, in athymic nude mice bearing SW480 cell xenografts, DIM-C-pPhC$_6$H$_5$ (20 and 40 mg/kg/d) inhibits tumor growth and immunostaining of tumors shows both overexpression of caspase-3 and NAG-1 in the treated groups. These data demonstrate that PPARγ-active C-DIMs inhibit colon cancer cell/tumor growth and confirm that

PPARγ agonists are an important class of compounds for potential applications in the treatment of colon cancer.

Materials and Methods

Cell lines, plasmids, chemicals and reagents

The SW480 human colon cancer cell line was provided by Dr. S. Hamilton (M.D Anderson Cancer Center, Houston, TX). SW480 cells were maintained in Dulbecco's Modified Eagle's Medium nutrient mixture F-12 Ham (DMEM:Ham's F-12; Sigma, St. Louis, MO) with phenol red supplemented with 0.22% sodium bicarbonate, 0.011% sodium pyruvate and 5% fetal bovine serum (FBS) and 10 ml/L of 100X antibiotic antimycotic solution (Sigma). The Gal4 reporter containing 5X Gal4 DBD (Gal4Luc) was kindly provided by Dr. Marty Mayo (University of North Carolina, Chapel Hill, NC). Gal4DBD-PPARγ construct (GAL4-PPARγ) was a gift of Dr. Jennifer L. Oberfield (Glaxo Wellcome Research and Development, Research Triangle Park, NC) and chimeric pM-PPARγ coactivator-1 (PGC1) was a gift of Dr. Bruce M. Spiegelman (Harvard University, Boston, MA). The PPARγ$_2$-VP16 fusion plasmid (VP-PPARγ) contained the DEF region of PPARγ (amino acids 183–505) fused to the pVP16 expression vector and the GAL4-coactivator fusion plasmids pM-SRC1, pMAIBI, pMTIFII, pM-DRIP205, pMTRAP220 and pM-CARM-1 were kindly provided by Dr. Shigeaki Kato (University of Tokyo, Tokyo, Japan). Rosiglitazone was purchased from LKT Laboratories, Inc. (St. Paul, MN). Horseradish peroxidase substrate for Western blot analysis was purchased from NEN Life Science Products (Boston, MA). Cell lysis buffer and luciferase reagent were purchased from Promega (Madison, WI), and β-

galactosidase (β-gal) reagent was from Tropix (Bedford, MA). Antibodies for cyclin D1 (sc-718), p27 (sc-528), phospho-Akt (sc-7985R), Akt (sc-8312), Bcl2 (sc-7382), Bax (sc20067), caveolin 1 (sc-894), and PARP (sc-8007) were purchased from Santa Cruz Biotechnology (Santa Cruz, CA). NAG-1 antibodies were obtained from Upstate Biotechnology (Lake Placid, NY); monoclonal anti-β-actin was purchased from Sigma (St. Louis, MO).

Cell proliferation assay

Cells were plated at a density of 2 x 10^4/well in 12-well plates and replaced the next day with DMEM:Ham's F-12 media containing 2.5% charcoal-stripped FBS and either vehicle (DMSO) or the indicated ligand and concentration. Fresh media and compounds were added every 48 hr. Cells were counted at the indicated times using a Coulter Z1 cell counter. Each experiment was carried out in triplicate and results are expressed as means ± SE for each determination.

Transfection and luciferase assay

SW480 cells were plated in 12-well plates at 1 x 10^5 cells/well in DME-F12 media supplemented with 2.5% charcoal-stripped FBS. After growth for 16 hr, various amounts of DNA, i.e. Gal4Luc (0.4 μg), b-gal 0.04 μg), VP-PPARγ (0.04 μg), pM SRC1 (0.04 μg), pMTIFII (0.04 μg), pMAIBI (0.04 μg), pMDRIP205 (0.04 μg), and pMCARM-1 (0.04 μg) were transfected by lipofectamine (Invitrogen) according to the manufacturer's protocol. Briefly, 2 μL of lipofectamine was mixed with 50 μL of serum-free medium. Appropriate concentrations of plasmid DNA were mixed with 50 μL of serum-free medium. The lipofectamine solution was then mixed with the DNA

solution and the mixture was allowed to incubate at room temperature for 45 min to form the DNA/lipofectamine complex. In the mean time, cells grown in the presence DME-F12 media supplemented with 2.5% charcoal-stripped FBS were washed with serum free DME-F12 media and then 400 μL of serum free media was added. Following 45 min incubation, the lipofectamine/DNA complex was carefully dropped over the cells and incubated for 5 - 6 hr at 37°C. Five hr after transfection, the transfection mix was replaced with complete media containing either vehicle (DMSO) or the indicated ligand for 20 to 22 hr. Cells were then lysed with 100 μL of 1X reporter lysis buffer, and 30 μL of cell extract were used for luciferase and β-gal assays. A Lumicount luminometer (PerkinElmer Life and Analytical Sciences) was used to quantitate luciferase and β-gal activities, and the luciferase activities were normalized to β-gal activity.

Western blot analysis

SW480 cells were seeded in DMEM:Ham's F-12 media containing 2.5% charcoal-stripped FBS for 24 hr and then treated with either the vehicle (DMSO) or the indicated compounds. Whole cell lysates were obtained using high salt buffer [50 mM HEPES, 500 mM NaCl, 1.5 mM $MgCl_2$, 1 mM EGTA, 10% glycerol, 1% Triton X-100 (pH 7.5), and 5 μL/ml of Protease Inhibitor Cocktail (Sigma-Aldrich)]. Protein samples were incubated at 100°C for 2 - 3 min, separated on 10% SDS-PAGE at 120 V for 3 - 4 hr in 1X running buffer [25 mM Tris-base, 192 mM glycine, and 0.1% SDS (pH 8.3)], and transferred to polyvinylidene difluoride membrane (PVDF, Bio-Rad, Hercules, CA) at 0.1 V for 16 hr at 4°C in 1X transfer buffer (48 mM Tris-HCl, 39 mM glycine, and 0.025% SDS). The PVDF membrane was blocked in 5% TBST-Blotto [10 mM Tris-

HCl, 150 mM NaCl (pH 8.0), 0.05% Triton X-100, and 5% non-fat dry milk] with gentle shaking for 30 min and incubated in fresh 5% TBST-Blotto with 1:1000 (for CD1, p27, Bcl2, Bax and caveolin 1), 1:500 (for PARP and NAG-1) and 1: 5000 (for β-actin) primary antibody overnight with gentle shaking at 4°C. After washing with TBST for 10 min, the PVDF membrane was incubated with secondary antibody (1:5000) in 5% TBST-Blotto for 90 min. The membrane was washed with TBST for 10 min and incubated with 10 ml of chemiluminiscence substrate (PerkinElmer Life Sciences) for 1.0 min and exposed to Kodak X-OMAT AR autoradiography film (Eastman Kodak, Rochester, NY).

Xenograft experiment

Male athymic BALB/c nude mice (aged 4 - 6 weeks) were purchased from Harlan (Indianapolis, IN). Mice were housed and maintained in laminar flow cabinets under specific pathogen-free conditions. SW480 cells were concentrated to 2 x 10^6 per 200 µL and injected s.c. into the left flank of each mouse using a 30-gauge needle. Six days after cell inoculation, animals were divided into three equal groups of 10 mice each. The first group received 70 µL of vehicle (corn oil) by oral gavage and the second and third groups of animals received 20 and 40 mg/kg/day doses of DIM-C-pPhC$_6$H$_5$ in vehicle, every second day. The mice were weighed, and tumor areas were also measured every other day. Final body and tumor weights were determined at the end of the dosing regimen, and selected tissues were further examined by routine H & E staining and immunohistochemical analysis.

Immunohistochemistry

Tissue sections (4-5 μm thick) mounted on poly-L-lysine-coated slide were deparaffinized by standard methods. Endogenous peroxidase was blocked by the use of 3% hydrogen peroxide in PBS for 10 min. Antigen retrieval for NAG-1 staining was performed for 7.5 min in 10 mm sodium citrate buffer (pH 6) heated at 95°C in a steamer, followed by cooling for 15 min. The slides were washed with PBS and incubated for 30 min at room temperature with a protein blocking solution (Biostain Rabbit IgG system, Biomeda, Foster City, CA). Excess blocking solution was drained, and the samples were incubated overnight at 4°C with one of the following: a 1:100 dilution of activated caspase-3 antibody; or 1:100 dilution of NAG-1 antibody. Sections were then incubated with biotinylated secondary antibody followed by steptavidin (Biostain Rabbit IgG system, Biomeda, Foster City, CA). The color was developed by exposing the peroxidase to diaminobenzidine reagent (Vector Laboratories, Burlingame, CA), which forms a brown reaction product. The sections were then counterstained with Gill's hematoxylin. Activated caspase-3 and NAG-1 expression were identified by the brown colored cytoplasmic staining.

Assesment of apoptotic cells

Four slides per group were stained and apoptotic cells were identified by the dark brown cytoplasmic staining. Ten microscopic fields in each slide were counted for cytoplasmic staining and averaged.

Results

Inhibition of cell proliferation and activation of PPARγ

Previous studies in colon and pancreatic cancer cells showed that PPARγ-active C-DIMs inhibit cell growth (394, 395) and results in Figure 5.1 also show the DIM-C-pPhCF$_3$, DIM-C-pPhtBu and DIM-C-pPhC$_6$H$_5$ inhibit SW480 cancer cell proliferation. IC$_{50}$ values varied between 1 - 10 μM and the relative order of potency was DIM-C-pPhCF$_3$ > DIM-C-pPhtBu > DIM-C-pPhC$_6$H$_5$. In contrast, 1 - 10 μM rosiglitazone did not significantly affect growth of SW480 cells. Activation of PPARγ was also investigated in SW480 cells transfected with chimeric PPARγ-Gal4 and a Gal4 response element reporter plasmid containing five tandem Gal4 response elements linked to a luciferase reporter gene.

The results showed that DIM-C-pPhCF$_3$, DIM-C-pPhtBu and DIM-C-pPhC$_6$H$_5$ significantly induced transactivation with a maximal 17-fold increase observed for 10 μM DIM-C-pPhCF$_3$, whereas a < 4-fold induction of luciferase activity was observed for rosiglitazone (Fig. 5.2A). We also investigated ligand-induced interactions of PPARγ with a panel of coactivators in a mammalian two-hybrid assay in SW480 cells (Fig. 5.2B). The results show that the PPARγ-active C-DIMs induce interactions between PPARγ and PGC-1 and similar results were obtained for the compounds in previous studies in HCT-15 cells, whereas in HT-29 cells, PGC-1 - PPARγ interactions were induced by DIM-C-pPhCF$_3$ and DIM-C-pPhtBu, but not DIM-C-pPhC$_6$H$_5$ (393). In contrast to results obtained in HT-29/HCT-15 cells, the PPARγ-active C-DIMs also
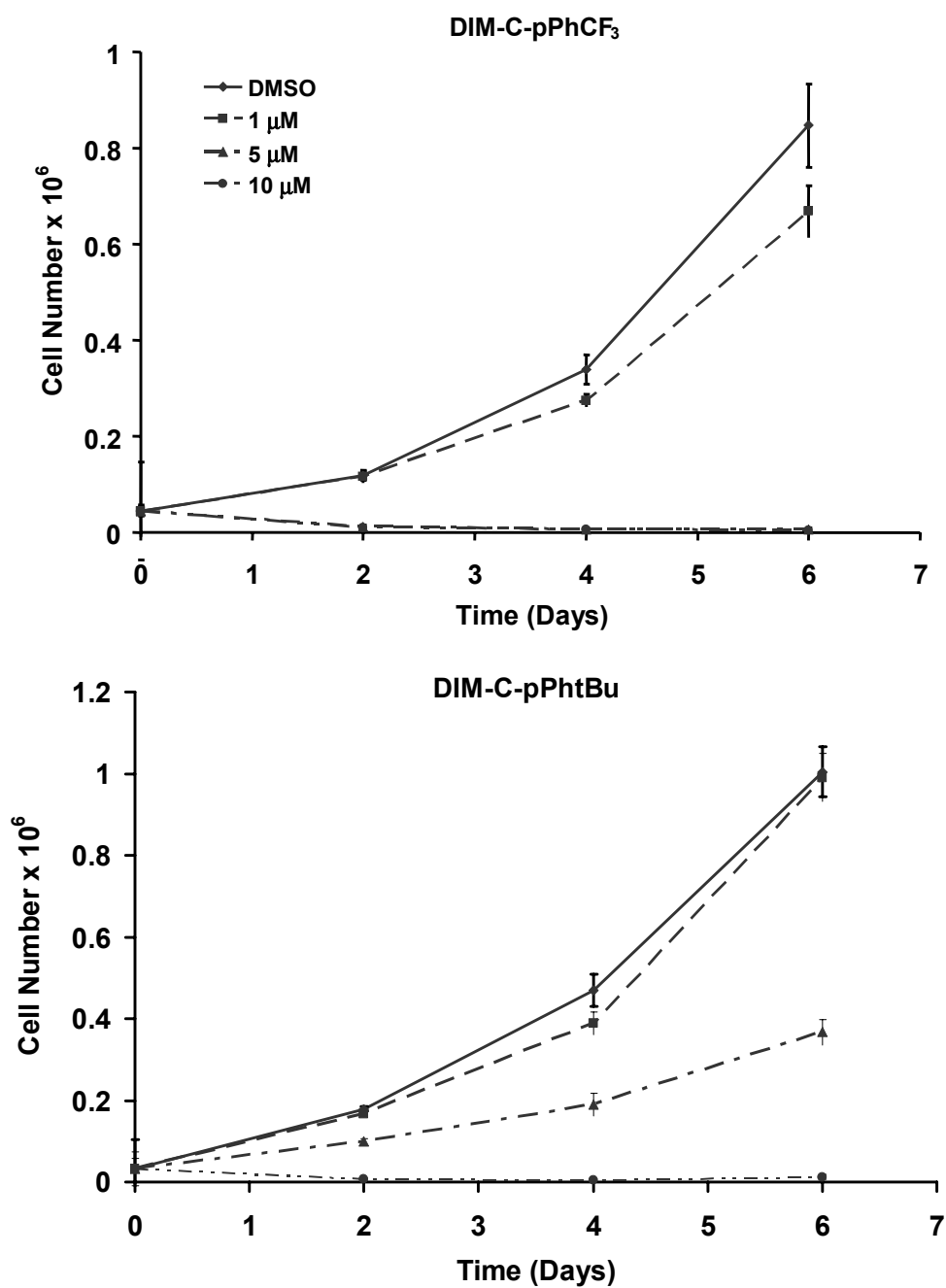
Fig. 5.1. Cell proliferation assays. SW480 cells were treated with DIM-C-pPhCF$_3$ [A], DIM-C-pPhtBu [B], DIM-C-pPhC$_6$H$_5$ [C] or rosiglitazone [D], and cell numbers were determined after 2, 4 and 6 days as described in the Materials and Methods. Significant ($p < 0.05$) inhibition of cell proliferation was observed for the C-DIMs (≥ 5 µM) and results are expressed as means $\pm$ SE for three replicate determinations for each treatment group.
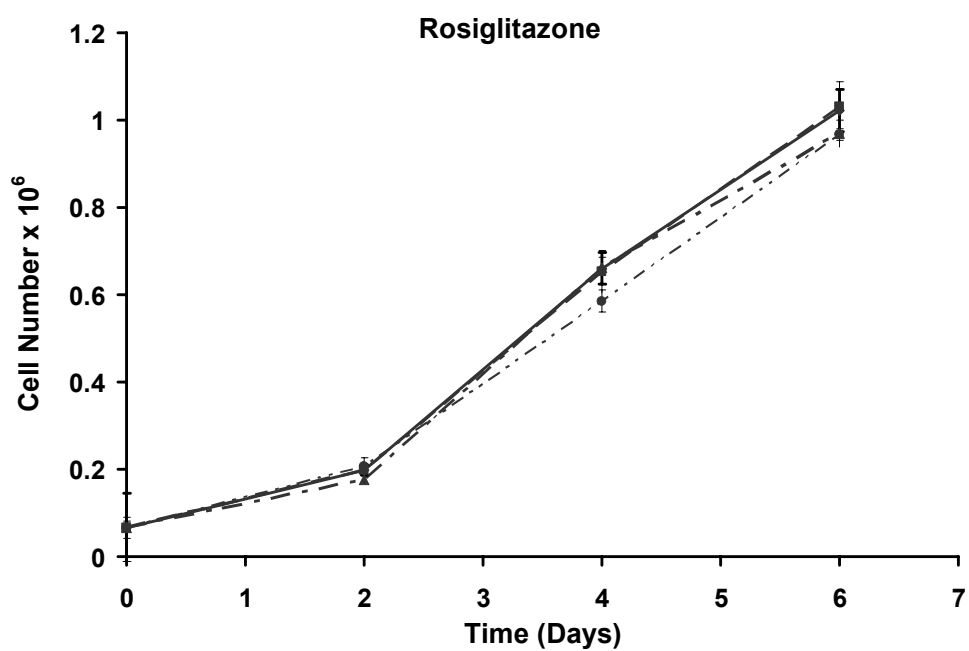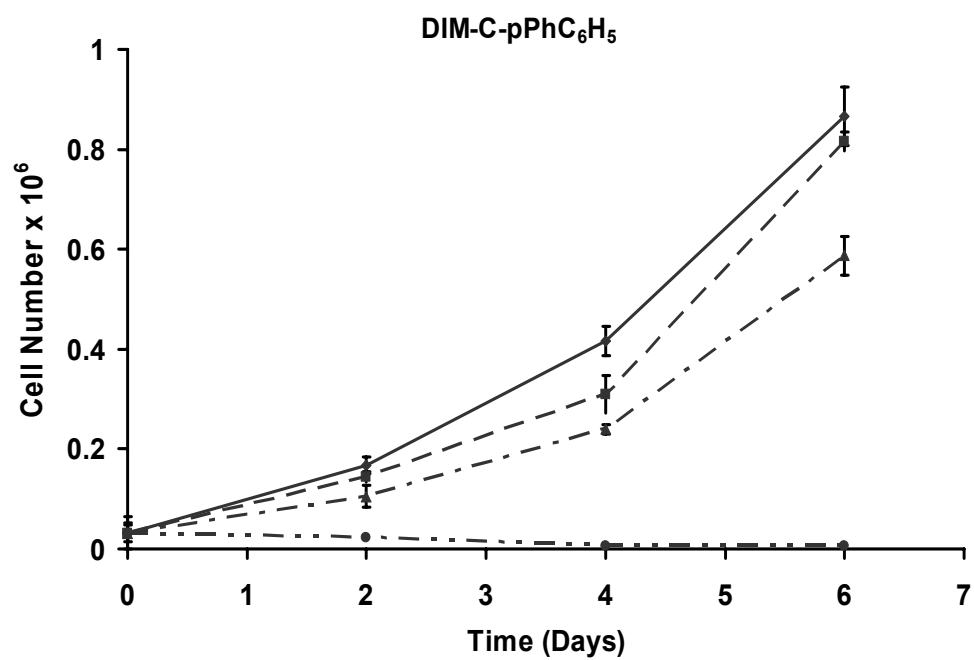
Fig. 5.1 Continued
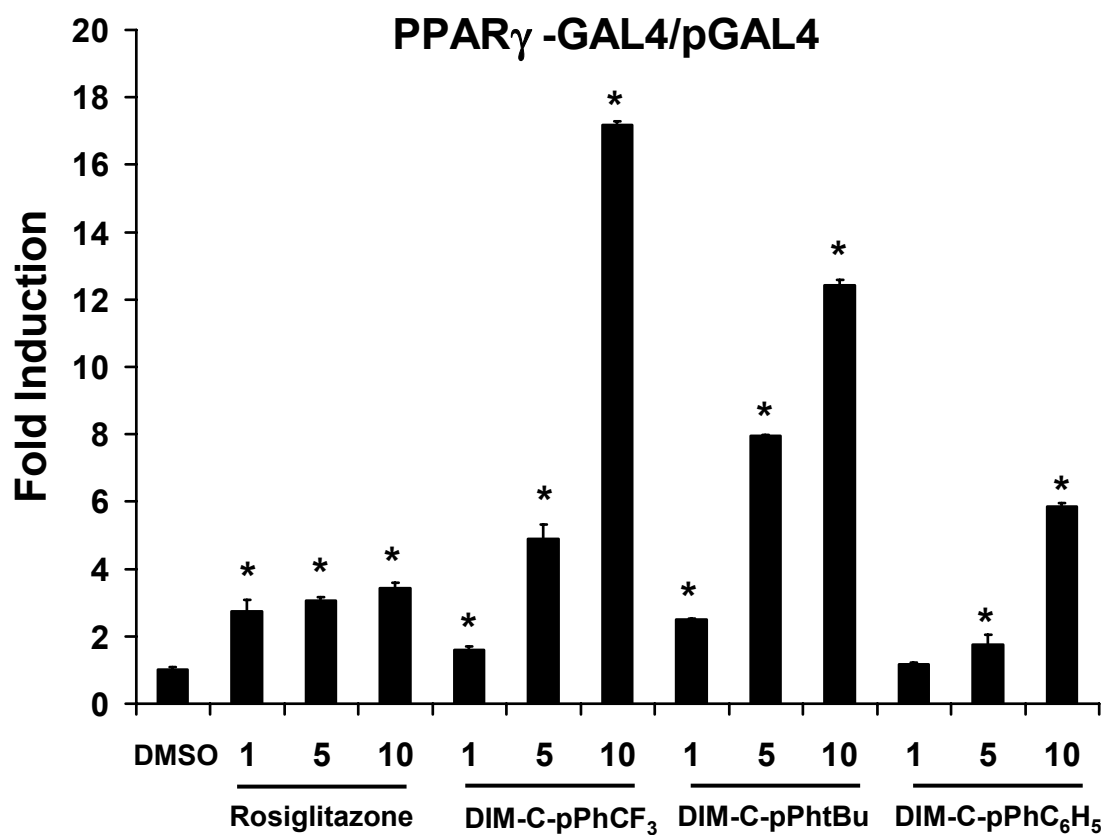
Fig. 5.2. C-DIMs activate PPARγ. [A] Transactivation. SW480 cells were transfected with PPARγ/Gal4/pGal4, treated with DMSO or different concentrations of compounds, and luciferase activity determined as described in the Materials and Methods. [B] Mammalian two-hybrid assay. SW480 cells were transfected with GAL4 chimeras, VP-PPARγ (LBD) and pGAL4-luc, treated with various compounds, and luciferase activity determined as described in the Materials and Methods. Results [A / B] are expressed as means ± SE for three replicate determinations for each treatment group and significant ($p < 0.05$) induction is indicated by asterisks.
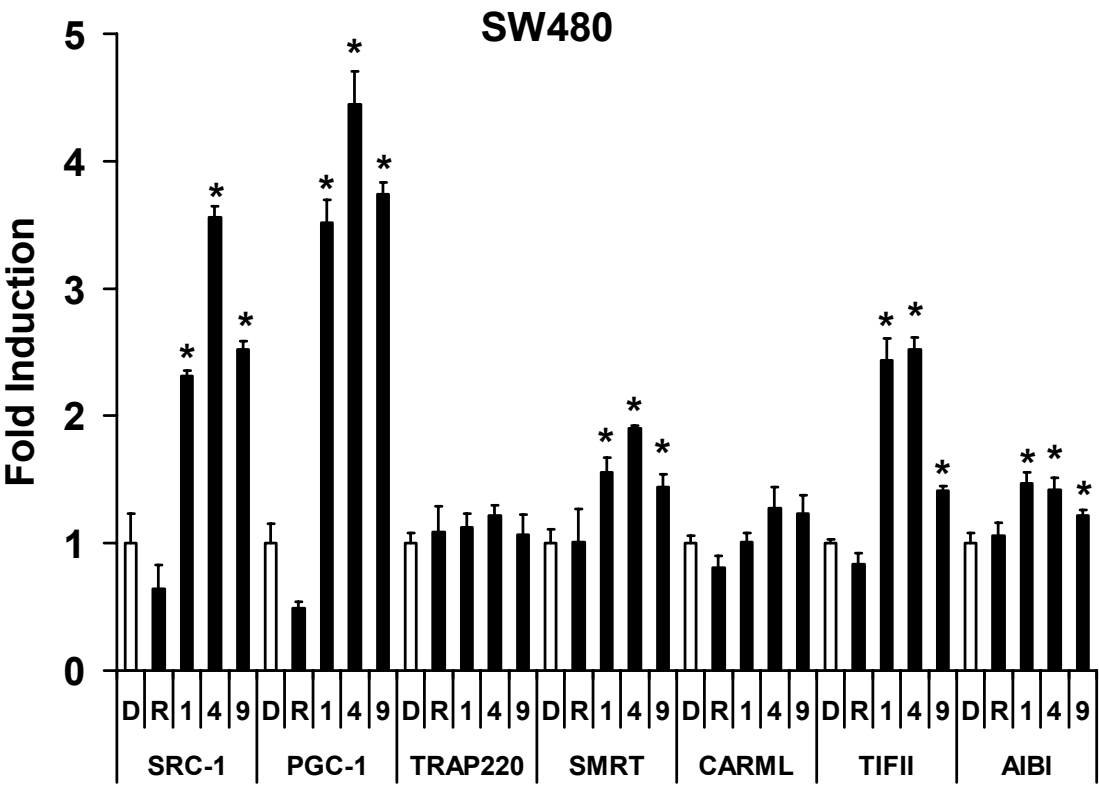
Fig. 5.2 Continued

significantly induced interactions of PPARγ with SRC-1, SRC-2 and the corepressor SMRT and this pattern of ligand-induced PPARγ-coactivator/corepressor interactions clearly differentiated between the effects of these compounds in SW480 and other colon cancer cells. In addition, rosiglitazone was inactive in the mammalian two hybrid assay in SW480 cells and this assay distinguished between the activities of this compound and the PPARγ-active C-DIMs.

Effects of PPARγ-active C-DIMs on expression of proteins associated with cell

proliferation and cell death

The effects of two prototypical PPARγ-active C-DIMs on expression of various cell cycle proteins and apoptosis (PARP cleavage) was investigated in SW480 cells treated with 5 - 10 μM Dim-C-pPhCF$_3$, DIM-C-pPhC$_6$H$_5$ or rosiglitazone for 24 hr (Fig. 5.3A). The PPARγ-active C-DIMs enhanced p27 expression and downregulated cyclin D1 protein only at the highest concentration and this was also accompanied by PARP cleavage. Previous studies with different structural classes of PPARγ agonists have reported induction of p27 in colon and other cancer cell lines, and we have also observed cyclin D1 downregulation and PARP cleavage in other cancer cell lines treated with C-DIM compounds (359, 393-395, 436, 437). There were minimal compound-induced changes in bax levels and decreased expression of bcl-2 at the 10 μM concentrations of DIM-C-pPhCF$_3$ and DIM-C-pPhC$_6$H$_5$, whereas up to 10 μM rosiglitazone did not affect expression of apoptotic or cell cycle proteins. The growth inhibitory effects of
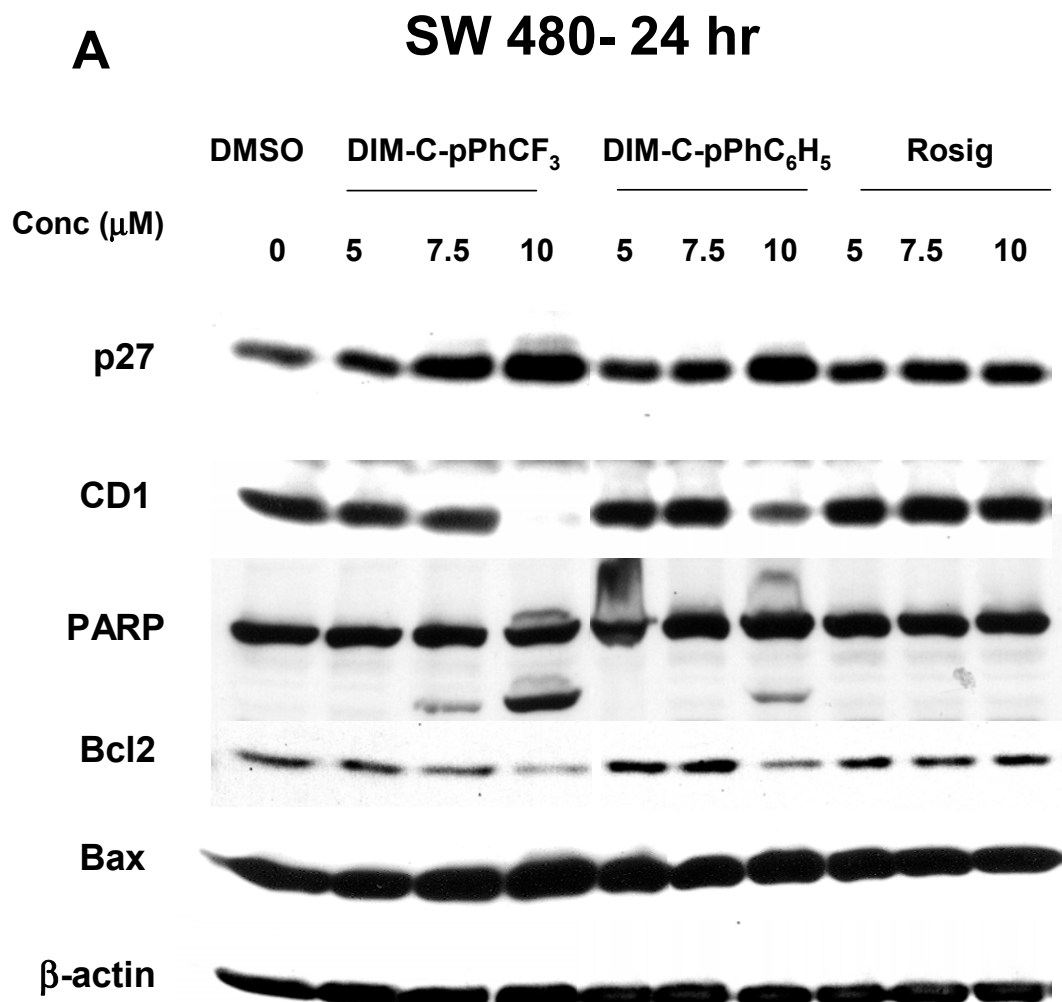
Fig. 5.3. Cell cycle proteins, caveolin-1 expression and Akt phosphorylation. [A] Cell cycle proteins. SW480 cells were treated with different concentrations of compounds for 24 hr, and whole cell lysates were analyzed by Western blot analysis as described in the Materials and Methods. Induction of caveolin-1 [B / C], Akt phosphorylation [D], and inhibition by GW9662 [C / D]. SW480 cells were treated with different concentrations of compounds alone or in combination, and whole cell lysates were analyzed by Western blot analysis as indicated in the Materials and Methods. β-Actin was used as a loading control for these experiments and levels of bax and p21 proteins [A] were unchanged in all treatment groups.

SW 480 - 96 hr

B

C　　　　　　**SW 480 – 96 hr**

D　　　　　　**SW 480 - 96hr**
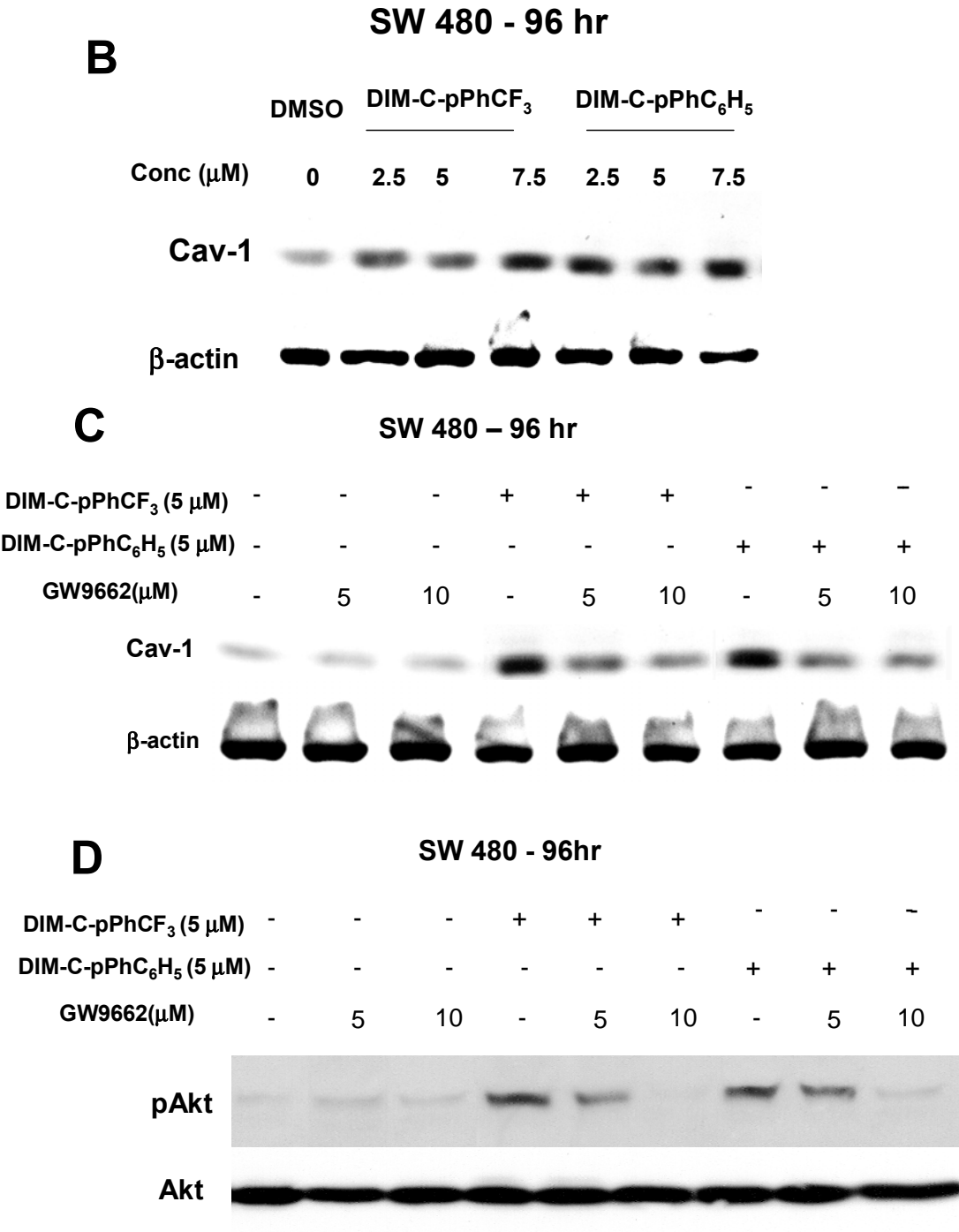
Fig. 5.3 Continued

PPARγ-active C-DIMs in HT-29 and HCT-15 cells have been linked, in part, to induction of caveolin-1 (393) and the results in Figure 5.3B show that at doses as low as 2.5 μM, there was induction of caveolin-1 in SW480 cells. This is a response that was not observed until 48 hr after treatment and only minimal apoptosis was induced in the 7.5 μM DIM-C-pPhCF$_3$ treatment group, suggesting that caveolin-1 was primarily associated with growth inhibitory responses observed at lower concentrations ($\leq$ 7.5 μM). Induction of caveolin-1 by 5 μM DIM-C-pPhCF$_3$ and DIM-C-pPhC$_6$H$_5$ was inhibited after cotreatment with the PPARγ antagonist GW9662 (Fig. 5.3C), demonstrating that this response was PPARγ-dependent, and this was previously observed in HT-29 and HCT-15 cells (393). We also recently reported that PPARγ-dependent induction of caveolin-1 was observed in SW480 cells treated with CDDO and related compounds (396) and this was accompanied by induction of PI3-K-dependent phosphorylation of Akt. The results in Figure 5.3D also show that 5 μM DIM-C-pPhCF$_3$ and DIM-C-pPhC$_6$H$_5$ also induce Akt phosphorylation and in SW480 cells cotreated with GW9662, there was a dose-dependent decrease in Akt phosphorylation. Thus, the PPARγ-active C-DIMs coordinately induced caveolin-1 and phospho-Akt in SW480 cells and it has been reported that combined activation of caveolin-1 and PI3-K enhances the effects of agents that decrease cancer cell survival (364, 438).

The role of PPARγ in mediating DIM-C-pPhCF$_3$- and DIM-C-pPhC$_6$H$_5$-induced apoptosis was investigated in SW480 cells cotreated with C-DIMs and the PPARγ antagonist GW9662 (Fig. 5.4A). The results show that GW9662 did not affect induced

PARP cleavage, suggesting that this response was PPARγ-independent and similar results were observed for cyclin D1 downregulation. Interestingly, we also observed that at higher concentrations (> 7.5 μM) of C-DIMs that induce apoptosis in SW480 cells (Fig. 5.4A), there is a loss of caveolin-1 induction by these same compounds (Fig. 5.4B). The reason for this concentration-dependent switch between PPARγ-dependent and -independent responses is unknown; however, we have also observed similar responses for CDDO and related compounds. Recent studies in this laboratory show that PPARγ-active C-DIMs induced cell death through activation of endoplasmic reticulum (ER) stress in pancreatic cancer cells (437) or through induction of NAG-1 in HCT116 colon cancer cells (436). Results in Figure 5.4C show that induction of apoptosis in SW480 cells treated with DIM-C-pPhCF$_3$ or DIM-C-pPhC$_6$H$_5$ for 24 hr is not accompanied by induction of the stress protein GRP78.

NAG-1 is a transforming growth factor β (TGFβ)-like peptide which is induced by C-DIMs and many other growth inhibitory agents including rosiglitazone in selected cell lines including HCT-116 colon cancer cells. Preliminary studies did not detect induction of NAG-1 by C-DIMs in SW480 cells (437); however, repetition of this experiment with a different antibody showed that within 24 hr after treatment with DIM-C-pPhCF$_3$ or DIM-C-pPhC$_6$H$_5$, there was induction of NAG-1 protein (Fig. 5.5A). Moreover, in SW480 cells cotreated with PPARγ-active C-DIMs (5 - 10 μM) plus the PPARγ agonist GW9662 (10 μM), the antagonist did not block induction of NAG-1 (Fig. 5.5B), suggesting that this response was PPARγ-independent as previously

A   **SW 480 - 24hr**

GW9662 (µM)	-	10	-	10	-	10	-	10	-	10	-	10	-	10	-	10
DIM-C-pPhC$_6$H$_5$ (µM)	-	-	7.5	7.5	10	10	15	15	-	-	-	-	-	-	-	-
DIM-C-pPhCF$_3$ (µM)	-	-	-	-	-	-	-	-	5	5	7.5	7.5	10	10	15	15

PARP

β-Actin
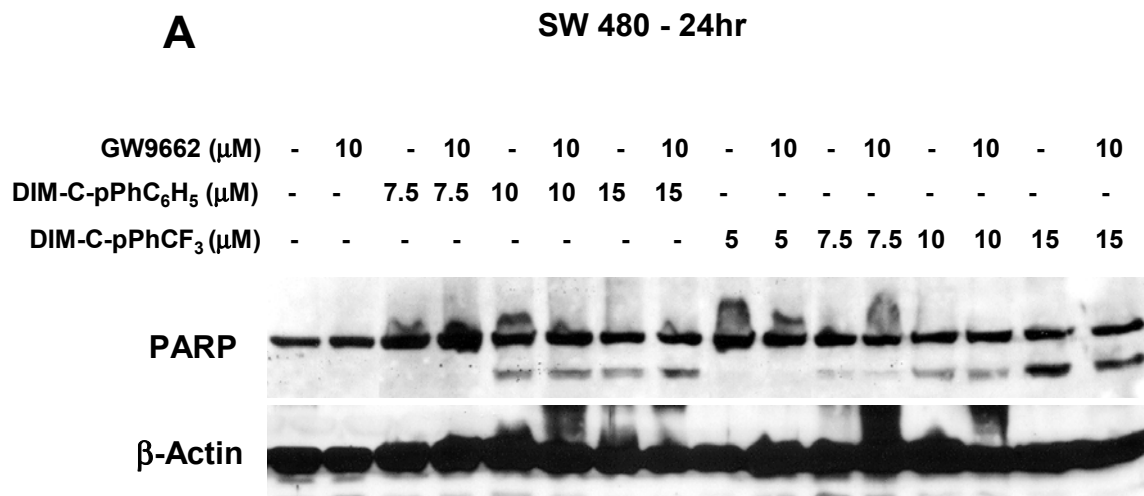
Fig. 5.4. Effects of higher concentrations of C-DIMs on PARP cleavage [A], caveolin-1 [B], GRP78 [C] expression. SW480 cells were treated with different compounds (alone or combined) for 24 [A and C] or 72 [B] hr, and whole cell lysates were assayed by Western blot analysis as described in the Materials and Methods. β-Actin served as a loading control for all experiments.

B

C

SW 480 - 24 hrs

Fig. 5.4 Continued

A   **SW 480**

24 hr	DMSO	DIM-C-pPhC$_6$H$_5$				DIM-C-pPhCF$_3$			
Conc (µM)	0	2.5	5	7.5	10	2.5	5	7.5	10

NAG-1

β-actin
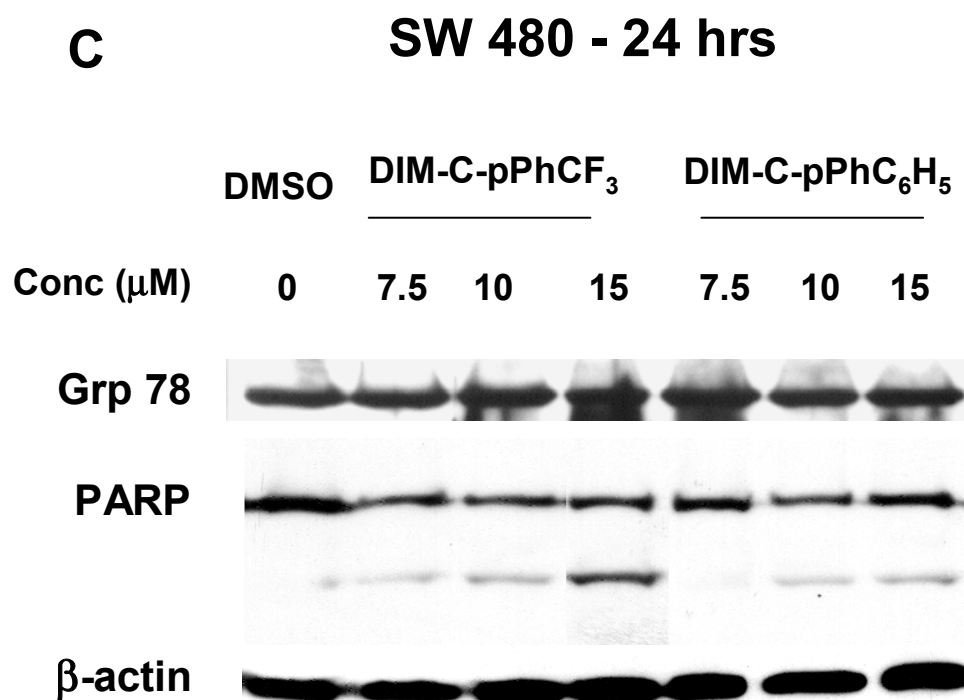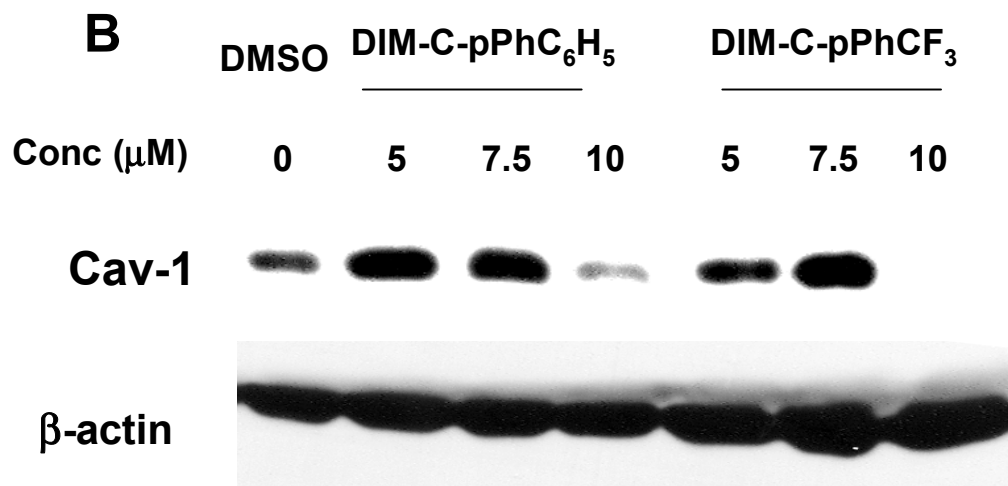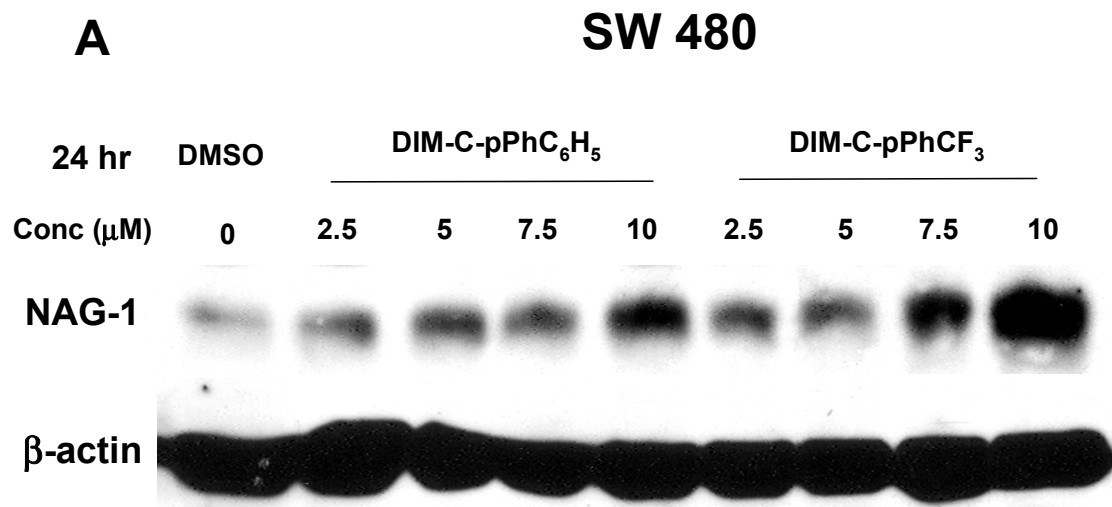
Fig. 5.5. Induction of NAG-1 by C-DIM compounds. SW480 cells were treated for 24 hr with DIM-C-pPhCF$_3$ or DIM-C-pPhC$_6$H$_5$ alone [A] or in combination with GW9662 [B] or for 96 hr [C]. Whole cell lysates were analyzed for NAG-1 expression by Western blot analysis as described in the Materials and Methods. β-Actin was used as a loading control for these experiments.

B   **SW 480**

24 hr

DIM-C-pPhCF₃ (μM)	-	-	-	-	-	-	-	-	5	5	7.5	7.5	10	10
DIM-C-pPhC₆H₅ (μM)	-	-	5	5	7.5	7.5	10	10	-	-	-	-	-	-
GW9662(μM)	-	10	-	10	-	10	-	10	-	10	-	10	-	10

NAG-1

β-actin

C

| 96 hr | DMSO | DIM-C-pPhC₆H₅ | | | | DIM-C-pPhCF₃ | | | |
| Conc (μM) | 0 | 2.5 | 5 | 7.5 | 10 | 2.5 | 5 | 7.5 | 10 |

NAG-1

β-actin
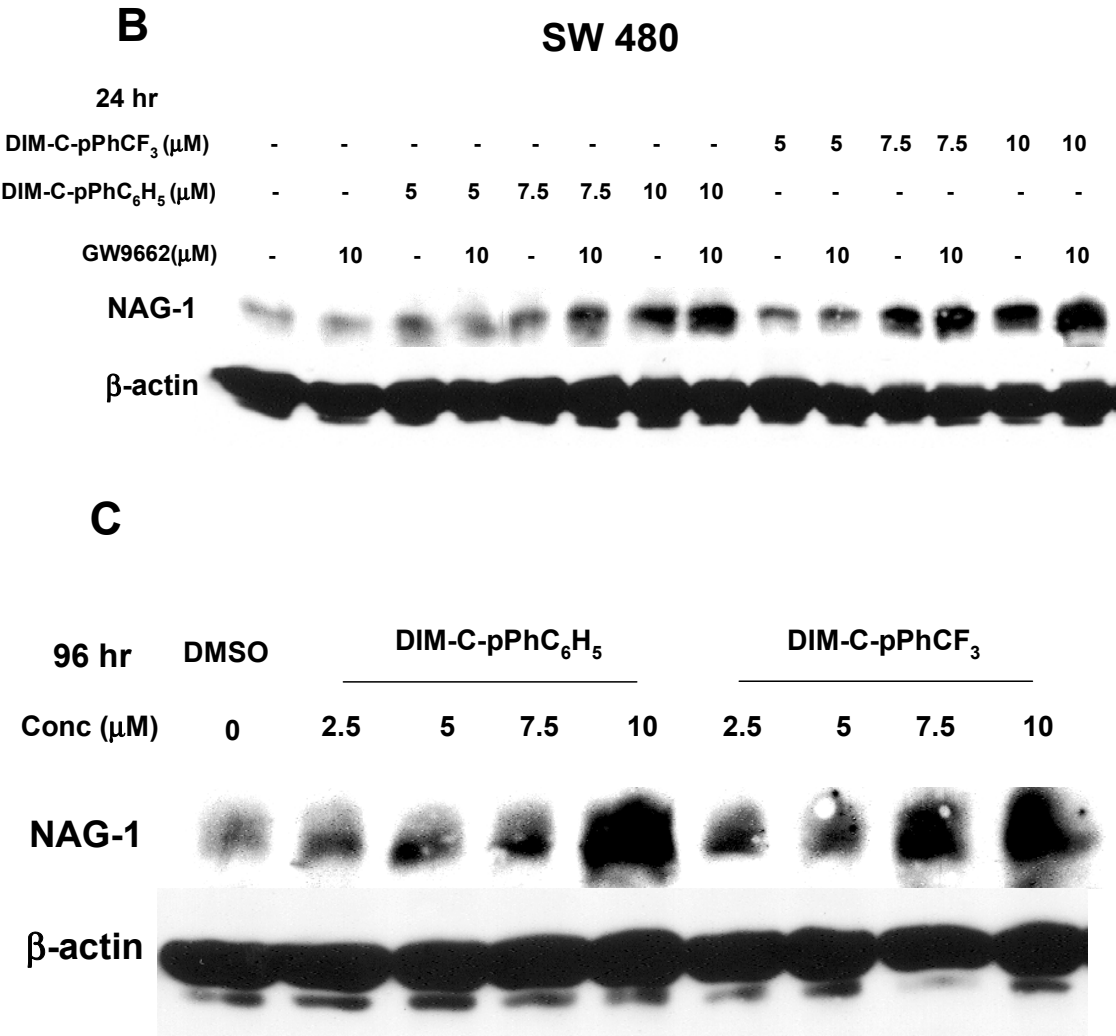
Fig. 5.5 Continued

reported in HCT-116 cells (437). We also observed induction of NAG-1 after treatment with C-DIMs for 96 hr (Fig. 5.5C) and at both the 24 and 96 hr time points, effective doses were in the 7.5 - 10 µM range.

The *in vivo* antitumorigenic activity of PPARγ-active C-DIMs was further investigated in male athymic nude mice bearing SW480 cell xenografts. After palpable tumors were first observed (< 15 mm^2), animals were treated with corn oil (70 µL/mouse) or DIM-C-pPhC$_6$H$_5$ (20 or 40 mg/kg) in corn oil by oral gavage every second day for 21 days and tumor areas were determined. The results (Fig. 5.6A) show that tumor areas were significantly decreased after treatment with DIM-C-pPhC$_6$H$_5$ compared to the corn oil (control) group and after sacrifice, tumor weights were also decreased in both treatment groups (Fig. 5.6B). We also investigated the effects of DIM-C-pPhC$_6$H$_5$ (40 mg/kg/d) on expression of the apoptotic gene caspase 3 (Figs. 5.6C and 5.6D) and NAG-1 in tumors by immunohistochemical analysis. DIM-C-pPhC$_6$H$_5$ significantly induced active caspase 3 expression compared to control (corn oil) tumors (Fig. 5.6C). NAG-1 was not detected in tumors from control animals, whereas massive expression (brown staining) of NAG-1 was detected in tumors from DIM-C-pPhC$_6$H$_5$-treated mice (Fig. 5.6D), suggesting an important role for this protein in the antitumorigenic activity of this C-DIM compound. These data complement the *in vitro* studies and demonstrate that PPARγ-active C-DIMs inhibit colon cancer cell/tumor growth and these compounds are being developed for future clinical applications.
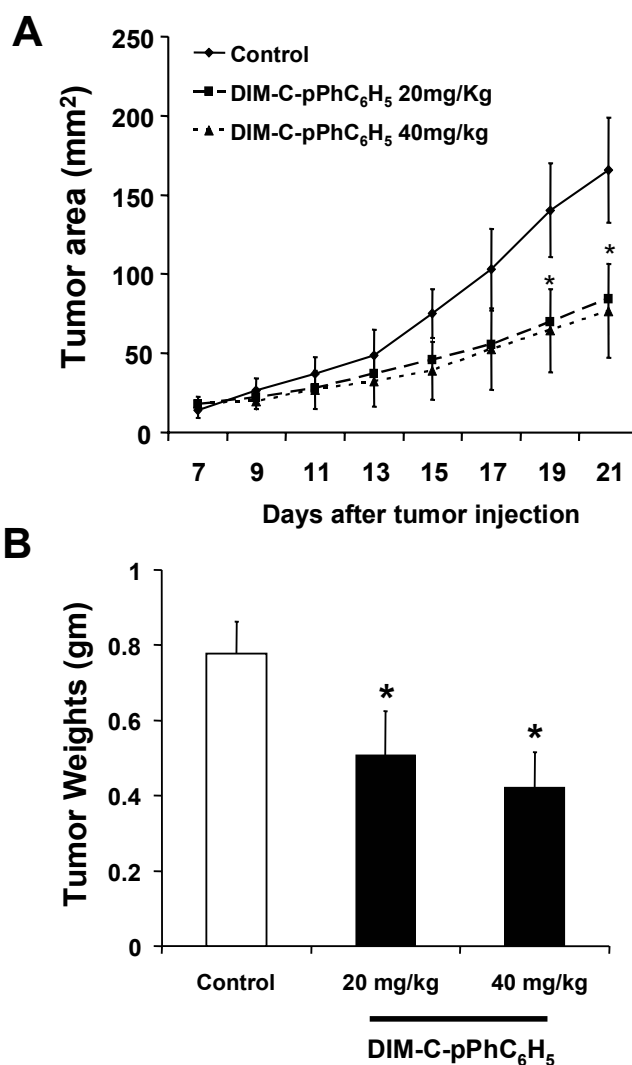
Fig. 5.6. *In vivo* antitumorigenic activity of DIM-C-pPhC$_6$H$_5$. Tumor areas [A] and weights [B]. When palpable tumors were first observed (15 mm^2), athymic nude mice bearing SW480 colon cancer cell xenografts were administered corn oil (control) or DIM-C-pPhC$_6$H$_5$ (20 or 40 mg/kg/d) in corn oil by oral gavage, and tumor areas and weights were determined as described in the Materials and Methods. Results are expressed as means ± SE for 10 animals for each treatment group, and a significant (p < 0.05) decrease in tumor areas and weights in the treatment groups compared to the corn oil (control) group is indicated by an asterisk. [C] Active caspase 3 expression. Active caspase 3 expression was quantitated by immunohistochemical analysis of caspase 3 in tumor sections from control and treated (DIM-C-pPhC$_6$H$_5$, 40 mg/kg/d) mice as described in the Materials and Methods. Arrows indicate positive caspase 3 staining. [D] Immunohistochemical analysis of NAG-1. Tumors from control or DIM-C-pPhC$_6$H$_5$-treated mice were analyzed for NAG-1 expression by immunohistochemistry as described in the Materials and Methods. There were no significant differences in animal weight gain, organ weights or histopathology in any of the treatment groups.

C

Active
Caspase-3

Control   Treated

D

NAG-1

Control   Treated
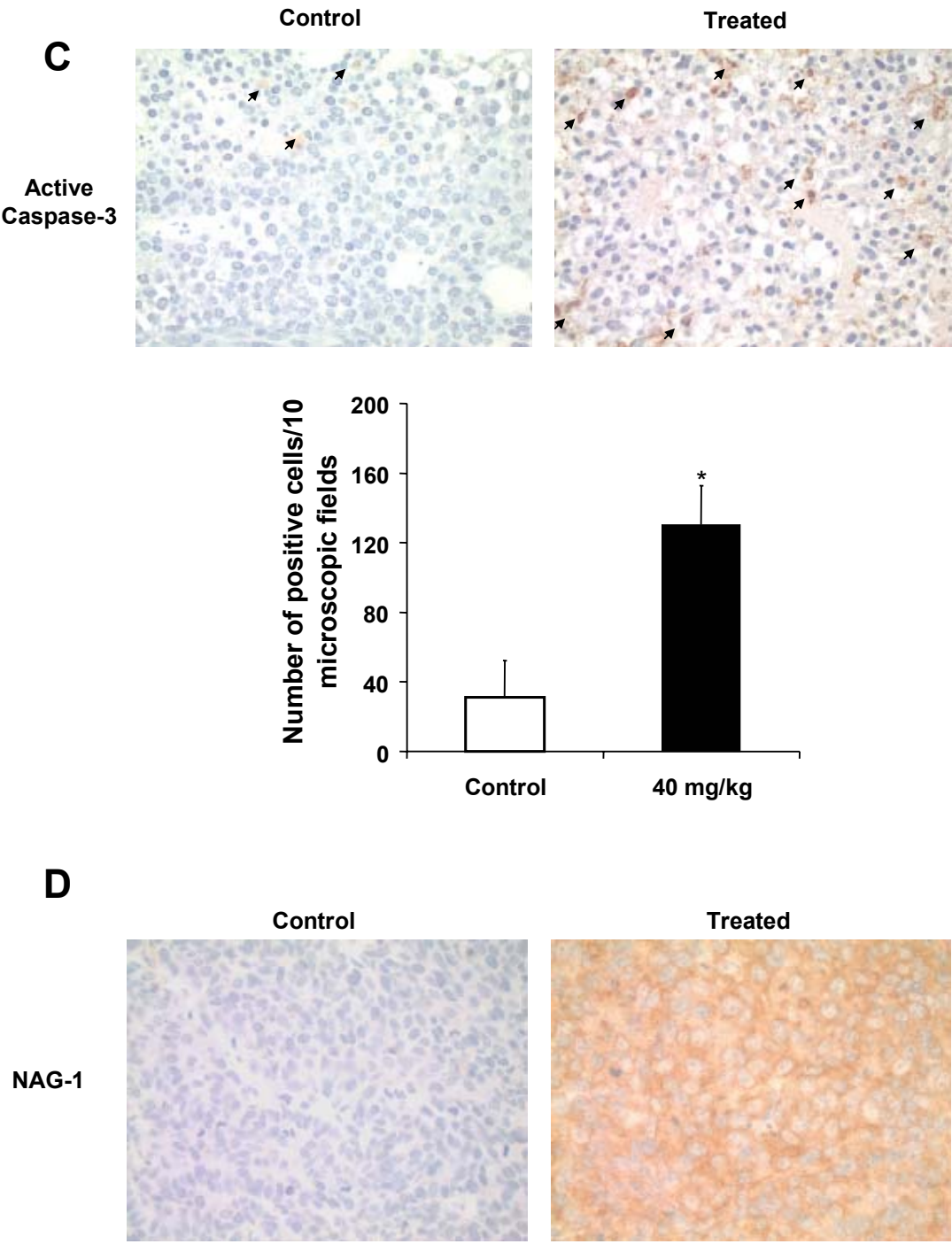
Fig. 5.6 Continued

Discussion

Several studies report that PPARγ agonists inhibit growth of colon cancer cells; however, their induced responses and mechanisms of action are dependent on multiple factors including ligand structure, cell context and wild-type or variant PPARγ expression. For example, troglitazone (a TZD), PGJ2 and PPARγ-active C-DIMs induce the TGFβ-like peptide NAG-1 in HCT-116 cells and GW9662 inhibits the effects of PGJ2 but had no effect on troglitazone or the PPARγ-active C-DIMs (303, 436). Although troglitazone, DIM-C-pPhCF$_3$, DIM-C-pPhtBu and DIM-C-pPhC$_6$H$_5$ induce NAG-1 through prior activation of early growth response gene (303, 436), the former response is dependent on activation of mitogen-activated protein kinase, whereas the C-DIMs activate Egr-1 and NAG-1 through induction of PI3-K. Dubois and coworkers (360, 362, 373) have reported that the effects of rosiglitazone on cell proliferation and differentiation in several colon cancer cell lines were dependent on their expression of wild-type or mutant K422Q PPARγ where rosiglitazone responsiveness was observed only in cells (e.g. HT-29) expressing wild-type receptor (362).

PPARγ-active C-DIMs inhibit growth of HT-29 and HCT-15 colon cancer cell lines expressing wild-type and mutant PPARγ, respectively, and these compounds also induce caveolin-1 in both cell lines (393). The results in Figures 5.1 and 5.2 demonstrate that the C-DIM compounds but not rosiglitazone inhibit SW480 cancer cell growth and induced PPARγ-dependent transactivation. These data are similar to those previously reported in rosiglitazone-nonresponsive HCT-15 cells, suggesting that

SW480 cells may also express mutant PPARγ which is not responsive to the growth inhibitory effects of rosiglitazone.

The short-term effects of DIM-C-pPhCF$_3$ and DIM-C-pPhC$_6$H$_5$ on cell cycle protein expression and apoptosis in SW480 (Fig. 5.4) vs. HT-29/HCT-15 cells (393) were different. Growth inhibitory concentrations (5.0 and 7.5 µM) did not affect p21 or cyclin D1 expression in SW480, HT-29 or HCT-15 cells, whereas p27 protein levels were slightly elevated in SW480 cells after treatment with 7.5 µM DIM-C-pPhCF$_3$ and 10 µM DIM-C-pPhCF$_3$ and DIM-C-pPhC$_6$H$_5$. Another major difference observed in this study with SW480 cells was the induction of apoptosis and downregulation of cyclin D1 after treatment with 10 µM DIM-C-pPhCF$_3$ and DIM-C-pPhC$_6$H$_5$ for 24 hr, whereas these responses were not observed in HT-29 or HCT-15 cells (393).

Despite the cell context-dependent differences in the effects of PPARγ-active C-DIMs in colon cancer cells, the results in Figure 5.3 demonstrate that PPARγ-active C-DIMs induce caveolin-1 expression in SW480 cells after prolonged treatment (3 d) with concentrations as low as 2.5 µM. This response in SW480 cells was inhibited by GW9662 and similar results were observed for PPARγ-active C-DIMs and also for CDDO and related compounds in colon cancer cells (393, 396). In this study, we also observed PPARγ-dependent upregulation of phospho-Akt in SW480 cells and similar results have been observed for CDDO and related compounds in the same cell line (396). The induction of caveolin-1 at the lower doses (< 7.5 µM) of DIM-C-pPhCF$_3$ and DIM-C-pPhC$_6$H$_5$ is consistent with the growth inhibitory effects of these compounds

since caveolin-1 expression has been linked to inhibition of colon cancer cell/tumor proliferation in both *in vitro* and *in vivo* models (398, 399). The observation that DIM-C-pPhCF$_3$ and DIM-C-pPhC$_6$H$_5$ induce PI3-K dependent phosphorylation of Akt, which is normally a cell survival pathway, was also consistent with the observed growth inhibitory effects of these compounds. PI3-K and caveolin-1 coexpression sensitizes HeLa and 293 cells to the cytotoxicity of arsenite and hydrogen peroxide (438) and sensitizes L929 cells to tumor necrosis factor α-induced cell death (364).

Several studies show that PPARγ agonists induce both receptor-dependent and independent responses (303, 359, 391, 393-397, 436, 437) and in this study these pathways are separable at different concentrations of C-DIMs. At low concentrations (> 7.5 μM), DIM-C-pPhCF$_3$ and DIM-C-pPhC$_6$H$_5$ induce receptor-dependent upregulation of caveolin-1 (Fig. 5.3), whereas at higher concentrations (> 7.5 μM), these same compounds induce apoptosis which was not inhibited by GW9662, a PPARγ antagonist (Fig. 5.4A). Similar results were observed for CDDO and related compounds in SW480 cells (396). Interestingly, there appears to be a narrow concentration range for the switch between receptor-dependent and receptor-independent responses. Moreover, induction of PPARγ-dependent caveolin-1 expression by ≥ 7.5 μM DIM-C-pPhCF$_3$ or DIM-C-pPhC$_6$H$_5$ is lost in cells treated with 10 μM concentrations of these same compounds (Fig. 5.4B) where extensive apoptosis is observed. In other cell lines, we have recently shown that C-DIMs induce ER stress which leads to activation of DR5 and the extrinsic pathway for apoptosis (436); however, this response was not observed in SW480 cells (Fig. 5.4C). In contrast, both DIM-C-pPhC$_6$H$_5$ and DIM-C-pPhCF$_3$

induced NAG-1 expression at concentrations ($\geq$ 7.5 µM) similar to those required for induction of apoptosis (PARP cleavage) and both responses were PPARγ-independent. Moreover, previous studies have demonstrated that NAG-1 induces apoptosis and activation of caspases in cancer cell lines (402, 439), suggesting that PPARγ-independent induction of apoptosis in SW480 cells by C-DIM compounds is due to upregulation of NAG-1 expression. These *in vitro* responses are also duplicated in the athymic nude mouse xenograft studies where DIM-C-pPhC$_6$H$_5$ not only inhibits tumor growth but induces caspase 3 and NAG-1 expression in the tumors (Fig. 5.6)

In summary, our results show that PPARγ-active C-DIMs inhibit SW480 cell proliferation and inhibit colon tumor growth in an athymic nude mouse xenograft model (Fig. 5.6). The effectiveness of C-DIMs as anticancer agents is enhanced by their activation of both receptor-dependent and -independent pathways and this dual mechanism of action is shared by other classes of PPARγ agonists. Ongoing studies in this laboratory are focused on development of new and more potent C-DIM analogs for treatment of colon cancer and on determining the receptor-independent mechanisms of action of C-DIMs and related PPARγ agonists.

CHAPTER VI

ACTIVATION OF NUR77 BY SELECTED 1,1-BIS(3'-INDOLYL)-1-(*p*-SUBSTITUTEDPHENYL)METHANES INDUCES APOPTOSIS THROUGH NUCLEAR PATHWAYS*

Introduction

The nuclear receptor superfamily of eukaryotic transcription factors encompasses steroid hormone and other nuclear receptors for which ligands have been identified and orphan receptors with no known ligands (440-446). Nuclear receptors share common structural features which include an N-terminal A/B domain, containing activation function-1 (AF-1), and a C-terminal E domain, which contains AF-2 and the ligand binding domain (LBD). Nuclear receptors also have a DNA binding domain [DBD, (C)], a variable hinge (D), and C-terminal F regions. Ligand activation of class 1 steroid hormone receptors induces homo- or heterodimer formation which interact with consensus or nonconsensus palindromic response elements. In contrast, class 2 receptors form heterodimers with the retinoic X receptor (RXR) as a common partner, whereas class 3 and 4 orphan receptors act as homodimers or monomers and bind to direct response element repeats or single sites, respectively. The DBDs of nuclear receptors all

---

*Reprinted with permission from "Activation of Nur77 by selected 1,1-bis(3'-indolyl)-1-(p-substituted phenyl)methanes induces apoptosis through nuclear pathways" by Chintharlapalli S, Burghardt R, Papineni S, Ramaiah S, Yoon K, Safe S. J Biol Chem 2005;280:24903-24914. Copyright 2005 by American Society for Biochemistry and Molecular Biology.

contain two zinc finger motifs that interact with similar half-site motifs; however, these interactions vary with the number of half-sites (1 or 2), their orientation, and spacing. Differences in nuclear receptor action are also determined by their other domains which dictate differences in ligand binding, receptor dimerization and interaction with other nuclear cofactors.

Most orphan receptors were initially cloned and identified as members of the nuclear receptor family based on their domain structure and endogenous or exogenous ligands have subsequently been identified for many of these proteins (444-446). The nerve growth factor I-B (NGFI-B) family of orphan receptors were initially characterized as immediate early genes induced by nerve growth factor in PC12 cells and the three members of this family include NGFI-Bα (Nur77), NGFI-Bβ (Nurr1), NGFI-Bγ (Nor1) (447-449).

Nur77 plays an important role in thymocyte-negative selection and in T-cell receptor (TCR)-mediated apoptosis in thymocytes (327, 450), and overexpression of Nur77 in transgenic mice resulted in high levels of apoptosis in thymocytes (451, 452). In cancer cells, several mechanisms for Nur77-mediated apoptosis have been described and differences between studies may be due to the apoptosis-inducing agent or cell line (453-459). For example, the retinoid 6-[3-(1-adamantyl)-4-hydroxyphenyl]-2-naphthalene carboxylic acid (CD437) and 12-*O*-tetradecanoylphorbol-13-acetate (TPA) induce translocation of Nur77 from the nucleus to the mitochondria where Nur77 binds Bcl-2 to form a pro-apoptotic complex (453, 454). In contrast, it has been suggested that TPA-induced Nur77 in LNCaP prostate cancer cells activates transcription of E2F1

which is also pro-apoptotic (459). These studies are examples of ligand-independent pathways where Nur77 expression is induced and/or Nur77 protein undergoes intracellular translocation since ligands for this receptor have hitherto not been reported. This paper shows that 1,1-bis(3'-indolyl)-1-(*p*-substitutedphenyl)methanes containing trifluoromethyl, hydrogen and methoxy substituents induce Nur77-dependent transactivation in Panc-28 pancreatic and other cancer cell lines. Nur77 agonists also induce typical cellular signatures of apoptosis including PARP cleavage and induction of TRAIL, and both ligand-dependent transactivation and induction of apoptosis were associated with the action of nuclear Nur77. This study shows for the first time that ligand-dependent activation of the orphan receptor Nur77 induces apoptosis in cancer cells, suggesting that Nur77 agonists represent a new class of anticancer drugs.

Materials and Methods

Cell lines and reagents

Panc-28, Panc-1, MiaPaCa-2, LNCaP, MCF-7, HT-29 and HCT-15 cancer cell lines were obtained from the American Type Culture Collection (Manassas, VA). RKO, DLD-1 and SW-480 colon cancer cells were provided by Dr. S. Hamilton, and KU7 and 253-JB-V-33 bladder cells were provided by Dr. A. Kamat (M.D. Anderson Cancer Center, Houston, TX). The C-substituted DIMs were synthesized in this laboratory as previously described (359). Antibodies for PARP (sc8007), Sp1 (sc-59) and TRAIL (sc7877) were purchased from Santa Cruz Biotechnology (Santa Cruz, CA) and Nur77 (IMG-528) from Imgenex (San Diego, CA). The GAL 4 reporter containing five GAL4 response elements (pGAL4) was provided by Dr. Marty Mayo (University of North

Carolina, Chapel Hill, NC). The GAL4-Nur77 (full length) and GAL4-Nur77 (E/F) chimeras were provided by Dr. Jae W. Lee (Baylor College of Medicine, Houston, TX) and Dr. T. Perlmann (Ludwig Institute for Cancer Research, Stockholm, Sweden) respectively, and Dr. Lee also provided the Nur77 response element-luciferase (NurRE-Luc) reporter construct. The GAL-4-coactivator fusion plasmids pM-SRC1, pMSRC2, pMSRC3, pM-DRIP205 and pMCARM-1 were kindly provided by Dr. Shigeaki Kato (University of Tokyo, Tokyo, Japan). For RNA interference assays, we used a non-specific scrambled (iScr) oligonucleotide as described (460). The small inhibitory RNA for Nur77 (iNur77) was identical to the reported oligonucleotide (454) and these were purchased from Dharmacon Research (Lafayette, CO). Leptomycin B (LMB) was obtained from Sigma (St Louis, MO) and caspase inhibitors were purchased from BD Pharminogen (San Diego, CA). The following oligonucleotides were prepared by IDT (Coralville, IA) and were used in gel mobility shift assays; NBRE:5'-GAT CCT CGT GCG AAA AGG TCA AGC GCT A-3'; NurRE:5'- GAT CCT AGT GAT ATT TAC CTC CAA ATG CCA GGA-3'.

Transfection assays

Transfection assays were essentially carried out as previously described using Lipofectamine Plus reagent (Invitrogen, Carlsbad, CA) and luciferase activities were normalized to β-galactosidase activity. For RNA interference studies, cells were transfected with small inhibitor RNAs for 36 hr to ensure protein knockdown prior to the standard transfection and treatment protocols (359, 460). Results are expressed as means ± SE for at least three replicate determinations for each treatment group.

Mammalian two-hybrid assay

Panc-28 cells were plated in 12-well plates at 1×10^5 cells/well in DME-F12 media supplemented with 2.5% charcoal-stripped FBS. After growth for 16 hr, various amounts of DNA, i.e. Gal4Luc (0.4 µg), β-gal (0.04 µg), VP-Nur77(E/F) (0.04 µg), pM SRC1 (0.04 µg), pMSRC2 (0.04 µg), pMSRC3 (0.04 µg), pMDRIP205 (0.04 µg) and pMCARM-1 (0.04 µg) were transfected by Lipofectamine (Invitrogen) according to the manufacturer's protocol. After 5 hr of transfection, the transfection mix was replaced with complete media containing either vehicle (DMSO) or the indicated ligand for 20-22 hr. Cells were then lysed with 100 ml of 1X reporter lysis buffer, and 30 µl of cell extract were used for luciferase and β-Gal assays. Lumicount was used to quantitate luciferase and β-Gal activities, and the luciferase activities were normalized to β-Gal activity.

Cell growth and apoptosis assays

The different cancer cell lines were cultured under standardized conditions. Panc-28 cells were grown in DMEM:Ham's F-12 media containing 2.5% charcoal stripped fetal bovine serum, and cells were treated with DMSO and different concentrations of test compounds as indicated. For longer term cell survival studies, the media was changed every second day, and values were presented for a 4 day experiment. For all other assays, cytosolic, nuclear fractions, or whole cell lysates were obtained at various time points, analyzed by Western blot analysis, and bands were quantitated as previously described (359, 460). Immunocytochemical analysis was determined using Nur77 antibodies as previously reported (460).

Gel shift assay

Cells were seeded in DME/F12 medium supplemented with 2.5% charcoal-stripped serum and treated with 10 µM DIM-C-pPhOCH$_3$ for 30 min. Nuclear extracts were obtained using NE-PER nuclear and cytoplasmic extraction reagents (Pierce Chemical Co.). Oligonucleotides were synthesized, purified, and annealed, and 5 pmol of specific oligonucleotides were ^{32}P-labeled at the 5'-end using T$_4$ polynucleotide kinase and [$^{32}\gamma$P]ATP. Nuclear extracts were incubated in HEPES with ZnCl$_2$ and 1 µg poly deoxyinosine-deoxycytidine for 5 min; 100-fold excess of unlabeled wild-type or mutant oligonucleotides were added for competition experiments and incubated for 5 min. The mixture was incubated with labeled DNA probe for 15 min on ice. The reaction mixture was loaded onto a 5% polyacrylamide gel and ran at 150 V for 2 hr. The gel was dried and protein DNA complexes were visualized by autoradiography using a Molecular Dynamics, Inc. Storm 860 instrument (Molecular Dynamics Inc., Sunnyvale CA).

Annexin-V staining

Detection of phosphatidylserine on the outside of the cell membrane, a unique and early marker for apoptosis, was performed using a commercial kit (Vybrant Apoptosis Assay Kit #2; Molecular Probes, Eugene, OR). Panc-28 cells were cultured as described above, and treated with 10 µM DIM-C-pPhOCH$_3$ or camptothecin for 6, 12 and 24 hrs. Binding of annexin V-Alexa-488 conjugate and propidium iodide (PI) was performed according to the manufacturer's instructions. After binding and washing, cells were observed under phase contrast and epifluorescent illumination using a 495-nm excitation filter and a 520-nm absorption filter for annexin V-Alexa 488 and a 546-nm

excitation filter and a 590-nm absorption filter for PI. Healthy cells were unstained by either dye; cells in early stages of apoptosis were stained only by annexin V, while dead cells were stained by annexin V and PI. The assay was repeated on three separate Panc-28 cell preparations.

Quantitative real-time PCR

cDNA was prepared from the Panc-28 cell line using a combination of oligodeoxythymidylic acid (Oligo d(T)$_{16}$), and dNTP mix (Applied Biosystems) and Superscript II (Invitrogen). Each PCR was carried out in triplicate in a 20-µl volume using Sybr Green Mastermix (Applied Biosystems) for 15 min at 95°C for initial denaturing, followed by 40 cycles of 95°C for 30 s and 60°C for 1 min in the ABI Prism 7700 Sequence Detection System. The ABI Dissociation Curves software was used following a brief thermal protocol (95°C 15 s and 60°C 20 s, followed by a slow ramp to 95°C) to control for multiple species in each PCR amplification. Values for each gene were normalized to expression levels of TBP. The sequences of the primers used for RT-PCR were as follows: TRAIL forward, 5'-CGT GTA CTT TAC CAA CGA GCT GA-3', reverse, 5'-ACG GAG TTG CCA CTT GAC TTG-3'; and TBP forward, 5'-TGC ACA GGA GCC AAG AGT GAA-3', reverse, 5'-CAC ATC ACA GCT CCC CAC CA-3'.

Xenograft experiment

Male athymic nude mice (BALB/c, ages 8-12 weeks) were purchased from Harlan (Indianapolis, IN). The mice were housed and maintained in laminar flow cabinets under specific pathogen-free conditions. Panc-28 cells were harvested from

subconfluent cultures by trypsinization and washed. Panc-28 cells (2×10^6) were injected subcutaneously into each mouse on both flanks using a 30-gauge needle. The tumors were allowed to grow for 11 days until tumors were palpable. Mice were then randomized into two groups of seven mice per group and dosed by oral gavage with either corn oil or DIM-C-pPhOCH$_3$ every second day. The volume of corn oil was 75 μl, and the dose of DIM-C-pPhOCH$_3$ was 25 mg/kg/day. The mice were weighed, and tumor areas were also measured every other day. Final body and tumor weights were determined at the end of the dosing regiment, and selected tissues were further examined by routine H & E staining and immunohistochemical analysis for apoptosis using the TUNEL assay.

Results

Nur77 expression and structure-dependent activation by C-substituted DIMs

Studies in this laboratory have been investigating the anticarcinogenic activities of a series of ring-substituted 3,3'-diindolylmethanes (DIMs) and methylene (C)-substituted DIMs, and many of these compounds were active *in vivo* and in cell culture assays (359, 393, 461, 462). Some members of a series of C-substituted DIMs activated peroxisome proliferator-activated receptor γ (PPARγ) but not PPARα, retinoic acid receptor (RAR), retinoic X receptor (RXR), estrogen receptor α, or the aryl hydrocarbon receptor (AhR). Previous studies have linked Nur77 to decreased cell survival and activation of cell death pathways by apoptosis-inducing agents in some cancer cell lines (453-459), and we therefore investigated expression of Nur77 in cancer cell lines and the effects of a series of eleven C-substituted DIMs on Nur77 activation/translocation.

Figure 6.1A summarizes Western blot analysis of Nur77 in whole cell lysates from 12 different cancer cell lines derived from pancreatic, prostate, breast, colon and bladder tumors. Only the 253 JB-V-33 bladder cancer cell line exhibited relatively low expression of Nur77, and the antibodies and electrophoretic conditions gave two immunostained bands as previously reported in other studies. Western blot analysis of the other NGFI-B proteins showed variable expression of Nurr1, and Nor1 was not detectable in these cancer cell lines. Similar results were also obtained in Jurkat T-cell leukemia cells. Structure-dependent activation of Nur77 by a series of eleven C-substituted DIMs was investigated in Panc-28 cells transfected with a GAL4-Nur77 (full length) chimera and a reporter construct containing five GAL4 response elements linked to a luciferase reporter gene (pGAL4). The results (Fig. 6.1B) showed that three compounds containing p-trifluoromethyl (DIM-C-pPhCF$_3$) and methoxy (DIM-C-pPhOCH$_3$) substituents or the unsubstituted phenyl group (DIM-C-Ph) activated luciferase activity. Similar results were also obtained in Panc-28 cells transfected with a construct containing a Nur response element (NurRE) (Fig. 6.1C), and these same compounds also activated GAL4-Nur77/pGAL4 and NurRE in MiaPaCa-1 pancreatic, HCT-15 colon, and MCF-7 breast cancer cells. The structure-dependent activation of Nur77 was also investigated using DIM-C-pPhOCH$_3$ as a model and the position of the methoxyl group was changed to the *meta* (DIM-C-mPhOCH$_3$) and *ortho* (DIM-C-oPhOCH$_3$) positions (Fig. 6.1D). Only the *para-* substituted compound was active. We also investigated N-methyl and 2-methyl indole ring-substituted analogs of DIM-C-pPhOCH$_3$, DIM-C-Ph, and DIM-C-pPhCF$_3$) and these compounds did not activate
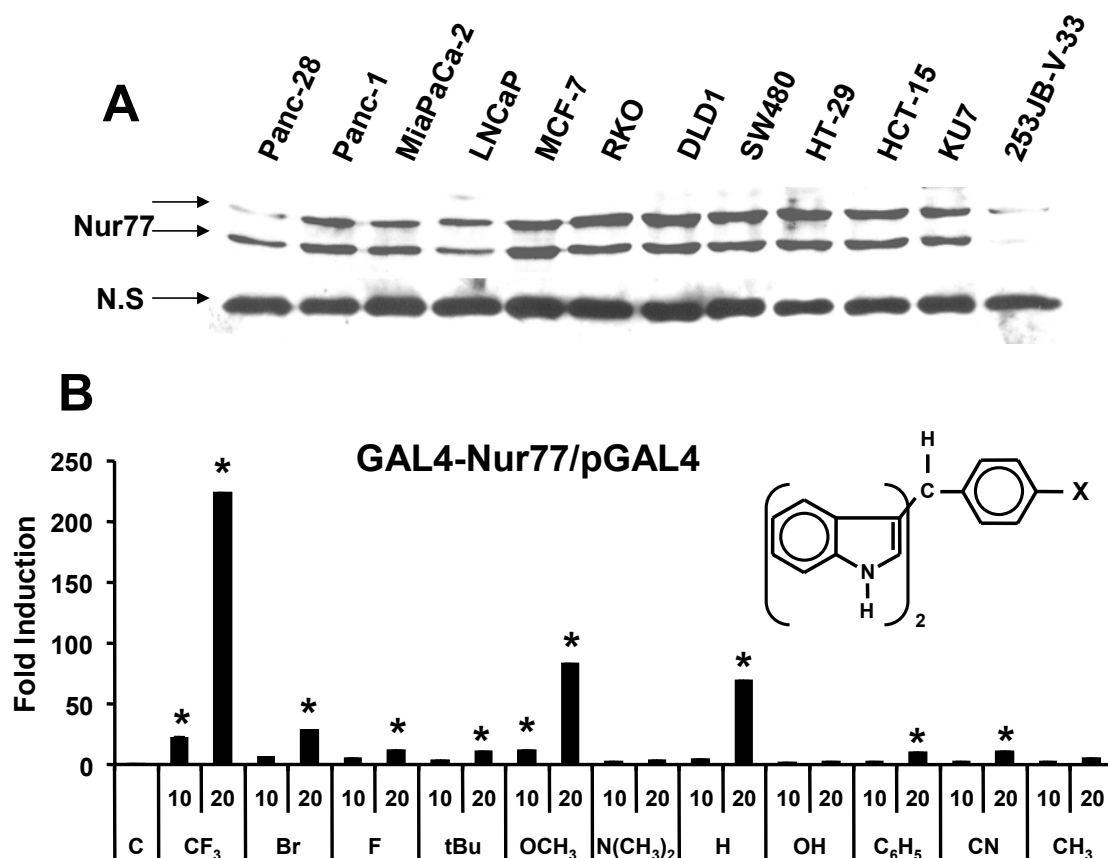
Fig. 6.1. Nur77 expression and activation in cancer cell lines. [A] Nur77 protein expression. Whole cell lysates from 12 different cancer cell lines were analyzed for Nur77, Nurr1 and Nor1 by Western blot analysis as described in the Materials and Methods. Nor1 protein was not detected in these cell lines. Activation of Gal4-Nur77 [B] and NuRE [C] Panc-28 cells were treated with 10 or 20 μM of the various compounds, transfected with GAL4-Nur77/pGAL4 or NuRE, and luciferase activity determined as described in the Materials and Methods. [D] Nur77 activation by isomeric DIM-C-PhOCH3 compounds. Panc-28 cells were treated with 10 or 20 μM of the DIM-C-PhOCH3 isomers, transfected with GAL4-Nur77/pGAL4 and luciferase activity determined as described in the Materials and Methods. Results are expressed as means ± SE for at least 3 separate determinations for each treatment group and significant ($p < 0.05$) induction is indicated by an asterisk.

Fig. 6.1 Continued

Nur77. These results demonstrate that activation of Nur77 by C-DIMs was structure-dependent and sensitive to substitution on the phenyl and indole rings. Thus, at least three C-substituted DIMs activate Nur77; one of these compounds (DIM-C-pPhCF$_3$) also activates PPARγ (359, 393), whereas DIM-C-pPhOCH$_3$ and DIM-C-Ph are PPARγ-inactive (359). DIM-C-pPhOH was inactive in both transactivation assays and, at higher concentrations, decreased activity lower than observed in solvent (DMSO) control.

Characterization and interactions of C-DIMs that activate and inhibit Nur77-mediated

transactivation

The role of the LBD or E/F region in ligand-induced transactivation of Nur77 was investigated in Panc-28 cells transfected with pGAL4 and a chimeric GAL4-Nur77(E/F) construct containing only the E/F domain of Nur77. Treatment of Panc-28 cells with different concentrations (5 - 15 μM) of DIM-C-pPhCF$_3$, DIM-C-pPhOCH$_3$ and DIM-C-Ph induced luciferase activity, whereas no response was observed in cells treated with Nur77-inactive DIM-C-pPhOH (Fig. 6.2A). These results are the first to identify a series of compounds that directly activate Nur77(LBD)-dependent transactivation in Panc-28 or any other cancer cell line. The role of Nur77 in mediating transactivation was further investigated in Panc-28 cells treated with 10 or 20 μM DIM-C-pPhOCH$_3$ or DIM-C-Ph and transfected with pNurRE, a non-specific "scrambled" small inhibitory RNA (iScr), or small inhibitory RNA for Nur77 (iNur77). The results (Fig. 6.2B) showed decreased Nur77 protein in whole cell lysates and a 90-100% decrease in ligand-induced transactivation over the different concentrations of compounds, thus confirming the role of Nur77 in mediating this response. As noted
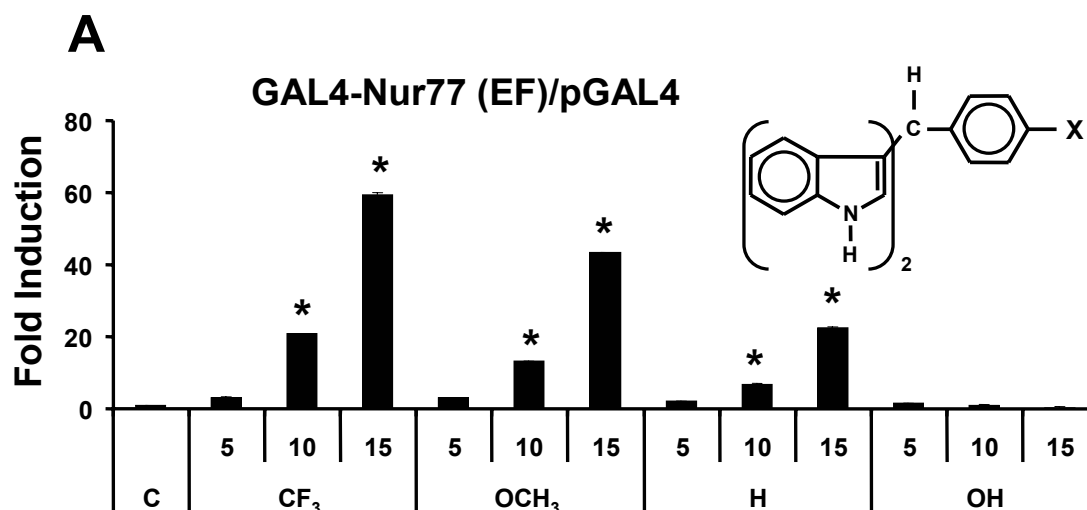
Fig. 6.2. Activation of Nur77. [A] Activation of GAL4-Nur77(E/F)/pGAL4. The effects of the various compounds was essentially determined as described in Figure 1; however, a truncated GAL4 chimera expressing only the E/F domain of Nur77 was used in this experiment. [B] Effects of iNur77 on transactivation. Cells were treated with DIM-C-pPhOCH$_3$ or DIM-C-Ph, transfected with NuRE and iNur77 or iScr (non-specific), and luciferase activity determined as described. Similar results were obtained for DIM-C-pPhCF$_3$. Nur77 antagonist activity of DIM-C-pPhOH [C], DIM-C-mPhOH [D], and DIM-C-oPhOH [E]. Cells were transfected with GAL4-Nur77/pGAL4 and different concentrations of the DIM-C-PhOH isomers and the Nur77 agonists, and luciferase activity determined as described in the Materials and Methods. Significant (p < 0.05) inhibition of transactivation is indicated (**). Results are expressed as means ± SE for at least 3 separate determinations for each treatment group and significant (p < 0.05) induction (*) or inhibition by iNur77 or DIM-C-pPhOH (**) is indicated.
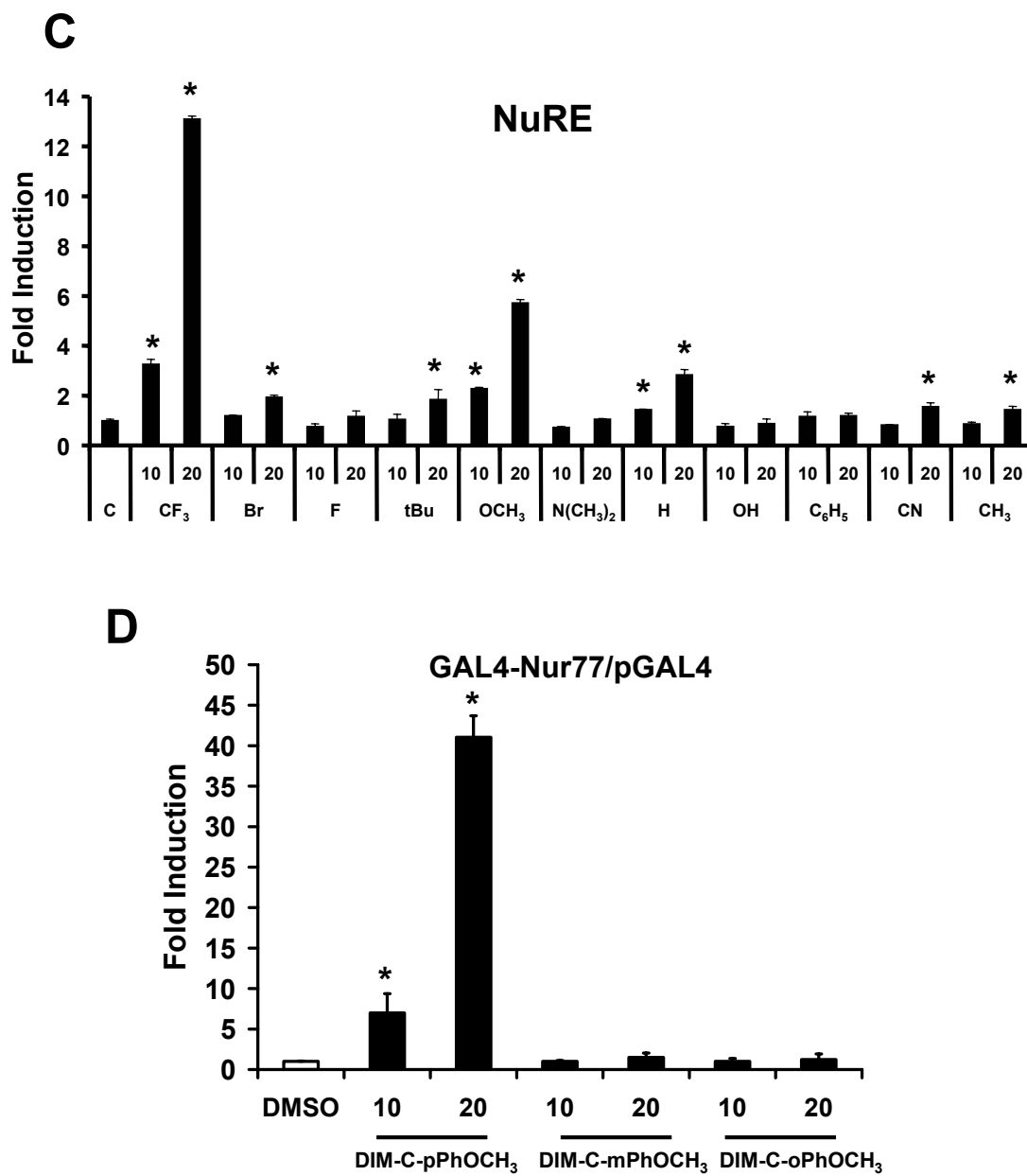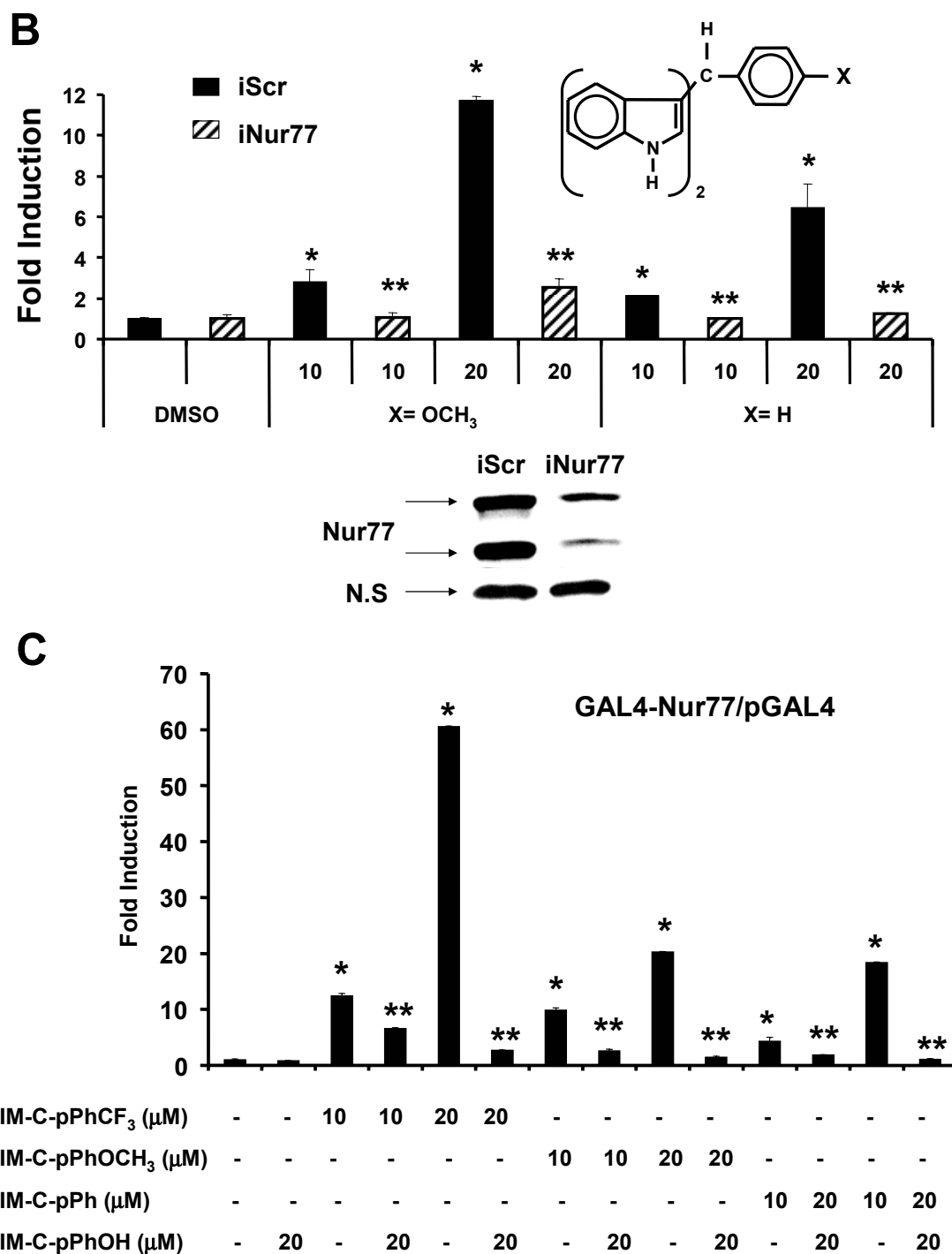
Fig. 6.2 Continued
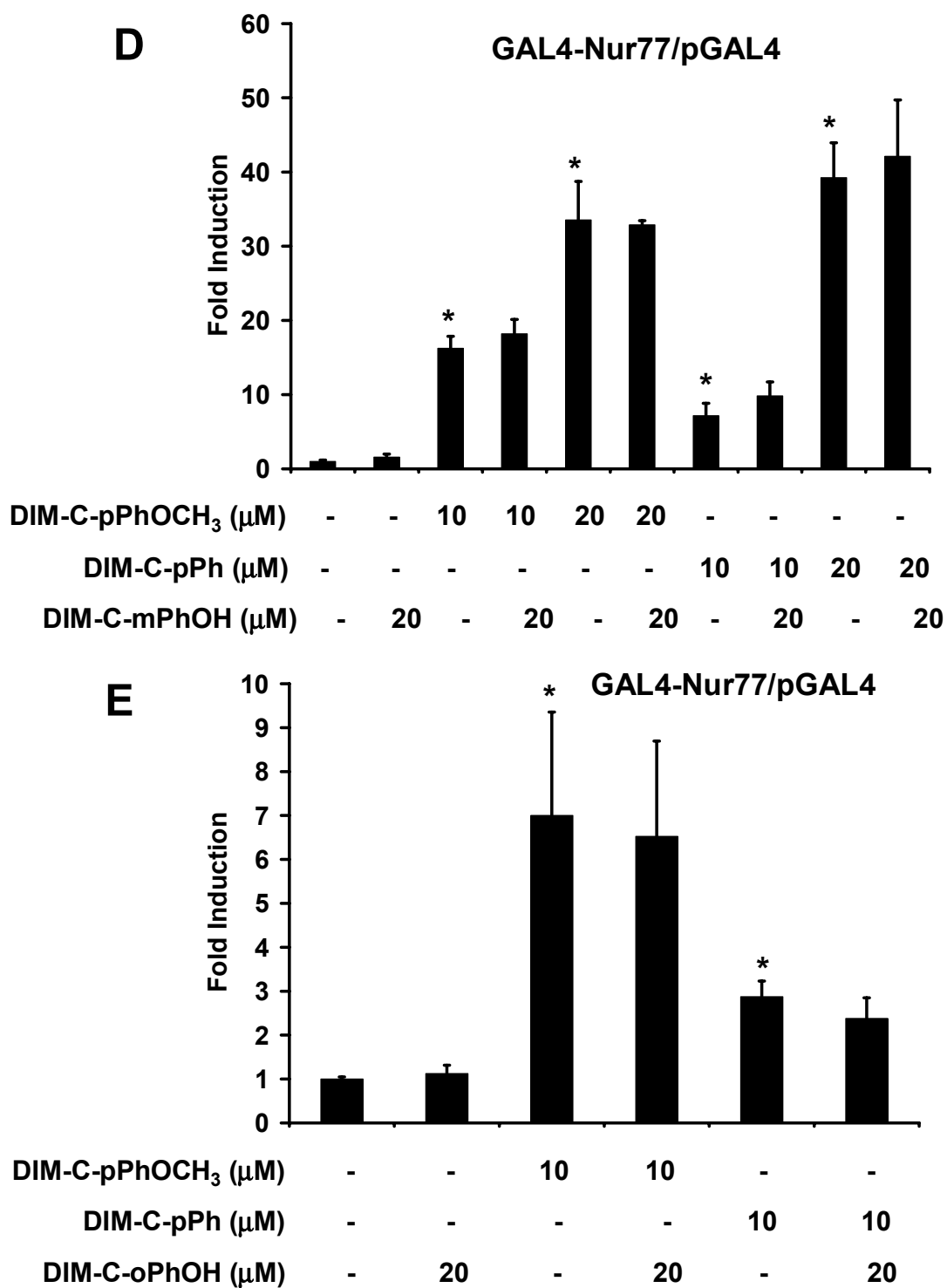
Fig. 6.2 Continued

above, one compound which contained a *p*-hydroxy substituent (DIM-C-pPhOH) did not induce activity (Fig. 6.1B) and DIM-C-pPhOH was further investigated as a potential Nur77 antagonist. Panc-28 cells were transfected with GAL4-Nur77/pGAL4 and cotreated with DIM-C-pPhOH and Nur77 agonists DIM-C-pPhCF$_3$, DIM-C-pPhOCH$_3$, and DIM-C-pH (Fig. 6.2C). The results show that DIM-C-pPhOH antagonizes activation of Nur77 by all three C-DIM compounds. The structural specificity of Nur77 antagonists was further investigated using *meta*-hydroxy (DIM-C-mPhOH) and *ortho*-hydroxy (DIM-C-oPhOH) analogs. DIM-C-mPhOH (10 or 20 μM) did not inhibit DIM-C-pPhOCH$_3$- or DIM-C-Ph-induced transactivation (Fig. 6.2D). DIM-C-oPhOH also did not exhibit Nur77 antagonist activity (Fig. 6.2E); however, high doses (20 μM) of both Nur77 agonists and DIM-C-oPhOH were toxic. Thus, activation of Nur77 by C-DIMs was E/F domain-dependent and Nur77 activation was inhibited by DIM-C-pPhOH; moreover, both activation and inhibition of Nur77-mediated transactivation was dependent on the structure of the C-DIM compounds.

Nur77 DNA-binding and C-DIM-induced Nur77-coactivator interactions

Incubation of nuclear extracts from Panc-28 cells treated with DMSO or DIM-C-pPhOCH$_3$ with ^{32}P-labeled NBRE and NurRE (lanes 1, 2, and 5, 6, respectively) gave retarded bands in EMSA assays (Fig. 6.3A). Retarded band intensities were decreased after incubation with 100-fold excess NurRE (lane 3) or NBRE (lane 7) but not by mutant NurRE (lane 4) or mutant NBRE (lane 8) oligonucleotides. These results show that nuclear extracts containing Nur77 bind NurRE and NBRE as dimers and monomers, respectively, and this corresponds to their migration in the EMSA assay. Results

obtained for nuclear extracts from solvent-treated cells show that formation of the retarded bands is ligand-independent and the retarded band pattern corresponds to previous studies using nuclear extracts from cells or *in vitro* translated Nur77 (463, 464). Extracts from cells treated with Nur77-active C-substituted DIMs gave retarded band intensities similar to that observed for solvent-treated extracts suggesting minimal ligand-dependent loss of nuclear Nur77 in these cells.

Ligand-dependent activation of nuclear receptors is dependent on interaction of the bound receptor with coactivators (465-467) and Figures 6.3B – 6.3D summarize results of a mammalian two-hybrid assay in Panc-28 cells transfected with VP-Nur77 (ligand binding domain) and GAL4-coactivator chimeras. Ligand-induced Nur77-coactivator interactions were determined using a construct (pGAL4) containing 5 GAL4 response elements. Coactivators used in this study include SRC-1, SRC-2 (TIFII), SRC-3 (AIB1), PGC-1, TRAP220 and CARM-1. A GAL4-repressor (SMRT) chimera was also included in the assay. All three ligands induced transactivation in cells transfected with GAL4-SRC-1, GAL4-PGC-1 and GAL4-TRAP220 chimeras. DIM-C-pPhOCH$_3$ induced transactivation in cells transfected with GAL4-SRC-3 and GAL4-CARM-1 was slightly activated by DIM-C-pPhOCH$_3$ and DIM-C-pPhCF$_3$. The results demonstrate that although there were some ligand-dependent differences in transactivation observed for GAL4-SRC-3 and GAL4-CARM-1; however, the most significant interactions between VP-Nur77 and GAL4 chimeras expressing SRC-1, PGC-1 and TRAP220 were induced by all three compounds.

A
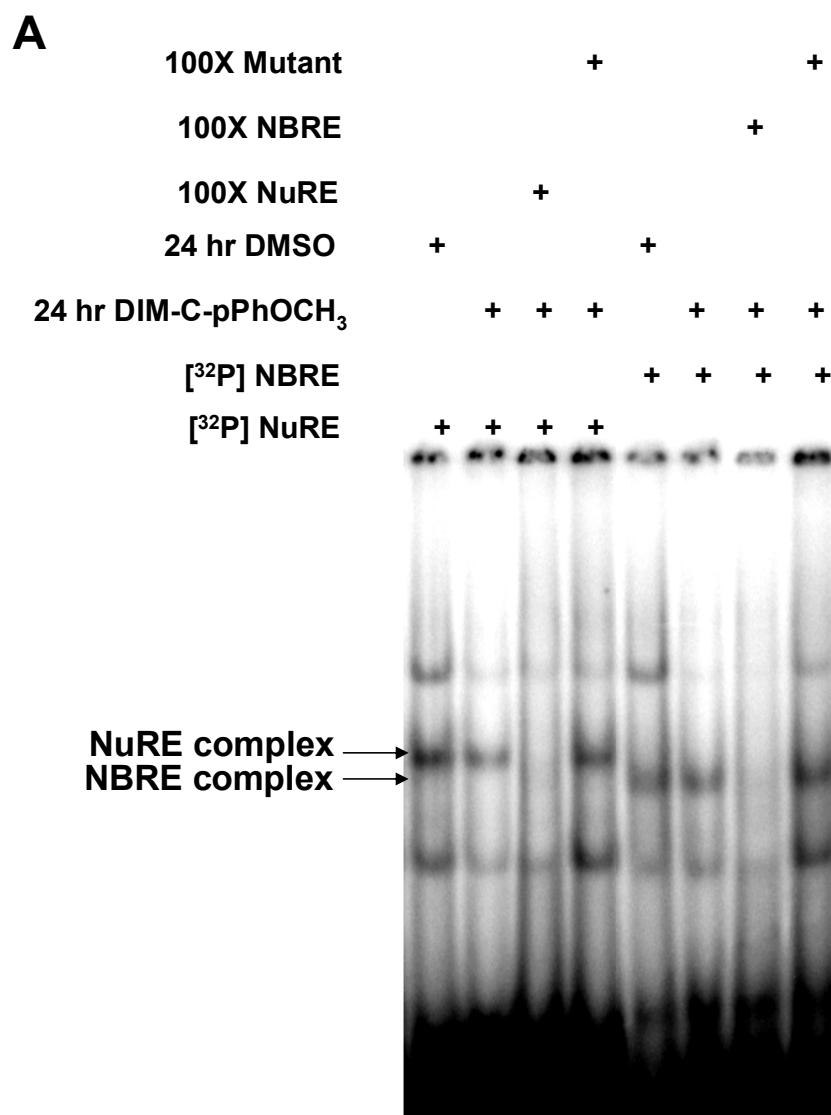
Fig. 6.3. DNA binding of Nur77 and ligand-induced coactivator-Nur77 interactions. [A] Gel mobility shift assay. Cells were treated with DMSO or Nur77 agonists for 0.5 hr, nuclear extracts were incubated with ^{32}P-labeled NurRE and NBRE, and formation of retarded bands was determined in a gel mobility shift assay as described in the Materials and Methods. Arrows denote the specifically bound bands. GAL4-coactivator interactions with VP-Nur77(E/F) in Panc-28 cells treated with DIM-C-pPhCF$_3$ [B], DIM-C-pPhOCH$_3$ [C], and DIM-C-Ph [D]. Cells were transfected with the pGAL4, VP-Nur77(E/F) and GAL4-coactivator/repressor (chimera) constructs, treated with the Nur77 agonists, and luciferase activity determined as described in the Materials and Methods. Significant (p < 0.05) induction of luciferase activity is indicated (*) and results are expressed as means ± SE for three separate determinations for each treatment group.
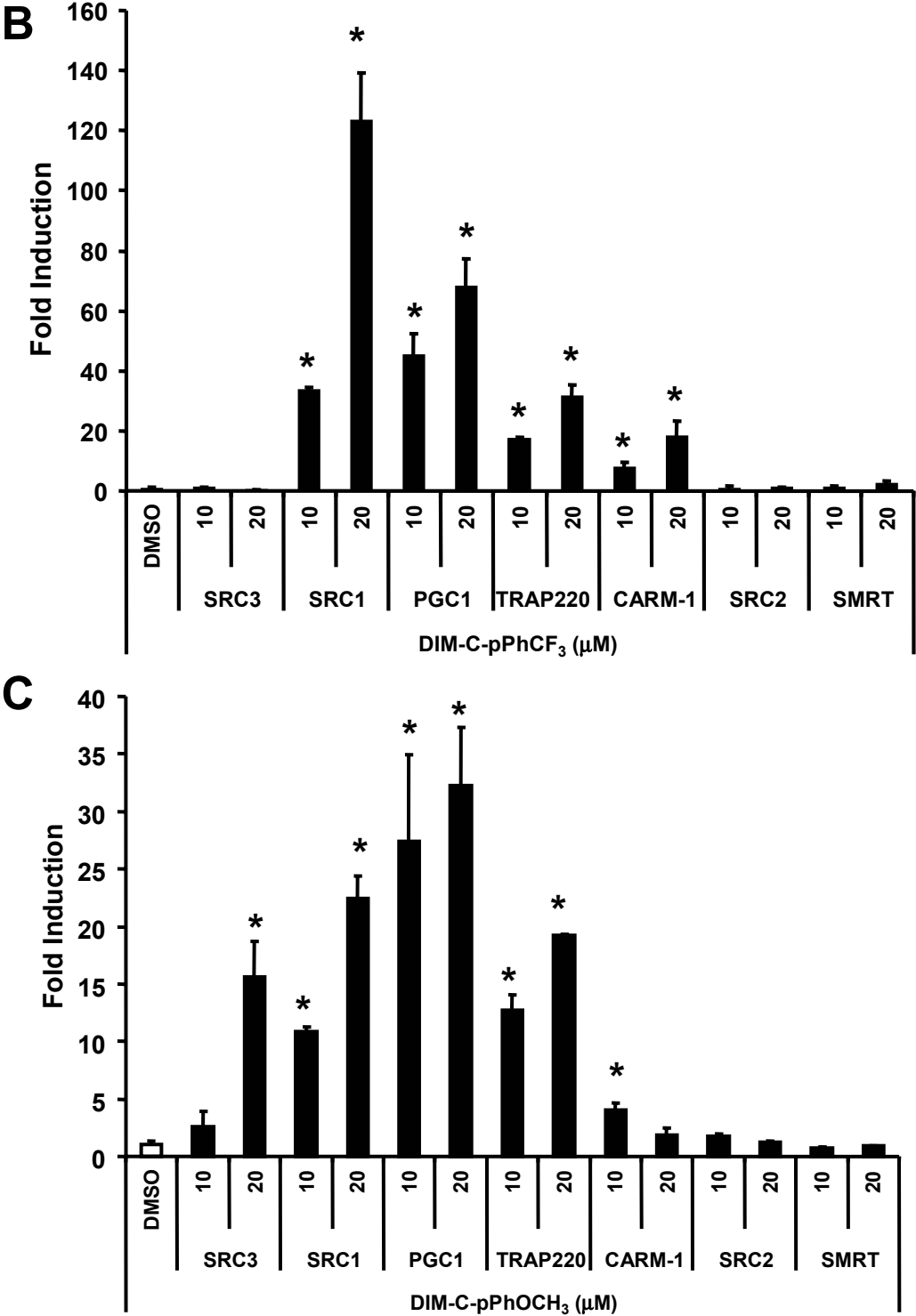
Fig. 6.3 Continued

D
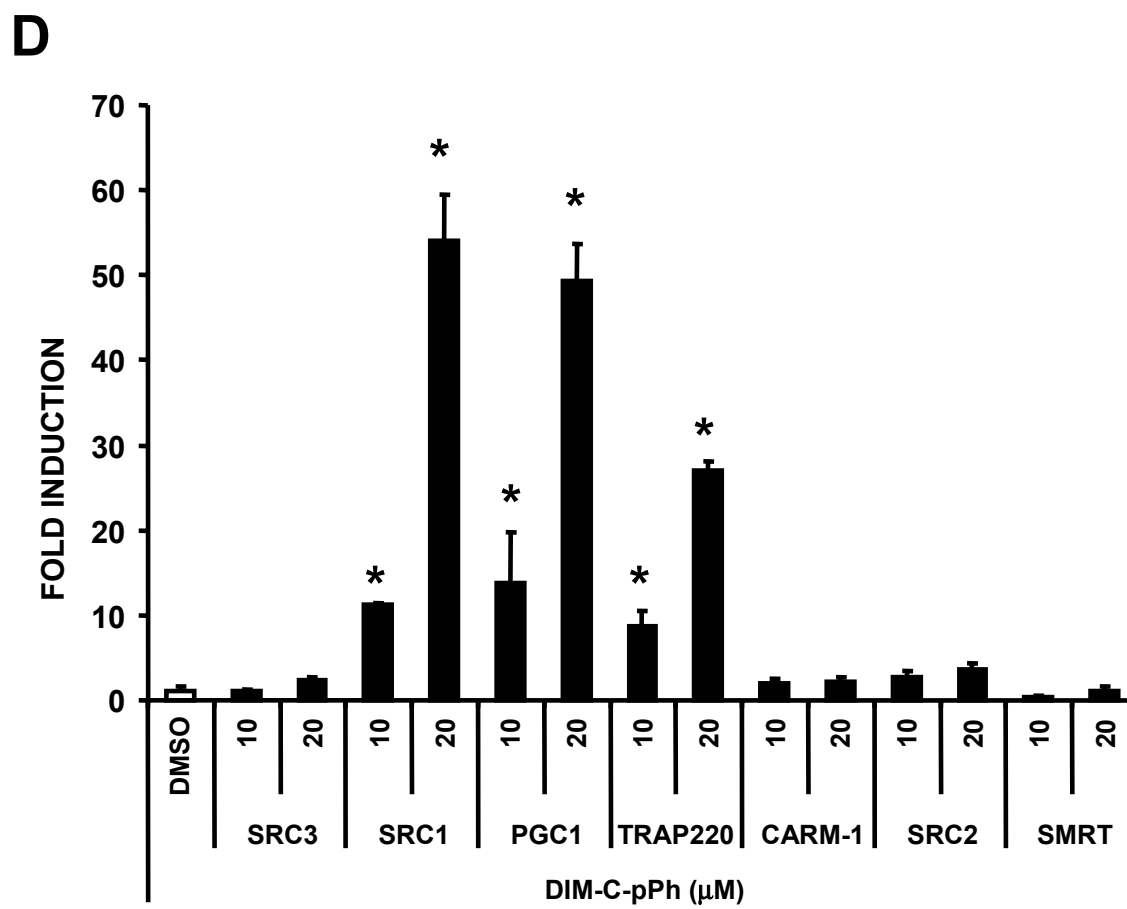
Fig. 6.3 Continued

Effects of Nur77-active C-DIMs on cell survival and apoptosis and role of nuclear

Nur77

In several cancer cell lines transfected with Nur77-GFP constructs, treatment with apoptosis and differentiation-inducing agents results in rapid translocation of Nur77 into the cytosol/mitochondria (453-458). Similar results have been observed in BGC-823 human gastric cancer cells where endogenous Nur77 is nuclear and TPA induced Nur77 translocation into the cytosol and this was accompanied by apoptosis but not by Nur77-dependent transactivation (455). Results summarized in Figure 6.4A show immunostaining of Nur77 in the nucleus of Panc-28 cells treated with DMSO and Nur77-active DIM-C-pPhCF$_3$, DIM-C-pPhOCH$_3$ and DIM-C-Ph for 6 hr, and comparable results were obtained in Panc-28, MiaPaCa and LNCaP cells after treatment for 6 or 12 hr. In all cases, Nur77 remained in the nucleus, and cells exhibited a compacted nuclear staining pattern typically observed in cells activated for cell death pathways. In a separate experiment, Panc-28 cells were treated with 10 or 20 µM DIM-C-pPhCF$_3$, DIM-C-pPhOCH$_3$ and DIM-C-Ph or 10 µM DIM-C-pPhOH for 12 hr, and Nur77 protein levels were determined by Western blot analysis of cytosolic and nuclear extracts (Fig. 6.4B). These results also confirm that Nur77, in the presence or absence of C-substituted DIM agonists, is a nuclear protein and ligand-induced Nur77 translocation from the nucleus is not observed. Sp1 is a nuclear protein and was used as a control to ensure efficient separation of the two extracts and Sp1 was identified only in the nuclear fraction (Fig. 6.4B).

Nur77 agonists significantly decreased survival of Panc-28 cells (Fig. 6.5A), and
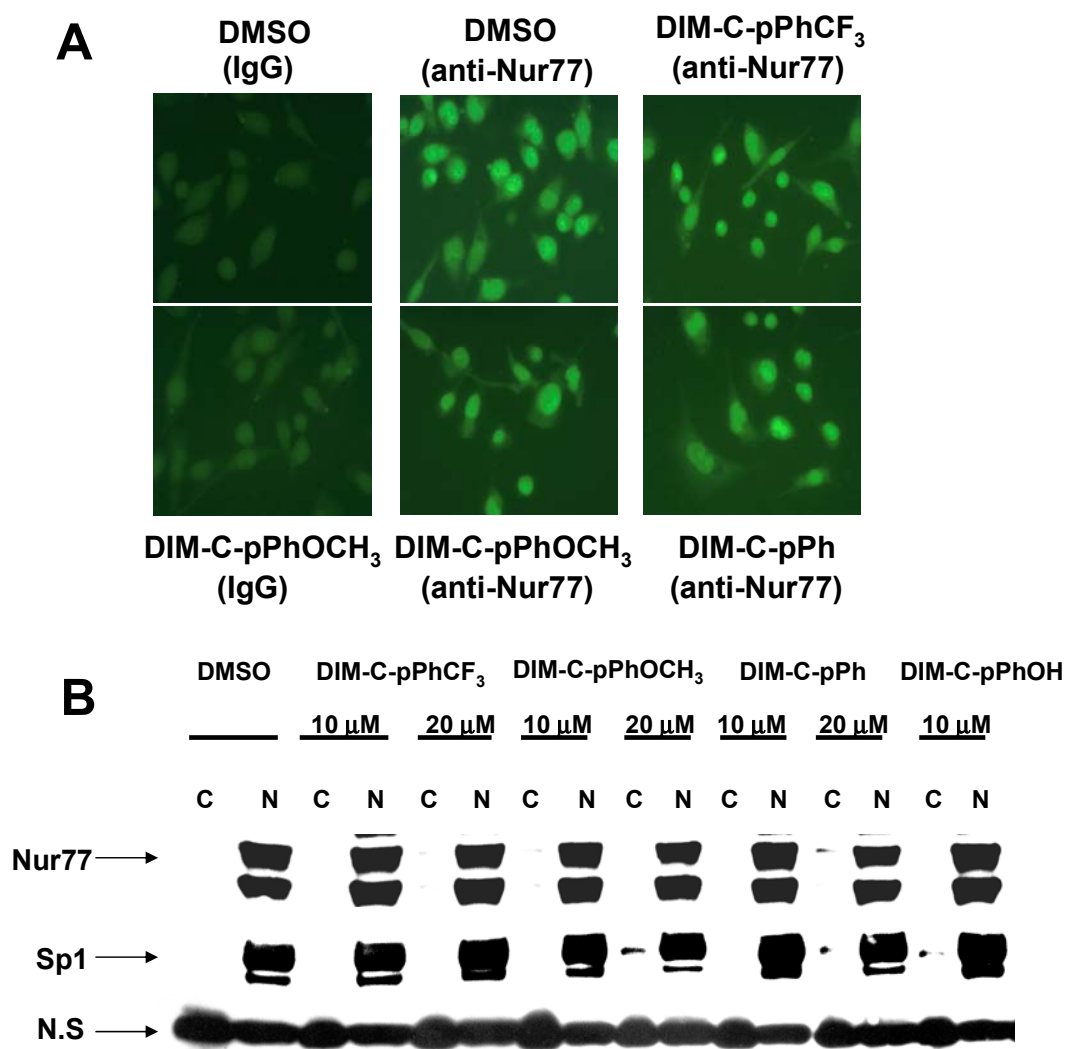
Fig. 6.4. Nuclear localization of Nur77. [A] Immunostaining. Panc-28 cells were treated with DMSO or 10 µM Nur77 agonists for 6 hr, and cells were immunostained for Nur77 as described in the Materials and Methods. Nur77 staining was not observed in cells treated with non-specific IgG. [B] Nuclear localization in subcellular fractions. Panc-28 cells were treated with the various compounds for 12 hr and Nur77 protein expression in cytosolic and nuclear extracts were determined by Western blot analysis. Sp1 protein and a non-specific (NS) band serve as loading controls, and Sp1, a nuclear protein, also serves as a control for separation of nuclear and cytosolic extracts.
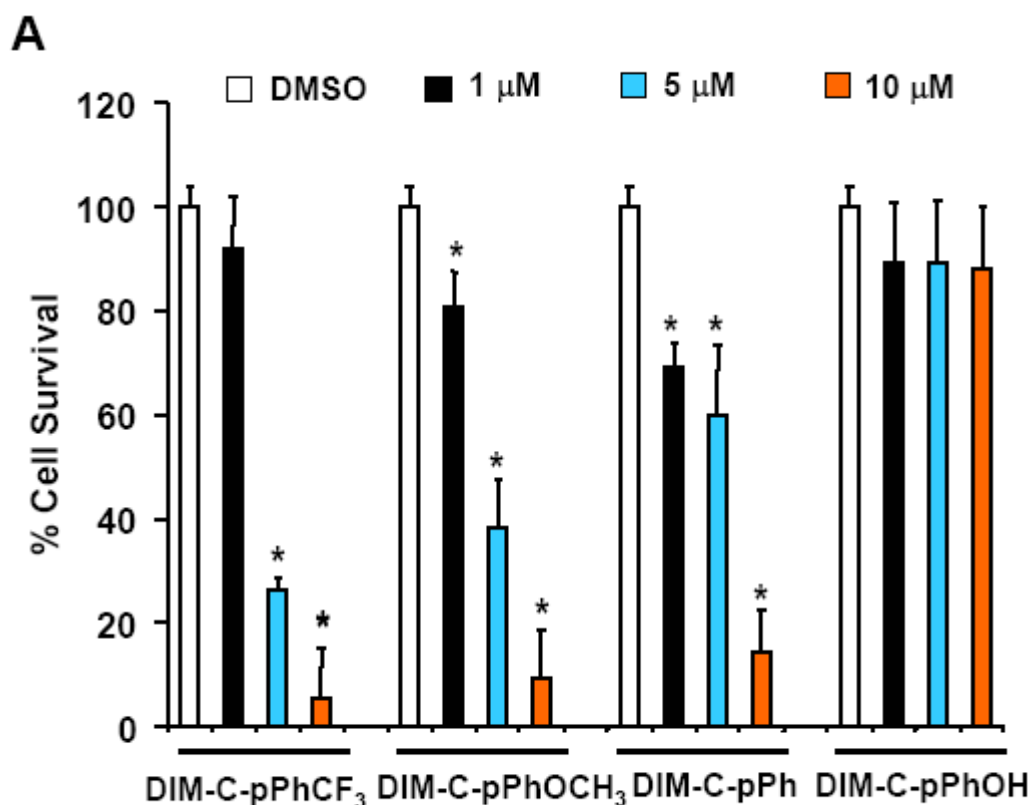
Fig. 6.5. Nur77 agonists decrease cell survival and induce apoptosis. [A] Cell survival. Panc-28 cells determined as described in the Materials and Methods. Results are expressed as means ± SE for 3 separate determinations for each treatment group, and a significant ($p < 0.050$ decrease in cell survival is indicated by an asterisk (*). DIM-C-pPhOH inhibited cell growth only after treatment for 96 or 144 hr; however, this compound did not induce cell death at any time point. [B] Effects of Nur77 agonists on PARP cleavage in Panc-28. Cells were treated with the different compounds alone or with LMB and PARP cleavage was determined by Western blot analysis of whole cell lysates as described in the Materials and Methods. Bax and bcl-2 (not shown) protein levels were not affected by treatment and NS (non-specific) protein served as a loading control. [C] Annexin staining. Panc-28 cells were treated with camptothecin (positive control) or DIM-C-pPhOCH$_3$ for 6 hr, and annexin staining was determined as described in the Materials and Methods. Approximately 30 - 40% of cells treated with DIM-C-pPhOCH$_3$ exhibited annexin staining. Induction of apoptosis in LNCaP, MiaPaCa-1 and MCF-7 cells [D] or Panc-28 cells [E] treated with Nur77 agonists alone or in combination with LMB, respectively. Cells were treated essentially as described [A] and PARP cleavage determined by Western blot analysis as described in the Materials and Methods.

B

PARP 112kDa →
PARP 85kDa →
Bax →
N.S →

DMSO | DIM-C-pPhCF₃ | DIM-C-pPhOCH₃ | DIM-C-Ph | DIM-C-pPhOH
10 μM | 20 μM | 10 μM | 20 μM | 10 μM | 20 μM | 20 μM

C

CAMPTOTHECIN 10μM

Annexin V Staining · Phase-Contrast · Overlay
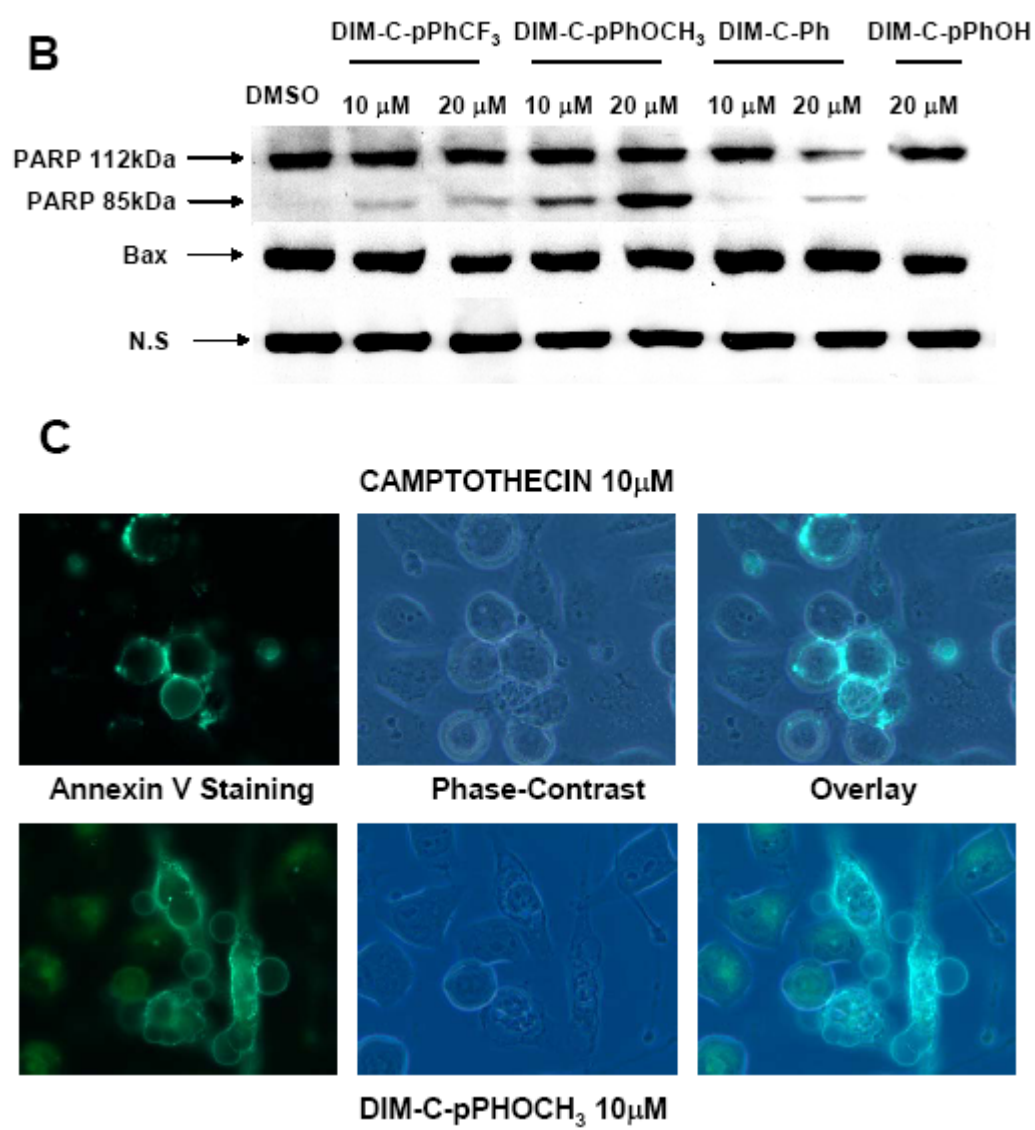
DIM-C-pPHOCH₃ 10μM
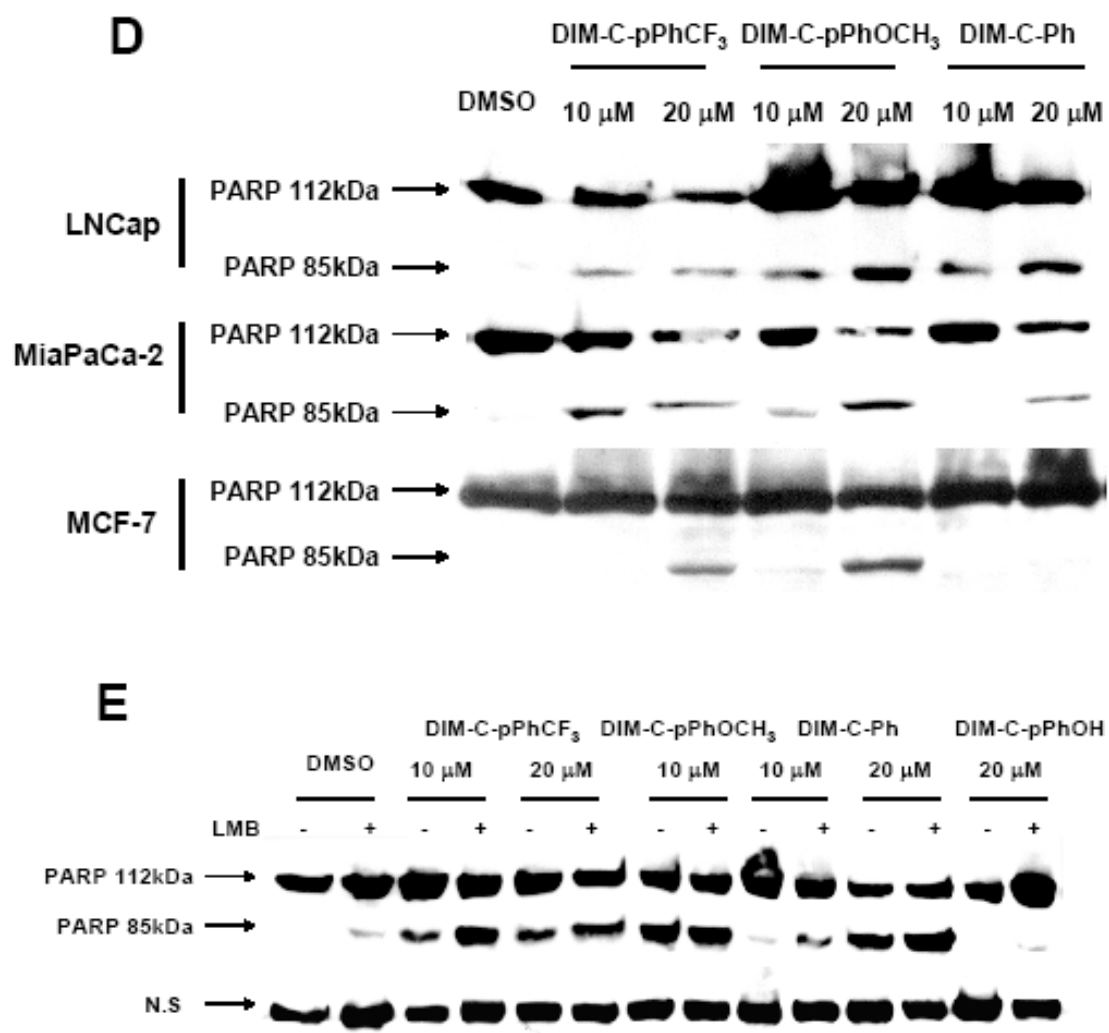
Fig. 6.5 Continued

Fig. 6.5 Continued

IC_{50} values for DIM-C-pPhCF$_3$, DIM-C-pPhOCH$_3$ and DIM-C-Ph were between 1 - 5 μM, whereas DIM-C-pPhOH did not affect cell survival. At longer time points (4 and 6 days), DIM-C-pPhOH slightly inhibited cell proliferation; however, induction of cell death was not observed for this compound at concentrations as high as 20 μM. Decreased cell survival is also observed for agents that induce apoptosis and/or Nur77 nuclear to cytosolic translocation in cancer cells (453-458). Results illustrated in Figure 6.5B show that treatment of Panc-28 cells with Nur77 agonists induced cleavage of PARP, whereas the Nur77-inactive DIM-C-pPhOH did not induce this response. PARP cleavage is associated with activation of cell death pathways; however, this was not accompanied by changes in levels of bax (Fig. 6.5B) or bcl-2 proteins. Moreover, treatment of Panc-28 cells with 10 and 20 μM DIM-C-pPhOCH$_3$ for 8 and 12 hr showed a time- and dose-dependent increase of annexin V-stained cells using a green-fluorescent Alexa Fluor 488 probe (Fig. 6.5C). The effects of camptothecin (positive control for apoptosis) and DIM-C-pPhOCH$_3$ were comparable. After treatment with DIM-C-pPhOCH$_3$ for 6 hr, annexin V-stained cells were significantly increased, plasma membrane blebbing was observed, and there was minimal PI staining. However, after 12 hr, PI staining was increased. Induction of PARP cleavage by Nur77 agonists was also observed in other pancreatic (MiaPaCa-2), prostate (LNCaP) and breast (MCF-7) cancer cell lines (Fig. 6.5D). Induction of PARP cleavage by the Nur77-active compounds in Panc-28 cells was not accompanied by changes in Nur77 expression (Fig. 6.4B), and this was in contrast to TPA which activates nuclear pathways by inducing Nur77 expression (459). Using a protocol comparable to that outlined in Figure 6.5B,
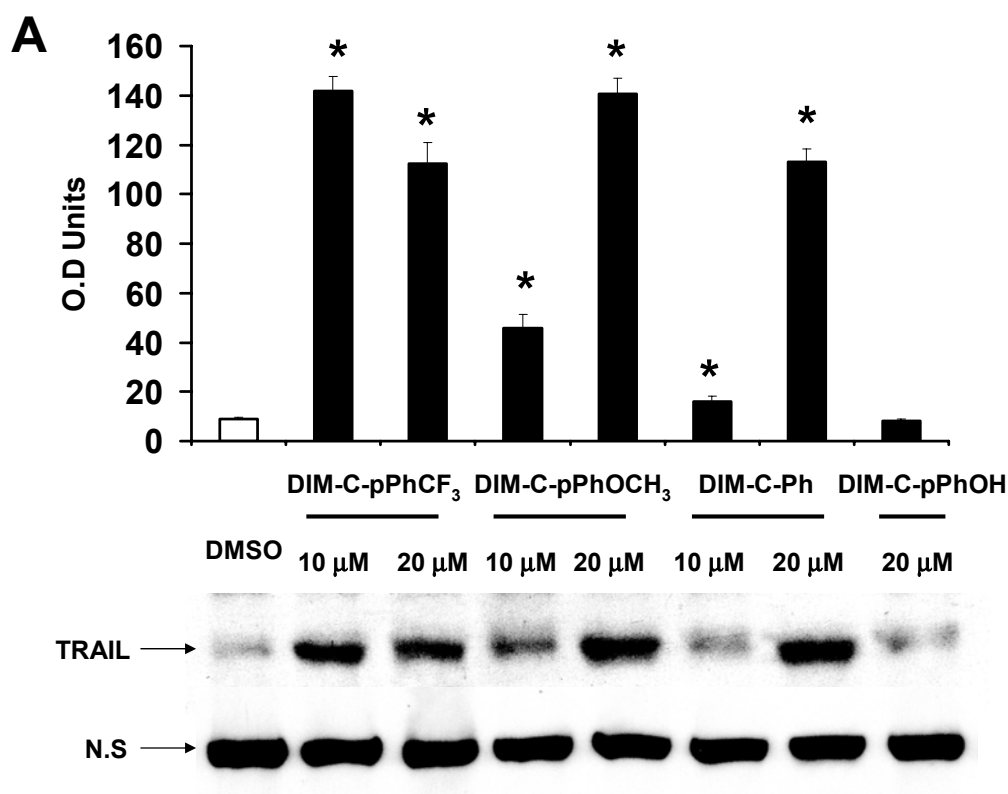
Fig. 6.6. Induction of TRAIL and PARP cleavage in Panc-28 cells is dependent on Nur77. [A] Induction of TRAIL. Cells were treated with Nur77 agonists and levels of TRAIL protein in whole cell lysates were determined by Western blot analysis as described in the Materials and Methods. Results are expressed as means ± SE for 3 separate determinations and significant ($p < 0.05$) induction is indicated. [B] Induction of TRAIL mRNA. Panc-28 cells were treated with 10 or 20 μM DIM-C-pPhOCH$_3$ or DIM-C-Ph for 12 hr, and TRAIL mRNA levels were determined by RT-PCR as described in the Materials and Methods. Results are expressed as means ± SE for 3 separate determinations for each treatment group as significant ($p < 0.05$) is indicated by an asterisk. [C] Effects of caspase inhibitors. Cells were treated and analyzed essentially as described in [A]; however cells were also cotreated with caspase 8 and pancaspase inhibitors Z-IETD or Z-VAD-FMK, respectively. Both inhibitors partially decreased PARP cleavage. [D] Effects of iNur77 on TRAIL expression and PARP cleavage. Panc-28 cells were treated with DMSO or 10 μM DIM-C-pPhOCH$_3$ for 24 hr, transfected with iNur77 or iScr (non-specific), and whole cell lysates were analyzed by Western blot analysis as described in the materials and methods. Results are expressed as means ± SE for 3 separate determinations for each treatment group and significant ($p < 0.05$) induction (*) or inhibition by iNur77 (**) is indicated. [E] Inhibition of induced PARP cleavage and TRAIL by DIM-C-pPhOH. Panc-28 cells were treated with 10 μM DIM-C-pPhOCH$_3$ or DIM-C-Ph alone or in the presence of 20 μM DIM-C-pPhOH, and PARP cleavage and TRAIL protein expression were determined by Western blot analysis as described in the Materials and Methods.
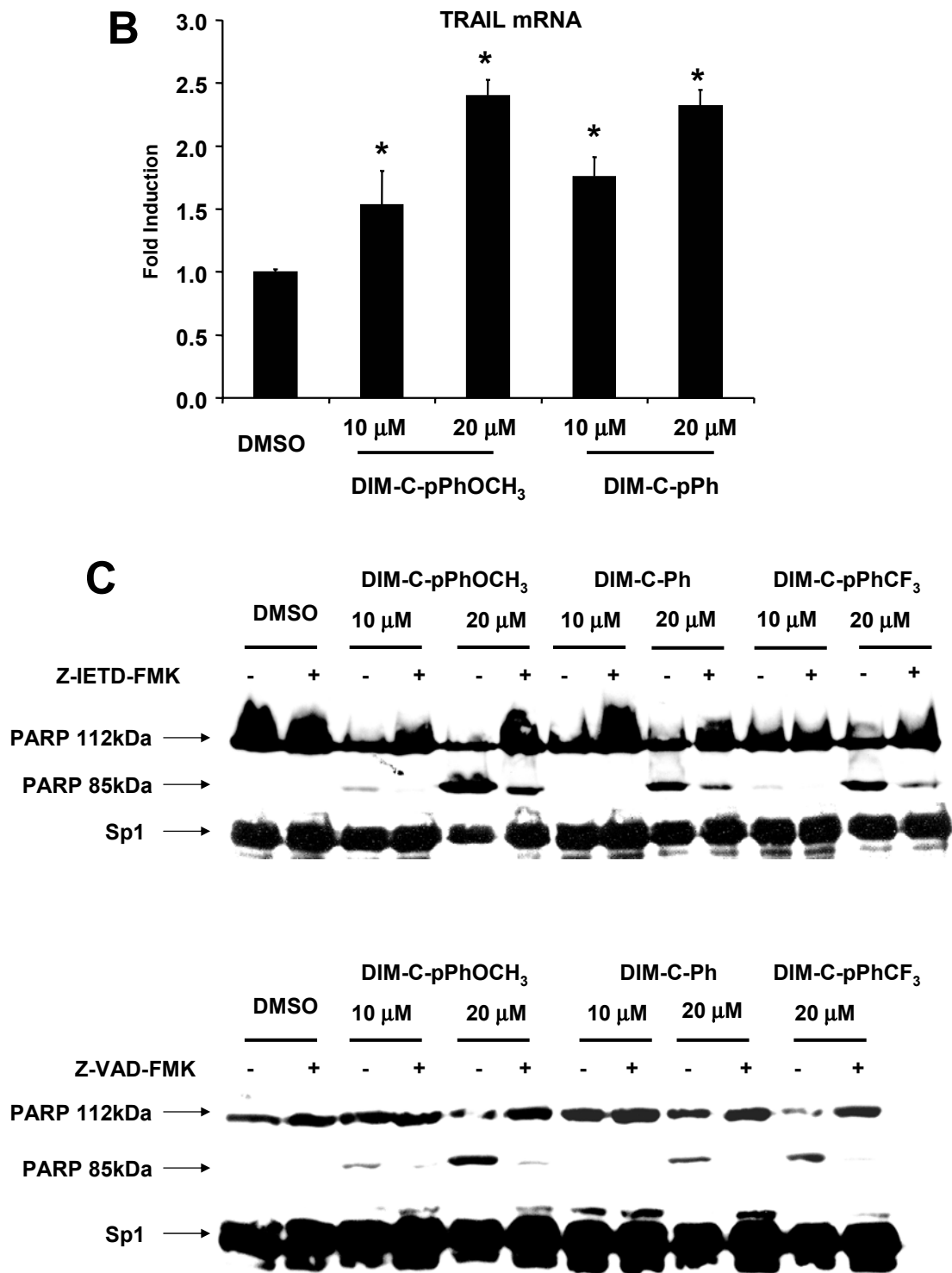
Fig. 6.6 Continued

Fig. 6.6 Continued

E

DIM-C-pPhOCH$_3$ (10 μM)	-	-	+	+	-	-
DIM-C-pPh (10 μM)	-	-	-	-	+	+
DIM-C-pPhOH (20 μM)	-	+	-	+	-	+

PARP 114kDa ➞

PARP 84kDa ➞

TRAIL ➞

β-actin ➞
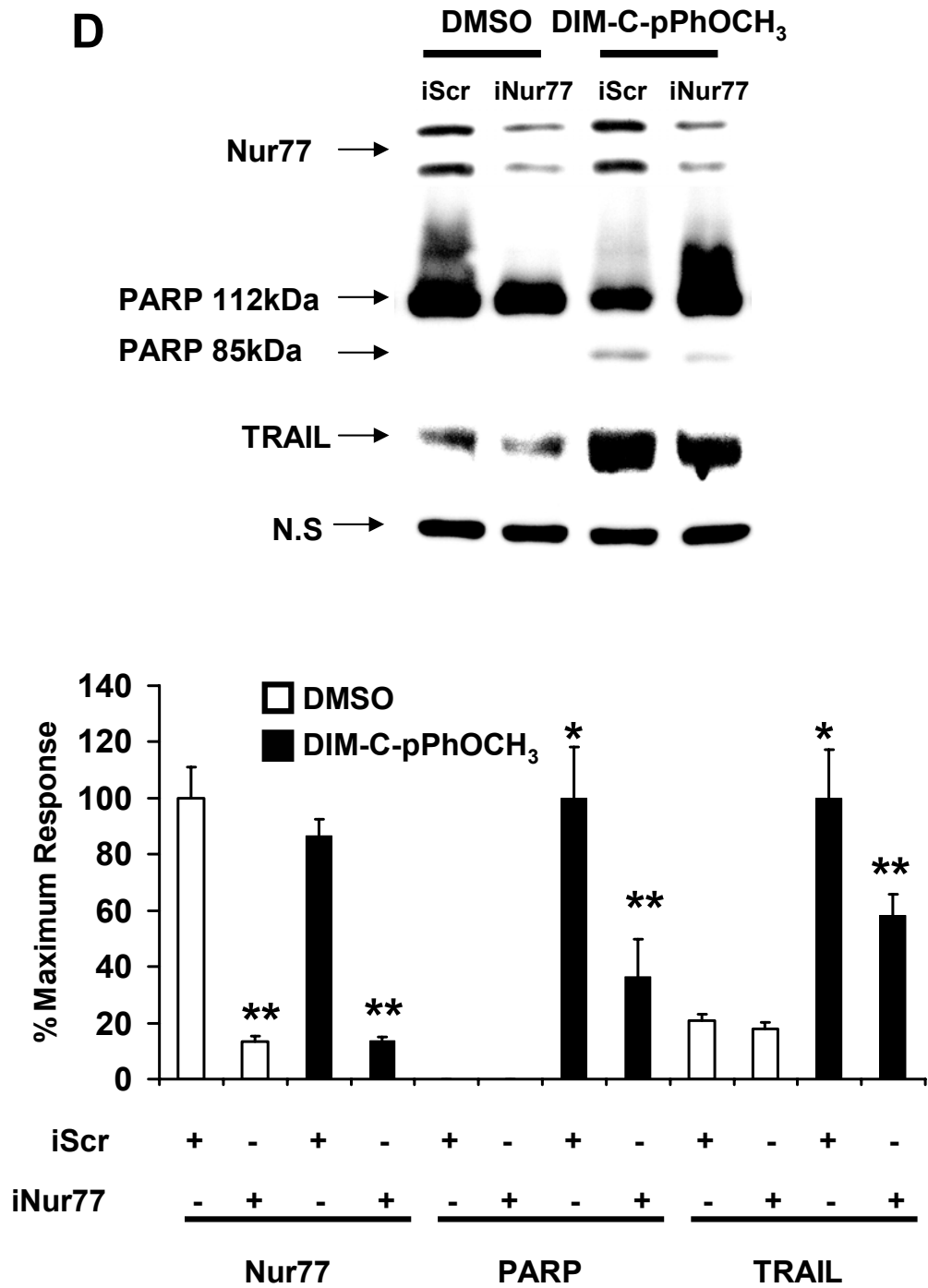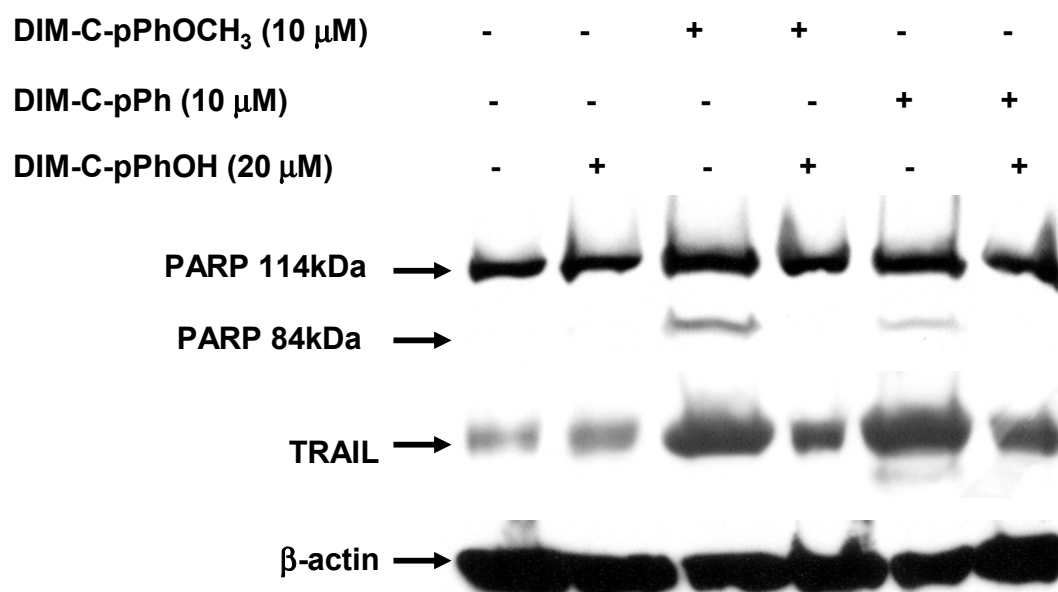
Fig. 6.6 Continued

the induction of PARP cleavage by the Nur77 agonists in Panc-28 cells was not affected by the nuclear export inhibitor leptomycin B (LMB) (1 ng/ml) (Fig. 6.5E). LMB alone slightly induced PARP cleavage and, for some cells cotreated with LMB plus Nur77 agonists, there was enhanced PARP cleavage. In contrast, previous studies showed that LMB inhibits apoptosis in cells treated with apoptosis-inducing agents that activate nuclear-cytosol/mitochondrial translocation of Nur77 (453, 454). These results demonstrate that activation of nuclear Nur77 by C-substituted DIMs induces apoptosis in Panc-28 and other cancer cell lines; however, evidence for activation of the intrinsic apoptotic pathways was not observed.

<p align="center">*Nur77-active C-DIMs induce TRAIL*</p>

In thymocytes, there is evidence that Nur77-induced apoptosis is linked to transcriptional activation (468), and microarray studies in thymocytes undergoing Nur77-dependent apoptosis identified several apoptosis-related genes including *fasL* and *TRAIL* (469). Results in Figure 6.6A show that Nur77 agonists that induce PARP cleavage also induce TRAIL (but not fasL) protein expression in Panc-28 cells, suggesting that this response may be a direct or indirect downstream target of Nur77 agonists in cancer cells. The Nur77-inactive DIM-C-pPhOH did not induce TRAIL. In addition, DIM-C-pPhOCH$_3$ or DIM-C-Ph induced TRAIL mRNA levels in Panc-28 cells (Fig. 6.6B). Since TRAIL activates the extrinsic apoptosis pathway and activation of caspase 8, we also investigated the effect of a caspase 8 inhibitor (Z-IETD-FMK) and the pan-caspase inhibitor (Z-VAD-FMK) on induction of PARP cleavage by Nur77

agonists (Fig. 6.6C). The results show that both inhibitors blocked (60 - 90%) induction of PARP cleavage by Nurr7 agonists.

The role of Nur77 in mediating induction of TRAIL and PARP cleavage by DIM-C-pPhOCH$_3$ was further investigated in Panc-28 cells transfected with non-specific RNA (iScr) and iNur77 (Fig. 6.6D). Levels of Nur77, PARP cleavage, and TRAIL proteins were determined by Western blot analysis of whole cell extracts and the results showed that iNurr significantly decreased levels of all three proteins. In addition, cotreatment of Panc-28 cells with DIM-C-pPhOH$_3$ or DIM-C-Ph and the Nur77 antagonist DIM-C-pPhOH (Fig. 6.6E) showed that the latter compound also inhibited induction of PARP cleavage and TRAIL protein expression induced by Nur77 agonists. These results demonstrate that Nur77 agonists induce apoptosis pathways in cancer cells through transcriptional (nuclear) mechanisms, and at least one of the induced proteins (TRAIL) activates an extrinsic apoptotic pathway. In summary, selected C-substituted DIMs have now been identified as ligands for the orphan receptor Nur77 and activation of this receptor is associated with decreased cancer cell survival, induction of TRAIL and apoptosis.

Inhibition of tumor growth in athymic nude mice bearing Panc-28 cell xenografts

Approximately 11 days after injection of Panc-28 cells, palpable tumors were detected and the mice were administered corn oil (control) or DIM-C-pPhOCH3 (in corn oil) at a dose of 25 mg/kg/day, which was given by oral gavage. The animals were treated every second day, and tumor areas were determined over the duration of the experiment. The results (Fig. 6.7A) showed that DIM-C-pPhOCH$_3$ significantly
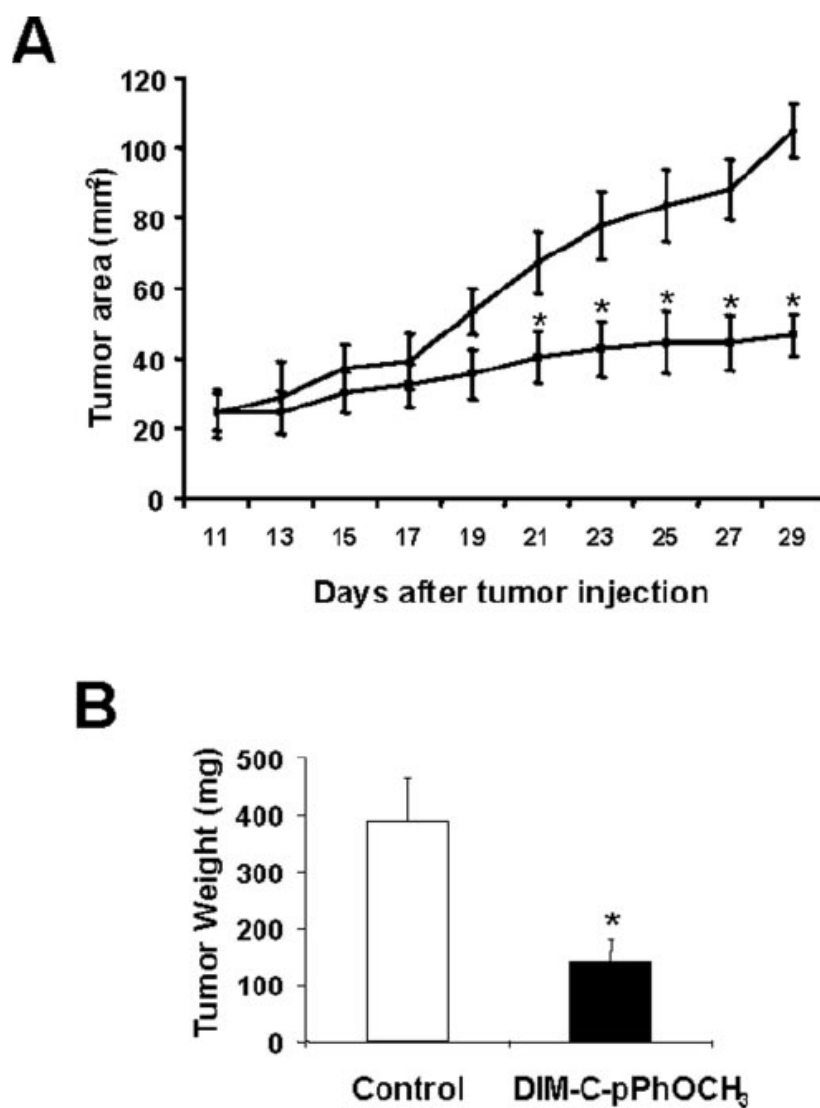
Fig. 6.7. Inhibition of tumor growth by DIM-C-pPhOCH$_3$. Tumor areas (*A*) and weights (*B*). Male athymic nude mice bearing Panc-28 cell xenografts were treated every second day with corn oil and DIM-C-pPhOCH$_3$ in corn oil as described under "Materials and Methods." The overall dose of DIM-C-pPhOCH$_3$ was 25 mg/kg/day. Significant ($p < 0.05$) inhibition of tumor areas and weights is indicated by an *asterisk*. H&E stainings of muscle and brain tissue from control and treated animals were similar, and tumors from control and treated animals exhibited apoptosis (data not shown).

213

inhibited tumor growth (area), and this was also complemented by a parallel decrease in tumor weights (Fig. 6.7B). Analysis of tumors from control and treated animals (TUNEL assay) indicated similar levels of apoptosis. Animal weight gain and organ weights were comparable in both treatment groups, and there were no apparent signs of toxicity in the DIM-C-pPhOCH3-treated mice compared with the corn oil controls. The mouse brain and muscle express relatively high levels of Nur77 (470), and examination of brain regions by H&E staining did not indicate any differences between the control (corn oil) and DIM-C-pPhOCH3-treated animals.

Discussion

Nur77 is widely expressed in multiple tissues and has been identified as a critical mediator of T-cell receptor-dependent apoptosis in T-lymphocytes and T-hybridoma cells (471, 472). Expression of dominant negative or antisense Nur77 blocked T-cell receptor-mediated apoptosis in T-hybridoma cells and extensive apoptosis of thymocytes was observed in transgenic mice overexpressing full length Nur77 (451, 452). Activation of cell death in macrophages is associated with increased expression of Nur77 and decreased cell death was observed in Nur77-deficient macrophages (473). A recent study (474) show that cadmium acetate induced apoptosis in WI-38 human lung fibroblasts and A549 human lung carcinoma cells and this was also accompanied by induction of Nur77. Moreover, transfection with dominant-negative Nur77 protected the cells against cadmium-induced apoptosis.

Ongoing studies in the laboratory with a series of C-substituted DIMs indicate that these compounds inhibit growth or induce cell death of multiple cancer cell lines,

and some of these analogs including DIM-C-pPhCF$_3$ activate PPARγ (359, 393). However, several PPARγ-inactive C-substituted DIMs also decreased cell survival of several cancer cell lines (e.g. Fig. 6.5A) and inhibited carcinogen-induced mammary tumor growth in female Sprague-Dawley rats. Nur77 was considered as a possible target for C-DIM compounds based on results of several studies with retinoids, apoptosis and differentiation-inducing agents that also inhibit cell growth and activate extranuclear Nur77 (453-458). Initial studies confirmed Nur77 protein expression in 12 prostate, colon, bladder, pancreatic and breast cancer cell lines (Fig. 6.1A). Results of screening a panel of structurally-diverse C-substituted DIMs shows that DIM-C-pPhCF$_3$ and two PPARγ-inactive analogs, DIM-C-pPhOCH$_3$ and DIM-C-Ph, activate Nur77-dependent transactivation in Panc-28 and other cancer cell lines transfected with GAL4-Nur77 (full length) or NuRE (Figs. 6.1B and 6.1C). Moreover, ligand-induced transcriptional activation is observed with GAL4-Nur77(E/F) chimeras (Fig. 6.2C) in which only the ligand binding domain of Nur77 is expressed. The role of Nur77 in mediating ligand-dependent transactivation was confirmed in studies showing that these responses were inhibited by either iNur77 (small inhibitory RNA) (Fig. 2B) or DIM-C-pPhOH which exhibited Nur77 antagonist activity (Fig. 6.2C). Previous studies on the crystal structure of the mouse Nurr1 LBD (475) and the *Drosophila* Nurr1 homolog DHR38 (476) show that the ligand binding pocket (LBP) is occupied by bulky hydrophobic amino acid side-chains. Moreover, due to the high sequence homology among NGFI-B family proteins, it has been suggested that Nur77, Nurr1 and Nor-1 may represent a class of orphan receptors that function independently of ligand binding (477). In contrast, this study

shows that selected C-DIM compounds uniquely induce nuclear Nur77-mediated transactivation; this induction response is observed through the E/F domain of Nur77 (Fig. 6.1C) and can be inhibited by DIM-C-pPhOH, a Nur77 antagonist (Figs. 6.2 and 6.5). Moreover, both activation of Nur77 and Nur77 antagonist activities by C-DIMs were highly structure-dependent (Figs. 6.1 and 6.2). These results suggest that the active C-DIM compounds interact with the E/F domain of Nur77 and induce conformational changes, resulting in binding to the LBP or other sites within the C-terminal region of Nur77. Currently, we are examining critical ligand interaction sites within the E/F domain of Nur77 by deletion/mutation analysis and by crystallization of the Nur77 LBD in the presence or absence of the C-DIM ligands.

Several studies have reported activation of Nur77-dependent transactivation in different cell lines and these responses primarily involve the AF-1 domain of Nur77 and activation by kinases (464, 478, 479). For example, induction of Nur77-dependent transactivation was observed for the coactivator ASC-2 in CV-1 and HeLa cells; however, this effect was dependent on calcium/calmodulin-dependent protein kinase IV and did not involve direct ASC-2-Nur77 interactions (478). Transactivation mediated by Nur77 homodimers is enhanced by protein kinase A and SRC1-3 in CV-1 and AtT-20 cells and these responses were AF-1-dependent (464). Another report also confirmed that Nur77 transactivation in C2C12 and COS-1 cells was enhanced by SRCs and other coactivators, and involved direct interactions of coactivators with the A/B (and not E/F) domain of Nur77 (479). These observations were consistent with the crystal structure of Nurr1 which lacks the "classical binding site for coactivators" (475). However, ligand-

dependent activation of Nur77 E/F domain observed in this study (Fig. 6.1C) should also be accompanied by interactions with some nuclear receptor coactivators/coregulators. Initial studies sowed that in the absence of ligand, VP-Nur77(E/F) did not interact with GAL-4-coactivators (PGF-1, CARM-1, SRC1-3, TRAP 220) or GALR-SMRT chimeras; however, DIM-C-pPhCF$_3$, DIM-C-pPhOCH$_3$ and DIM-C-Ph induced interactions between several common nuclear receptor coactivators (PGC-1, SRC-1 and TRAP220) and the LBD (E/F) of Nur77 in mammalian two-hybrid assays (Figs. 6.3B – 6.3D). These results are consistent with other studies on activation of nuclear receptors by ligands and their interactions with specific coactivators through binding receptor E/F domains. For example, our recent studies with PPARγ-active C-substituted DIMs in colon cancer cells show that ligand-induced PPARγ(E/F domain)-coactivator interactions in mammalian two-hybrid assays primarily involved PGC-1 (393), whereas C-DIM-induced Nur77-coactivator interactions in Panc-28 cells involve multiple coactivators. Although the crystal structure of unliganded Nurr1 shows that this receptor does not contain a classical coactivator interaction site in the E/F domain (helix 12), novel coactivator interactions surfaces have recently been identified between helices 11 and 12 in Nurr1 (480). This region is similar in human Nur77 and current studies are investigating C-DIM-induced interaction surfaces between the E/F domain of Nur77 and coactivators. In summary, the transactivation and coactivator-Nur77 interactions induced by DIM-C-pPhCF$_3$, DIM-C-pPhOCH$_3$ and DIM-C-Ph are consistent with results obtained for other ligand-activated nuclear receptors suggesting that selected C-

substituted DIMs are a novel class of compounds that induce E/F domain-dependent activation of Nur77.

Treatment of Panc-28 cells with Nur77-active C-substituted DIMs agonists decreased cell survival (Fig. 6.4A) and induced nuclear condensation within 48 and 24 hr, respectively and this is typically observed in cells undergoing cell death. We therefore further examined Nur77-mediated induction of PARP cleavage which is a well-characterized downstream marker of activated cell death pathways. PARP cleavage was induced in Panc-28 cells treated with Nur77 agonists (Fig. 6.5B), and similar results were observed in other pancreatic, prostate and breast cancer cell lines (Fig. 6.5D). Annexin V staining was also observed in Panc-28 cells treated with Nur77-active C-DIMs (Fig. 6.5C) and these data further confirm induction of apoptosis in these cancer cell lines. Previous studies report that induction of cell death pathways by apoptosis-inducing agents in some cancer cell lines is accompanied by translocation of Nur77 from the nucleus to the cytosol/mitochondria, and this has been linked to cytochrome c release and direct interaction of Nur77 with bcl-2 (453-458). In contrast, we observed that treatment of Panc-28 cells with Nur77-active C-DIMs resulted only in formation of a nuclear complex (Figs. 6.4A and 6.4B). Moreover, inhibition of nuclear export of Nur77 by LMB did not affect PARP cleavage induced by Nur77-active C-DIMs (Fig. 6.5E) suggesting that this response is mediated through nuclear Nur77. This nuclear pathway for induction of apoptosis is in contrast to the effects observed for TPA and CD437 which induce nuclear export of Nur77 in cancer cell lines and inhibition of Nur77 nuclear export by LMB inhibits induction of apoptosis (453, 454). These results clearly

distinguish between the induction of cell death pathways in cancer cells through ligand-dependent activation of nuclear Nur77 (this study) and through induction of Nur77 nuclear translocation (453-458).

Overexpression of Nur77 in thymocytes induces expression of several genes associated with apoptosis (469), and at least one of the genes, TRAIL (protein and mRNA), is also induced by Nur77 agonists in Panc-28 cells (Figs. 6.6A and 6.6B). RNA interference assays with iNur77 (Fig. 6.6D) and inhibition studies with the Nur77 antagonist DIM-C-pPhOH (Fig. 6.6E) demonstrate that induction of TRAIL and PARP cleavage by DIM-C-pPhOCH$_3$ and DIM-C-Ph are Nur77-dependent. Thus, the nuclear action of Nur77 agonists in cancer cell lines is comparable to the transcriptionally-dependent pathway observed in T-cells overexpressing Nur77 (469). TRAIL typically activates caspase 8 and the extrinsic pathways of apoptosis and the caspase 8 inhibitor Z-IETD-FMK significantly blocks (>60%) induction of PARP cleavage by Nur77 agonists (Fig. 6.5C). The pancaspase inhibitor Z-VAD-FMK blocked >90% of induced PARP cleavage suggesting that although TRAIL may be a major Nur77-induced gene in Panc-28 cells, other pro-apoptotic genes may also be induced and these are currently being investigated. We also observed in xenograft experiments that DIM-C-pPhOCH$_3$ inhibited tumor growth in athymic nude mice bearing Panc-28 cell xenografts (Fig. 6.7).

In summary, results of this study have identified a novel group of C-substituted DIMs that activate the orphan receptor Nur77 through the E/F domain. These results are in contrast to previous reports showing that kinase/coactivator-dependent activation of Nur77 was primarily AF-1-dependent (460, 478, 479). It has also been reported that

nuclear receptor coactivators interact with the N-terminal A/B but not E/F domains of Nur77 and in the absence of C-DIM compounds, coactivator-Nur7(E/F) interactions were not observed in this study. However, DIM-C-pPhCF$_3$, DIM-C-Ph and DIM-C-pPhOCH$_3$ induced coactivator interactions with the E/F domain of Nur77 (Fig. 6.3) and this was consistent with Nur77 (nuclear)-dependent transactivation. Activation of Nur77 by selected C-DIMs is associated with decreased cancer cell survival, induction of apoptosis, and induced expression of the apoptotis gene/protein TRAIL. These results suggest that C-DIM ligands that activate Nur77 are a potential new class of anticancer agents and their activities and mechanisms of action in other cancer cell lines are currently being investigated.

CHAPTER VII

2-CYANO-3,12-DIOXOOLEAN-1,9-DIEN-28-OIC ACID (CDDO) AND

RELATED COMPOUNDS INHIBIT GROWTH OF COLON CANCER CELLS

THROUGH PEROXISOME PROLIFERATOR-ACTIVATED RECEPTOR γ-

DEPENDENT AND -INDEPENDENT PATHWAYS*

Introduction

2-Cyano-3,12-dioxooleana-1,9-dien-28-oic acid (CDDO) is a synthetic triterpenoid-derived compound structurally-related to the pentacyclic triterpenoids oleanolic and ursolic acids which exhibit anti-inflammatory and anticarcinogenic activities (481-483). CDDO and related compounds inhibit growth of multiple cancer cell lines, induced differentiation and inhibited inducible nitric oxide synthase (iNOS) and cyclooxygenase 2 activities (432, 433, 481, 483-486). CDDO and the methyl ester derivative (CDDO-Me) bound peroxisome-proliferator-activated receptor γ (PPARγ) and CDDO induced transactivation in CV-1 cells transfected with PPARγ-responsive GAL4-PPARγ or PPRE (promoter) constructs (487). CDDO alone or in combination with the RXR agonist LG100268 induced 3T3-L1 differentiation, whereas CDDO-Me was inactive in this assay. It was suggested that CDDO was a PPARγ agonist, whereas

CDDO-Me exhibited partial antagonist activity (487).

CDDO, CDDO-Me and an imidazole ester (CDDO-Im) decrease cancer cell survival, and their cell context-dependent responses and mechanisms of action have been investigated (488-495). These triterpenoid compounds are potent inducers of differentiation and apoptosis in leukemia cells; however, their pro-apoptotic effects were somewhat variable among different cell lines. CDDO-Me induced intrinsic apoptotic pathways in HL-60 cells and enhanced responses were observed after cotreatment with RXR ligands (491). CDDO-induced apoptosis in HL-60 and U937 cells were inhibited by dominant negative PPARγ expression and the PPARγ antagonist N-(4'-aminopyridyl-2-chloro-5-nitrobenzamide (T007) (494). CDDO and related compounds also induced caspase 8-dependent pathways in leukemia cells (489, 490, 492-494), and this may be due, in part, to downregulation of FLIP, an endogenous inhibitor of caspase-8 activation. CDDO also induced apoptosis in leukemia cells through enhanced oxidative stress (493) and loss of mitochondrial membrane potential (495). In breast cancer cells, CDDO inhibits growth of ER-positive and ER-negative cells and tumor growth in athymic nude mouse models and this correlated with modulation of genes associated with cell cycle progression, apoptosis and ER stress (496). In COLO 16 human skin cancer cells, CDDO induced apoptosis and this was due, in part, to ER stress and direct mitochondrial effects that disrupted calcium homeostasis (497). CDDO-Me induced both the intrinsic and extrinsic apoptosis pathway in lung cancer cell lines (498, 499), and a caspase 8-dependent apoptotic pathway was activated by CDDO in human osteosarcoma cells (500). CDDO also inhibited growth of several ovarian cancer cell lines that express

PPARγ and, since cotreatment with the PPARγ antagonist T007 did not block the effects of CDDO, it was concluded that this response was PPARγ-independent (363, 501).

This study reports the effects of CDDO compound on SW-480 and other colon cancer cell lines and investigates the concentration-dependent induction of PPARγ-dependent and -independent responses. Growth inhibitory IC_{50} values for CDDO-Me and CDDO-Im were ≤ 0.2 μM in SW-480, HCT-116 and HT-29 colon cancer cells, whereas IC_{50} values for CDDO were ≤ 0.5 μM after 6 days of growth. CDDO, CDDO-Im and CDDO-Me also induced PPARγ-dependent transactivation and coactivator-PPARγ interactions in mammalian two-hybrid assays in SW-480 cells. In the same cell lines, CDDO and related compounds induce PPARγ-dependent upregulation of the tumor suppressor gene caveolin-1 and PPARγ-independent apoptosis and these responses were activated over distinct and separable concentrations in SW-480 cells.

Materials and Methods

Cell culture

Human colon cancer cell lines SW480 and HT-29 were provided by M.D. Anderson Cancer Center; HCT-116 cells were obtained from American Type Culture Collection (Manassas, VA). SW480 and HT-29 cells were maintained in Dulbecco's Modified Eagle's Medium nutrient mixture F-12 Ham (DMEM:Ham's F-12; Sigma, St. Louis, MO) with phenol red supplemented with 0.22% sodium bicarbonate, 0.011% sodium pyruvate and 5% fetal bovine serum (FBS) (Intergen, Purchase, NY) and 10 ml/L of 100X antibiotic antimycotic solution (Sigma). HCT-116 cells were maintained in RPMI-1640 medium (Sigma) supplemented with 0.22% sodium bicarbonate, 0.011%

sodium pyruvate, 0.45% glucose, 0.24% HEPES, 10% FBS and 10 ml/L of 100X antibiotic antimycotic solution (Sigma).

Chemicals, reagents, plasmids and antibodies

The PPARγ antagonist *N*-(4'-aminopyridyl)-2-chloro-5-nitrobenzamide (T007) was synthesized in this laboratory and confirmed by gas chromatography-mass spectrometry. CCDO compounds were provided by Dr. Edward Sausville (Developmental Therapeutics Program, National Cancer Institute, Bethesda, MD) through the Rapid Access to Intervention Developmental Program. Horseradish peroxidase substrate for Western blot analysis was purchased from NEN Life Science Products (Boston, MA). Cell lysis buffer, and luciferase reagent were purchased from Promega (Madison, WI), and β-galactosidase (β-gal) reagent was from Tropix (Bedford, MA). Small inhibitory RNA (siRNA) duplexes were prepared by Dharmacon Research (Lafayette, CO). Previous studies in this laboratory have reported oligonucleotide sequences for PPARγ and lamin A/C siRNA (359). The Gal4 reporter containing 5X Gal4 DBD (Gal4Luc) was kindly provided by Dr. Marty Mayo (University of North Carolina, Chapel Hill, NC). Gal4DBD-PPARγ construct (gPPARγ) was a gift of Dr. Jennifer L. Oberfield (Glaxo Wellcome Research and Development, Research Triangle Park, NC) and PPARγ expression plasmid and pM-PPARγ coactivator-1 (PGC1) were gifts of Dr. Bruce M. Spiegelman (Harvard University, Boston, MA). The PPRE-luc construct contains three tandem PPARγ response elements (PPREs) with a minimal TATA sequence in pGL2. The PPARγ2-VP16 fusion plasmid (VP-PPARγ) contained the DEF region of PPARγ (amino acids 183–505) fused to the pVP16 expression vector and

the GAL4-coactivator fusion plasmids pM-SRC1, pMSRC2, pMSRC3, pM-DRIP205 and pM-CARM-1 were kindly provided by Dr. Shigeaki Kato (University of Tokyo, Tokyo, Japan). Antibodies for caveolin-1 (sc-894), PARP (sc-8007), Akt and phospho-Akt were purchased from Santa Cruz Biotechnology (Santa Cruz, CA). Monoclonal anti-β-actin was purchased from Sigma (St. Louis, MO).

Cell proliferation assay

Cells (2×10^4) were plated in 12-well plates and media was replaced the next day with DMEM:Ham's F-12 media containing 2.5% charcoal-stripped FBS and either vehicle (DMSO) or the indicated ligand and dissolved in DMSO. Fresh media and compounds were added every 48 hr. Cells were counted at the indicated times using a Coulter Z1 cell counter. The proliferation of SW480 cells was also carried out as described above using the colorimetric WST1 assay according to the manufacturer's instructions (Roche, Mannheim, Germany). Cells (4000/well) were seeded in 96 well plates and assayed after 48 hr. Each experiment was carried out at least three times and results are expressed as means ± SE for each determination.

Transfection and luciferase assay

Colon cancer cells (1×10^5) were seeded onto 24-well plates in DME-F12 media supplemented with 2.5% charcoal-stripped FBS and grown overnight. Transient transfections were performed using LipofectAmine reagent (Invitrogen) according to the protocol provided by the manufacturer. For transfections with siRNA for PPARγ, the RNA concentration was 75 nM and Oligofectamine transfection regent (Invitrogen) was used. Cotransfections were performed using Gal4Luc (0.4 μg), β-gal 0.04 μg),

Gal4DBD-PPARγ (0.04 µg), VP-PPARγ (0.04 µg), pM SRC1 (0.04 µg), pMSRC2 (0.04 µg), pMSRC3 (0.04 µg), pMPGC-1 (0.04 µg), pMDRIP205 (0.04 µg) and pMCARM-1 (0.04 µg). After 5 hr of transfection, the transfection mix was replaced with complete media containing either vehicle (DMSO) or the indicated ligand for 20-22 hr. Cells were then lysed with 100 µl of 1X reporter lysis buffer and 30 µl of cell extract were used for luciferase and β-galactosidase assays. A Packard Lumicount luminator (Packard Instruments Co., Downers Grove, IL) was used to quantitate luciferase and β-galactosidase activities, and the luciferase activities were normalized to β-galactosidase activity.

Western blot analysis

SW480, HT-29 and HCT-116 (3 x 10^5) cells were seeded in six-well plates in DMEM:Ham's F-12 media containing 2.5% charcoal-stripped FBS for 24 hr and then treated with either the vehicle (DMSO) or the indicated compounds. Whole cell lysates were obtained using high salt buffer [50 mM HEPES, 500 mM NaCl, 1.5 mM MgCl$_2$, 1 mM EGTA, 10% glycerol and 1% Triton X-100 pH 7.5 and 5 µl/ml of Protease Inhibitor Cocktail (Sigma)]. Protein samples were incubated at 100°C for 2 min, separated on 10% SDS-PAGE at 120 V for 3-4 hr in 1 X running buffer [25 mM Tris-base, 192 mM glycine, and 0.1% SDS (pH 8.3)], and transferred to polyvinylidene difluoride membrane (PVDF, Bio-Rad, Hercules, CA) at 0.1 V for 16 hr at 4°C in 1 X transfer buffer (48 mM Tris-HCl, 39 mM glycine, and 0.025% SDS). The PVDF membrane was blocked in 5% TBST-Blotto [10 mM Tris-HCl, 150 mM NaCl (pH 8.0), 0.05% Triton X-100 and 5% non-fat dry milk] with gentle shaking for 30 min and incubated in fresh

5% TBST-Blotto with 1:1000 (for caveolin-1), 1:250 (for PARP), 1:5000 (for β-actin) primary antibody overnight with gentle shaking at 4°C. After washing with TBST for 10 min, the PVDF membrane was incubated with secondary antibody (1:5000) in 5% TBST-Blotto for 90 min. The membrane was washed with TBST for 10 min and incubated with 10 ml of chemiluminiscence substrate (PerkinElmer Life Sciences) for 1.0 min and exposed to Kodak X-OMAT AR autoradiography film (Eastman Kodak, Rochester, NY). Band intensities were evaluated by scanning laser densitometry (Sharp Electronics Corporation, Mahwah, NJ) using Zero-D Scanalytics software (Scanalytics Corporation, Billerica, MA).

Results

Initial studies investigated the effects of CDDO, CDDO-Me and CDDO-Im on growth of SW-480, HT-29 and HCT-116 colon cancer cells. Cells were treated with different concentrations of the test compounds on days 0, 2 and 4 (media and compounds were changed every 2 days) and cell numbers were determined 2, 4 and 6 days after treatment. Significant inhibition of cell proliferation was observed for all compounds after treatment for 2 and 4 days, and IC_{50} values were ≤ 0.2 µM for CDDO-Me and CDDO-Im and ≤ 0.5 µM for CDDO in all three cell lines. Cell survival results after treatment with the CDDO compounds (Fig. 7.1) were derived from the growth inhibition curves, and the percent cell survival was the ratio of the number of cells in the treated/DMSO (solvent) groups at each time point. Higher concentrations of these compounds decreased cell numbers below the initial number of attached cells (i.e. cell death) and after 96 hr, the concentrations of CDDO, CDDO-Me and CDDO-Im that

induced cell death in all three cell lines were 1.0-2.5, 0.2 and 0.2 µM, respectively. CDDO decreased proliferation of SW480 cells using the WST-1 colorimetric assay (Fig. 7.1D), and cotreatment of CDDO plus 5.0 µM T007 (PPARγ antagonist) significantly reversed the growth inhibitory effects of CDDO. The results demonstrate a role for PPARγ in mediating the effects of CDDO in this assay.

PPARγ-dependent transactivation assays

Previous studies showed that CDDO and related compounds activate PPARγ (487) and this was further investigated in SW-480 cells transfected a GAL4-PPARγ chimericexpression plasmid and a reporter construct (pGAL4) containing 5 tandem GAL4 response elements linked to a luciferase reporter gene. The results (Fig. 7.2A) show that CDDO, CDDO-Me and CDDO-Im induced a concentration-dependent increase in luciferase activity and significant induction was observed at concentrations as low as 0.2, 0.025 and 0.025 µM, respectively. Both CDDO and CDDO-Me induced a maximal 35- to 45-fold increase in luciferase activity; the maximal induced value for CDDO-Im was lower (< 30-fold); however, this may be due to toxicity of this compound at the higher concentrations or differential recruitment of coactivators or corepressors. Ligand-induced transactivation in SW-480 cells transfected with GAL4-PPARγ/pGAL4 was also inhibited by the PPARγ antagonist T007 (Fig. 7.2B). Maximal induction of luciferase activity by CDDO (2.5 µM), CDDO-Me (0.5 µM) and CDDO-Im (0.5 µM) was inhibited in cells cotreated with 5 µM T007. Similar results were observed at lower concentrations of the CDDO compounds and also with the PPARγ antagonist GW9660.

The CDDO compounds also induced transactivation in SW-480 cells transfected with a

construct (PPRE₃-luc) containing three tandem PPARγ response elements linked to
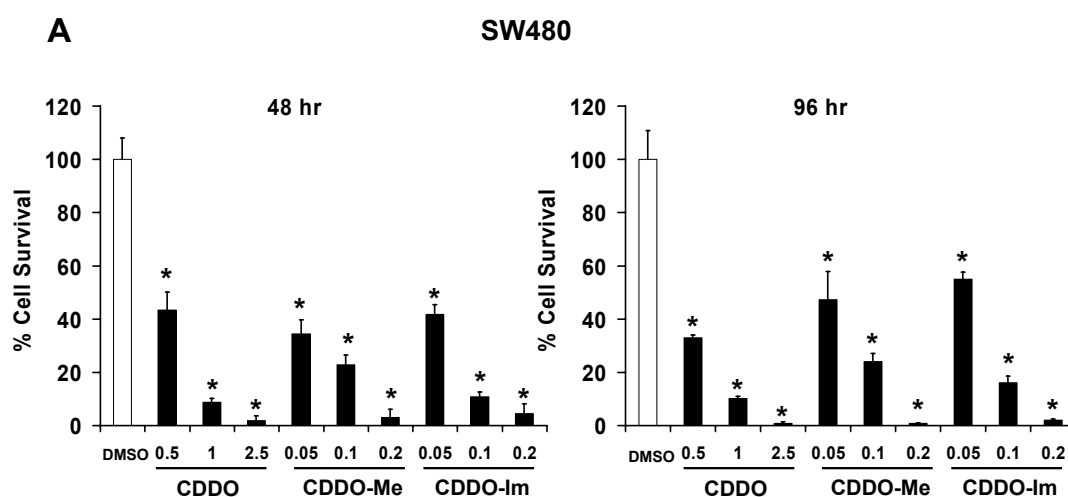
Fig. 7.1. Effects of CDDO and related esters on colon cancer cell survival and proliferation. SW-480 (A), HT-29 (B) and HCT-116 (C) cells were treated with different concentrations of CDDO, CDDO-Me or CDDO-Im for 48 or 96 hr, and this percent cell survival was determined as described in the Materials and Methods. Solvent (DMSO)-treated cells survival was set at 100% and significantly ($p < 0.05$) decreased cell numbers after treatment are indicated by an asterisk. The percent cell survival is derived from the treated/control (DMSO) cell number ratios. (D) Effects of T007 on CDDO-induced cell proliferation. SW480 cells were treated with different concentrations of CDDO and 5 µM T007 for 48 hr, and cell proliferation was determined colorimetrically using the cell proliferation reagent WST-1 as described in the Materials and Methods. Significant ($p < 0.05$) inhibition of cell proliferation by CDDO is indicated by an asterisk (*) and reversal of these effects by 5 µM T007 is indicated (**).

B

HT-29

C

HCT-116

Fig. 7.1. Continued

D
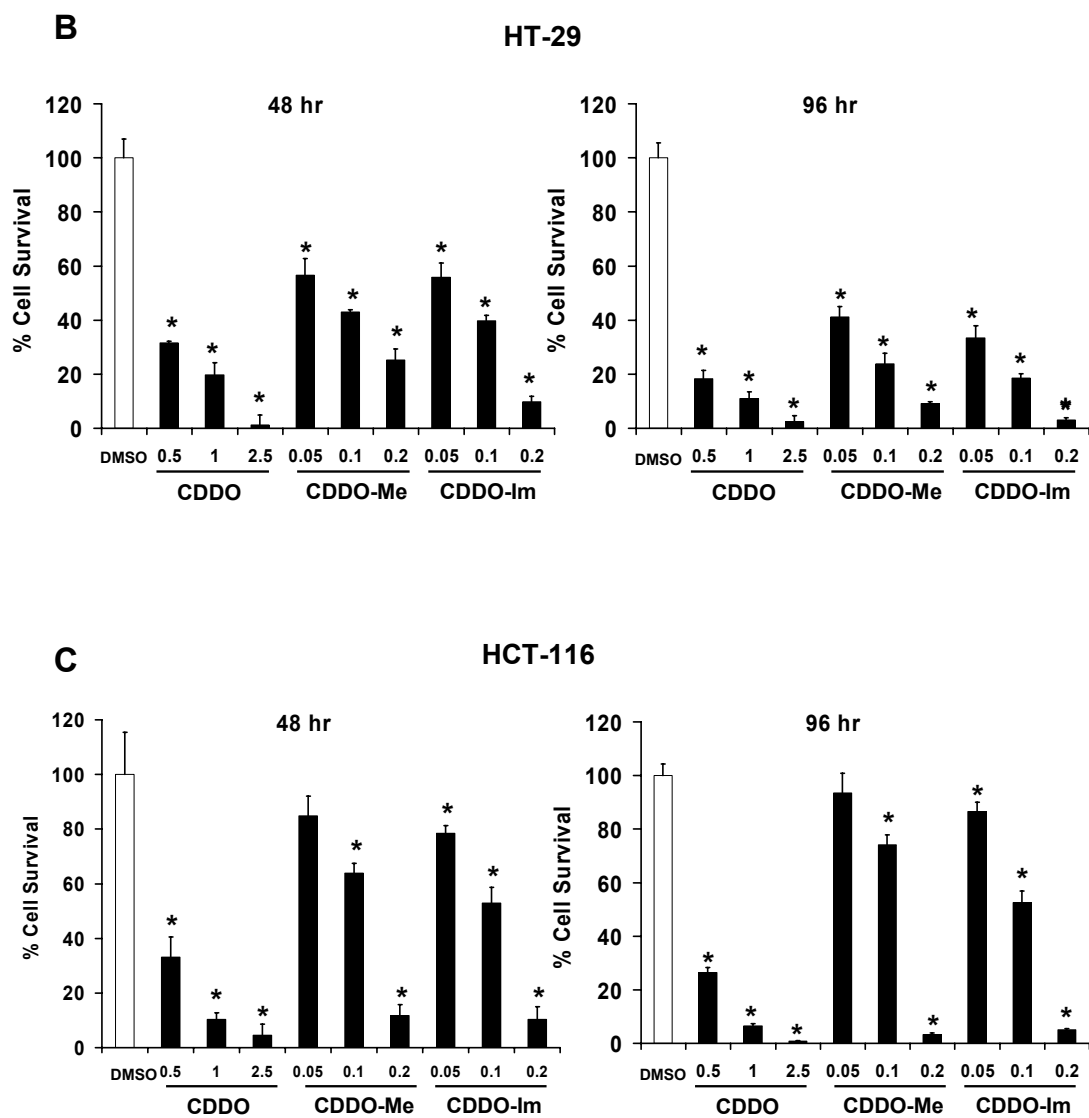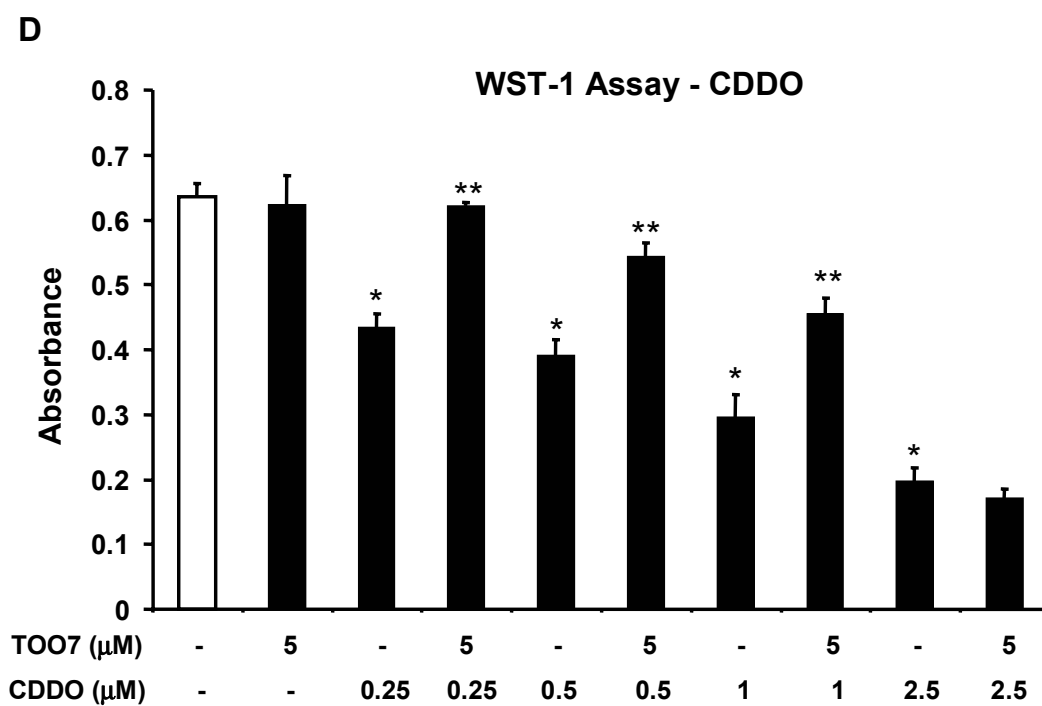
Fig. 7.1. Continued
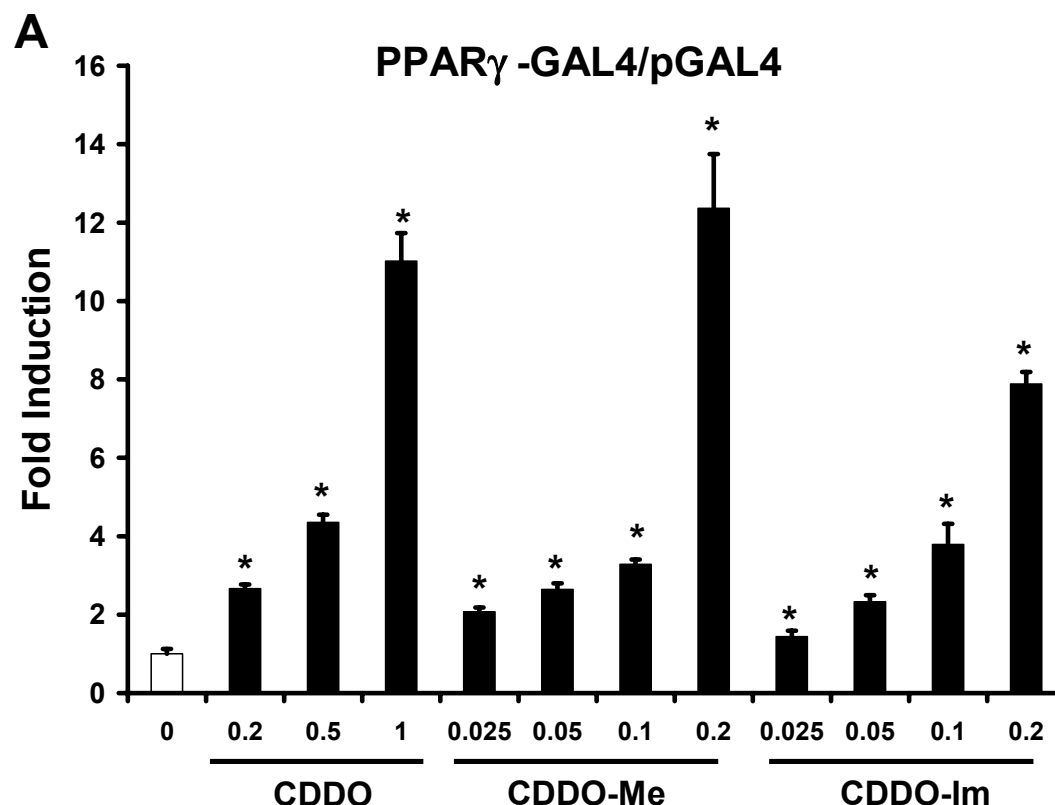
Fig. 7.2. PPARγ-dependent transactivation by CDDO, CDDO-Me and CDDO-Im in SW-480 cells. Activation of PPARγ-GAL4/pGAL4 (A) and inhibition by T007 (B). SW-480 cells were transfected with PPARγ-GAL4/pGAL4, treated with different concentrations of CDDO compounds and luciferase activity determined as described in the Materials and Methods. In a separate experiment, cells were treated with CDDO (2.5 µM), CDDO-Me (0.5 and 1.0 µM), or CDDO-Im (0.2 and 0.5 µM) alone or in combination with 5 µM T007. Significant ($p < 0.05$) induction by CDDO, CDDO-Me and CDDO-Im is indicated by an asterisk and inhibition by T007 is also indicated (**). (C) Activation of PPRE$_3$-luc. SW-480 cells were transfected with PPRE$_3$-luc, treated with CDDO compounds and luciferase activity determined as described in the Materials and Methods. Significant ($p < 0.05$) induction is indicated by an asterisk. (D) RNA interference assay. Cells were transfected with PPRE-luc, treated with the different CDDO compounds, and small inhibitory RNA for lamin (non-specific control) or PPARγ and luciferase activity determined as described in the Materials and Methods. Significant ($p < 0.05$) induction by PPARγ agonist (*) and inhibition after cotransfection with iPPARγ (**) is indicated. All experiments (A - D) are expressed as means ± SE for at least three separate determinations for each treatment group.

B

C

Fig. 7.2 Continued

D
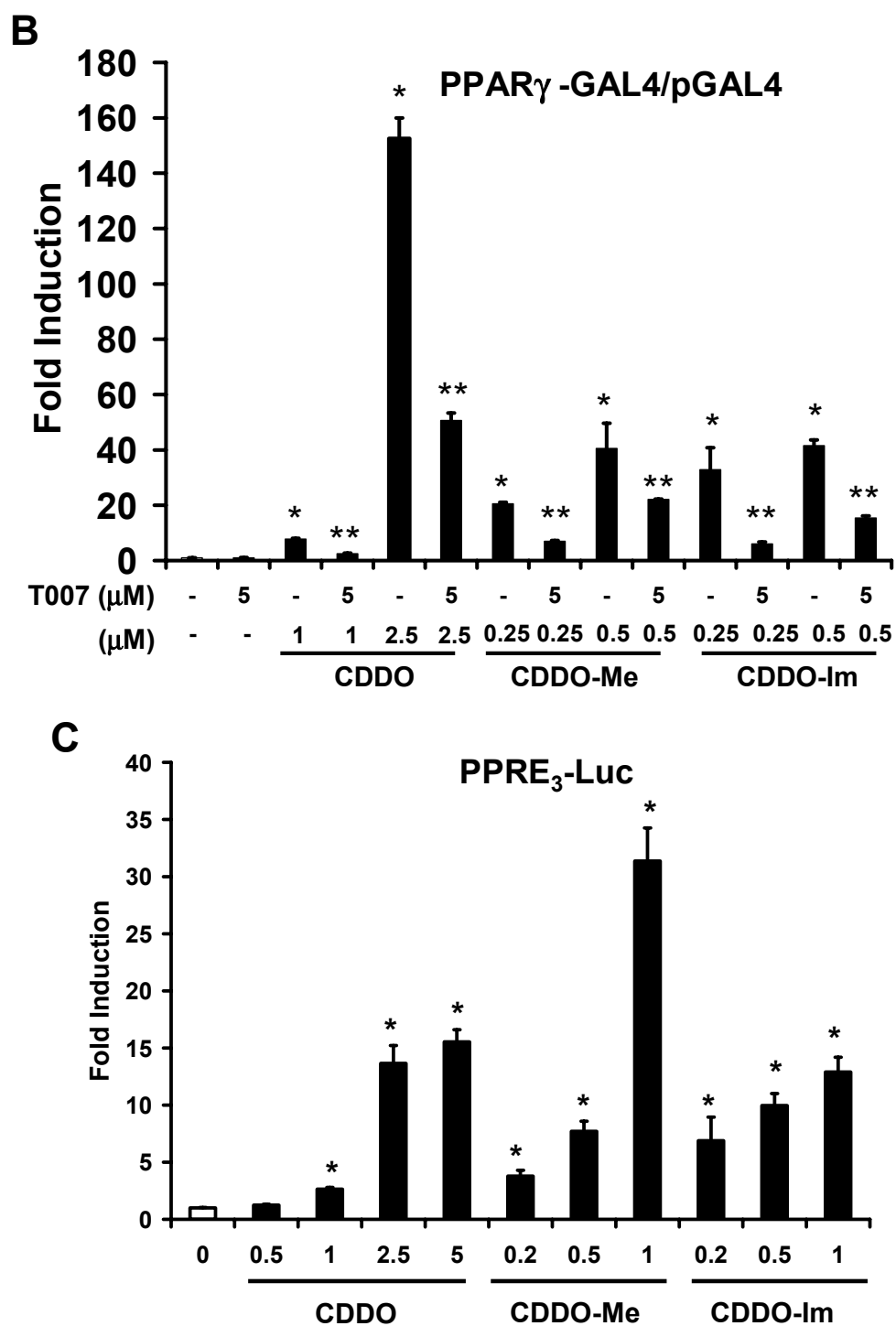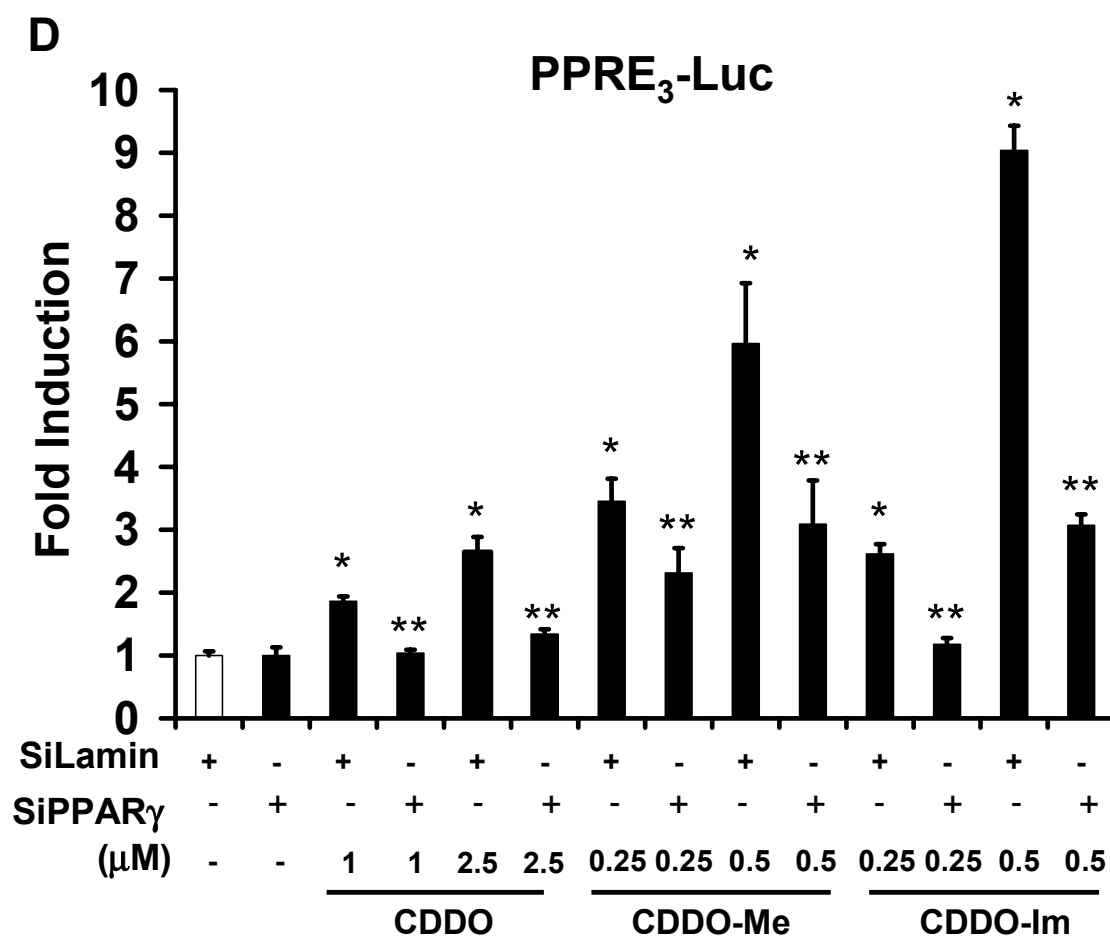
Fig. 7.2 Continued

firefly luciferase. The results (Fig. 7.2C) show that CDDO, CDDO-Me and CDDO-Im significantly induce transactivation at concentrations of 1.0, 0.2 and 0.2 μM, respectively, and maximal induction (> 30-fold) was observed for CDDO-Me. Transactivation induced by CDDO compounds in SW-480 cells transfected with PPRE-luc was inhibited after cotransfection with iPPARγ (Fig. 7.2D), and this correlates with comparable inhibition of PPARγ-dependent gene expression induced by other PPARγ agonists using iPPARγ (393). These results confirm that CDDO, CDDO-Me and CDDO-Im activate PPARγ-dependent transactivation in SW-480 colon cancer cells.

Induction of PPARγ-coactivator interactions by CDDO and related compounds

Previous reports show that different classes of PPARγ agonist induce structure-dependent interactions of PPARγ with coactivators in mammalian two hybrid experiments (363, 393) and therefore the effects of CDDO compounds were investigated in a mammalian two hybrid assay in SW-480 cells transfected with pGAL4, VP-PPARγ and GAL4-coactivators/GAL4-SMRT (corepressor). The results show that CDDO, CDDO-Me and CDDO-Im induce VP-PPARγ - pM coactivator interactions in SW-480 cells transfected with SRC-1, SRC-2, TRAP 220, CARM-1 and PGC-1 (Fig. 7.3). In contrast, CDDO and CDDO-Me but not CDDO-Im enhanced PPARγ-SRC-3 interaction; however, it is possible that higher concentrations of CDDO-Im would induce transactivation. We also investigated interactions with the corepressor SMRT and the results indicate that all three compound increased transactivation but CDDO-Im was
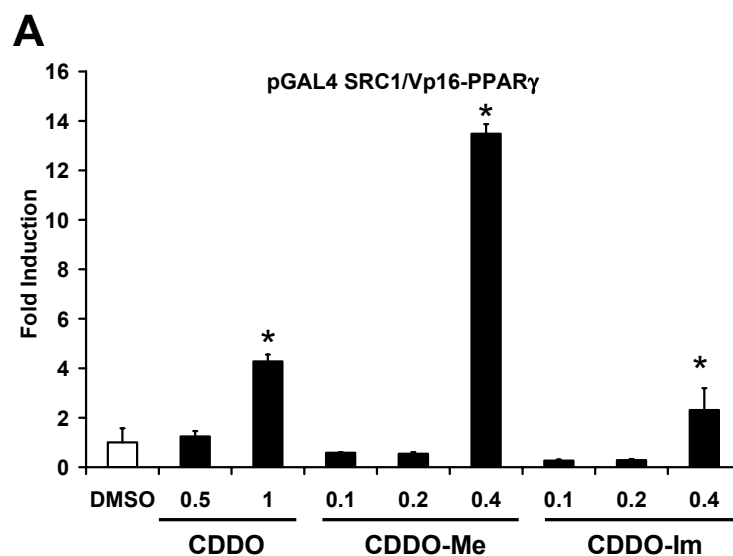
Fig 7.3. CDDO-, CDDO-Me- and CDDO-Im-induced PPARγ-coactivator interactions in SW-480 cells. Ligand-induced interactions with SRC-1 (A), SRC-2 (B), SRC-3 (C), TRAP 220 (D), PGC-1(E), CARM-1 (F), and SMRT (G). Cells were transfected with VP-PPARγ and GAL4-coactivator chimeric expression plasmids, treated with the CDDO compounds, and luciferase activity determined as described in the Materials and Methods. Results are expressed as means ± SE for at least three separate determinations for each treatment group and significant (p < 0.05) induction as indicated by an asterisk.
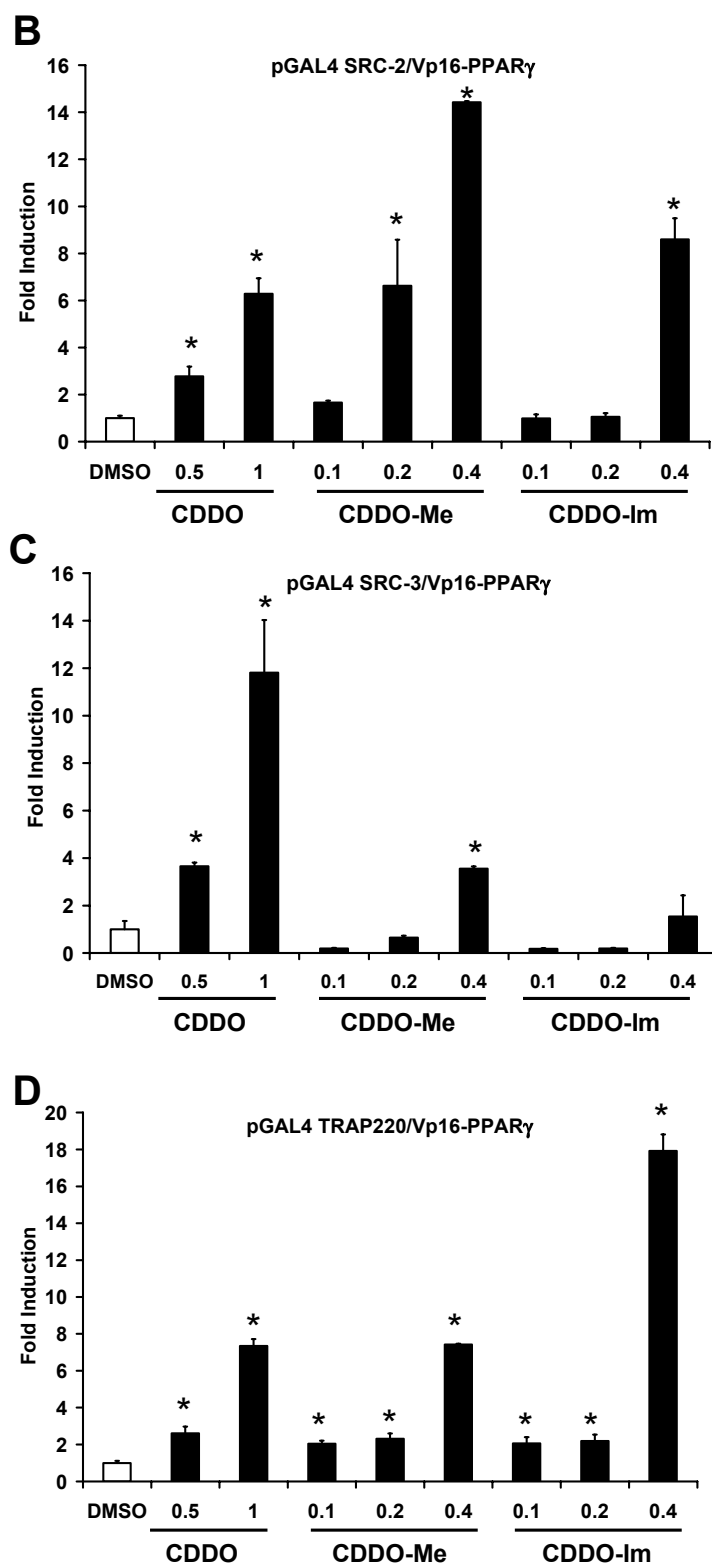
Fig. 7.3 Continued
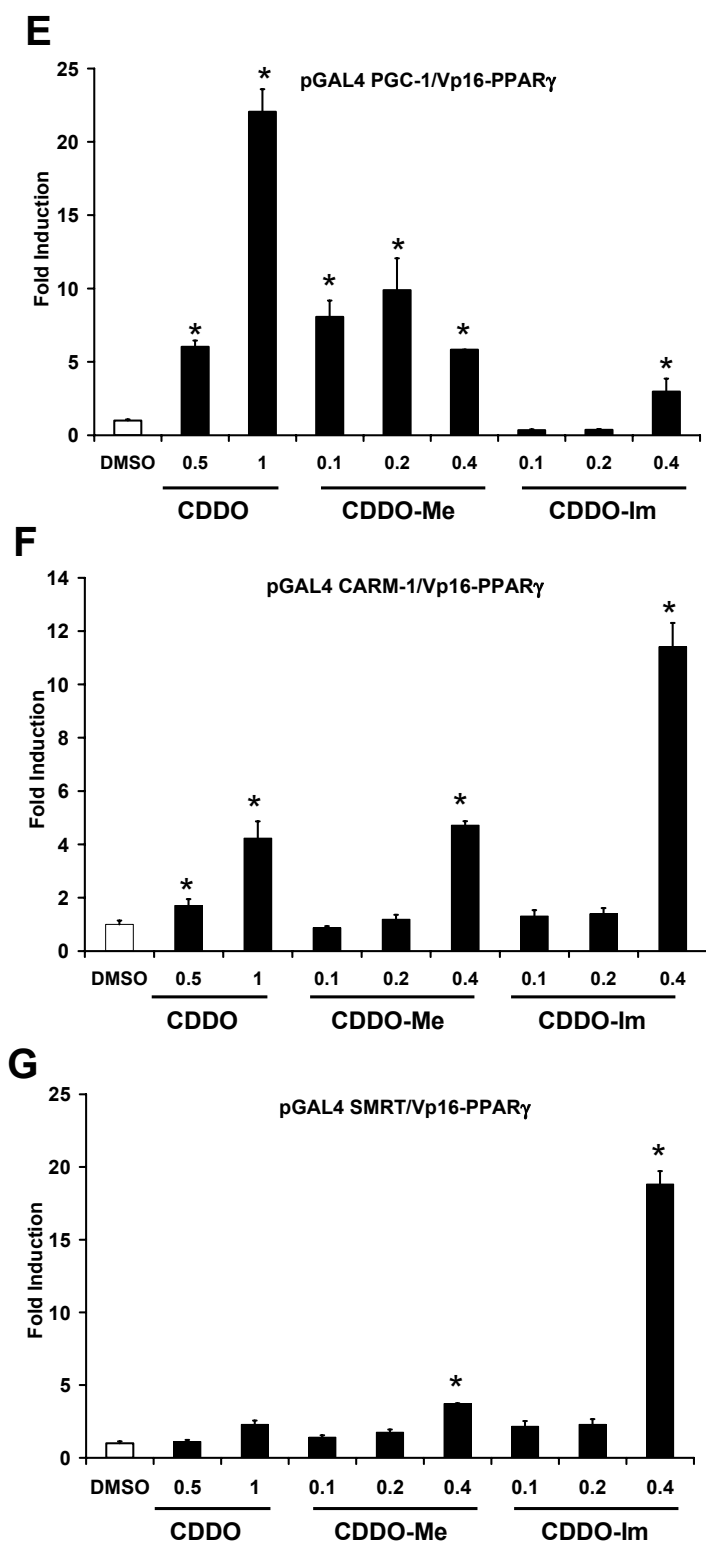
Fig. 7.3 Continued

significantly more active than CDDO or CDDO-Im. These results confirm that CDDO and related esters induce interactions between VP-PPARγ with pM-coactivators in SW-480 cells and differences between compounds were primarily concentration-dependent.

CDDO compounds induce caveolin-1 in colon cancer cells

Caveolin-1 is a tumor suppressor gene in colon cancer cells and previous reports show that PPARγ agonists induce this response in some colon cancer cell lines (364, 393). The results illustrated in Figure 7.4A show that after treatment of SW-480 cells with CDDO (0.25 - 0.5 μM), CDDO-Me (0.025 - 0.1 μM) and CDDO-Im (0.5 - 0.1 μM) for 3 days, caveolin-1 was induced by all three compounds. In contrast, induction of PARP cleavage, a marker of apoptosis was not observed at these concentrations. A slight increase in p27 was observed, and cyclin D1 was unchanged by these treatments. In a separate experiment, SW-480 cells were treated with the CDDO compounds or T007 alone and in combination for 3 days and caveolin-1 protein expression was determined (Figs. 7.4B – 7.4D). The results show that 5 μM T007 alone did not affect levels of caveolin-1 protein; however, in cells cotreated with CDDO, CDDO-Me or CDDO-Im plus T007, there was a decrease in caveolin-1 protein expression compared to cells treated with the CDDO compounds alone. These results complement the transactivation studies and demonstrate that induction of caveolin-1 by the CDDO compounds was inhibited by the PPARγ antagonist T007. Induction of caveolin-1 by CDDO, CDDO-Me and CDDO-Im was also determined in HT-29 (Fig. 7.5A) and HCT-116 (Fig. 5B) cells, and induction was observed in both colon cancer cell lines, The

A

B
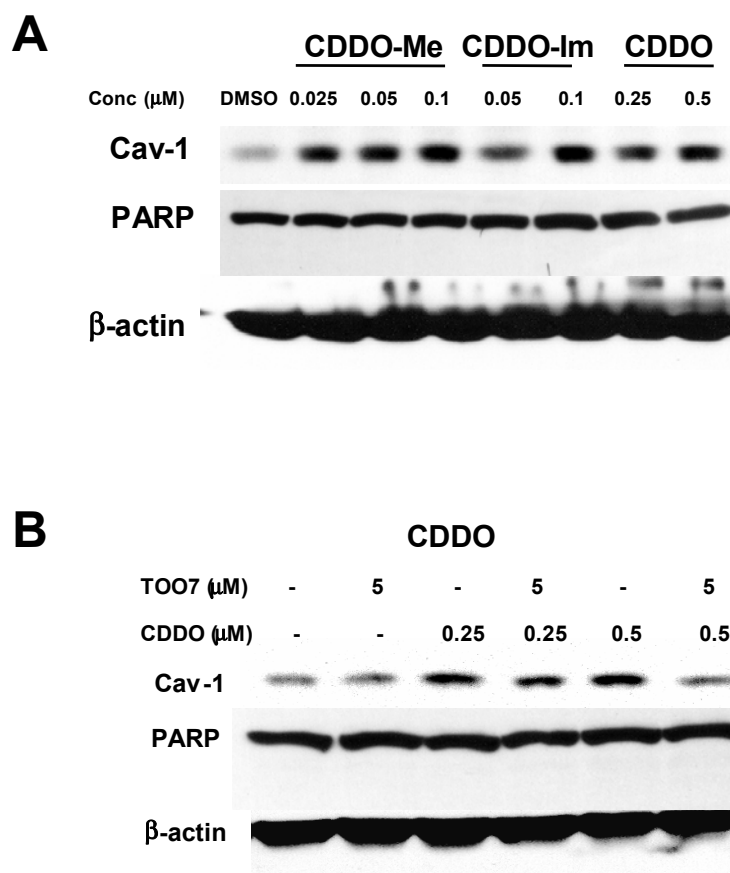
Fig 7.4. Induction of caveolin-1, Akt phosphorylation, and PARP cleavage by CDDO and related esters in SW-480 cells. (A) Induction of caveolin-1 and PARP cleavage. SW-480 cells were treated with CDDO, CDDO-Me and CDDO-Im for 3 days and caveolin-1 and PARP cleavage proteins were determined by Western blot analysis of whole cell lysates as described in the Materials and Methods. T007 inhibition of caveolin-1 induction by CDDO (B), CDDO-Me (C), and CDDO-Im (D). Cells were treated with the compounds alone or in combination with 5 μM T007 as described in (A), and whole cell lysates were analyzed by Western blot analysis. β-Actin served as a loading control for these experiments. (E) CDDO compounds induce Akt phosphorylation. Cells were treated with the CDDO compounds as described in (A), and Akt/phospho-Akt were determined by Western blot analysis as described in the Materials and Methods.

240

C

CDDO-Me

| TOO7 (µM) | - | 5 | - | 5 | - | 5 |
| CDDO-Me (µM) | - | - | 0.05 | 0.05 | 0.1 | 0.1 |

Cav-1

PARP

β-actin

D

CDDO-Im

| TOO7 (µM) | - | 5 | - | 5 | - | 5 |
| CDDO-Im (µM) | - | - | 0.05 | 0.05 | 0.1 | 0.1 |

Cav-1

PARP

β-actin

E

CDDO-Me   CDDO-Im   CDDO

| Conc (µM) | DMSO | 0.025 | 0.05 | 0.1 | 0.05 | 0.1 | 0.25 | 0.5 |

p-Akt

Akt
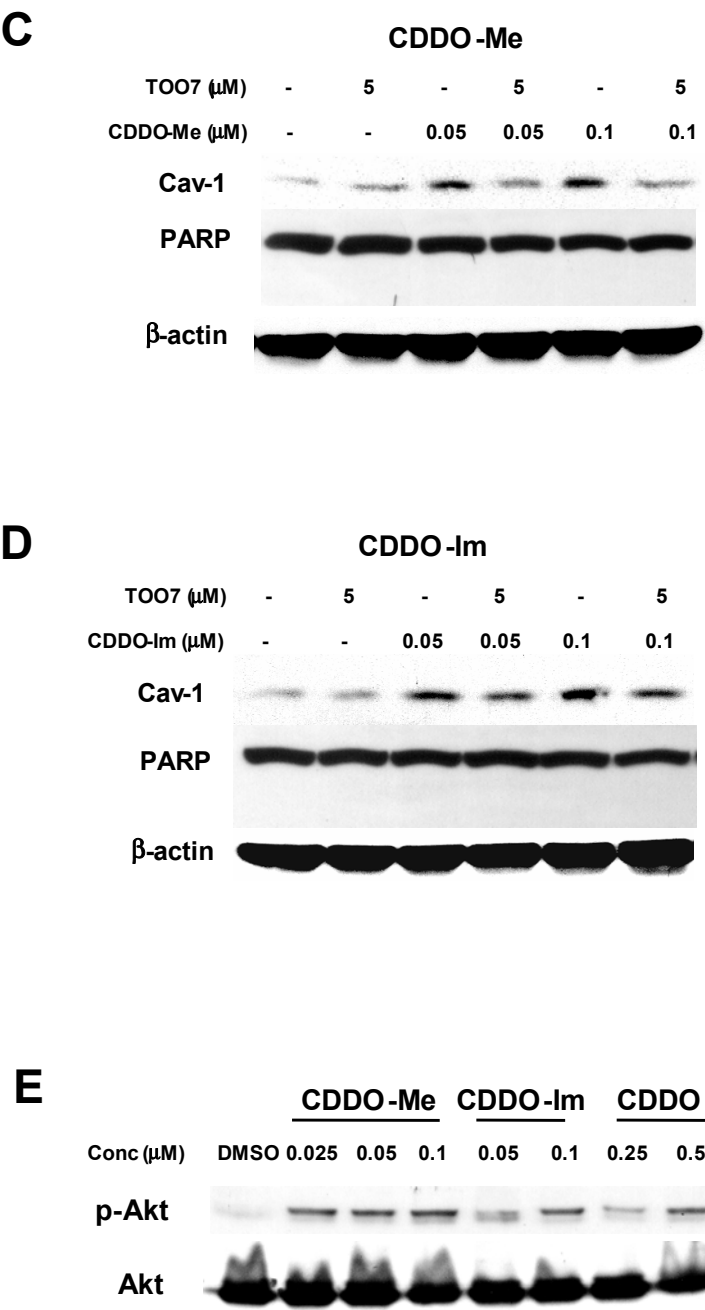
Fig. 7.4 Continued
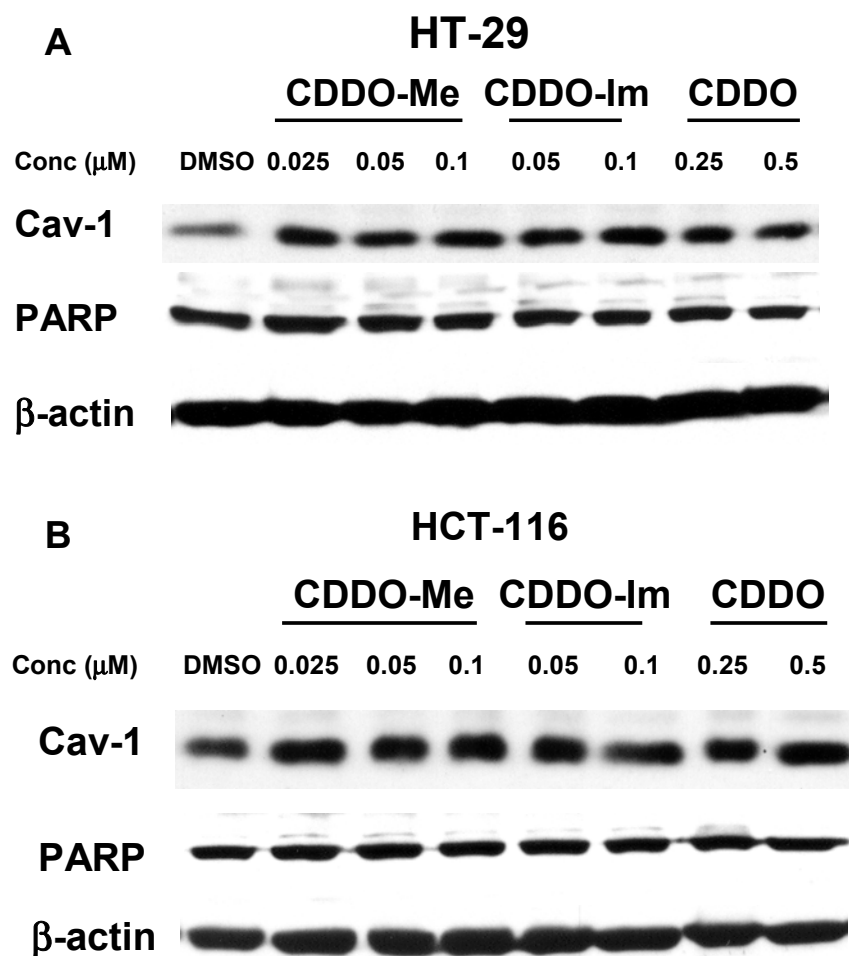
Fig. 7.5. Induction of caveolin-1 and PARP cleavage by CDDO compounds in colon cancer cell lines. Induction by CDDO, CDDO-Me and CDDO-Im in HT-29 (A) and HCT-116 (B) cells. Cells were treated with different concentrations of CDDO and related esters for 3 days, and whole cell lysates were analyzed by Western blot analysis as described in the Materials and Methods. (C) Higher concentrations of CDDO, CDDO-Me and CDDO-Im induce PPARγ-independent PARP cleavage in SW-480 cells. SW-480 cells were treated for 1 day with the indicated doses of CDDO compounds alone or in combination with 5.0 μM T007 and PARP cleavage was determined by Western blot analysis of whole cell lysates as described in the Materials and Methods. β-Actin served as a loading control.

242

C   SW480

TOO7 (µM)	-	5	-	5	-	5	-	5	-	5	-	5	-	5	-	5
CDDO (µM)	-	-	2.5	2.5	-	-	-	-	-	-	-	-	-	-	-	-
CDDO-Me (µM)	-	-	-	-	0.2	0.2	0.5	0.5	1	1	-	-	-	-	-	-
CDDO-Im (µM)	-	-	-	-	-	-	-	-	-	-	0.2	0.2	0.5	0.5	1	1

PARP 112kDa→

PARP 85kDa→

β-Actin
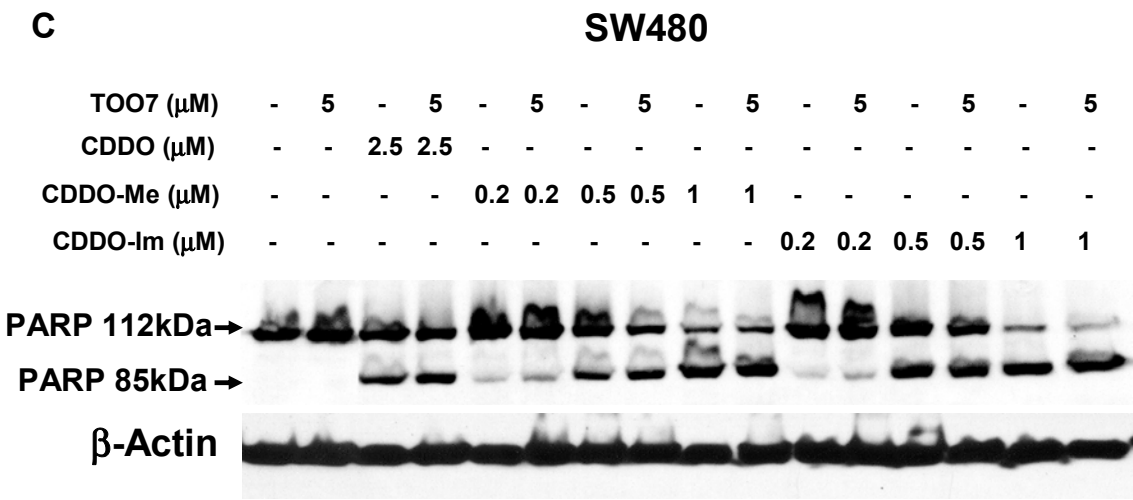
Fig. 7.5 Continued

effects of caveolin-1 induction by CDDO compounds on levels of phospho-Erk in SW480 cells were minimal. However, these compounds induced phosphatidylinositol-3-kinase (PI3-K)-dependent phosphorylation of Akt (Fig. 7.4E), and this was consistent with results of a recent study in human 293 and HeLa cells overexpressing caveolin-1 (398). PARP cleavage was minimal or not observed at the concentrations of CDDO compounds used in this experiment.

Cell survival studies (Fig. 7.1) indicated that higher concentrations of CDDO and related esters induced cell death and therefore we further investigated induction of PARP cleavage in SW-480 cells treated with 0.5 - 2.5 μM CDDO and 0.2 - 1.0 μM CDDO-Me and CDDO-Im for 1 day (Fig. 7.5C). Longer treatment (i.e. 3 days) could not be determined due to extensive cell death and minimal cell survival. These results demonstrate that the higher concentrations of CDDO and related esters induced PARP cleavage and this was consistent with the cell survival studies. In contrast, the PPARγ antagonist T007 did not inhibit induced PARP cleavage, suggesting that this response was PPARγ-independent. Moreover, at these higher concentrations, there was also a significant downregulation of cyclin D1, and this response was also not affected by T007 (data not shown). These results demonstrate that CDDO and related esters induce PPARγ-dependent and -independent responses associated with growth inhibition/cell death in colon cancer cells, and these mechanistic differences are concentration-dependent.

Discussion

PPARγ is expressed in tumors from multiple tissues and cancer cell lines (257), and chemicals that activate PPARγ have been extensively investigated for their efficacy in cancer chemotherapy [reviewed in (355, 357, 383-385, 502)]. PPARγ agonists typically decrease cancer cell survival due to induction of differentiation genes and apoptosis and modulation of genes/proteins linked to G1 → S phase progression. It is somewhat paradoxical that induction of these responses by PPARγ agonists, such as the thiazolidinediones (TZDs), 15-deoxy-Δ12,14-prostaglandin J2 (PGJ2), and CDDO compounds, appears to be both PPARγ-dependent and -independent and the relative contributions of these pathways are often not well defined. For example, troglitazone inhibits growth and induces apoptosis in colon cancer cell lines and induces early growth response-1 (Egr-1) gene expression which in turn activates downstream growth inhibitory effects (397). This response was unique to troglitazone among PPARγ agonists and was induced via PPARγ-independent pathways.

CDDO, CDDO-Me and CDDO-Im activate PPARγ in transactivation assays and CDDO-induced apoptosis was inhibited by dominant negative PPARγ in myeloid HL-60 cells and by T007 in myeloid U937 cells (494). In another study, CDDO-Im induced differentiation in leukemia cells that was not inhibited by the PPARγ antagonist GW9662 (500) and T007 did not affect inhibition of SKOV3 ovarian cancer cell growth by CDDO (501). Thus, it is clear that CDDO and related compounds activate PPARγ-dependent and -independent pathways that inhibit cancer cell growth and this dual action

may be beneficial for cancer chemotherapy. Results of this study demonstrate that CDDO, CDDO-Me and CDDO-Im also inhibit growth and survival of colon cancer cells (Fig. 7.1) and we have primarily used SW-480 cells as a model for determining activation of PPARγ-dependent and -independent pathways by CDDO and related esters.

CDDO, CDDO-Me and CDDO-Im activate PPARγ-dependent transactivation (Fig. 7.2) and coactivator interactions (Fig. 7.3) and differences between compounds were primarily associated with the fold-induction response where induction was lower for CDDO-Im due to the higher toxicity of this compound. Previous studies indicate that induced transactivation in the mammalian two hybrid assay using VP-PPARγ and GAL4-coactivators was both structure and coactivator-dependent (364, 393). For example, a series of 1,1-bis(3'-indolyl)-1-(*p*-substitutedphenyl)methanes [methylene-substituted 1,1-bis(3'-indolyl)methanes (C-DIMs)], that activate PPARγ, primarily induced interactions of PPARγ primarily with PGC-1 in colon cancer cell lines (393), whereas CDDO, CDDO-Me and CDDO-Im induced interactions with several coactivators including SRC-1, SRC-2, CARM-1, TRAP 220 and PGC-1. The main distinguishing feature among the CDDO compounds was the failure of CDDO-Im to induce PPARγ-SRC-3 interactions with VP-PPARγ and the relatively high activity of CDDO-Im to induce PPARγ interactions with the co-repressor SMRT. These differences among CDDO compounds in PPARγ-dependent interactions with coactivators might result in some tissue/cell selectivity in their PPARγ dependent responses.

PPARγ agonists such as TZDs, PGJ2 and C-DIMs typically inhibit genes/proteins associated with cell cycle progression and differentiation in cancer cell lines and these responses may be receptor dependent or independent. Previous studies in colon cancer cell lines with C-DIMs showed that these compounds had minimal effects on critical cell cycle proteins cyclin D1, p21 and p27 (393); and similar results were observed in this study at the lower concentrations of CDDO compounds. The induction of caveolin-1 by PGJ2, C-DIMs and TZDs has been observed in colon cancer cell lines (364, 393) and overexpression of caveolin-1 inhibits colon cancer cell growth *in vitro* and tumor growth in athymic nude mice (364, 375, 393). Results in Figures 7.4 and 7.5 show that CDDO, CDDO-Me and CDDO-Im significantly induce caveolin-1 in colon cancer cells at concentrations that also inhibit cell growth (Figs. 7.1). Moreover, in SW-480 cells, the induced caveolin-1 expression is inhibited by the PPARγ antagonist T007. The relatively low concentrations of CDDO, CDDO-Me and CDDO-Im that inhibit SW-480 cell proliferation induce minimal to non-detectable apoptosis as indicated by PARP cleavage (Figs. 7.4, 7.5A and 7.5B). We also observed that CDDO compounds induced PI3-K-dependent Akt phosphorylation which is normally associated with increased cell survival. However, a recent report (398) showed that overexpression of caveolin-1 in human 293 and HeLa cells also resulted in upregulation of the PI3-K/Akt pathway which sensitized the cells to stress-induced cytotoxicity.

In contrast, higher concentrations of CDDO compounds induce apoptosis and PARP cleavage; however, this response was PPARγ-independent and not inhibited by T007 (Fig. 7.5C). Moreover, at the higher concentrations of CDDO, CDDO-Me and

CDDO-Im, there was also a marked decrease in cyclin D1 protein expression which was also not inhibited by T007. Similar results have also been observed in this laboratory after treatment of breast cancer cells by PGJ2, TZDs and C-DIMs (359, 361). These data demonstrate that CDDO and related esters inhibit colon cancer cell growth through both PPARγ-dependent and -independent pathways which are observed at different concentrations and are linked to growth inhibition and cell death, respectively.

Previous reports of mechanistic differences regarding the role of PPARγ agonists in mediating growth inhibitory responses in different cancer cell lines may be explained, in part, by results of this study. CDDO and related esters are a unique example of a specific structural class of PPARγ agonists that induce both PPARγ-dependent (caveolin induction) and -independent (apoptosis) responses over a relatively narrow dose range in colon cancer cells. It is possible that the antimitogenic and anticarcinogenic activities of PPARγ agonists may be enhanced when the dose ranges for their PPARγ-dependent and -independent responses are similar, and this may contribute to the high potencies observed for CDDO, CDDO-Me and CDDO-Im in colon cancer cell lines. Currently, we are investigating the dose-dependent effects of thiazolidinediones, CDDO and related esters and C-DIMs in different cancer cell lines to determine their relative potencies in activating PPARγ-dependent and -independent pathways. This approach will provide important mechanistic insights into the activities of these compounds and their potential clinical applications for cancer chemotherapy.

CHAPTER VIII

SUMMARY

1,1-Bis(3'indolyl)-1-1(*p*-substitutedphenyl)methanes containing *p*-trifluoromethyl (DIM-C-pPhCF$_3$), *p-t*-butyl (DIM-C-pPhtBu), and *p*-phenyl (DIM-C-pPhC$_6$H$_5$) groups induce peroxisome proliferator-activated receptor γ (PPARγ)-mediated transactivation in HT-29, HCT-15, HCT-116, RKO and SW480 colon cancer cell lines and, KU7 and 253JB-V33 bladder cancer cell lines. Rosiglitazone also induces transactivation in these cell lines and inhibited growth of HT-29 cells which express wild-type PPARγ, but not HCT-15 cells which express mutant (K422Q) PPARγ. In contrast, DIM-C-pPhCF$_3$, DIM-C-pPhtBu and DIM-C-pPhC$_6$H$_5$ inhibited growth of both HT-29 and HCT-15 cells with IC$_{50}$ (50% growth inhibition) values ranging from 1 to 10 μM. Rosiglitazone and diindolylmethane (DIM) analogs did not affect expression of cyclin D1, p21 or p27 protein levels or apoptosis in HCT-15 or HT-29 cells but induced keratin 18 in both cell lines. However, rosiglitazone induced caveolins 1 and 2 in HT-29 but not HCT-15 cells, whereas these differentiation markers were induced by DIM-C-pPhCF$_3$ and DIM-C-pPhC$_6$H$_5$ in both cell lines. Since overexpression of caveolin 1 is known to suppress colon cancer cell and tumor growth, the growth inhibitory effects of rosiglitazone and the DIM compounds are associated with PPARγ-dependent induction of caveolins.

These PPARγ-active compounds also inhibited the proliferation of KU7 and 253J-BV bladder cancer cells, and the corresponding IC$_{50}$ values were 5-10 μM and 1-5 μM, respectively. In the less responsive KU7 cells, the PPARγ agonists induced

caveolin-1 but no changes in the cell cycle proteins cyclin D1, p27, or p21; in 253J-BV cells, the PPARγ agonists did not affect caveolin-1, cyclin D1, or p27 expression but did induce p21 protein. In KU7 cells, induction of caveolin-1 by each of the PPARγ agonists was significantly downregulated after cotreatment with the PPARγ antagonist GW9662. DIMC-pPhCF3 (60 mg/kg 3 times a week for 4 weeks) inhibited the growth of implanted KU7 orthotopic and subcutaneous tumors by 32% and 60%, respectively, and produced a corresponding decrease in proliferation index. Treatment of KU7 cells with DIM-C-pPhCF3 also elevated caveolin-1 expression by 25-30%, suggesting a role for this protein in mediating the antitumorigenic activity of DIM-C-pPhCF3 in bladder cancer.

The PPARγ-active 1,1-bis-(3'-indolyl)-1-(*p*-substitutedphenyl)methanes containing *p*-trifluoromethyl (DIM-C-pPhCF$_3$), *p-t*-butyl (DIM-C-pPhtBu), and phenyl (DIM-C-pPhC$_6$H$_5$) substituents had minimal effects on expression of cell cycle proteins and did not induce caveolin-1 in HCT-116 cells. However, these compounds induced NSAID-activated gene-1 (NAG-1) and apoptosis in HCT-116 cells and, in time-course studies, the PPARγ agonists maximally induced early growth response-1 (Egr-1) protein within 2 hr, whereas a longer time course was observed for induction of NAG-1 protein. These data, coupled with deletion and mutation analysis of both the Egr-1 and NAG-1 gene promoters, indicate that activation of NAG-1 by these compounds was dependent on prior induction of Egr-1, and induction of these responses were PPARγ-independent. Results of kinase inhibitor studies also demonstrated that activation of Egr-1/NAG-1 by methylene-substituted diindolylmethanes (C-DIMs) was phosphatidylinositol-3-kinase-

dependent, and this represents a novel receptor-independent pathway for C-DIM-induced growth inhibition and apoptosis in colon cancer cells.

At concentrations from 2.5 - 7.5 µM, the PPARγ agonists induce caveolin-1 and phosphorylation of Akt and cotreatment with the PPARγ antagonist GW9662 inhibited the induction response in SW480 colon cancer cells. In contrast, higher concentrations (10 µM) of DIM-C-pPhCF$_3$ and DIM-C-pPhC$_6$H$_5$ induce apoptosis which is PPARγ-independent and this was accompanied by loss of caveolin-1 induction but induction of pro-apoptotic nonsteroidal anti-inflammatory drug activated gene-1 (NAG-1). In athymic nude mice bearing SW480 cell xenografts, DIM-C-pPhC$_6$H$_5$ inhibits tumor growth at doses of 20 and 40 mg/kg/day and immunohistochemical staining of the tumors showed induction of apoptosis and NAG-1 expression. Thus, the indole-derived PPARγ active compounds induce both receptor-dependent and -independent responses in SW480 cells which are separable over a narrow range of concentrations and this dual mechanism of action enhances their antiproliferative and anticancer activities.

Nur77 is an orphan receptor and a member of the nerve growth factor-I-B subfamily of the nuclear receptor family of transcription factors. Based on the results of transactivation assays in pancreatic and other cancer cell lines, we have now identified for the first time Nur77 agonists typified by 1,1-bis(3-indolyl)-1-(*p*-anisyl)methane that activate GAL4-Nur77 chimeras expressing wild-type and the ligand binding domain (E/F) of Nur77. In Panc-28 pancreatic cancer cells, Nur77 agonists activate the nuclear receptor, and downstream responses include decreased cell survival and induction of cell death pathways, including tumor necrosis factor-related apoptosis-inducing ligand

(TRAIL) and poly(ADP-ribose) polymerase (PARP) cleavage. Moreover, the transactivation and apoptotic responses are also induced in other pancreatic, prostate, and breast cancer cells that express Nur77. In Panc-28 cells, small inhibitory RNA for Nur77 reverses ligand-dependent transactivation and induction of TRAIL and PARP cleavage. Nur77 agonists also inhibit tumor growth *in vivo* in athymic mice bearing Panc-28 cell xenografts. These results identify compounds that activate Nur77 through the ligand binding domain and show that ligand-dependent activation of Nur77 through nuclear pathways in cancer cells induces cell death and these compounds are a novel class of anticancer agents.

2-Cyano-3,12-dioxoolean-1,9-dien-28-oic acid (CDDO) and the corresponding methyl (CDDO-Me) and imidazole (CDDO-Im) esters induce peroxisome proliferator-activated receptor gamma (PPARγ)-dependent transactivation in SW-480 colon cancer cells, and these responses were inhibited by small inhibitory RNA for PPARγ (iPPARγ). Moreover, in a mammalian two-hybrid assay using VP-PPARγ and GAL4-coactivator/corepressor chimeras and a construct (pGAL4) containing five tandem GAL4 response elements, CDDO, CDDO-Me and CDDO-IM induce transactivation and PPARγ interaction with multiple coactivators. A major difference among the three PPARγ agonists was the higher activity of CDDO-Im to induce PPARγ interactions with the corepressor SMRT. CDDO, CDDO-Me and CDDO-Im inhibited SW-480, HCT-116 and HT-29 colon cancer cell proliferation at low concentrations and induced cell death at higher concentrations. Growth inhibition at lower concentrations correlated with induction of the tumor suppressor gene caveolin-1 which is known to inhibit colon

cancer cell growth. Induction of caveolin-1 by CDDO, CDDO-Me and CDDO-Im was inhibited by the PPARγ antagonist N-(4'-aminopyridyl-2-chloro-5-nitrobenzamide (T007), whereas higher doses induced apoptosis (PARP cleavage) which was not inhibited by T007. These results illustrate that CDDO-, CDDO-Me and CDDO-Im induce both PPARγ-dependent and -independent responses in colon cancer cells and activation of these pathways are separable and concentration-dependent for all three compounds.

REFERENCES

1. Beato M, Herrlich P, Schutz G. Steroid hormone receptors: many actors in search of a plot. Cell 1995;83:851-857.

2. Blumberg B, Evans RM. Orphan nuclear receptors-new ligands and new possibilities. Genes Dev 1998;12:3149-3155.

3. Evans RM. The steroid and thyroid hormone receptor superfamily. Science 1988;240:889-895.

4. Mangelsdorf DJ, Thummel C, Beato M, Herrlich P, Schutz G, et al. The nuclear receptor superfamily: the second decade. Cell 1995;83:835-839.

5. Robinson-Rechavi M, Carpentier AS, Duffraisse M, Laudet V. How many nuclear hormone receptors are there in the human genome? Trends Genet 2001;17:554-556.

6. Robinson-Rechavi M, Laudet V. Bioinformatics of nuclear receptors. Methods Enzymol 2003;364:95-118.

7. Adams MD, Celniker SE, Holt RA, Evans CA, Gocayne JD, et al. The genome sequence of *Drosophila melanogaster*. Science 2000;287:2185-2195.

8. Sluder AE, Mathews SW, Hough D, Yin VP, Maina CV. The nuclear receptor superfamily has undergone extensive proliferation and diversification in nematodes. Genome Res 1999;9:103-120.

9. A unified nomenclature system for the nuclear receptor superfamily. Cell 1999;97:161-163.

10. Gronemeyer H, Gustafsson JA, Laudet V. Principles for modulation of the nuclear receptor superfamily. Nat Rev Drug Discov 2004;3:950-964.

11. Giguere V, Hollenberg SM, Rosenfeld MG, Evans RM. Functional domains of the human glucocorticoid receptor. Cell 1986;46:645-652.

12. Hollenberg SM, Giguere V, Segui P, Evans RM. Colocalization of DNA-binding and transcriptional activation functions in the human glucocorticoid receptor. Cell 1987;49:39-46.

13. Dahlman-Wright K, Baumann H, McEwan IJ, Almlof T, Wright AP, et al. Structural characterization of a minimal functional transactivation domain from the human glucocorticoid receptor. Proc Natl Acad Sci U S A 1995;92:1699-1703.

14. McEwan IJ, Wright AP, Dahlman-Wright K, Carlstedt-Duke J, Gustafsson JA. Direct interaction of the tau 1 transactivation domain of the human glucocorticoid receptor with the basal transcriptional machinery. Mol Cell Biol 1993;13:399-407.

15. Lehrman SR, Tuls JL, Lund M. Peptide alpha-helicity in aqueous trifluoroethanol: correlations with predicted alpha-helicity and the secondary structure of the corresponding regions of bovine growth hormone. Biochemistry 1990;29:5590-5596.

16. Schwabe JW, Chapman L, Finch JT, Rhodes D. The crystal structure of the estrogen receptor DNA-binding domain bound to DNA: how receptors discriminate between their response elements. Cell 1993;75:567-578.

17. Tjian R, Maniatis T. Transcriptional activation: a complex puzzle with few easy pieces. Cell 1994;77:5-8.

18. Henriksson A, Almlof T, Ford J, McEwan IJ, Gustafsson JA, et al. Role of the Ada adaptor complex in gene activation by the glucocorticoid receptor. Mol Cell Biol 1997;17:3065-3073.

19. Ford J, McEwan IJ, Wright AP, Gustafsson JA. Involvement of the transcription factor IID protein complex in gene activation by the N-terminal transactivation domain of the glucocorticoid receptor *in vitro*. Mol Endocrinol 1997;11:1467-1475.

20. Zeiner M, Gehring U. A protein that interacts with members of the nuclear hormone receptor family: identification and cDNA cloning. Proc Natl Acad Sci U S A 1995;92:11465-11469.

21. Onate SA, Tsai SY, Tsai MJ, O'Malley BW. Sequence and characterization of a coactivator for the steroid hormone receptor superfamily. Science 1995;270:1354-1357.

22. Chakravarti D, LaMorte VJ, Nelson MC, Nakajima T, Schulman IG, et al. Role of CBP/P300 in nuclear receptor signalling. Nature 1996;383:99-103.

23. Luisi BF, Xu WX, Otwinowski Z, Freedman LP, Yamamoto KR, et al. Crystallographic analysis of the interaction of the glucocorticoid receptor with DNA. Nature 1991;352:497-505.

24. Freedman LP, Yamamoto KR, Luisi BF, Sigler PB. More fingers in hand. Cell 1988;54:444.

25. Freedman LP, Luisi BF, Korszun ZR, Basavappa R, Sigler PB, et al. The function and structure of the metal coordination sites within the glucocorticoid receptor DNA binding domain. Nature 1988;334:543-546.

26. Hard T, Kellenbach E, Boelens R, Maler BA, Dahlman K, et al. Solution structure of the glucocorticoid receptor DNA-binding domain. Science 1990;249:157-160.

27. Schwabe JW, Neuhaus D, Rhodes D. Solution structure of the DNA-binding domain of the oestrogen receptor. Nature 1990;348:458-461.

28. Knegtel RM, Katahira M, Schilthuis JG, Bonvin AM, Boelens R, et al. The solution structure of the human retinoic acid receptor-beta DNA-binding domain. J Biomol NMR 1993;3:1-17.

29. Lee MS, Kliewer SA, Provencal J, Wright PE, Evans RM. Structure of the retinoid X receptor alpha DNA binding domain: a helix required for homodimeric DNA binding. Science 1993;260:1117-1121.

30. Aranda A, Pascual A. Nuclear hormone receptors and gene expression. Physiol Rev 2001;81:1269-1304.

31. Ylikomi T, Bocquel MT, Berry M, Gronemeyer H, Chambon P. Cooperation of proto-signals for nuclear accumulation of estrogen and progesterone receptors. EMBO J 1992;11:3681-3694.

32. Guiochon-Mantel A, Delabre K, Lescop P, Milgrom E. Nuclear localization signals also mediate the outward movement of proteins from the nucleus. Proc Natl Acad Sci U S A 1994;91:7179-7183.

33. Walker D, Htun H, Hager GL. Using inducible vectors to study intracellular trafficking of GFP-tagged steroid/nuclear receptors in living cells. Methods 1999;19:386-393.

34. Hager GL, Lim CS, Elbi C, Baumann CT. Trafficking of nuclear receptors in living cells. J Steroid Biochem Mol Biol 2000;74:249-254.

35. Greschik H, Moras D. Structure-activity relationship of nuclear receptor-ligand interactions. Curr Top Med Chem 2003;3:1573-1599.

36. Moras D, Gronemeyer H. The nuclear receptor ligand-binding domain: structure and function. Curr Opin Cell Biol 1998;10:384-391.

37. Bourguet W, Ruff M, Chambon P, Gronemeyer H, Moras D. Crystal structure of the ligand-binding domain of the human nuclear receptor RXR-alpha. Nature 1995;375:377-382.

38. Brzozowski AM, Pike AC, Dauter Z, Hubbard RE, Bonn T, et al. Molecular basis of agonism and antagonism in the oestrogen receptor. Nature 1997;389:753-758.

39. Renaud JP, Rochel N, Ruff M, Vivat V, Chambon P, et al. Crystal structure of the RAR-gamma ligand-binding domain bound to all-trans retinoic acid. Nature 1995;378:681-689.

40. Wagner RL, Apriletti JW, McGrath ME, West BL, Baxter JD, et al. A structural role for hormone in the thyroid hormone receptor. Nature 1995;378:690-697.

41. Wurtz JM, Bourguet W, Renaud JP, Vivat V, Chambon P, et al. A canonical structure for the ligand-binding domain of nuclear receptors. Nat Struct Biol 1996;3:206.

42. Rochel N, Wurtz JM, Mitschler A, Klaholz B, Moras D. The crystal structure of the nuclear receptor for vitamin D bound to its natural ligand. Mol Cell 2000;5:173-179.

43. Green S, Chambon P. Nuclear receptors enhance our understanding of transcription regulation. Trends Genet 1988;4:309-314.

44. Nagpal S, Friant S, Nakshatri H, Chambon P. RARs and RXRs: evidence for two autonomous transactivation functions (AF-1 and AF-2) and heterodimerization *in vivo*. EMBO J 1993;12:2349-2360.

45. vom Baur E, Zechel C, Heery D, Heine MJ, Garnier JM, et al. Differential ligand-dependent interactions between the AF-2 activating domain of nuclear receptors and the putative transcriptional intermediary factors mSUG1 and TIF1. EMBO J 1996;15:110-124.

46. Tasset D, Tora L, Fromental C, Scheer E, Chambon P. Distinct classes of transcriptional activating domains function by different mechanisms. Cell 1990;62:1177-1187.

47. Danielian PS, White R, Lees JA, Parker MG. Identification of a conserved region required for hormone dependent transcriptional activation by steroid hormone receptors. EMBO J 1992;11:1025-1033.

48. McInerney EM, Tsai MJ, O'Malley BW, Katzenellenbogen BS. Analysis of estrogen receptor transcriptional enhancement by a nuclear hormone receptor coactivator. Proc Natl Acad Sci U S A 1996;93:10069-10073.

49. Montano MM, Muller V, Trobaugh A, Katzenellenbogen BS. The carboxy-terminal F domain of the human estrogen receptor: role in the transcriptional activity of the receptor and the effectiveness of antiestrogens as estrogen antagonists. Mol Endocrinol 1995;9:814-825.

50. Nichols M, Rientjes JM, Stewart AF. Different positioning of the ligand-binding domain helix 12 and the F domain of the estrogen receptor accounts for functional differences between agonists and antagonists. EMBO J 1998;17:765-773.

51. Yamamoto KR. Steroid receptor regulated transcription of specific genes and gene networks. Annu Rev Genet 1985;19:209-252.

52. Strahle U, Klock G, Schutz G. A DNA sequence of 15 base pairs is sufficient to mediate both glucocorticoid and progesterone induction of gene expression. Proc Natl Acad Sci U S A 1987;84:7871-7875.

53. Arriza JL, Weinberger C, Cerelli G, Glaser TM, Handelin BL, et al. Cloning of human mineralocorticoid receptor complementary DNA: structural and functional kinship with the glucocorticoid receptor. Science 1987;237:268-275.

54. Ham J, Thomson A, Needham M, Webb P, Parker M. Characterization of response elements for androgens, glucocorticoids and progestins in mouse mammary tumour virus. Nucleic Acids Res 1988;16:5263-5276.

55. Darbre P, Page M, King RJ. Androgen regulation by the long terminal repeat of mouse mammary tumor virus. Mol Cell Biol 1986;6:2847-2854.

56. Cato AC, Miksicek R, Schutz G, Arnemann J, Beato M. The hormone regulatory element of mouse mammary tumour virus mediates progesterone induction. EMBO J 1986;5:2237-2240.

57. Cato AC, Weinmann J. Mineralocorticoid regulation of transcription of transfected mouse mammary tumor virus DNA in cultured kidney cells. J Cell Biol 1988;106:2119-2125.

58. Umesono K, Murakami KK, Thompson CC, Evans RM. Direct repeats as selective response elements for the thyroid hormone, retinoic acid, and vitamin D3 receptors. Cell 1991;65:1255-1266.

59. Mangelsdorf DJ, Evans RM. The RXR heterodimers and orphan receptors. Cell 1995;83:841-850.

60. Zhao Q, Chasse SA, Devarakonda S, Sierk ML, Ahvazi B, et al. Structural basis of RXR-DNA interactions. J Mol Biol 2000;296:509-520.

61. Rastinejad F, Wagner T, Zhao Q, Khorasanizadeh S. Structure of the RXR-RAR DNA-binding complex on the retinoic acid response element DR1. EMBO J 2000;19:1045-1054.

62. Pratt WB, Toft DO. Steroid receptor interactions with heat shock protein and immunophilin chaperones. Endocr Rev 1997;18:306-360.

63. Horlein AJ, Naar AM, Heinzel T, Torchia J, Gloss B, et al. Ligand-independent repression by the thyroid hormone receptor mediated by a nuclear receptor co-repressor. Nature 1995;377:397-404.

64. Chen JD, Evans RM. A transcriptional co-repressor that interacts with nuclear hormone receptors. Nature 1995;377:454-457.

65. Damm K, Thompson CC, Evans RM. Protein encoded by v-erbA functions as a thyroid-hormone receptor antagonist. Nature 1989;339:593-597.

66. Sap J, Munoz A, Schmitt J, Stunnenberg H, Vennstrom B. Repression of transcription mediated at a thyroid hormone response element by the v-erb-A oncogene product. Nature 1989;340:242-244.

67. Graupner G, Wills KN, Tzukerman M, Zhang XK, Pfahl M. Dual regulatory role for thyroid-hormone receptors allows control of retinoic-acid receptor activity. Nature 1989;340:653-656.

68. Meyer ME, Gronemeyer H, Turcotte B, Bocquel MT, Tasset D, et al. Steroid hormone receptors compete for factors that mediate their enhancer function. Cell 1989;57:433-442.

69. Hollenberg SM, Evans RM. Multiple and cooperative trans-activation domains of the human glucocorticoid receptor. Cell 1988;55:899-906.

70. Tora L, White J, Brou C, Tasset D, Webster N, et al. The human estrogen receptor has two independent nonacidic transcriptional activation functions. Cell 1989;59:477-487.

71. Horwitz KB, Jackson TA, Bain DL, Richer JK, Takimoto GS, et al. Nuclear receptor coactivators and corepressors. Mol Endocrinol 1996;10:1167-1177.

72. Hong H, Kohli K, Trivedi A, Johnson DL, Stallcup MR. GRIP1, a novel mouse protein that serves as a transcriptional coactivator in yeast for the hormone binding domains of steroid receptors. Proc Natl Acad Sci U S A 1996;93:4948-4952.

73. Kalkhoven E, Valentine JE, Heery DM, Parker MG. Isoforms of steroid receptor co-activator 1 differ in their ability to potentiate transcription by the oestrogen receptor. EMBO J 1998;17:232-243.

74. Hong H, Kohli K, Garabedian MJ, Stallcup MR. GRIP1, a transcriptional coactivator for the AF-2 transactivation domain of steroid, thyroid, retinoid, and vitamin D receptors. Mol Cell Biol 1997;17:2735-2744.

75. Torchia J, Rose DW, Inostroza J, Kamei Y, Westin S, et al. The transcriptional co-activator p/CIP binds CBP and mediates nuclear-receptor function. Nature 1997;387:677-684.

76. Voegel JJ, Heine MJ, Tini M, Vivat V, Chambon P, et al. The coactivator TIF2 contains three nuclear receptor-binding motifs and mediates transactivation through CBP binding-dependent and -independent pathways. EMBO J 1998;17:507-519.

77. Anzick SL, Kononen J, Walker RL, Azorsa DO, Tanner MM, et al. AIB1, a steroid receptor coactivator amplified in breast and ovarian cancer. Science 1997;277:965-968.

78. Chen H, Lin RJ, Schiltz RL, Chakravarti D, Nash A, et al. Nuclear receptor coactivator ACTR is a novel histone acetyltransferase and forms a multimeric activation complex with P/CAF and CBP/p300. Cell 1997;90:569-580.

79. Kim HJ, Lee SK, Na SY, Choi HS, Lee JW. Molecular cloning of xSRC-3, a novel transcription coactivator from *Xenopus*, that is related to AIB1, p/CIP, and TIF2. Mol Endocrinol 1998;12:1038-1047.

80. McKenna NJ, Lanz RB, O'Malley BW. Nuclear receptor coregulators: cellular and molecular biology. Endocr Rev 1999;20:321-344.

81. Collingwood TN, Urnov FD, Wolffe AP. Nuclear receptors: coactivators, corepressors and chromatin remodeling in the control of transcription. J Mol Endocrinol 1999;23:255-275.

82. Heery DM, Kalkhoven E, Hoare S, Parker MG. A signature motif in transcriptional co-activators mediates binding to nuclear receptors. Nature 1997;387:733-736.

83. Darimont BD, Wagner RL, Apriletti JW, Stallcup MR, Kushner PJ, et al. Structure and specificity of nuclear receptor-coactivator interactions. Genes Dev 1998;12:3343-3356.

84. Nolte RT, Wisely GB, Westin S, Cobb JE, Lambert MH, et al. Ligand binding and co-activator assembly of the peroxisome proliferator-activated receptor-gamma. Nature 1998;395:137-143.

85. Huang ZJ, Edery I, Rosbash M. PAS is a dimerization domain common to *Drosophila* period and several transcription factors. Nature 1993;364:259-262.

86. Chen H, Lin RJ, Xie W, Wilpitz D, Evans RM. Regulation of hormone-induced histone hyperacetylation and gene activation via acetylation of an acetylase. Cell 1999;98:675-686.

87. Korzus E, Torchia J, Rose DW, Xu L, Kurokawa R, et al. Transcription factor-specific requirements for coactivators and their acetyltransferase functions. Science 1998;279:703-707.

88. Onate SA, Boonyaratanakornkit V, Spencer TE, Tsai SY, Tsai MJ, et al. The steroid receptor coactivator-1 contains multiple receptor interacting and activation domains that cooperatively enhance the activation function 1 (AF1) and AF2 domains of steroid receptors. J Biol Chem 1998;273:12101-12108.

89. Koh SS, Chen D, Lee YH, Stallcup MR. Synergistic enhancement of nuclear receptor function by p160 coactivators and two coactivators with protein methyltransferase activities. J Biol Chem 2001;276:1089-1098.

90. Spencer TE, Jenster G, Burcin MM, Allis CD, Zhou J, et al. Steroid receptor coactivator-1 is a histone acetyltransferase. Nature 1997;389:194-198.

91. Liu Z, Wong J, Tsai SY, Tsai MJ, O'Malley BW. Sequential recruitment of steroid receptor coactivator-1 (SRC-1) and p300 enhances progesterone receptor-dependent initiation and reinitiation of transcription from chromatin. Proc Natl Acad Sci U S A 2001;98:12426-12431. Epub 12001 Oct 12416.

92. Roth SY, Denu JM, Allis CD. Histone acetyltransferases. Annu Rev Biochem 2001;70:81-120.

93. Glass CK, Rosenfeld MG. The coregulator exchange in transcriptional functions of nuclear receptors. Genes Dev 2000;14:121-141.

94. Chan HM, La Thangue NB. p300/CBP proteins: HATs for transcriptional bridges and scaffolds. J Cell Sci 2001;114:2363-2373.

95. Bannister AJ, Kouzarides T. The CBP co-activator is a histone acetyltransferase. Nature 1996;384:641-643.

96. Ogryzko VV, Schiltz RL, Russanova V, Howard BH, Nakatani Y. The transcriptional coactivators p300 and CBP are histone acetyltransferases. Cell 1996;87:953-959.

97. Kraus WL, Manning ET, Kadonaga JT. Biochemical analysis of distinct activation functions in p300 that enhance transcription initiation with chromatin templates. Mol Cell Biol 1999;19:8123-8135.

98. Berger SL. Histone modifications in transcriptional regulation. Curr Opin Genet Dev 2002;12:142-148.

99. Yang XJ, Ogryzko VV, Nishikawa J, Howard BH, Nakatani Y. A p300/CBP-associated factor that competes with the adenoviral oncoprotein E1A. Nature 1996;382:319-324.

100. Manning ET, Ikehara T, Ito T, Kadonaga JT, Kraus WL. p300 forms a stable, template-committed complex with chromatin: role for the bromodomain. Mol Cell Biol 2001;21:3876-3887.

101. Kamei Y, Xu L, Heinzel T, Torchia J, Kurokawa R, et al. A CBP integrator complex mediates transcriptional activation and AP-1 inhibition by nuclear receptors. Cell 1996;85:403-414.

102. Kraus WL, Wong J. Nuclear receptor-dependent transcription with chromatin. Is it all about enzymes? Eur J Biochem 2002;269:2275-2283.

103. Dilworth FJ, Fromental-Ramain C, Yamamoto K, Chambon P. ATP-driven chromatin remodeling activity and histone acetyltransferases act sequentially during transactivation by RAR/RXR *in vitro*. Mol Cell 2000;6:1049-1058.

104. Hassan AH, Neely KE, Workman JL. Histone acetyltransferase complexes stabilize swi/snf binding to promoter nucleosomes. Cell 2001;104:817-827.

105. Daujat S, Bauer UM, Shah V, Turner B, Berger S, et al. Crosstalk between CARM1 methylation and CBP acetylation on histone H3. Curr Biol 2002;12:2090-2097.

106. Zhang X, Zhou L, Cheng X. Crystal structure of the conserved core of protein arginine methyltransferase PRMT3. EMBO J 2000;19:3509-3519.

107. Teyssier C, Chen D, Stallcup MR. Requirement for multiple domains of the protein arginine methyltransferase CARM1 in its transcriptional coactivator function. J Biol Chem 2002;277:46066-46072.

108. Chen D, Huang SM, Stallcup MR. Synergistic, p160 coactivator-dependent enhancement of estrogen receptor function by CARM1 and p300. J Biol Chem 2000;275:40810-40816.

109. Fondell JD, Ge H, Roeder RG. Ligand induction of a transcriptionally active thyroid hormone receptor coactivator complex. Proc Natl Acad Sci U S A 1996;93:8329-8333.

110. Fondell JD, Guermah M, Malik S, Roeder RG. Thyroid hormone receptor-associated proteins and general positive cofactors mediate thyroid hormone receptor function in the absence of the TATA box-binding protein-associated factors of TFIID. Proc Natl Acad Sci U S A 1999;96:1959-1964.

111. Rachez C, Lemon BD, Suldan Z, Bromleigh V, Gamble M, et al. Ligand-dependent transcription activation by nuclear receptors requires the DRIP complex. Nature 1999;398:824-828.

112. Rachez C, Suldan Z, Ward J, Chang CP, Burakov D, et al. A novel protein complex that interacts with the vitamin D3 receptor in a ligand-dependent manner and enhances VDR transactivation in a cell-free system. Genes Dev 1998;12:1787-1800.

113. Hittelman AB, Burakov D, Iniguez-Lluhi JA, Freedman LP, Garabedian MJ. Differential regulation of glucocorticoid receptor transcriptional activation via AF-1-associated proteins. EMBO J 1999;18:5380-5388.

114. Yuan CX, Ito M, Fondell JD, Fu ZY, Roeder RG. The TRAP220 component of a thyroid hormone receptor- associated protein (TRAP) coactivator complex interacts directly with nuclear receptors in a ligand-dependent fashion. Proc Natl Acad Sci U S A 1998;95:7939-7944.

115. Zhu Y, Qi C, Jain S, Rao MS, Reddy JK. Isolation and characterization of PBP, a protein that interacts with peroxisome proliferator-activated receptor. J Biol Chem 1997;272:25500-25506.

116. Rachez C, Gamble M, Chang CP, Atkins GB, Lazar MA, et al. The DRIP complex and SRC-1/p160 coactivators share similar nuclear receptor binding determinants but constitute functionally distinct complexes. Mol Cell Biol 2000;20:2718-2726.

117. Ren Y, Behre E, Ren Z, Zhang J, Wang Q, et al. Specific structural motifs determine TRAP220 interactions with nuclear hormone receptors. Mol Cell Biol 2000;20:5433-5446.

118. Kim K, Thu N, Saville B, Safe S. Domains of estrogen receptor alpha (ERalpha) required for ERalpha/Sp1-mediated activation of GC-rich promoters by estrogens and antiestrogens in breast cancer cells. Mol Endocrinol 2003;17:804-817.

119. Paige LA, Christensen DJ, Gron H, Norris JD, Gottlin EB, et al. Estrogen receptor (ER) modulators each induce distinct conformational changes in ER alpha and ER beta. Proc Natl Acad Sci U S A 1999;96:3999-4004.

120. Wu Q, Burghardt R, Safe S. Vitamin D-interacting protein 205 (DRIP205) coactivation of estrogen receptor alpha (ERalpha) involves multiple domains of both proteins. J Biol Chem 2004;279:53602-53612.

121. Ito M, Roeder RG. The TRAP/SMCC/Mediator complex and thyroid hormone receptor function. Trends Endocrinol Metab 2001;12:127-134.

122. Puigserver P, Wu Z, Park CW, Graves R, Wright M, et al. A cold-inducible coactivator of nuclear receptors linked to adaptive thermogenesis. Cell 1998;92:829-839.

123. Vega RB, Huss JM, Kelly DP. The coactivator PGC-1 cooperates with peroxisome proliferator-activated receptor alpha in transcriptional control of nuclear genes encoding mitochondrial fatty acid oxidation enzymes. Mol Cell Biol 2000;20:1868-1876.

124. Puigserver P, Adelmant G, Wu Z, Fan M, Xu J, et al. Activation of PPARgamma coactivator-1 through transcription factor docking. Science 1999;286:1368-1371.

125. Tcherepanova I, Puigserver P, Norris JD, Spiegelman BM, McDonnell DP. Modulation of estrogen receptor-alpha transcriptional activity by the coactivator PGC-1. J Biol Chem 2000;275:16302-16308.

126. Schreiber SN, Knutti D, Brogli K, Uhlmann T, Kralli A. The transcriptional coactivator PGC-1 regulates the expression and activity of the orphan nuclear receptor estrogen-related receptor alpha (ERRalpha). J Biol Chem 2003;278:9013-9018.

127. Knutti D, Kressler D, Kralli A. Regulation of the transcriptional coactivator PGC-1 via MAPK-sensitive interaction with a repressor. Proc Natl Acad Sci U S A 2001;98:9713-9718.

128. Delerive P, Wu Y, Burris TP, Chin WW, Suen CS. PGC-1 functions as a transcriptional coactivator for the retinoid X receptors. J Biol Chem 2002;277:3913-3917.

129. Wu Y, Delerive P, Chin WW, Burris TP. Requirement of helix 1 and the AF-2 domain of the thyroid hormone receptor for coactivation by PGC-1. J Biol Chem 2002;277:8898-8905.

130. Meirhaeghe A, Crowley V, Lenaghan C, Lelliott C, Green K, et al. Characterization of the human, mouse and rat PGC1 beta (peroxisome-proliferator-activated receptor-gamma co-activator 1 beta) gene *in vitro* and *in vivo*. Biochem J 2003;373:155-165.

131. Li D, Desai-Yajnik V, Lo E, Schapira M, Abagyan R, et al. NRIF3 is a novel coactivator mediating functional specificity of nuclear hormone receptors. Mol Cell Biol 1999;19:7191-7202.

132. Mahajan MA, Samuels HH. A new family of nuclear receptor coregulators that integrate nuclear receptor signaling through CREB-binding protein. Mol Cell Biol 2000;20:5048-5063.

133. Lee SK, Anzick SL, Choi JE, Bubendorf L, Guan XY, et al. A nuclear factor, ASC-2, as a cancer-amplified transcriptional coactivator essential for ligand-

dependent transactivation by nuclear receptors *in vivo*. J Biol Chem 1999;274:34283-34293.

134. Caira F, Antonson P, Pelto-Huikko M, Treuter E, Gustafsson JA. Cloning and characterization of RAP250, a novel nuclear receptor coactivator. J Biol Chem 2000;275:5308-5317.

135. Ko L, Chin WW. Nuclear receptor coactivator thyroid hormone receptor-binding protein (TRBP) interacts with and stimulates its associated DNA-dependent protein kinase. J Biol Chem 2003;278:11471-11479.

136. Zhu Y, Kan L, Qi C, Kanwar YS, Yeldandi AV, et al. Isolation and characterization of peroxisome proliferator-activated receptor (PPAR) interacting protein (PRIP) as a coactivator for PPAR. J Biol Chem 2000;275:13510-13516.

137. Yeh S, Chang C. Cloning and characterization of a specific coactivator, ARA70, for the androgen receptor in human prostate cells. Proc Natl Acad Sci U S A 1996;93:5517-5521.

138. Muller JM, Isele U, Metzger E, Rempel A, Moser M, et al. FHL2, a novel tissue-specific coactivator of the androgen receptor. EMBO J 2000;19:359-369.

139. Lanz RB, McKenna NJ, Onate SA, Albrecht U, Wong J, et al. A steroid receptor coactivator, SRA, functions as an RNA and is present in an SRC-1 complex. Cell 1999;97:17-27.

140. Xu J, Liao L, Ning G, Yoshida-Komiya H, Deng C, et al. The steroid receptor coactivator SRC-3 (p/CIP/RAC3/AIB1/ACTR/TRAM-1) is required for normal

growth, puberty, female reproductive function, and mammary gland development. Proc Natl Acad Sci U S A 2000;97:6379-6384.

141. Philibert RA, King BH, Winfield S, Cook EH, Lee YH, et al. Association of an X-chromosome dodecamer insertional variant allele with mental retardation. Mol Psychiatry 1998;3:303-309.

142. Dotzlaw H, Moehren U, Mink S, Cato AC, Iniguez Lluhi JA, et al. The amino terminus of the human AR is target for corepressor action and antihormone agonism. Mol Endocrinol 2002;16:661-673.

143. Jackson TA, Richer JK, Bain DL, Takimoto GS, Tung L, et al. The partial agonist activity of antagonist-occupied steroid receptors is controlled by a novel hinge domain-binding coactivator L7/SPA and the corepressors N-CoR or SMRT. Mol Endocrinol 1997;11:693-705.

144. Liao G, Chen LY, Zhang A, Godavarthy A, Xia F, et al. Regulation of androgen receptor activity by the nuclear receptor corepressor SMRT. J Biol Chem 2003;278:5052-5061.

145. Shang Y, Hu X, DiRenzo J, Lazar MA, Brown M. Cofactor dynamics and sufficiency in estrogen receptor-regulated transcription. Cell 2000;103:843-852.

146. Zhang X, Jeyakumar M, Petukhov S, Bagchi MK. A nuclear receptor corepressor modulates transcriptional activity of antagonist-occupied steroid hormone receptor. Mol Endocrinol 1998;12:513-524.

147. Nagy L, Kao HY, Love JD, Li C, Banayo E, et al. Mechanism of corepressor binding and release from nuclear hormone receptors. Genes Dev 1999;13:3209-3216.

148. Perissi V, Staszewski LM, McInerney EM, Kurokawa R, Krones A, et al. Molecular determinants of nuclear receptor-corepressor interaction. Genes Dev 1999;13:3198-3208.

149. Heinzel T, Lavinsky RM, Mullen TM, Soderstrom M, Laherty CD, et al. A complex containing N-CoR, mSin3 and histone deacetylase mediates transcriptional repression. Nature 1997;387:43-48.

150. Guenther MG, Barak O, Lazar MA. The SMRT and N-CoR corepressors are activating cofactors for histone deacetylase 3. Mol Cell Biol 2001;21:6091-6101.

151. Yu J, Li Y, Ishizuka T, Guenther MG, Lazar MA. A SANT motif in the SMRT corepressor interprets the histone code and promotes histone deacetylation. EMBO J 2003;22:3403-3410.

152. Thiagalingam S, Cheng KH, Lee HJ, Mineva N, Thiagalingam A, et al. Histone deacetylases: unique players in shaping the epigenetic histone code. Ann N Y Acad Sci 2003;983:84-100.

153. Giguere V. Orphan nuclear receptors: from gene to function. Endocr Rev 1999;20:689-725.

154. Mangelsdorf DJ, Borgmeyer U, Heyman RA, Zhou JY, Ong ES, et al. Characterization of three RXR genes that mediate the action of 9-cis retinoic acid. Genes Dev 1992;6:329-344.

155. Devchand PR, Ijpenberg A, Devesvergne B, Wahli W. PPARs: nuclear receptors for fatty acids, eicosanoids, and xenobiotics. Adv Exp Med Biol 1999;469:231-236.

156. Niesor EJ, Flach J, Lopes-Antoni I, Perez A, Bentzen CL. The nuclear receptors FXR and LXRalpha: potential targets for the development of drugs affecting lipid metabolism and neoplastic diseases. Curr Pharm Des 2001;7:231-259.

157. Tu H, Okamoto AY, Shan B. FXR, a bile acid receptor and biological sensor. Trends Cardiovasc Med 2000;10:30-35.

158. Peet DJ, Janowski BA, Mangelsdorf DJ. The LXRs: a new class of oxysterol receptors. Curr Opin Genet Dev 1998;8:571-575.

159. Honkakoski P, Sueyoshi T, Negishi M. Drug-activated nuclear receptors CAR and PXR. Ann Med 2003;35:172-182.

160. Fitzgerald ML, Moore KJ, Freeman MW. Nuclear hormone receptors and cholesterol trafficking: the orphans find a new home. J Mol Med 2002;80:271-281. Epub 2002 Mar 2007.

161. Zazopoulos E, Lalli E, Stocco DM, Sassone-Corsi P. DNA binding and transcriptional repression by DAX-1 blocks steroidogenesis. Nature 1997;390:311-315.

162. Rosen ED, Spiegelman BM. PPARgamma: a nuclear regulator of metabolism, differentiation, and cell growth. J Biol Chem 2001;276:37731-37734.

163. Puddu P, Puddu GM, Muscari A. Peroxisome proliferator-activated receptors: are they involved in atherosclerosis progression? Int J Cardiol 2003;90:133-140.

164. Xing G, Zhang L, Zhang L, Heynen T, Yoshikawa T, et al. Rat PPAR delta contains a CGG triplet repeat and is prominently expressed in the thalamic nuclei. Biochem Biophys Res Commun 1995;217:1015-1025.

165. Chen F, Law SW, O'Malley BW. Identification of two mPPAR related receptors and evidence for the existence of five subfamily members. Biochem Biophys Res Commun 1993;196:671-677.

166. Zhu Y, Alvares K, Huang Q, Rao MS, Reddy JK. Cloning of a new member of the peroxisome proliferator-activated receptor gene family from mouse liver. J Biol Chem 1993;268:26817-26820.

167. Aperlo C, Pognonec P, Saladin R, Auwerx J, Boulukos KE. cDNA cloning and characterization of the transcriptional activities of the hamster peroxisome proliferator-activated receptor haPPAR gamma. Gene 1995;162:297-302.

168. Schmidt A, Endo N, Rutledge SJ, Vogel R, Shinar D, et al. Identification of a new member of the steroid hormone receptor superfamily that is activated by a peroxisome proliferator and fatty acids. Mol Endocrinol 1992;6:1634-1641.

169. Sher T, Yi HF, McBride OW, Gonzalez FJ. cDNA cloning, chromosomal mapping, and functional characterization of the human peroxisome proliferator activated receptor. Biochemistry 1993;32:5598-5604.

170. Greene ME, Blumberg B, McBride OW, Yi HF, Kronquist K, et al. Isolation of the human peroxisome proliferator activated receptor gamma cDNA: expression in hematopoietic cells and chromosomal mapping. Gene Expr 1995;4:281-299.

171. Dreyer C, Krey G, Keller H, Givel F, Helftenbein G, et al. Control of the peroxisomal beta-oxidation pathway by a novel family of nuclear hormone receptors. Cell 1992;68:879-887.

172. Yoshikawa T, Brkanac Z, Dupont BR, Xing GQ, Leach RJ, et al. Assignment of the human nuclear hormone receptor, NUC1 (PPARD), to chromosome 6p21.1-p21.2. Genomics 1996;35:637-638.

173. Blanquart C, Barbier O, Fruchart JC, Staels B, Glineur C. Peroxisome proliferator-activated receptors: regulation of transcriptional activities and roles in inflammation. J Steroid Biochem Mol Biol 2003;85:267-273.

174. Koeffler HP. Peroxisome proliferator-activated receptor gamma and cancers. Clin Cancer Res 2003;9:1-9.

175. Lee CH, Olson P, Evans RM. Minireview: lipid metabolism, metabolic diseases, and peroxisome proliferator-activated receptors. Endocrinology 2003;144:2201-2207.

176. Kliewer SA, Umesono K, Noonan DJ, Heyman RA, Evans RM. Convergence of 9-cis retinoic acid and peroxisome proliferator signalling pathways through heterodimer formation of their receptors. Nature 1992;358:771-774.

177. Desvergne B, Wahli W. Peroxisome proliferator-activated receptors: nuclear control of metabolism. Endocr Rev 1999;20:649-688.

178. Palmer CN, Hsu MH, Griffin HJ, Johnson EF. Novel sequence determinants in peroxisome proliferator signaling. J Biol Chem 1995;270:16114-16121.

179. A IJ, Jeannin E, Wahli W, Desvergne B. Polarity and specific sequence requirements of peroxisome proliferator-activated receptor (PPAR)/retinoid X receptor heterodimer binding to DNA. A functional analysis of the malic enzyme gene PPAR response element. J Biol Chem 1997;272:20108-20117.

180. Juge-Aubry C, Pernin A, Favez T, Burger AG, Wahli W, et al. DNA binding properties of peroxisome proliferator-activated receptor subtypes on various natural peroxisome proliferator response elements. Importance of the 5'-flanking region. J Biol Chem 1997;272:25252-25259.

181. Osada S, Tsukamoto T, Takiguchi M, Mori M, Osumi T. Identification of an extended half-site motif required for the function of peroxisome proliferator-activated receptor alpha. Genes Cells 1997;2:315-327.

182. DiRenzo J, Soderstrom M, Kurokawa R, Ogliastro MH, Ricote M, et al. Peroxisome proliferator-activated receptors and retinoic acid receptors differentially control the interactions of retinoid X receptor heterodimers with ligands, coactivators, and corepressors. Mol Cell Biol 1997;17:2166-2176.

183. Hsu MH, Palmer CN, Song W, Griffin KJ, Johnson EF. A carboxyl-terminal extension of the zinc finger domain contributes to the specificity and polarity of peroxisome proliferator-activated receptor DNA binding. J Biol Chem 1998;273:27988-27997.

184. Willson TM, Brown PJ, Sternbach DD, Henke BR. The PPARs: from orphan receptors to drug discovery. J Med Chem 2000;43:527-550.

185. Zhu Y, Qi C, Korenberg JR, Chen XN, Noya D, et al. Structural organization of mouse peroxisome proliferator-activated receptor gamma (mPPAR gamma) gene: alternative promoter use and different splicing yield two mPPAR gamma isoforms. Proc Natl Acad Sci U S A 1995;92:7921-7925.

186. Fajas L, Auboeuf D, Raspe E, Schoonjans K, Lefebvre AM, et al. The organization, promoter analysis, and expression of the human PPARgamma gene. J Biol Chem 1997;272:18779-18789.

187. Fajas L, Fruchart JC, Auwerx J. PPARgamma3 mRNA: a distinct PPARgamma mRNA subtype transcribed from an independent promoter. FEBS Lett 1998;438:55-60.

188. Forman BM, Tontonoz P, Chen J, Brun RP, Spiegelman BM, et al. 15-Deoxy-delta 12, 14-prostaglandin J2 is a ligand for the adipocyte determination factor PPAR gamma. Cell 1995;83:803-812.

189. Fitzpatrick FA, Wynalda MA. Albumin-catalyzed metabolism of prostaglandin D2. Identification of products formed *in vitro*. J Biol Chem 1983;258:11713-11718.

190. Powell WS. 15-Deoxy-delta12,14-PGJ2: endogenous PPARgamma ligand or minor eicosanoid degradation product? J Clin Invest 2003;112:828-830.

191. Nosjean O, Boutin JA. Natural ligands of PPARgamma: are prostaglandin J(2) derivatives really playing the part? Cell Signal 2002;14:573-583.

192. Bell-Parikh LC, Ide T, Lawson JA, McNamara P, Reilly M, et al. Biosynthesis of 15-deoxy-delta12,14-PGJ2 and the ligation of PPARgamma. J Clin Invest 2003;112:945-955.

193. Chawla A, Barak Y, Nagy L, Liao D, Tontonoz P, et al. PPAR-gamma dependent and independent effects on macrophage-gene expression in lipid metabolism and inflammation. Nat Med 2001;7:48-52.

194. Straus DS, Pascual G, Li M, Welch JS, Ricote M, et al. 15-deoxy-delta 12,14-prostaglandin J2 inhibits multiple steps in the NF-kappa B signaling pathway. Proc Natl Acad Sci U S A 2000;97:4844-4849.

195. Rossi A, Kapahi P, Natoli G, Takahashi T, Chen Y, et al. Anti-inflammatory cyclopentenone prostaglandins are direct inhibitors of IkappaB kinase. Nature 2000;403:103-108.

196. Berger J, Bailey P, Biswas C, Cullinan CA, Doebber TW, et al. Thiazolidinediones produce a conformational change in peroxisomal proliferator-activated receptor-gamma: binding and activation correlate with antidiabetic actions in db/db mice. Endocrinology 1996;137:4189-4195.

197. Heneka MT, Landreth GE, Feinstein DL. Role for peroxisome proliferator-activated receptor-gamma in Alzheimer's disease. Ann Neurol 2001;49:276.

198. Wang Y, Porter WW, Suh N, Honda T, Gribble GW, et al. A synthetic triterpenoid, 2-cyano-3,12-dioxooleana-1,9-dien-28-oic acid (CDDO), is a ligand for the peroxisome proliferator-activated receptor gamma. Mol Endocrinol 2000;14:1550-1556.

199. Theocharis S, Margeli A, Vielh P, Kouraklis G. Peroxisome proliferator-activated receptor-gamma ligands as cell-cycle modulators. Cancer Treat Rev 2004;30:545-554.

200. Qin C, Morrow D, Stewart J, Spencer K, Porter W, et al. A new class of peroxisome proliferator-activated receptor gamma (PPARgamma) agonists that inhibit growth of breast cancer cells: 1,1-Bis(3'-indolyl)-1-(p-substituted phenyl)methanes. Mol Cancer Ther 2004;3:247-260.

201. Tontonoz P, Hu E, Graves RA, Budavari AI, Spiegelman BM. mPPAR gamma 2: tissue-specific regulator of an adipocyte enhancer. Genes Dev 1994;8:1224-1234.

202. Tontonoz P, Hu E, Spiegelman BM. Stimulation of adipogenesis in fibroblasts by PPAR gamma 2, a lipid-activated transcription factor. Cell 1994;79:1147-1156.

203. Schoonjans K, Peinado-Onsurbe J, Lefebvre AM, Heyman RA, Briggs M, et al. PPARalpha and PPARgamma activators direct a distinct tissue-specific transcriptional response via a PPRE in the lipoprotein lipase gene. EMBO J 1996;15:5336-5348.

204. Jiang C, Ting AT, Seed B. PPAR-gamma agonists inhibit production of monocyte inflammatory cytokines. Nature 1998;391:82-86.

205. Li M, Pascual G, Glass CK. Peroxisome proliferator-activated receptor gamma-dependent repression of the inducible nitric oxide synthase gene. Mol Cell Biol 2000;20:4699-4707.

206. Marx N, Mach F, Sauty A, Leung JH, Sarafi MN, et al. Peroxisome proliferator-activated receptor-gamma activators inhibit IFN-gamma-induced expression of the T cell-active CXC chemokines IP-10, Mig, and I-TAC in human endothelial cells. J Immunol 2000;164:6503-6508.

207. Ricote M, Li AC, Willson TM, Kelly CJ, Glass CK. The peroxisome proliferator-activated receptor-gamma is a negative regulator of macrophage activation. Nature 1998;391:79-82.

208. Gelman L, Fruchart JC, Auwerx J. An update on the mechanisms of action of the peroxisome proliferator-activated receptors (PPARs) and their roles in inflammation and cancer. Cell Mol Life Sci 1999;55:932-943.

209. Kodera Y, Takeyama K, Murayama A, Suzawa M, Masuhiro Y, et al. Ligand type-specific interactions of peroxisome proliferator-activated receptor gamma with transcriptional coactivators. J Biol Chem 2000;275:33201-33204.

210. Xu HE, Lambert MH, Montana VG, Parks DJ, Blanchard SG, et al. Molecular recognition of fatty acids by peroxisome proliferator-activated receptors. Mol Cell 1999;3:397-403.

211. Uppenberg J, Svensson C, Jaki M, Bertilsson G, Jendeberg L, et al. Crystal structure of the ligand binding domain of the human nuclear receptor PPARgamma. J Biol Chem 1998;273:31108-31112.

212. Auwerx J. PPARgamma, the ultimate thrifty gene. Diabetologia 1999;42:1033-1049.

213. Dowell P, Peterson VJ, Zabriskie TM, Leid M. Ligand-induced peroxisome proliferator-activated receptor alpha conformational change. J Biol Chem 1997;272:2013-2020.

214. Shalev A, Siegrist-Kaiser CA, Yen PM, Wahli W, Burger AG, et al. The peroxisome proliferator-activated receptor alpha is a phosphoprotein: regulation by insulin. Endocrinology 1996;137:4499-4502.

215. Juge-Aubry CE, Hammar E, Siegrist-Kaiser C, Pernin A, Takeshita A, et al. Regulation of the transcriptional activity of the peroxisome proliferator-activated receptor alpha by phosphorylation of a ligand-independent trans-activating domain. J Biol Chem 1999;274:10505-10510.

216. Zhang B, Berger J, Zhou G, Elbrecht A, Biswas S, et al. Insulin- and mitogen-activated protein kinase-mediated phosphorylation and activation of peroxisome proliferator-activated receptor gamma. J Biol Chem 1996;271:31771-31774.

217. Camp HS, Tafuri SR. Regulation of peroxisome proliferator-activated receptor gamma activity by mitogen-activated protein kinase. J Biol Chem 1997;272:10811-10816.

218. Hu E, Kim JB, Sarraf P, Spiegelman BM. Inhibition of adipogenesis through MAP kinase-mediated phosphorylation of PPARgamma. Science 1996;274:2100-2103.

219. Gabbay RA, Sutherland C, Gnudi L, Kahn BB, O'Brien RM, et al. Insulin regulation of phosphoenolpyruvate carboxykinase gene expression does not require activation of the Ras/mitogen-activated protein kinase signaling pathway. J Biol Chem 1996;271:1890-1897.

220. Keller H, Dreyer C, Medin J, Mahfoudi A, Ozato K, et al. Fatty acids and retinoids control lipid metabolism through activation of peroxisome proliferator-activated

receptor-retinoid X receptor heterodimers. Proc Natl Acad Sci U S A 1993;90:2160-2164.

221. Gearing KL, Gottlicher M, Teboul M, Widmark E, Gustafsson JA. Interaction of the peroxisome-proliferator-activated receptor and retinoid X receptor. Proc Natl Acad Sci U S A 1993;90:1440-1444.

222. Vu-Dac N, Schoonjans K, Kosykh V, Dallongeville J, Heyman RA, et al. Retinoids increase human apolipoprotein A-11 expression through activation of the retinoid X receptor but not the retinoic acid receptor. Mol Cell Biol 1996;16:3350-3360.

223. Poirier H, Braissant O, Niot I, Wahli W, Besnard P. 9-cis-retinoic acid enhances fatty acid-induced expression of the liver fatty acid-binding protein gene. FEBS Lett 1997;412:480-484.

224. Mukherjee R, Davies PJ, Crombie DL, Bischoff ED, Cesario RM, et al. Sensitization of diabetic and obese mice to insulin by retinoid X receptor agonists. Nature 1997;386:407-410.

225. Mukherjee R, Strasser J, Jow L, Hoener P, Paterniti JR, Jr., et al. RXR agonists activate PPARalpha-inducible genes, lower triglycerides, and raise HDL levels *in vivo*. Arterioscler Thromb Vasc Biol 1998;18:272-276.

226. Tontonoz P, Graves RA, Budavari AI, Erdjument-Bromage H, Lui M, et al. Adipocyte-specific transcription factor ARF6 is a heterodimeric complex of two nuclear hormone receptors, PPAR gamma and RXR alpha. Nucleic Acids Res 1994;22:5628-5634.

227. Barak Y, Nelson MC, Ong ES, Jones YZ, Ruiz-Lozano P, et al. PPAR gamma is required for placental, cardiac, and adipose tissue development. Mol Cell 1999;4:585-595.

228. Kubota N, Terauchi Y, Miki H, Tamemoto H, Yamauchi T, et al. PPAR gamma mediates high-fat diet-induced adipocyte hypertrophy and insulin resistance. Mol Cell 1999;4:597-609.

229. Rosen ED, Sarraf P, Troy AE, Bradwin G, Moore K, et al. PPAR gamma is required for the differentiation of adipose tissue *in vivo* and *in vitro*. Mol Cell 1999;4:611-617.

230. Masugi J, Tamori Y, Kasuga M. Inhibition of adipogenesis by a COOH-terminally truncated mutant of PPARgamma2 in 3T3-L1 cells. Biochem Biophys Res Commun 1999;264:93-99.

231. Gurnell M, Wentworth JM, Agostini M, Adams M, Collingwood TN, et al. A dominant-negative peroxisome proliferator-activated receptor gamma (PPARgamma) mutant is a constitutive repressor and inhibits PPARgamma-mediated adipogenesis. J Biol Chem 2000;275:5754-5759.

232. Tontonoz P, Hu E, Devine J, Beale EG, Spiegelman BM. PPAR gamma 2 regulates adipose expression of the phosphoenolpyruvate carboxykinase gene. Mol Cell Biol 1995;15:351-357.

233. Schoonjans K, Watanabe M, Suzuki H, Mahfoudi A, Krey G, et al. Induction of the acyl-coenzyme A synthetase gene by fibrates and fatty acids is mediated by a

peroxisome proliferator response element in the C promoter. J Biol Chem 1995;270:19269-19276.

234. Martin G, Schoonjans K, Lefebvre AM, Staels B, Auwerx J. Coordinate regulation of the expression of the fatty acid transport protein and acyl-CoA synthetase genes by PPARalpha and PPARgamma activators. J Biol Chem 1997;272:28210-28217.

235. Sfeir Z, Ibrahimi A, Amri E, Grimaldi P, Abumrad N. Regulation of FAT/CD36 gene expression: further evidence in support of a role of the protein in fatty acid binding/transport. Prostaglandins Leukot Essent Fatty Acids 1997;57:17-21.

236. Hotamisligil GS, Murray DL, Choy LN, Spiegelman BM. Tumor necrosis factor alpha inhibits signaling from the insulin receptor. Proc Natl Acad Sci U S A 1994;91:4854-4858.

237. Hofmann C, Lorenz K, Braithwaite SS, Colca JR, Palazuk BJ, et al. Altered gene expression for tumor necrosis factor-alpha and its receptors during drug and dietary modulation of insulin resistance. Endocrinology 1994;134:264-270.

238. Ribon V, Johnson JH, Camp HS, Saltiel AR. Thiazolidinediones and insulin resistance: peroxisome proliferatoractivated receptor gamma activation stimulates expression of the CAP gene. Proc Natl Acad Sci U S A 1998;95:14751-14756.

239. Day C. Thiazolidinediones: a new class of antidiabetic drugs. Diabet Med 1999;16:179-192.

240. Hauner H. The mode of action of thiazolidinediones. Diabetes Metab Res Rev 2002;18 Suppl 2:S10-15.

241. Ranganathan S, Kern PA. Thiazolidinediones inhibit lipoprotein lipase activity in adipocytes. J Biol Chem 1998;273:26117-26122.

242. Wang M, Wise SC, Leff T, Su TZ. Troglitazone, an antidiabetic agent, inhibits cholesterol biosynthesis through a mechanism independent of peroxisome proliferator-activated receptor-gamma. Diabetes 1999;48:254-260.

243. Colville-Nash PR, Qureshi SS, Willis D, Willoughby DA. Inhibition of inducible nitric oxide synthase by peroxisome proliferator-activated receptor agonists: correlation with induction of heme oxygenase 1. J Immunol 1998;161:978-984.

244. Willson TM, Cobb JE, Cowan DJ, Wiethe RW, Correa ID, et al. The structure-activity relationship between peroxisome proliferator-activated receptor gamma agonism and the antihyperglycemic activity of thiazolidinediones. J Med Chem 1996;39:665-668.

245. Tsukamoto H, Hishinuma T, Suzuki N, Tayama R, Hiratsuka M, et al. Thiazolidinediones increase arachidonic acid release and subsequent prostanoid production in a peroxisome proliferator-activated receptor gamma-independent manner. Prostaglandins Other Lipid Mediat 2004;73:191-213.

246. Crosby MB, Svenson JL, Zhang J, Nicol CJ, Gonzalez FJ, et al. Peroxisome proliferation-activated receptor (PPAR)gamma is not necessary for synthetic PPARgamma agonist inhibition of inducible nitric-oxide synthase and nitric oxide. J Pharmacol Exp Ther 2005;312:69-76.

247. Nagy L, Tontonoz P, Alvarez JG, Chen H, Evans RM. Oxidized LDL regulates macrophage gene expression through ligand activation of PPARgamma. Cell 1998;93:229-240.

248. Tontonoz P, Nagy L, Alvarez JG, Thomazy VA, Evans RM. PPARgamma promotes monocyte/macrophage differentiation and uptake of oxidized LDL. Cell 1998;93:241-252.

249. Ricote M, Huang J, Fajas L, Li A, Welch J, et al. Expression of the peroxisome proliferator-activated receptor gamma (PPARgamma) in human atherosclerosis and regulation in macrophages by colony stimulating factors and oxidized low density lipoprotein. Proc Natl Acad Sci U S A 1998;95:7614-7619.

250. Marx N, Sukhova G, Murphy C, Libby P, Plutzky J. Macrophages in human atheroma contain PPARgamma: differentiation-dependent peroxisomal proliferator-activated receptor gamma(PPARgamma) expression and reduction of MMP-9 activity through PPARgamma activation in mononuclear phagocytes *in vitro*. Am J Pathol 1998;153:17-23.

251. Febbraio M, Podrez EA, Smith JD, Hajjar DP, Hazen SL, et al. Targeted disruption of the class B scavenger receptor CD36 protects against atherosclerotic lesion development in mice. J Clin Invest 2000;105:1049-1056.

252. Marx N, Schonbeck U, Lazar MA, Libby P, Plutzky J. Peroxisome proliferator-activated receptor gamma activators inhibit gene expression and migration in human vascular smooth muscle cells. Circ Res 1998;83:1097-1103.

253. Itami A, Watanabe G, Shimada Y, Hashimoto Y, Kawamura J, et al. Ligands for peroxisome proliferator-activated receptor g inhibit growth of pancreatic cancers both *in vitro* and *in vivo*. Int J Cancer 2001;94:370.

254. Takahashi N, Okumura T, Motomura W, Fujimoto Y, Kawabata I, et al. Activation of PPAR g inhibits cell growth and induces apoptosis in human gastric cancer cells. FEBS Lett. 1999;455:135.

255. Inoue K, Kawahito Y, Tsubouchi Y, Kohno M, Yoshimura R, et al. Expression of peroxisome proliferator-activated receptor g in renal cell carcinoma and growth inhibition by its agonists. Biochem and Biophys Res Commun 2001;287:727.

256. Kubota T, Koshizuka K, Williamson EA, Asou H, Said JW, et al. Ligand for peroxisome proliferator-activated receptor g (troglitazone) has potent antitumor effect against human prostate cancer both *in vitro* and *in vivo*. Cancer Res 1998;58:3344.

257. Ikezoe T, Miller CW, Kawano S, Heaney A, Williamson EA, et al. Mutational analysis of the peroxisome proliferator-activated receptor g gene in human malignancies. Cancer Res 2001;61:5307.

258. Fajas L, Debril MB, Auwerx J. Peroxisome proliferator-activated receptor-gamma: from adipogenesis to carcinogenesis. J Mol Endocrinol 2001;27:1-9.

259. Altiok S, Xu M, Spiegelman BM. PPARgamma induces cell cycle withdrawal: inhibition of E2F/DP DNA-binding activity via down-regulation of PP2A. Genes Dev 1997;11:1987-1998.

260. Wakino S, Kintscher U, Kim S, Yin F, Hsueh WA, et al. Peroxisome proliferator-activated receptor gamma ligands inhibit retinoblastoma phosphorylation and G1--> S transition in vascular smooth muscle cells. J Biol Chem 2000;275:22435-22441.

261. Morrison RF, Farmer SR. Role of PPARgamma in regulating a cascade expression of cyclin-dependent kinase inhibitors, p18(INK4c) and p21(Waf1/Cip1), during adipogenesis. J Biol Chem 1999;274:17088-17097.

262. Kawa S, Nikaido T, Unno H, Usuda N, Nakayama K, et al. Growth inhibition and differentiation of pancreatic cancer cell lines by PPAR gamma ligand troglitazone. Pancreas 2002;24:1-7.

263. Itami A, Watanabe G, Shimada Y, Hashimoto Y, Kawamura J, et al. Ligands for peroxisome proliferator-activated receptor gamma inhibit growth of pancreatic cancers both *in vitro* and *in vivo*. Int J Cancer 2001;94:370-376.

264. Koga H, Sakisaka S, Harada M, Takagi T, Hanada S, et al. Involvement of p21(WAF1/Cip1), p27(Kip1), and p18(INK4c) in troglitazone-induced cell-cycle arrest in human hepatoma cell lines. Hepatology 2001;33:1087-1097.

265. Hupfeld CJ, Weiss RH. TZDs inhibit vascular smooth muscle cell growth independently of the cyclin kinase inhibitors p21 and p27. Am J Physiol Endocrinol Metab 2001;281:E207-216.

266. Yin F, Wakino S, Liu Z, Kim S, Hsueh WA, et al. Troglitazone inhibits growth of MCF-7 breast carcinoma cells by targeting G1 cell cycle regulators. Biochem Biophys Res Commun 2001;286:916-922.

267. Tontonoz P, Singer S, Forman BM, Sarraf P, Fletcher JA, et al. Terminal differentiation of human liposarcoma cells induced by ligands for peroxisome proliferator-activated receptor gamma and the retinoid X receptor. Proc Natl Acad Sci U S A 1997;94:237-241.

268. Kubota T, Koshizuka K, Williamson EA, Asou H, Said JW, et al. Ligand for peroxisome proliferator-activated receptor gamma (troglitazone) has potent antitumor effect against human prostate cancer both *in vitro* and *in vivo*. Cancer Res 1998;58:3344-3352.

269. Brockman JA, Gupta RA, Dubois RN. Activation of PPARgamma leads to inhibition of anchorage-independent growth of human colorectal cancer cells. Gastroenterology 1998;115:1049-1055.

270. Sarraf P, Mueller E, Jones D, King FJ, DeAngelo DJ, et al. Differentiation and reversal of malignant changes in colon cancer through PPARgamma. Nat Med 1998;4:1046-1052.

271. Kitamura S, Miyazaki Y, Shinomura Y, Kondo S, Kanayama S, et al. Peroxisome proliferator-activated receptor gamma induces growth arrest and differentiation markers of human colon cancer cells. Jpn J Cancer Res 1999;90:75-80.

272. Chang TH, Szabo E. Induction of differentiation and apoptosis by ligands of peroxisome proliferator-activated receptor gamma in non-small cell lung cancer. Cancer Res 2000;60:1129-1138.

273. Guan YF, Zhang YH, Breyer RM, Davis L, Breyer MD. Expression of peroxisome proliferator-activated receptor gamma (PPARgamma) in human transitional bladder cancer and its role in inducing cell death. Neoplasia 1999;1:330-339.

274. Sato H, Ishihara S, Kawashima K, Moriyama N, Suetsugu H, et al. Expression of peroxisome proliferator-activated receptor (PPAR)gamma in gastric cancer and inhibitory effects of PPARgamma agonists. Br J Cancer 2000;83:1394-1400.

275. Demetri GD, Fletcher CD, Mueller E, Sarraf P, Naujoks R, et al. Induction of solid tumor differentiation by the peroxisome proliferator-activated receptor-gamma ligand troglitazone in patients with liposarcoma. Proc Natl Acad Sci U S A 1999;96:3951-3956.

276. Elnemr A, Ohta T, Iwata K, Ninomia I, Fushida S, et al. PPARgamma ligand (thiazolidinedione) induces growth arrest and differentiation markers of human pancreatic cancer cells. Int J Oncol 2000;17:1157-1164.

277. Chattopadhyay N, Singh DP, Heese O, Godbole MM, Sinohara T, et al. Expression of peroxisome proliferator-activated receptors (PPARS) in human astrocytic cells: PPARgamma agonists as inducers of apoptosis. J Neurosci Res 2000;61:67-74.

278. Lefebvre M, Paulweber B, Fajas L, Woods J, McCrary C, et al. Peroxisome proliferator-activated receptor gamma is induced during differentiation of colon epithelium cells. J Endocrinol 1999;162:331-340.

279. Gupta RA, Brockman JA, Sarraf P, Willson TM, DuBois RN. Target genes of peroxisome proliferator-activated receptor gamma in colorectal cancer cells. J Biol Chem 2001;276:29681-29687.

280. Scherer PE, Lewis RY, Volonte D, Engelman JA, Galbiati F, et al. Cell-type and tissue-specific expression of caveolin-2. Caveolins 1 and 2 co-localize and form a stable hetero-oligomeric complex *in vivo*. J Biol Chem 1997;272:29337-29346.

281. Scherer PE, Lisanti MP, Baldini G, Sargiacomo M, Mastick CC, et al. Induction of caveolin during adipogenesis and association of GLUT4 with caveolin-rich vesicles. J Cell Biol 1994;127:1233-1243.

282. Kilgore MW, Tate PL, Rai S, Sengoku E, Price TM. MCF-7 and T47D human breast cancer cells contain a functional peroxisomal response. Mol Cell Endocrinol 1997;129:229-235.

283. Pignatelli M, Cortes-Canteli M, Lai C, Santos A, Perez-Castillo A. The peroxisome proliferator-activated receptor gamma is an inhibitor of ErbBs activity in human breast cancer cells. J Cell Sci 2001;114:4117-4126.

284. Mueller E, Sarraf P, Tontonoz P, Evans RM, Martin KJ, et al. Terminal differentiation of human breast cancer through PPAR gamma. Mol Cell 1998;1:465-470.

285. Burgermeister E, Tencer L, Liscovitch M. Peroxisome proliferator-activated receptor-gamma upregulates caveolin-1 and caveolin-2 expression in human carcinoma cells. Oncogene 2003;22:3888-3900.

286. Konopleva M, Andreeff M. Role of peroxisome proliferator-activated receptor-gamma in hematologic malignancies. Curr Opin Hematol 2002;9:294-302.

287. Haydon RC, Zhou L, Feng T, Breyer B, Cheng H, et al. Nuclear receptor agonists as potential differentiation therapy agents for human osteosarcoma. Clin Cancer Res 2002;8:1288-1294.

288. Panigrahy D, Shen LQ, Kieran MW, Kaipainen A. Therapeutic potential of thiazolidinediones as anticancer agents. Expert Opin Investig Drugs 2003;12:1925-1937.

289. Debril MB, Renaud JP, Fajas L, Auwerx J. The pleiotropic functions of peroxisome proliferator-activated receptor gamma. J Mol Med 2001;79:30-47.

290. Clay CE, Monjazeb A, Thorburn J, Chilton FH, High KP. 15-Deoxy-delta12,14-prostaglandin J2-induced apoptosis does not require PPARgamma in breast cancer cells. J Lipid Res 2002;43:1818-1828.

291. Elstner E, Muller C, Koshizuka K, Williamson EA, Park D, et al. Ligands for peroxisome proliferator-activated receptorgamma and retinoic acid receptor inhibit growth and induce apoptosis of human breast cancer cells *in vitro* and in BNX mice. Proc Natl Acad Sci U S A 1998;95:8806-8811.

292. Clay CE, Atsumi GI, High KP, Chilton FH. Early *de novo* gene expression is required for 15-deoxy-Delta 12,14-prostaglandin J2-induced apoptosis in breast cancer cells. J Biol Chem 2001;276:47131-47135.

293. Zander T, Kraus JA, Grommes C, Schlegel U, Feinstein D, et al. Induction of apoptosis in human and rat glioma by agonists of the nuclear receptor PPARgamma. J Neurochem 2002;81:1052-1060.

294. Toyoda M, Takagi H, Horiguchi N, Kakizaki S, Sato K, et al. A ligand for peroxisome proliferator activated receptor gamma inhibits cell growth and induces apoptosis in human liver cancer cells. Gut 2002;50:563-567.

295. Shimada T, Kojima K, Yoshiura K, Hiraishi H, Terano A. Characteristics of the peroxisome proliferator activated receptor gamma (PPARgamma) ligand induced apoptosis in colon cancer cells. Gut 2002;50:658-664.

296. Eibl G, Wente MN, Reber HA, Hines OJ. Peroxisome proliferator-activated receptor gamma induces pancreatic cancer cell apoptosis. Biochem Biophys Res Commun 2001;287:522-529.

297. Ohta K, Endo T, Haraguchi K, Hershman JM, Onaya T. Ligands for peroxisome proliferator-activated receptor gamma inhibit growth and induce apoptosis of human papillary thyroid carcinoma cells. J Clin Endocrinol Metab 2001;86:2170-2177.

298. Kim Y, Suh N, Sporn M, Reed JC. An inducible pathway for degradation of FLIP protein sensitizes tumor cells to TRAIL-induced apoptosis. J Biol Chem 2002;277:22320-22329.

299. Laurora S, Pizzimenti S, Briatore F, Fraioli A, Maggio M, et al. Peroxisome proliferator-activated receptor ligands affect growth-related gene expression in human leukemic cells. J Pharmacol Exp Ther 2003;305:932-942.

300. Abe A, Kiriyama Y, Hirano M, Miura T, Kamiya H, et al. Troglitazone suppresses cell growth of KU812 cells independently of PPARgamma. Eur J Pharmacol 2002;436:7-13.

301. Liu DC, Zang CB, Liu HY, Possinger K, Fan SG, et al. A novel PPAR alpha/gamma dual agonist inhibits cell growth and induces apoptosis in human glioblastoma T98G cells. Acta Pharmacol Sin 2004;25:1312-1319.

302. Perez-Ortiz JM, Tranque P, Vaquero CF, Domingo B, Molina F, et al. Glitazones differentially regulate primary astrocyte and glioma cell survival. Involvement of reactive oxygen species and peroxisome proliferator-activated receptor-gamma. J Biol Chem 2004;279:8976-8985.

303. Baek SJ, Kim JS, Nixon JB, DiAugustine RP, Eling TE. Expression of NAG-1, a transforming growth factor-α superfamily member, by troglitazone requires the early growth response gene EGR-1. J Biol Chem 2004;279:6883.

304. Yin F, Bruemmer D, Blaschke F, Hsueh WA, Law RE, et al. Signaling pathways involved in induction of GADD45 gene expression and apoptosis by troglitazone in human MCF-7 breast carcinoma cells. Oncogene 2004;23:4614-4623.

305. Melichar B, Konopleva M, Hu W, Melicharova K, Andreeff M, et al. Growth-inhibitory effect of a novel synthetic triterpenoid, 2-cyano-3,12-dioxoolean-1,9-dien-28-oic acid, on ovarian carcinoma cell lines not dependent on peroxisome proliferator-activated receptor-gamma expression. Gynecol Oncol 2004;93:149-154.

306. Palakurthi SS, Aktas H, Grubissich LM, Mortensen RM, Halperin JA. Anticancer effects of thiazolidinediones are independent of peroxisome proliferator-activated receptor gamma and mediated by inhibition of translation initiation. Cancer Res 2001;61:6213-6218.

307. Milbrandt J. Nerve growth factor induces a gene homologous to the glucocorticoid receptor gene. Neuron 1988;1:183-188.

308. Hazel TG, Nathans D, Lau LF. A gene inducible by serum growth factors encodes a member of the steroid and thyroid hormone receptor superfamily. Proc Natl Acad Sci U S A 1988;85:8444-8448.

309. Law SW, Conneely OM, DeMayo FJ, O'Malley BW. Identification of a new brain-specific transcription factor, NURR1. Mol Endocrinol 1992;6:2129-2135.

310. Scearce LM, Laz TM, Hazel TG, Lau LF, Taub R. RNR-1, a nuclear receptor in the NGFI-B/Nur77 family that is rapidly induced in regenerating liver. J Biol Chem 1993;268:8855-8861.

311. Pena de Ortiz S, Jamieson GA, Jr. HZF-3, an immediate-early orphan receptor homologous to NURR1/NOT: induction upon membrane depolarization and seizures. Brain Res Mol Brain Res 1996;38:1-13.

312. Mages HW, Rilke O, Bravo R, Senger G, Kroczek RA. NOT, a human immediate-early response gene closely related to the steroid/thyroid hormone receptor NAK1/TR3. Mol Endocrinol 1994;8:1583-1591.

313. Ohkura N, Hijikuro M, Yamamoto A, Miki K. Molecular cloning of a novel thyroid/steroid receptor superfamily gene from cultured rat neuronal cells. Biochem Biophys Res Commun 1994;205:1959-1965.

314. Watson MA, Milbrandt J. Expression of the nerve growth factor-regulated NGFI-A and NGFI-B genes in the developing rat. Development 1990;110:173-183.

315. Williams GT, Lau LF. Activation of the inducible orphan receptor gene nur77 by serum growth factors: dissociation of immediate-early and delayed-early responses. Mol Cell Biol 1993;13:6124-6136.

316. Nakai A, Kartha S, Sakurai A, Toback FG, DeGroot LJ. A human early response gene homologous to murine nur77 and rat NGFI-B, and related to the nuclear receptor superfamily. Mol Endocrinol 1990;4:1438-1443.

317. Bandoh S, Tsukada T, Maruyama K, Ohkura N, Yamaguchi K. Differential expression of NGFI-B and RNR-1 genes in various tissues and developing brain of the rat: comparative study by quantitative reverse transcription-polymerase chain reaction. J Neuroendocrinol 1997;9:3-8.

318. Liu ZG, Smith SW, McLaughlin KA, Schwartz LM, Osborne BA. Apoptotic signals delivered through the T-cell receptor of a T-cell hybrid require the immediate-early gene nur77. Nature 1994;367:281-284.

319. Woronicz JD, Calnan B, Ngo V, Winoto A. Requirement for the orphan steroid receptor Nur77 in apoptosis of T-cell hybridomas. Nature 1994;367:277-281.

320. Labelle Y, Zucman J, Stenman G, Kindblom LG, Knight J, et al. Oncogenic conversion of a novel orphan nuclear receptor by chromosome translocation. Hum Mol Genet 1995;4:2219-2226.

321. Maruyama K, Tsukada T, Bandoh S, Sasaki K, Ohkura N, et al. Expression of the putative transcription factor NOR-1 in the nervous, the endocrine and the immune systems and the developing brain of the rat. Neuroendocrinology 1997;65:2-8.

322. Wilson TE, Fahrner TJ, Johnston M, Milbrandt J. Identification of the DNA binding site for NGFI-B by genetic selection in yeast. Science 1991;252:1296-1300.

323. Wilson TE, Fahrner TJ, Milbrandt J. The orphan receptors NGFI-B and steroidogenic factor 1 establish monomer binding as a third paradigm of nuclear receptor-DNA interaction. Mol Cell Biol 1993;13:5794-5804.

324. Giguere V, McBroom LD, Flock G. Determinants of target gene specificity for ROR alpha 1: monomeric DNA binding by an orphan nuclear receptor. Mol Cell Biol 1995;15:2517-2526.

325. Wilson TE, Paulsen RE, Padgett KA, Milbrandt J. Participation of non-zinc finger residues in DNA binding by two nuclear orphan receptors. Science 1992;256:107-110.

326. Philips A, Lesage S, Gingras R, Maira MH, Gauthier Y, et al. Novel dimeric Nur77 signaling mechanism in endocrine and lymphoid cells. Mol Cell Biol 1997;17:5946-5951.

327. Winoto A. Genes involved in T-cell receptor-mediated apoptosis of thymocytes and T-cell hybridomas. Semin Immunol 1997;9:51.

328. Zetterstrom RH, Solomin L, Mitsiadis T, Olson L, Perlmann T. Retinoid X receptor heterodimerization and developmental expression distinguish the orphan nuclear receptors NGFI-B, Nurr1, and Nor1. Mol Endocrinol 1996;10:1656-1666.

329. Perlmann T, Jansson L. A novel pathway for vitamin A signaling mediated by RXR heterodimerization with NGFI-B and NURR1. Genes Dev 1995;9:769-782.

330. Forman BM, Umesono K, Chen J, Evans RM. Unique response pathways are established by allosteric interactions among nuclear hormone receptors. Cell 1995;81:541-550.

331. Fahrner TJ, Carroll SL, Milbrandt J. The NGFI-B protein, an inducible member of the thyroid/steroid receptor family, is rapidly modified posttranslationally. Mol Cell Biol 1990;10:6454-6459.

332. Hazel TG, Misra R, Davis IJ, Greenberg ME, Lau LF. Nur77 is differentially modified in PC12 cells upon membrane depolarization and growth factor treatment. Mol Cell Biol 1991;11:3239-3246.

333. Davis IJ, Hazel TG, Chen RH, Blenis J, Lau LF. Functional domains and phosphorylation of the orphan receptor Nur77. Mol Endocrinol 1993;7:953-964.

334. Li Y, Lau LF. Adrenocorticotropic hormone regulates the activities of the orphan nuclear receptor Nur77 through modulation of phosphorylation. Endocrinology 1997;138:4138-4146.

335. Katagiri Y, Hirata Y, Milbrandt J, Guroff G. Differential regulation of the transcriptional activity of the orphan nuclear receptor NGFI-B by membrane depolarization and nerve growth factor. J Biol Chem 1997;272:31278-31284.

336. Ordentlich P, Yan Y, Zhou S, Heyman RA. Identification of the antineoplastic agent 6-mercaptopurine as an activator of the orphan nuclear hormone receptor Nurr1. J Biol Chem 2003;278:24791-24799.

337. Wansa KD, Harris JM, Yan G, Ordentlich P, Muscat GE. The AF-1 domain of the orphan nuclear receptor NOR-1 mediates trans-activation, coactivator recruitment,

and activation by the purine anti-metabolite 6-mercaptopurine. J Biol Chem 2003;278:24776-24790.

338. Zetterstrom RH, Solomin L, Jansson L, Hoffer BJ, Olson L, et al. Dopamine neuron agenesis in Nurr1-deficient mice. Science 1997;276:248-250.

339. Saucedo-Cardenas O, Quintana-Hau JD, Le WD, Smidt MP, Cox JJ, et al. Nurr1 is essential for the induction of the dopaminergic phenotype and the survival of ventral mesencephalic late dopaminergic precursor neurons. Proc Natl Acad Sci U S A 1998;95:4013-4018.

340. DeYoung RA, Baker JC, Cado D, Winoto A. The orphan steroid receptor Nur77 family member Nor-1 is essential for early mouse embryogenesis. J Biol Chem 2003;278:47104-47109.

341. Lee SL, Wesselschmidt RL, Linette GP, Kanagawa O, Russell JH, et al. Unimpaired thymic and peripheral T cell death in mice lacking the nuclear receptor NGFI-B (Nur77). Science 1995;269:532-535.

342. Calnan BJ, Szychowski S, Chan FK, Cado D, Winoto A. A role for the orphan steroid receptor Nur77 in apoptosis accompanying antigen-induced negative selection. Immunity 1995;3:273-282.

343. Zhou T, Cheng J, Yang P, Wang Z, Liu C, et al. Inhibition of Nur77/Nurr1 leads to inefficient clonal deletion of self-reactive T cells. J Exp Med 1996;183:1879-1892.

344. Cheng LE, Chan FK, Cado D, Winoto A. Functional redundancy of the Nur77 and Nor-1 orphan steroid receptors in T-cell apoptosis. EMBO J 1997;16:1865-1875.

345. Liu W, Youn HD, Liu JO. Thapsigargin-induced apoptosis involves Cabin1-MEF2-mediated induction of Nur77. Eur J Immunol 2001;31:1757-1764.

346. Woronicz JD, Lina A, Calnan BJ, Szychowski S, Cheng L, et al. Regulation of the Nur77 orphan steroid receptor in activation-induced apoptosis. Mol Cell Biol 1995;15:6364-6376.

347. Youn HD, Sun L, Prywes R, Liu JO. Apoptosis of T cells mediated by Ca2+-induced release of the transcription factor MEF2. Science 1999;286:790-793.

348. Li Y, Lin B, Agadir A, Liu R, Dawson MI, et al. Molecular determinants of AHPN (CD437)-induced growth arrest and apoptosis in human lung cancer cell lines. Mol Cell Biol 1998;18:4719-4731.

349. Young CY, Murtha PE, Zhang J. Tumor-promoting phorbol ester-induced cell death and gene expression in a human prostate adenocarcinoma cell line. Oncol Res 1994;6:203-210.

350. Li H, Kolluri SK, Gu J, Dawson MI, Cao X, et al. Cytochrome c release and apoptosis induced by mitochondrial targeting of nuclear orphan receptor TR3. Science 2000;289:1159-1164.

351. Lin B, Kolluri SK, Lin F, Liu W, Han YH, et al. Conversion of Bcl-2 from protector to killer by interaction with nuclear orphan receptor Nur77/TR3. Cell 2004;116:527-540.

352. Wilson AJ, Arango D, Mariadason JM, Heerdt BG, Augenlicht LH. TR3/Nur77 in colon cancer cell apoptosis. Cancer Res 2003;63:5401-5407.

353. Mu X, Chang C. TR3 orphan nuclear receptor mediates apoptosis through up-regulating E2F1 in human prostate cancer LNCaP cells. J Biol Chem 2003;278:42840-42845.

354. Rosen ED, Spiegelman BM. PPAR g: a nuclear regulator of metabolism, differentiation, and cell growth. J Biol Chem 2001;276:37731-37734.

355. Willson RM, Lambert MH, Kliewer SA. Peroxisome proliferator-activated receptor g and metabolic disease. Annu.Rev.Biochem. 2001;70:341-367.

356. Lee CH, Olson P, Evans RM. Minireview: lipid metabolism, metabolic diseases, and peroxisome proliferator-activated receptors. Endocrinology 2003;144:2201-2207.

357. Murphy GJ, Holder JC. PPAR- g agonists: therapeutic role in diabetes, inflammation and cancer. Trends Pharmacol.Sci. 2000;21:469-474.

358. Sarraf P, Mueller E, Smith WM, Wright HM, Kum JB, et al. Loss-of-function mutations in PPAR g associated with human colon cancer. Mol.Cell 1999;3:799-804.

359. Qin C, Morrow D, Stewart J, Spencer K, Porter W, et al. A new class of peroxisome proliferator-activated receptor g (PPAR g) agonists that inhibit growth of breast cancer cells: 1,1-bis(3'-indolyl)-1-(p -substitutedphenyl)methanes. Mol.Cancer Therap 2004;3:247-259.

360. Gupta RA, Sarraf P, Mueller E, Brockman JA, Prusakiewicz JJ, et al. Peroxisome proliferator-activated receptor g -mediated differentiation: a mutation in colon

cancer cells reveals divergent and cell type-specific mechanisms. J Biol Chem 2003;278:22669-22677.

361.   Qin C, Burghardt R, Smith R, Wormke M, Stewart J, et al. Peroxisome proliferator-activated receptor g (PPAR g) agonists induce proteasome-dependent degradation of cyclin D1 and estrogen receptor à in MCF-7 breast cancer cells. Cancer Res 2003;63:958-964.

362. Brockman JA, Gupta RA, DuBois RN. Activation of PPAR g leads to inhibition of anchorage independent growth of human colorectal cancer cells. Gastroenterology 1998;115:1049-1055.

363. Kodera Y, Takeyama K, Murayama A, Suzawa M, Masuhiro Y, et al. Ligand type-specific interactions of peroxisome proliferator-activated receptor g with transcriptional coactivators. J Biol Chem 2000;275:33201-33204.

364.   Burgermeister E, Tencer L, Liscovitch M. Peroxisome proliferator-activated receptor- g upregulates caveolin-1 and caveolin-2 expression in human carcinoma cells. Oncogene 2003;22:3888-3900.

365. Chang TH, Szabo E. Induction of differentiation and apoptosis by ligands of peroxisome proliferator-activated receptor g in non-small cell lung cancer. Cancer Res 2000;60:1129-1138.

366. Elstner E, Muller C, Koshizuka K, Williamson EA, Park D, et al. Ligands for peroxisome proliferator-activated receptor gamma and retinoic acid receptor inhibit growth and induce apoptosis of human breast cancer cells in vitro and in BNX mice. Proc Natl Acad Sci U S A 1998;95:8806-8811.

367. Sarraf P, Mueller E, Jones D, King FJ, DeAngelo DJ, et al. Differentiation and reversal of malignant changes in colon cancer through PPAR g. Nat.Med. 1998;4:1046-1052.

368. Lefebvre A, Chen I, Desreumaux P, Najib J, Fruchart J, et al. Activation of the peroxisome proliferator-activated receptor g promotes the development of colon tumors in C57BL/6J-APCMin/+ mice. Nat Med 1998;4:1053-1057.

369. Saez E, Tontonoz P, Nelson MC, Alvarez JG, Ming UT, et al. Activators of the nuclear receptor PPAR g enhance colon polyp formation. Nat Med 1998;4:1058-1061.

370. Niho N, Takahashi M, Kitamura T, Shoji Y, Itoh M, et al. Concomitant suppression of hyperlipidemia and intestinal polyp formation in Apc -deficient mice by peroxisome proliferator-activated receptor ligands. Cancer Res 2003;63:6090-6095.

371. Girnun GD, Smith WM, Drori S, Sarraf P, Mueller E, et al. APC-dependent suppression of colon carcinogenesis by PPAR g. Proc Natl Acad Sci U S A 2002;99:13771-13776.

372. Kato M, Kusumi T, Tsuchida S, Tanaka M, Sasaki M, et al. Induction of differentiation and peroxisome proliferator-activated receptor g expression in colon cancer cell lines by troglitazone. J.Cancer Res.Clin.Oncol. 2004;130:73-79.

373. Gupta RA, Brockman JA, Sarraf P, Willson TM, DuBois RN. Target genes of peroxisome proliferator-activated receptor g in colorectal cancer cells. J Biol Chem 2001;276:29681-29687.

374. Kitamura S, Miyazaki Y, Shinomura Y, Kondo S, Kanayama S, et al. Peroxisome proliferator-activated receptor g induces growth arrest and differentiation markers of human colon cancer cells. Jpn J Cancer Res 1999;90:75-80.

375. Bender FC, Reymond MA, Bron C, Quest AF. Caveolin-1 levels are down-regulated in human colon tumors, and ectopic expression of caveolin-1 in colon carcinoma cell lines reduces cell tumorigenicity. Cancer Res 2000;60:5870-5878.

376. Geller NL, Sternberg CN, Penenberg D, Scher H, Yagoda A. Prognostic factors for survival of patients with advanced urothelial tumors treated with methotrexate, vinblastine, doxorubicin, and cisplatin chemotherapy. Cancer 1991;67:1525-1531.

377. Pagano F, Bassi P, Galetti TP, Meneghini A, Milani C, et al. Results of contemporary radical cystectomy for invasive bladder cancer: a clinicopathological study with an emphasis on the inadequacy of the tumor, nodes and metastases classification. J Urol 1991;145:45-50.

378. Sternberg CN, Yagoda A, Scher HI, Watson RC, Herr HW, et al. M-VAC (methotrexate, vinblastine, doxorubicin and cisplatin) for advanced transitional cell carcinoma of the urothelium. J Urol 1988;139:461-469.

379. Sternberg CN, Yagoda A, Scher HI, Watson RC, Geller N, et al. Methotrexate, vinblastine, doxorubicin, and cisplatin for advanced transitional cell carcinoma of the urothelium. Efficacy and patterns of response and relapse. Cancer 1989;64:2448-2458.

380. von der MH, Hansen SW, Roberts JT, Dogliotti L, Oliver T, et al. Gemcitabine and cisplatin versus methotrexate, vinblastine, doxorubicin, and cisplatin in advanced

or metastatic bladder cancer: results of a large, randomized, multinational, multicenter, phase III study. J Clin Oncol 2000;18:3068-3067.

381. Bellmunt J, Guillem V, Paz-Ares L, Gonzalez-Larriba JL, Carles J, et al. Phase I-II study of paclitaxel, cisplatin, and gemcitabine in advanced transitional-cell carcinoma of the urothelium. Spanish Oncology Genitourinary Group. J Clin Oncol 2000;18:3247-3255.

382. Hussain M, Vaishampayan U, Du W, Redman B, Smith DC. Combination paclitaxel, carboplatin, and gemcitabine is an active treatment for advanced urothelial cancer. J Clin Oncol 2001;19:2527-2533.

383. Fajas L, Debril MB, Auwerx J. Peroxisome proliferator-activated receptor- g: from adipogenesis to carcinogenesis. J Mol Endocrinol 2001;27:1-9.

384. Desvergne B, Wahli W. Peroxisome proliferator-activated receptors: nuclear control of metabolism. Endo Rev 1999;20:649-688.

385. Escher P, Wahli W. Peroxisome proliferator-activated receptors: insight into multiple cellular functions. Mutat Res 2000;448:121-138.

386. Guan Y. Targeting peroxisome proliferator-activated receptors (PPARs) in kidney and urologic disease. Minerva Urol Nefrol 2002;54:65.

387. Guan YF, Zhang YH, Breyer RM, Davis L, Breyer MD. Expression of peroxisome proliferator-activated receptor g (PPAR g) in human transitional bladder cancer and its role in inducing cell death. Neoplasia 1999;1:330-339.

388. Fauconnet S, Lascombe I, Chabannes E, Adessi GL, Desvergne B, et al. Differential regulation of vascular endothelial growth factor expression by

peroxisome proliferator-activated receptors in bladder cancer cells. J Biol Chem 2002;277:23534-23537.

389. Nakashiro KI, Hayashi Y, Kita A, Tamatani T, Chlenski A, et al. Role of peroxisome proliferator-activated receptor g and its ligands in non-neoplastic and neoplastic human urothelial cells. Am J Path 2001;159:591-597.

390. Clay CE, Namen AM, Atsumi G, Willingham MC, High KP, et al. Influence of J series prostaglandins on apoptosis and tumorigenesis of breast cancer cells. Carcinogenesis 1999;20:1905-1911.

391. Clay CE, Monjazeb A, Thorburn J, Chilton FH, High KP. 15-Deoxy- D (12,14)-prostaglandin J2-induced apoptosis does not require PPAR g in breast cancer cells. J Lipid Res 2002;43:1818-1828.

392. Campo PA, Das S, Hsiang CH, Bui T, Samuel CE, et al. Translational regulation of cyclin D1 by 15-deoxy- D (12,14)-prostaglandin J2. Cell Growth Differ 2002;13:409-420.

393. Chintharlapalli S, Smith Iii R, Samudio I, Zhang W, Safe S. 1,1-Bis(3'-indolyl)-1-(p -substitutedphenyl)methanes induce peroxisome proliferator-activated receptor g -mediated growth inhibition, transactivation and differentiation markers in colon cancer cells. Cancer Res 2004;64:5994-6001.

394. Hong J, Samudio I, Liu S, Abdelrahim M, Safe S. Peroxisome proliferator-activated receptor g -dependent activation of p21 in Panc-28 pancreatic cancer cells involves Sp1 and Sp4 proteins. Endocrinology 2004;145:5774-5785.

395. Contractor R, Samudio I, Estrov Z, Harris D, McCubrey JA, et al. A novel ring-substituted diindolylmethane 1,1-bis[3'-(5-methoxyindolyl)]-1-(p-t-butylphenyl)methane inhibits ERK activation and induces apoptosis in acute myeloid leukemia. Cancer Res 2005;65:2890-2901.

396. Chintharlapalli S, Papineni S, Konopleva M, Andreef M, Samudio I, et al. 2-Cyano-3,12-dioxoolean-1,9-dien-28-oic acid and related compounds inhibit growth of colon cancer cells through peroxisome proliferator-activated receptor g -dependent and -independent pathways. Mol Pharmacol 2005;68:119-128.

397. Baek SJ, Wilson LC, Hsi LC, Eling TE. Troglitazone, a peroxisome proliferator-activated receptor g (PPAR g) ligand, selectively induces the early growth response-1 gene independently of PPAR g. A novel mechanism for its anti-tumorigenic activity. J Biol Chem 2003;278:5845-5853.

398. Shack S, Wang XT, Kokkonen GC, Gorospe M, Longo DL, et al. Caveolin-induced activation of the phosphatidylinositol 3-kinase/Akt pathway increases arsenite cytotoxicity. Mol Cell Biol 2003;23:2407-2414.

399. Ono K, Iwanaga Y, Hirayama M, Kawamura T, Sowa N, et al. Contribution of caveolin-1 à and Akt to TNF-à-induced cell death. Am J Physiol Lung Cell Mol Physiol 2004;287:L201-209.

400. Tan J, Hall SH, Hamil KG, Grossman G, Petrusz P, et al. Protein inhibitor of activated STAT-1 (signal transducer and activator of transcription-1) is a nuclear receptor coregulator expressed in human testis. Mol Endocrinol 2000;14:14-24.

401. Li M, Baumeister P, Roy B, Phan T, Foti D, et al. ATF6 as a transcription activator of the endoplasmic reticulum stress element: thapsigargin stress-induced changes and synergistic interactions with NF-Y and YY1. Mol Cell Biol 2000;20:5096-5106.

402. Baek SJ, Kim KS, Nixon JB, Wilson LC, Eling TE. Cyclooxygenase inhibitors regulate the expression of a TGF-á superfamily member that has proapoptotic and antitumorigenic activities. Mol Pharmacol 2001;59:901-908.

403. Baek SJ, Horowitz JM, Eling TE. Molecular cloning and characterization of human nonsteroidal anti-inflammatory drug-activated gene promoter. Basal transcription is mediated by Sp1 and Sp3. J Biol Chem 2001;276:33384-33392.

404. Kim KS, Baek SJ, Flake GP, Loftin CD, Calvo BF, et al. Expression and regulation of nonsteroidal anti-inflammatory drug-activated gene (NAG-1) in human and mouse tissue. Gastroenterology 2002;122:1388-1398.

405. Bottone FG, Jr., Baek SJ, Nixon JB, Eling TE. Diallyl disulfide (DADS) induces the antitumorigenic NSAID-activated gene (NAG-1) by a p53-dependent mechanism in human colorectal HCT 116 cells. J Nutr 2002;132:773-778.

406. Baek SJ, Wilson LC, Eling TE. Resveratrol enhances the expression of non-steroidal anti-inflammatory drug-activated gene (NAG-1) by increasing the expression of p53. Carcinogenesis 2002;23:425-434.

407. Wilson LC, Baek SJ, Call A, Eling TE. Nonsteroidal anti-inflammatory drug-activated gene (NAG-1) is induced by genistein through the expression of p53 in colorectal cancer cells. Int J Cancer 2003;105:747-753.

408. Newman D, Sakaue M, Koo JS, Kim KS, Baek SJ, et al. Differential regulation of nonsteroidal anti-inflammatory drug-activated gene in normal human tracheobronchial epithelial and lung carcinoma cells by retinoids. Mol Pharmacol 2003;63:557-564.

409. Yamaguchi K, Lee SH, Eling TE, Baek SJ. Identification of nonsteroidal anti-inflammatory drug-activated gene (NAG-1) as a novel downstream target of phosphatidylinositol 3-kinase/AKT/GSK-3á pathway. J Biol Chem 2004;279:49617-49623.

410. Kim KS, Yoon JH, Kim JK, Baek SJ, Eling TE, et al. Cyclooxygenase inhibitors induce apoptosis in oral cavity cancer cells by increased expression of nonsteroidal anti-inflammatory drug-activated gene. Biochem Biophys Res Commun 2004;325:1298-1303.

411. Baek SJ, Kim JS, Jackson FR, Eling TE, McEntee MF, et al. Epicatechin gallate-induced expression of NAG-1 is associated with growth inhibition and apoptosis in colon cancer cells. Carcinogenesis 2004;25:2425-2432.

412. Baek SJ, Kim JS, Moore SM, Lee SH, Martinez J, et al. Cyclooxygenase inhibitors induce the expression of the tumor suppressor gene EGR-1, which results in the up-regulation of NAG-1, an antitumorigenic protein. Mol Pharmacol 2005;67:356-364.

413. Kim JS, Baek SJ, Sali T, Eling TE. The conventional nonsteroidal anti-inflammatory drug sulindac sulfide arrests ovarian cancer cell growth via the expression of NAG-1/MIC-1/GDF-15. Mol Cancer Ther 2005;4:487-493.

414. Lee SH, Kim JS, Yamaguchi K, Eling TE, Baek SJ. Indole-3-carbinol and 3,3'-diindolylmethane induce expression of NAG-1 in a p53-independent manner. Biochem Biophys Res Commun 2005;328:63-69.

415. Chen CC, Lee WR, Safe S. Egr-1 is activated by 17á-estradiol in MCF-7 cells by mitogen-activated protein kinase-dependent phosphorylation of ELK-1. J Cell Biochem 2004;93:1063-1074.

416. Motomura W, Okumura T, Takahashi N, Obara T, Kohgo Y. Activation of peroxisome proliferator-activated receptor gamma by troglitazone inhibits cell growth through the increase of p27 KiP1 in human pancreatic carcinoma cells. Cancer Res 2000;60:5558--5564.

417. Palakurthi SS, Aktas H, Grubissich LM, Mortensen RM, Halperin JA. Anticancer effects of thiazolidinediones are independent of peroxisome proliferator-activated receptor g and mediated by inhibition of translation initiation. Cancer Res 2001;61:6213-6218.

418. Sukhatme VP, Kartha S, Toback FG, Taub R, Hoover RG, et al. A novel early growth response gene rapidly induced by fibroblast, epithelial cell and lymphocyte mitogens. Oncogene Res 1987;1:343-355.

419. Christy B, Nathans D. DNA binding site of the growth factor-inducible protein Zif268. Proc Natl Aca Sci U S A 1989;86:8737-8741.

420. Sukhatme VP. Early transcriptional events in cell growth: the Egr family. J Am Soc Nephrol 1990;1:859-866.

421. Cicatiello L, Sica V, Bresciani F, Weisz A. Identification of a specific pattern of "immediate-early" gene activation induced by estrogen during mitogenic stimulation of rat uterine cells. Receptor. 1993;3:17-30.

422. Muthukkumar S, Nair P, Sells SF, Maddiwar NG, Jacob RJ, et al. Role of EGR-1 in thapsigargin-inducible apoptosis in the melanoma cell line A375-C6. Mol Cell Biol 1995;15:6262-6272.

423. Dziema H, Oatis B, Butcher GQ, Yates R, Hoyt KR, et al. The ERK/MAP kinase pathway couples light to immediate-early gene expression in the suprachiasmatic nucleus. Eur J Neurosci 2003;17:1617-1627.

424. Sarker KP, Lee KY. L6 myoblast differentiation is modulated by Cdk5 via the PI3K-AKT-p70S6K signaling pathway. Oncogene 2004;23:6064-6070.

425. Huang RP, Liu C, Fan Y, Mercola D, Adamson ED. Egr-1 negatively regulates human tumor cell growth via the DNA-binding domain. Cancer Res 1995;55:5054-5062.

426. Schopfer FJ, Lin Y, Baker PR, Cui T, Garcia-Barrio M, et al. Nitrolinoleic acid: an endogenous peroxisome proliferator-activated receptor g ligand. Proc Natl Acad Sci U S A 2005;102:2340-2345.

427. Rieusset J, Touri F, Michalik L, Escher P, Desvergne B, et al. A new selective peroxisome proliferator-activated receptor g antagonist with antiobesity and antidiabetic activity. Mol Endocrinol 2002;16:2628-2644.

428. Berger JP, Petro AE, Macnaul KL, Kelly LJ, Zhang BB, et al. Distinct properties and advantages of a novel peroxisome proliferator-activated protein g selective modulator. Mol Endocrinol 2003;17:662-676.

429. Koyama H, Miller DJ, Boueres JK, Desai RC, Jones AB, et al. (2R)-2-ethylchromane-2-carboxylic acids: discovery of novel PPARà/ g dual agonists as antihyperglycemic and hypolipidemic agents. J Med Chem 2004;47:3255-3263.

430. Acton JJ, III, Black RM, Jones AB, Moller DE, Colwell L, et al. Benzoyl 2-methyl indoles as selective PPAR g modulators. Bioorg Med Chem Lett 2005;15:357-362.

431. Liu K, Black RM, Acton JJ, III, Mosley R, Debenham S, et al. Selective PPAR g modulators with improved pharmacological profiles. Bioorg Med Chem Lett 2005;15:2437-2440.

432. Suh N, Wang Y, Honda T, Gribble GW, Dmitrovsky E, et al. A novel synthetic oleanane triterpenoid, 2-cyano-3,12-dioxoolean-1,9-dien-28-oic acid, with potent differentiating, antiproliferative, and anti-inflammatory activity. Cancer Res 1999;59:336-341.

433. Place AE, Suh N, Williams CR, Risingsong R, Honda T, et al. The novel synthetic triterpenoid, CDDO-imidazolide, inhibits inflammatory response and tumor growth *in vivo*. Clin Cancer Res 2003;9:2798-2806.

434. Osawa E, Nakajima A, Wada K, Ishimine S, Fujisawa N, et al. Peroxisome proliferator-activated receptor g ligands suppress colon carcinogenesis induced by azoxymethane in mice. Gastroenterology 2003;124:361-367.

435. Niho N, Takahashi M, Shoji Y, Takeuchi Y, Matsubara S, et al. Dose-dependent suppression of hyperlipidemia and intestinal polyp formation in Min mice by pioglitazone, a PPAR g ligand. Cancer Sci. 2003;94:960-964.

436. Chintharlapalli S, Papineni S, Baek SJ, Liu S, Safe S. 1,1-Bis(3'-indolyl)-1-(p -substitutedphenyl)methanes are peroxisome proliferator-activated receptor gamma agonists but decrease HCT-116 colon cancer cell survival through receptor-independent activation of early growth response-1 and NAG-1. Mol Pharmacol 2005:[Epub ahead of print].

437. Abdelrahim M, Newman K, Vanderlaag K, Samudio I, Safe S. 3,3'-Diindolylmethane (DIM) and derivatives induce apoptosis in pancreatic cancer cells through endoplasmic reticulum stress-dependent upregulation of DR5. Carcinogenesis 2005:in review.

438. Saidi JA, Chang DT, Goluboff ET, Bagiella E, Olsen G, et al. Declining sperm counts in the United States? A critical review. J Urol 1999;161:460-462.

439. Liu T, Bauskin AR, Zaunders J, Brown DA, Pankhurst S, et al. Macrophage inhibitory cytokine 1 reduces cell adhesion and induces apoptosis in prostate cancer cells. Cancer Res 2003;63:5034-5040.

440. Tsai MJ, O'Malley BW. Molecular mechanisms of action of steroid/thyroid receptor superfamily members. Annu Rev Biochem 1994;63:451-486.

441. Mangelsdorf DJ, Thummel C, Beato M, Herrlich P, Schutz G, et al. The nuclear receptor superfamily: the second decade. Cell 1995;83:835-839.

442. Beato M, Herrlich P, Schutz G. Steroid hormone receptors: many actors in search of a plot. Cell 1995;83:851-857.

443. Olefsky JM. Nuclear receptor minireview series. J Biol Chem 2001;276:36863-36864.

444. Enmark E, Gustafsson JA. Orphan nuclear receptors--the first eight years. Mol Endocrinol 1996;10:1293-1307.

445. Giguere V. Orphan nuclear receptors: from gene to function. Endo Rev 1999;20:689-725.

446. Mohan R, Heyman RA. Orphan nuclear receptor modulators. Curr Top Med Chem 2003;3:1637-1647.

447. Milbrandt J. Nerve growth factor induces a gene homologous to the glucocorticoid receptor gene. Neuron 1988;1:183-188.

448. Ryseck RP, Macdonald-Bravo H, Mattei MG, Ruppert S, Bravo R. Structure, mapping and expression of a growth factor inducible gene encoding a putative nuclear hormonal binding receptor. EMBO J 1989;8:3327-3335.

449. Nakai A, Kartha S, Sakurai A, Toback FG, DeGroot LJ. A human early response gene homologous to murine nur77 and rat NGFI-B, and related to the nuclear receptor superfamily. Mol Endocrinol 1990;4:1438-1443.

450. He YW. Orphan nuclear receptors in T lymphocyte development. J Leukoc Biol 2002;72:440-446.

451. Cheng LE, Chan FK, Cado D, Winoto A. Functional redundancy of the Nur77 and Nor-1 orphan steroid receptors in T-cell apoptosis. EMBO J 1997;16:1865-1875.

452. Calnan BJ, Szychowski S, Chan FK, Cado D, Winoto A. A role for the orphan steroid receptor Nur77 in apoptosis accompanying antigen-induced negative selection. Immunity 1995;3:273-282.

453. Li H, Kolluri SK, Gu J, Dawson MI, Cao X, et al. Cytochrome c release and apoptosis induced by mitochondrial targeting of nuclear orphan receptor TR3. Science 2000;289:1159-1164.

454. Lin B, Kolluri SK, Lin F, Liu W, Han YH, et al. Conversion of Bcl-2 from protector to killer by interaction with nuclear orphan receptor Nur77/TR3. Cell 2004;116:527-540.

455. Wu Q, Liu S, Ye XF, Huang ZW, Su WJ. Dual roles of Nur77 in selective regulation of apoptosis and cell cycle by TPA and ATRA in gastric cancer cells. Carcinogenesis 2002;23:1583-1592.

456. Holmes WF, Soprano DR, Soprano KJ. Early events in the induction of apoptosis in ovarian carcinoma cells by CD437: activation of the p38 MAP kinase signal pathway. Oncogene 2003;22:6377-6386.

457. Holmes WF, Soprano DR, Soprano KJ. Comparison of the mechanism of induction of apoptosis in ovarian carcinoma cells by the conformationally restricted synthetic retinoids CD437 and 4-HPR. J Cell Biochem 2003;89:262-278.

458. Wilson AJ, Arango D, Mariadason JM, Heerdt BG, Augenlicht LH. TR3/Nur77 in colon cancer cell apoptosis. Cancer Res 2003;63:5401-5407.

459. Mu X, Chang C. TR3 orphan nuclear receptor mediates apoptosis through up-regulating E2F1 in human prostate cancer LNCaP cells. J Biol Chem 2003;278:42840-42845.

460. Abdelrahim M, Samudio I, Smith R, Burghardt R, Safe S. Small inhibitory RNA duplexes for Sp1 mRNA block basal and estrogen-induced gene expression and cell cycle progression in MCF-7 breast cancer cells. J Biol Chem 2002;277:28815-288422.

461. McDougal A, Sethi-Gupta M, Ramamoorthy K, Sun G, Safe S. Inhibition of carcinogen-induced rat mammary tumor growth and other estrogen-dependent responses by symmetrical dihalo-substituted analogs of diindolylmethane. Cancer Letts 2000;151:169-179.

462. McDougal A, Wilson C, Safe S. Inhibition of 7,12-dimethylbenz[a]anthracene-induced rat mammary tumor growth by aryl hydrocarbon receptor agonists. Cancer Lett 1997;120:53-63.

463. Philips A, Lesage S, Gingras R, Maira MH, Gauthier Y, et al. Novel dimeric Nur77 signaling mechanism in endocrine and lymphoid cells. Mol Cell Biol 1997;17:5946-5951.

464. Maira M, Martens C, Batsche E, Gauthier Y, Drouin J. Dimer-specific potentiation of NGFI-B (Nur77) transcriptional activity by the protein kinase A pathway and AF-1-dependent coactivator recruitment. Mol Cell Biol 2003;23:763-776.

465. Rosenfeld MG, Glass CK. Coregulator codes of transcriptional regulation by nuclear receptors. J Biol Chem 2001;276:36865-36868.

466. Xu J, Li Q. Review of the *in vivo* functions of the p160 steroid receptor coactivator family. Mol Endocrinol 2003;17:1681-1692.

467. Smith CL, O'Malley BW. Coregulator function: a key to understanding tissue specificity of selected receptor modulators. Endo Rev 2004;25:45-71.

468. Kuang AA, Cado D, Winoto A. Nur77 transcription activity correlates with its apoptotic function *in vivo*. Eur J Immunol 1999;29:3722-3728.

469. Rajpal A, Cho YA, Yelent B, Koza-Taylor PH, Li D, et al. Transcriptional activation of known and novel apoptotic pathways by Nur77 orphan steroid receptor. EMBO J 2003;22:6526-6536.

470. Law SW, Conneely OM, DeMayo FJ, O'Malley BW. Identification of a new brain-specific transcription factor, NURR1. Mol Endocrinol 1992;6:2129-2135.

471. Liu ZG, Smith SW, McLaughlin KA, Schwartz LM, Osborne BA. Apoptotic signals delivered through the T-cell receptor of a T-cell hybrid require the immediate-early gene nur77. Nature 1994;367:281-284.

472. Woronicz JD, Calnan B, Ngo V, Winoto A. Requirement for the orphan steroid receptor Nur77 in apoptosis of T-cell hybridomas. Nature 1994;367:277-281.

473. Kim SO, Ono K, Tobias PS, Han J. Orphan nuclear receptor Nur77 is involved in caspase-independent macrophage cell death. J Exp Med 2003;197:1441-1452.

474. Shin HJ, Lee BH, Yeo MG, Oh SH, Park JD, et al. Induction of orphan nuclear receptor Nur77 gene expression and its role in cadmium-induced apoptosis in lung. Carcinogenesis 2004;25:1467-1475.

475. Wang Z, Benoit G, Liu J, Prasad S, Aarnisalo P, et al. Structure and function of Nurr1 identifies a class of ligand-independent nuclear receptors. Nature 2003;423:555-560.

476. Baker KD, Shewchuk LM, Kozlova T, Makishima M, Hassell A, et al. The Drosophila orphan nuclear receptor DHR38 mediates an atypical ecdysteroid signaling pathway. Cell 2003;113:731-742.

477. Benoit G, Malewicz M, Perlmann T. Digging deep into the pockets of orphan nuclear receptors: insights from structural studies. Trends Cell Biol. 2004;14:369-376.

478. Sohn YC, Kwak E, Na Y, Lee JW, Lee SK. Silencing mediator of retinoid and thyroid hormone receptors and activating signal cointegrator-2 as transcriptional coregulators of the orphan nuclear receptor Nur77. J Biol Chem 2001;276:43734-43739.

479. Wansa KD, Harris JM, Muscat GE. The activation function-1 domain of Nur77/NR4A1 mediates trans-activation, cell specificity, and coactivator recruitment. J Biol Chem 2002;277:33001-33011.

480. Codina A, Benoit G, Gooch JT, Neuhaus D, Perlmann T, et al. Identification of a novel co-regulator interaction surface on the ligand binding domain of Nurr1 using NMR footprinting. J Biol Chem 2004;279:53338-53345.

481. Nishino H, Nishino A, Takayasu J, Hasegawa T, Iwashima A, et al. Inhibition of the tumor-promoting action of 12-O-tetradecanoylphorbol-13-acetate by some oleanane-type triterpenoid compounds. Cancer Res 1988;48:5210-5215.

482. Huang MT, Ho CT, Wang ZY, Ferraro T, Lou YR, et al. Inhibition of skin tumorigenesis by rosemary and its constituents carnosol and ursolic acid. Cancer Res 1994;54:701-708.

483. Suh N, Honda T, Finlay HJ, Barchowsky A, Williams C, et al. Novel triterpenoids suppress inducible nitric oxide synthase (iNOS) and inducible cyclooxygenase (COX-2) in mouse macrophages. Cancer Res 1998;58:717-723.

484. Honda T, Finlay HJ, Gribble GW, Suh N, Sporn MB. New enone derivatives of oleanolic acid and ursolic acid as inhibitors of nitric oxide production in mouse macrophages. Bioorg Med Chem Lett 1997;7:1623-1628.

485. Honda T, Rounds BV, Gribble GW, Suh N, Wang Y, et al. Design and synthesis of 2-cyano-3,12-dioxoolean-1,9-dien-28-oic acid, a novel and highly active inhibitor of nitric oxide production in mouse macrophages. Bioorg Med Chem Lett 1998;8:2711-2714.

486. Honda T, Rounds BV, Bore L, Finlay HJ, Favaloro FG, Jr., et al. Synthetic oleanane and ursane triterpenoids with modified rings A and C: a series of highly active inhibitors of nitric oxide production in mouse macrophages. J Med Chem 2000;43:4233-4246.

487. Wang Y, Porter WW, Suh N, Honda T, Gribble GW, et al. A synthetic triterpenoid, 2-cyano-3,12-dioxooleana-1,9-dien-28-oic acid (CDDO), is a ligand for the peroxisome proliferator-activated receptor g. Mol Endocrinol 2000;14:1550-1556.

488. Ito Y, Pandey P, Place A, Sporn MB, Gribble GW, et al. The novel triterpenoid 2-cyano-3,12-dioxoolean-1,9-dien-28-oic acid induces apoptosis of human myeloid

leukemia cells by a caspase-8-dependent mechanism. Cell Growth Differ 2000;11:261-267.

489. Stadheim TA, Suh N, Ganju N, Sporn MB, Eastman A. The novel triterpenoid 2-cyano-3,12-dioxooleana-1,9-dien-28-oic acid (CDDO) potently enhances apoptosis induced by tumor necrosis factor in human leukemia cells. J Biol Chem 2002;277:16448-16455.

490. Pedersen IM, Kitada S, Schimmer A, Kim Y, Zapata JM, et al. The triterpenoid CDDO induces apoptosis in refractory CLL B cells. Blood 2002;100:2965-2972.

491. Konopleva M, Tsao T, Ruvolo P, Stiouf I, Estrov Z, et al. Novel triterpenoid CDDO-Me is a potent inducer of apoptosis and differentiation in acute myelogenous leukemia. Blood 2002;99:326-335.

492. Suh WS, Kim YS, Schimmer AD, Kitada S, Minden M, et al. Synthetic triterpenoids activate a pathway for apoptosis in AML cells involving downregulation of FLIP and sensitization to TRAIL. Leukemia 2003;17:2122-2129.

493. Ikeda T, Sporn M, Honda T, Gribble GW, Kufe D. The novel triterpenoid CDDO and its derivatives induce apoptosis by disruption of intracellular redox balance. Cancer Res 2003;63:5551-5558.

494. Konopleva M, Elstner E, McQueen TJ, Tsao T, Sudarikov A, et al. Peroxisome proliferator-activated receptor g and retinoid X receptor ligands are potent inducers of differentiation and apoptosis in leukemias. Mol Cancer Ther 2004;3:1249-1262.

495. Konopleva M, Tsao T, Estrov Z, Lee RM, Wang RY, et al. The synthetic triterpenoid 2-cyano-3,12-dioxooleana-1,9-dien-28-oic acid induces caspase-dependent and -independent apoptosis in acute myelogenous leukemia. Cancer Res 2004;64:7927-7935.

496. Lapillonne H, Konopleva M, Tsao T, Gold D, McQueen T, et al. Activation of peroxisome proliferator-activated receptor g by a novel synthetic triterpenoid 2-cyano-3,12-dioxooleana-1,9-dien-28-oic acid induces growth arrest and apoptosis in breast cancer cells. Cancer Res 2003;63:5926-5939.

497. Hail N, Jr., Konopleva M, Sporn M, Lotan R, Andreeff M. Evidence supporting a role for calcium in apoptosis induction by the synthetic triterpenoid 2-cyano-3,12-dioxooleana-1,9-dien-28-oic acid (CDDO). J Biol Chem 2004;279:11179-11187.

498. Kim KB, Lotan R, Yue P, Sporn MB, Suh N, et al. Identification of a novel synthetic triterpenoid, methyl-2-cyano-3,12-dioxooleana-1,9-dien-28-oate, that potently induces caspase-mediated apoptosis in human lung cancer cells. Mol Cancer Ther 2002;1:177-184.

499. Zou W, Liu X, Yue P, Zhou Z, Sporn MB, et al. c-Jun NH 2 -terminal kinase-mediated up-regulation of death receptor 5 contributes to induction of apoptosis by the novel synthetic triterpenoid methyl-2-cyano-3,12-dioxooleana-1,9-dien-28-oate in human lung cancer cells. Cancer Res 2004;64:7570-7578.

500. Ito Y, Pandey P, Sporn MB, Datta R, Kharbanda S, et al. The novel triterpenoid CDDO induces apoptosis and differentiation of human osteosarcoma cells by a caspase-8 dependent mechanism. Mol Pharmacol 2001;59:1094-1099.

501. Melichar B, Konopleva M, Hu W, Melicharova K, Andreeff M, et al. Growth-inhibitory effect of a novel synthetic triterpenoid, 2-cyano-3,12-dioxoolean-1,9-dien-28-oic acid, on ovarian carcinoma cell lines not dependent on peroxisome proliferator-activated receptor- g expression. Gynecol Oncol 2004;93:149-154.

502. Grommes C, Landreth GE, Heneka MT. Antineoplastic effects of peroxisome proliferator-activated receptor g agonists. Lancet Oncol 2004;5:419-429.

VITA

Name: Sudhakar Reddy Chintharlapalli

Mailing Address: Department of Veterinary Physiology & Pharmacology
                       4466 TAMU, College Station, TX 77843-4466

Education: 2005 **Doctor of Philosophy in Biochemistry**
                       Texas A&M University, College Station, TX (GPA 4.0/4.0)

                       2002 **Master of Science in Chemistry**
                       Texas A&M University, Kingsville, TX (GPA 4.0/4.0)

                       1999 **B.V.M.** (equivalent to DVM)
                       Acharya N. G. Ranga Agricultural University
                       Rajendranagar, India (GPA 3.8/4.0)

HONORS AND AWARDS:

2005   First place for best platform presentation in the life sciences category, Student Research Week, Texas A&M University, College Station
2005   Merck award presented at the Society of Toxicology Carcinogenesis Specialty Section Annual meeting, New Orleans, Louisiana.
2005   Second place for best platform presentation at the Gulf Coast Chapter Society of Toxicology, 2005 Annual Meeting, M. D. Anderson Cancer Center, Houston, Texas.
2004   Second place for best poster presentation in the Toxicology Graduate Student Symposium, College Station, Texas,
2002   First place for best poster presentation in the CANCER category. 2nd Biennial RIMI/NIH Research Symposium. Morgan State University, Baltimore, Maryland,
2002   Second place for best poster presentation at the 105th Annual Meeting of the Texas Academy of Science, Texas A&M International University, Laredo, Texas.
2000   RIMI-Research Infrastructure in Minority Institutions Fellowship, 2000-2002
2000   Dr. P. Rama Krishna Reddy Memorial Gold Medal for securing the highest GPA in the subject of Animal Genetics & Breeding.
1999   Sri O. Pulla Reddy (I.C.S) Memorial Medal for securing the highest OGPA in the College of Veterinary Science, Rajendranagar, Acharya N. G. Ranga Agricultural University.